Optimisation of a residential energy system with an embedded PV source

by

Tielman Nieuwoudt

Thesis presented in partial fulfilment of the requirements for the degree

Master of Science in Engineering at

Stellenbosch University

Supervisor: Prof. Hendrik Johannes Vermeulen

March 2016

Declaration

By submitting this thesis/dissertation electronically, I declare that the entirety of the work contained therein is my own, original work, that I am the sole author thereof (save to the extent explicitly otherwise stated), that reproduction and publication thereof by Stellenbosch University will not infringe any third party rights and that I have not previously in its entirety or in part submitted it for obtaining any qualification.

March 2016

Acknowledgements

The author gratefully acknowledges the contributions of the following individuals and institutions:

- My study leader, HJ Vermeulen, for the initial inspiration for the project and the guidance and commitment to simplify and improve presentation of the work.
- Those that have proved unwavering support to the author while working on the project: JH Nieuwoudt, CJ Nieuwoudt, L Viljoen and other friends and family.
- For the confidential data provided by T Willemse, acting on behalf of ESKOM.
- Stellenbosch University for the dedication to provide high quality research facilities.

Abstract

The economic viability of PhotoVoltaic (PV) systems for the residential sector remains one of the greatest barriers to PV adoption. Economic viability of PV systems can be expressed in terms of a wide array of financial indicators. The economic viability of a PV system can be difficult to interpret for potential PV system owners, due to the fact that financial indicators for PV systems can involve concepts such as inflation, changing electricity tariffs, time-of-use tariffs and feed-in tariffs. This project focuses on simple payback time and determines the effect of tariff structures, load schedule optimisation and battery storage on the payback time of PV systems. The project goes on to determine whether an optimal PV system rating exists for which the payback time is minimum.

For this purpose, a mathematical model is developed for a residential energy system. This mathematical model includes the subsystems present in a smart residential energy system, namely the non-controllable loads, controllable loads, battery storage, a PV system and the grid. The grid is associated with electricity tariffs, allowing for time-of-use tariffs as well as feed-in tariffs. The mathematical model can model the energy flow between subsystems. It provides a method of calculating energy cost for the residential energy system.

A software application that implements the above mathematical model is developed to explore the payback time of residential PV systems. The application takes as input a load profile, solar profile and grid connection tariff structure. It calculates the PV system payback time as a function of PV systems rating. An optimisation is implemented to identify the PV system rating with the minimum payback time.

Financial performance and optimisation results are presented for two sets of case studies. The first set of case studies is exploratory. Using simple input parameters, cause-and-effect relationships between input parameters and results established. The second set of case studies use representative input parameters to confirm that the observed cause-and-effect relationships are present in practical residential energy systems.

The project identifies important mathematical factors that determine PV system payback time depending on the use of tariff structure, the inclusion of load schedule optimisation and/or the inclusion of battery storage. It is concluded that for each residential energy system, an optimal PV system rating with a minimum payback time exists.

Opsomming

Die ekonomiese vatbaarheid van Photovoltaiese (PV) stelsels vir die residensiële sektor bly een van die grootste verhinderings tot PV installasies. Die begrip van ekonomiese vatbaarheid van PV stelsels word bemoeilik vir potensiële PV stelsel eienaars deurdat finansiële aanwysers vir PV stelsels konsepte insluit soos inflasie, veranderende electrisiteitspryse en tyd-afhanklike elektrisiteitaankoop en -verkoop tariewe. Die projek fokus op terugbetalingstydperk en bepaal hoe elektrisiteit-tariefstrukture, las-skedule optimering en batterykrag die terugbetaaltyd van PV stelsels beïnvloed. Die projek stel verder ondersoek in om te bepaal of ‘n optimale PV stelsel grootte met minimum terugbetalingstydperk bestaan.

Ten einde die doel te bereik is ‘n wiskudige model vir ‘n residensiële kragstelsel ontwikkel. Die wiskundige model sluit onderliggende stelsels in ‘n intelligente huiskragstelsel in, naamlik die nie-beheerbare laste, die beheerbare laste, batterykrag, die PV stelsel en die kragnetwerk. Die kragnetwerk word geassosieer met ‘n elektrisiteits-tariefstruktuur, wat toelaat vir tyd-van-die-dag verbruikstariewe en invoer tariewe. Die wiskundige model modelleer die vloei van energie tussen die onderliggende stelsels. Dit bied die geleentheid om koste aangaande die residensiële kragstelsels te bereken.

‘n Sagteware program wat die bogenoemde wiskundige model implementeer is ontwikkel om verkenningswerk te doen aangaande die terugbetaaltydperk van PV stelsels. Die program se invoer is ‘n lasprofiel, sonkragprofiel en die tariefstruktuure van die kragnetwerk. Die program bereken die terugbetalingstydperk as ‘n funksie van die PV stelsel grootte. ‘n Optimering identifiseer die PV stelsel te identifiseer met die minimum tergbetalingstydperk.

Finansiële prestasie- en optimeringsresultate word dan aangebied vir twee stelle gevallestudies. Die eerste stel is verkennend. Eenvoudige invoer parameters word gebruik om oorsaak-en-gevolg verhoudings tussen invoer parameters en resulate te verken. Die tweede stel gevallestudies gebruik verteenwoordigende invoer parameters om te bevestig dat die oorsaak-en-gevolg verhoudings wel teenwoordig is in praktiese residensiële kragstelsels.

Die projek identifiseer belangrike wiskundige faktore ten opsigte van PV stelsels se terugbetaaltyd na aanleiding van die betrokke tariefstruktuur, die gebruik van lasprofiel optimering en/of die insluiting van batterystelsels. Dit word bevind dat ‘n optimale PV stelsel grootte met minimum terugbetalings tydperk vir ‘n residensiële kragstelsel bestaan.

Contents

List of Figures

List of Tables

List of Appendix Figures

List of Appendix Tables

List of Symbols

$\boldsymbol{T}$	Array of time stamps of a 24 hour day
t_k	Timestamp value at index *k*
k	Index for timestamp values
N_K	The number of timestamps per day
$P(t)$	Instantaneous power usage function
$\widetilde{\boldsymbol{P}}$	Vector of averaged power profiles
$\tilde{P}_k$	Element of $\widetilde{\boldsymbol{P}}$ at index *k*
$\boldsymbol{E}$	Energy use profile set
E_k	Element of $\boldsymbol{E}$ at index *k*
i	Index for subsystems in the energy system topology
N_M	The number of subsystems in an energy system topology
$\boldsymbol{E}^I$	Subset of $\boldsymbol{E}$ that is imported
$\boldsymbol{R}^I$	Per-unit energy cost profile for imported energy
$\boldsymbol{C}^I$	Energy import cost set
c_{ik}^I	Energy import cost for subsystem *i* during averaging interval *k*
$C_i^{I\prime}$	Total cost of imported energy for subsystem i
$\boldsymbol{E}^E$	Subset of $\boldsymbol{E}$ that is exported
$\boldsymbol{R}^E$	Per-unit energy cost profile for exported energy
$\boldsymbol{C}^E$	Energy export cost set
c_{ik}^E	Energy export cost for subsystem *i* during averaging interval *k*
$C_i^{E\prime}$	Total cost of imported energy for subsystem *i*
C'_i	Net cost associated with subsystem *i*
$P_G(t)$	Instantaneous power flow to/from the grid
$P_{G\,max}$	Max allowed power flow to/from grid
$\boldsymbol{E}_G$	Energy transfer set for grid subsystem
$P_{PV}(t)$	Instantaneous power flow from PV panels
$P_{PV\,max}$	Max allowed power flow from PV panels
$\boldsymbol{E}_{PV}$	Energy transfer set for PV subsystem
$P_{LU}(t)$	Instantaneous power flow to non-schedulable loads
$P_{LU\,max}$	Max allowed power flow to non-schedulable loads
$\boldsymbol{E}_{LU}$	Energy transfer set for non-schedulable loads subsystem

$P_{LC}(t)$	Instantaneous power flow to schedulable loads
$P_{LC\,max}$	Max allowed power flow to schedulable loads
$\boldsymbol{E}_{LC}$	Energy transfer set for schedulable loads subsystem
$P_B(t)$	Instantaneous power flow to/from energy storage
$-P_{BD\,max}$	Max allowed power flow from the energy storage (discharge)
$P_{BC\,max}$	Max allowed power flow to the storage (charge)
$\boldsymbol{E}_B$	Energy transfer set for energy storage subsystem
E_{Bmin}	Minimum energy in the battery
E_{Bmax}	Maximum energy in the battery
B_R	Rating of the battery system
B_{DOD}	Depth-of-discharged allowed for the battery system
M	Index for each schedulable load in the set of schedulable loads
N_S	Total number of schedulable loads
P_{Lm}	The power rating of schedulable load *m*
$\boldsymbol{A}_{Lm}$	The set of operation cycles for load P_{Lm}
n	Index for operation cycles in the set of operation cycles $\boldsymbol{A}_{Lm}$
N_C	Total number of operation cycles in $\boldsymbol{A}_{Lm}$
T_{Amn}	The starting time of operation cycle *n* for schedulable load *m*
D_{Amn}	The duration of operation cycle *n* for schedulable load *m*
C_G'	Net cost of energy imported from of exported to the grid.
C'	Savings after system installation
I_C	Combined PV and battery storage capital cost
S_C	PV system capital cost
B_C	Battery storage system capital cost
T_{pb}	Payback period of the installed system
S_R	Battery system rating
$S_R min$	Lower bound for battery system rating optimisation
$S_R max$	Upper bound for battery system rating optimisation
B_R	Battery system rating
$B_R min$	Lower bound for battery system rating optimisation
$B_R max$	Upper bound for battery system rating optimisation
$S_{pu}(S_R)$	PV system per-watt (per-unit) cost
$\Delta\boldsymbol{E}^{\boldsymbol{I}}$	Fraction of energy from the $\boldsymbol{E}_{PV}$ set that is utilised locally
$\Delta\boldsymbol{E}^{\boldsymbol{E}}$	Fraction of energy from the $\boldsymbol{E}_{PV}$ set that is unused (possibly exported to the grid)
$\boldsymbol{F}_U$	PV energy utilisation factor

1 Project Overview

1.1 Introduction

Photovoltaic systems have long been a favoured method of lowering grid electricity consumption at residences. As repeatedly noted in published works on the subject [1-5], one of the key challenges towards mass adoption of this technology is the high investment cost and the uncertainty about whether or not the systems are economically viable. The question of economic viability quickly becomes complex: The acquisition of necessary information to determine the economic feasibility is but the first challenge. Armed with that knowledge, simulation software can be applied to attempt to predictively calculate the most economically sensible PV system available on the market. It is at this calculation attempt that this project seeks to answer the question: What is the optimal PV system rating to be installed at a residence to ensure maximum economic viability?

Investigating this question turns up a host of key questions to be answered, questions such as: What is the effect of installing a PV system with a higher or lower PV system rating? What is the effect of feed-in tariffs, whereby residences are remunerated for feeding their surplus electricity back into the grid? Are there significant advantages to installing appliances at a residence of which the load schedules can be controlled to try and minimise electricity cost?

This project aims to answer these questions amidst the various different residential electrical topologies and tariff schemes implemented throughout the world. Where traditionally a common scenario would be that the residential electricity system would simply consume energy from the grid and then be billed for this energy, the scenario can now be much more involved: Loads may constitute of both schedulable and non-schedulable loads, electricity tariffs have the possibility of being time-dependant (with schemes such as Time-of-Use tariffs [6, 7]), electricity may be fed electricity back into the grid for compensation [8, 9] and battery storage can adapt charge and discharge profiles to change the residential load profile.

The concepts stipulated above all contribute to more intelligent management of energy, which is a driving factor of the smart grid concept. The definition of a smart grid is varied and diverse [10-12]. A common idea among definitions is that it monitors and reports the grid state more intelligently, through which more intelligent management of electricity can be achieved. One view is that the smart grid is not a specific type of grid to be installed in the place of traditional grid systems, but that smart grids are rather a continual improvement of the current grid system. Consider the quote by Farhangi [10]: "…Utilities believe that investing in distribution automation will provide them with increasing capabilities over time…". This implies that the features/capabilities mentioned in the previous paragraph can independently be implemented in electric grid systems. Each of these features creates new opportunities for electricity consumers to manage and control their electricity consumption.

To deal with this increasing complexity and assist in the modelling thereof, the residence is modelled as *smart microgrid*. The concept of a smart microgrid, or equivalently a mini smart grid, is where the electricity system inside a residence is managed with smart technologies. A strong focus is placed in this project in the mathematical modelling of the smart microgrid. The only interaction this project will have with the electric utility grid is importing or exporting energy from or to it. The microgrid is then implemented, modelled, tweaked and in some cases fitted with optimisation software, all with the final goal of finding the optimal rating of a PV and possible battery system that maximises the economic viability of the installed system.

1.2 Project Motivation

Installing PV systems can be financially rewarding, but with the significant upfront cost this investment needs to be carefully analysed and understood. It's important to identify the factors that influence financial performance when a range of PV system ratings are considered. Two particular additions to a residential energy system are available that can impact the financial performance. These additions are energy storage and loads of which the load profile can be optimised and controlled. These additions allow greater flexibility of energy management within the residential energy system. A third factor that impacts financial performance in the modern electrical grid is the tariff structures. Tariff structures can implement time-of-use tariffs and feed-in tariffs. In the light of the discussed factors, this study will aim to determine the effects and dynamics of these factors on the financial performance of PV systems.

Installing PV systems at a residence is closely linked to the principle of Distributed Generation (DG) in a power system, whereas load scheduling is a mechanism which is discussed in literature as part of Demand Side Management (DSM). PV system installations contribute some of the advantages brought forward through DG [13-15]. DG is the generation of electricity on a small scale in a network, as opposed to the traditional centralised generation. The following advantages of renewable DG are briefly discussed [14]:

- Liberalisation of electricity markets

Distributed generation allows residents to become more independent of electricity suppliers to an extent by providing their own electricity.

- Environmental concerns:

Renewable energy generates electricity with less pollution, and furthermore the centralized pollution associated with large generation plants is lessened.

- Reduced transmission power and energy

Reducing the amount of electricity transported over the network by generating electricity at households self. This can lower transportation losses and additionally lower the strain on transmission systems under severe load conditions.

It is worth noting that there are also major challenges associated with DG, but these are not mentioned here as the scope of the project does not included grid stability and issues such as islanding networks during fault conditions.

Demand Side Management (DSM) encapsulates some of the concepts that will be brought forward when a PV system is installed in a residence. The concept of DSM is given concisely by Gellings [16] when he states that control is shifted from generation side to customer side:

> "In order to increase efficiency and hold the line on costs, utilities are now controlling, directly and indirectly, when and how the electric energy is used – shifting from a supply-side-only viewpoint to an integrated demand- and supply-side viewpoint."

How this can be an advantage to the grid utility is again stated by Gellings, albeit in a different publication [17], when he describes that DSM is the

> "Planning and implementation of utility activities designed to influence the time pattern and/or amount of electricity demand in ways that will increase customer satisfaction, and coincidentally produce the desired changes in the utility's system load shape."

DSM adapts load profile to improve the grid efficiency or stability through, among other factors, peak clipping and load shifting. These are applied through several methods, but included in this study is TOU rates and load control. The interaction of DSM with microgrid is briefly mentioned to be one of the driving factors for renewed interest in DSM [18].

The key motivation behind this project is twofold. The first motivation is to understand the important factors that influence financial performance of PV systems. The second motivation is to determine whether an optimal PV system rating exists for a given residential energy system. These are meant to provide a better understanding of the effect of installing PV systems and provide insight into how PV systems can become economically viable. Maximising the economic viability of renewable energies (as this project focuses on solar, that will be used as the representative of renewables) is of utmost importance as economics have been identified as one of the (if not *the*) barrier to adoption [1-5].

This project will contribute to a set of goals and producing positive side effects:

- Decreasing electricity cost through more efficient use of energy at a residence
- Providing insight to policy makers to encourage PV system installation by providing the effects of tariff structure on the financial performance of PV systems
- Developing analysis tools to predict the financial returns on investments, focusing on but not limited to PV systems

There are more barriers of adoption that this project would clarify. Some barriers as mentioned in literature that this project will address is [19]

- Complexity
- Inconvenience
- Observability

The importance of removing these barriers allow for better market penetration of renewable technologies especially when third-party solar systems are considered [5]. This project aims to, through presentation of clear graphical results and concise explanation of findings, contribute to understanding the financial implications of installing renewables at a residence.

1.3 Project Description

1.3.1 Research Objectives

The motivations for this project as discussed above gives rise the following objectives:

- Creating a mathematical model of PV system financial performance based on the parameters of a residential energy system. This model is the core of the work and will be applied to answer key questions and address the research tasks.
- Constructing PV system financial simulation software to calculate the financial performance of the residential PV system, using the developed mathematical model.
- Analysing, understanding and logically explaining the effect of the input parameters, the battery storage and controllable loads on the financial viability of residential PV systems.
- Investigate the possibility of using an optimisation algorithm to find an optimal PV system rating for a residential energy system.

The project requires research and development of a custom implementation of analytical software application. It will be able to take as input the residential energy system parameters calculate relevant financial indicators. The achievement of these objectives will provide insightful analysis tools and indicators. This will be applied to understand the effect of parameters of a residential energy system on the financial performance of PV systems. It will particularly provide insight into the installation of small scale renewable plants and battery banks at the residence.

1.3.2 Key Questions

The key questions that this project aims to answer are given as follows:

- What financial indicators provide relevant and realistic reflections of the economic viability of the PV system?
- How does the economic viability of PV systems vary over a range of system ratings? Several parameters of the environment in which the system operates should be considered, including:
    - The tariff system, allowing for time-of-use and feed-in tariffs
    - The load profile of the residence

  - The effect of including controllable loads
  - The expected solar irradiation profile for the specific location of the residence
  - Cost of installing a PV system
  - Cost of installing an energy storage system
- What are the important relationships between input parameters and results with regards to the financial viability of the PV system?
- Does an optimal rating exist for solar plants to maximum economic viability?
- What is the contribution of controllable loads toward the economic viability of PV systems?
- If energy storage is included in the system to try and improve efficiency, e.g. to store energy during cheap TOU tariff periods and offset more expensive energy use in more expensive TOU tariff periods, can it be successfully implemented improve the economic viability of PV systems?

1.3.3 **Research Tasks**

The research task to answer the key questions and achieve the research objectives are the following:

- Define a mathematical model for the residential energy systems, with consideration of the parameters that should be included in the system, and from which the financial performance of the PV systems can be calculated.
- Implement the mathematical model in a software application to simulate the residential energy system, the energy flows within this system and the electricity costs associated with the system.
- Acquire relevant research data with which realistic simulations can be run.
- Devise relevant analysis methods to analyse the results obtained by using the software application to simulate the residential energy system.
- Bind this application to a UI that makes it easier to input and access relevant information from the system.
- Construct relevant input parameters for a set of case studies, analyse it with the built application and provide results showing the findings through tables and graphs.

- Conduct case studies for residences with several different environmental factors, including
    - Different tariff structures both for drawing energy from the grid and feeding back into the grid.
    - Different solar profiles and different load profiles, unique to each residence

The case studies will present the information that answer the key questions for the various different parameters provided in each case study.

1.4 **Thesis Structure**

The rest of the document is structured as follows:

- Chapter 2: Literature Review

  The relevant literature concepts and topics are reviewed here. The review describes, amongst others, related works, PV system mechanics, energy storage mechanisms, optimisation algorithms, typical controllable loads and financial indicators.

- Chapter 3: Mathematical model

  The mathematical model that provides the interface between practical real-world systems and theoretical calculations is defined and specified in this chapter. The residential electrical topology is shown to contain *n subsystems*, and this is related to the residential electricity consumption, solar energy generation and total electricity cost.

- Chapter 4: Software Program Logic and structure

  The software implementation is presented here, setting out the program logic and structure between sections of the program (e.g. the sections for calculation, analysis and organisation of data storage).

- Chapter 5: Case Studies, Parameter Effects and Results

  This chapter aims to provide the information to answer the key questions. Each case study defines a residential energy system and the input parameters associated with it, including the tariff structures, load profiles, battery storage, etc. The software application then performs a simulation to present the results, including the energy flow and financial performance in the energy system. An analysis is done on the results to answer the key questions as set out above.

- Chapter 6: Conclusions and Recommendations

The final chapter draws the relationships between the findings from chapter 5 and the key questions and objects as set out in chapter 1. Recommendations are made on aspects that were identified in this project that could provide valuable insight if researched more in-depth.

2 Literature Study

2.1 Overview

The literature study presents previous work done on the subject of this project, as well presenting research on different fields from which features will be implemented in this project. Thereafter the different technical options to meet the project objectives are explored and a review of the recognised software design communication methodologies is given. The topics presented are:

- Previous work

A review of previous work in the field is presented. The focus of each related research project is discussed. The similarities and shortcomings of the research relevant to this project are discussed. Notable methodologies used in the related research are mentioned.

- Residential load modelling

This section explores the relevant methodologies of modelling energy flow in a residential energy system to optimise the PV system rating. Research is presented on how load profiles are typically modelled, and how the model is adapted when controllable loads are present in the residential energy system.

- Grid connection and tariffs

This section provides research on how residences connect to and interface with the grid. New developments and the introduction of Advanced Metering Infrastructure (AMI), that make more complex tariff structures possible, are researched. The feed-in tariff structure is explored to understand how electricity is exported back to the grid.

- Photovoltaic systems

Two fields of interest of PV systems in this project are presented. The first considers the typical components and connection topology of a residential PV system. The second is the matter on how to generate solar profiles for the household, both in an international and national context.

- Battery storage

Battery storage is a viable addition to a PV system and can possibly provide an additional dimension to the mathematical modelling of system rating optimisation. An overview is provided to indicate the relevant technologies for energy storage. Different parameters associated with battery storage that is relevant to this study are presented.

- Optimisation

A broad overview of the basic fields of optimisation is given. The basic methods of optimisation are considered. This provides necessary information to understand the design choices presented regarding controllable load optimisation and PV system rating optimisation.

- Financial indicators

The economic viability of PV systems is not bound to any specific financial indicator. A selection of the indicators relevant to PV systems are presented and discussed.

- Software development platforms

Specific characteristics of this project require a software engineering approach to understand the objective and develop a solution to reach this objective. Different development platforms are explored to determine what platforms will be used to develop the software application. The availability of the platforms and the support provided is considered to ensure successful development of the project.

- Unified modelling language

The designed software application is presented through the use of Unified Modelling Language (UML). The latest developments in the specification of the language are provided to ensure reporting on the software application design is done according to standard.

2.2 Previous work

Publications on the relationship between the load profile and economic viability of PV systems show that tariff and policy design have been studied closely in recent years. A 2011 study in California [20] used load data of 215 customers together with simulated solar profiles to study the effect of various policy decisions, with regards to feed-in tariffs, on the savings achieved by homeowners. Results indicated that savings achieved could differ with a factor of four based on the tariff policy chosen. Results were collected purely from a simulation; no mathematical equations were presented on which sensitivity analysis could be done for various parameters.

A 2007/2008 study in Japan [21] studied the economic optimisation and analysis of PV systems. This study included a mathematical model for the system to do a sensitivity analysis on the various parameters in the study. The objective of this study was to determine the minimum electricity cost per annum for a specific customer. The cost to the customer is a combination of the annualised PV system cost, the maintenance cost and purchasing electricity, while subtracting electricity sold to the grid. The study finds that an optimal PV system rating exists for each customer, depending on their specific inputs to the optimisation. The study uses a constant PV system purchase price over the range of PV systems rated 1 kW to 5 kW. It's found that the optimal PV system rating changes as the purchase price of the PV system changes. Sensitivity analysis is done on the system inputs with regards to payback time and levelised cost of energy.

A 2003 study from Japan [22] optimised a large PV system's rating by considering the fraction of the PV system energy utilisation locally (referred to as the "effectiveness factor"). This is then applied at a very rudimentary level to determine a PV system rating on which the rest of the research in the paper is based on.

2.3 Residential Load Modelling

2.3.1 Load monitoring and load profile forecast

Load monitoring is the process of continuously assessing the load curve of one or more appliances. The most widely praised and referenced work in this field was done by George Hart [23]. His work has since been improved on and is revised continuously. Hart focuses on non-intrusive load monitoring, where sensors are installed either between wall sockets and electrical plugs, or on the distribution board. This is opposed to intrusive monitoring, where sensors are installed inside an appliance, and possibly injects electrical signals into the electrical network.

Load monitoring usually captures information from multiple appliances. The challenge in identifying individual loads is the diversity of the appliances. Hart suggested the following classification of individual loads:

- On/Off loads – loads operating at fixed power when on
- Finite State Machine - loads that go through states using different power levels
- Continuously variable – loads with infinite number of states

But the classification remains a challenge. Figure 2-1 gives some indication of the variety in load appliances that has to be extracted from an aggregated load profile. Research has built upon Hart's work, diversifying and improving classifications to suit the load profile of modern appliances. Techniques used to accurately detect these loads typically use steady-state analysis, transient analysis or Fast Fourier Transforms (FFT's) [24, 25].

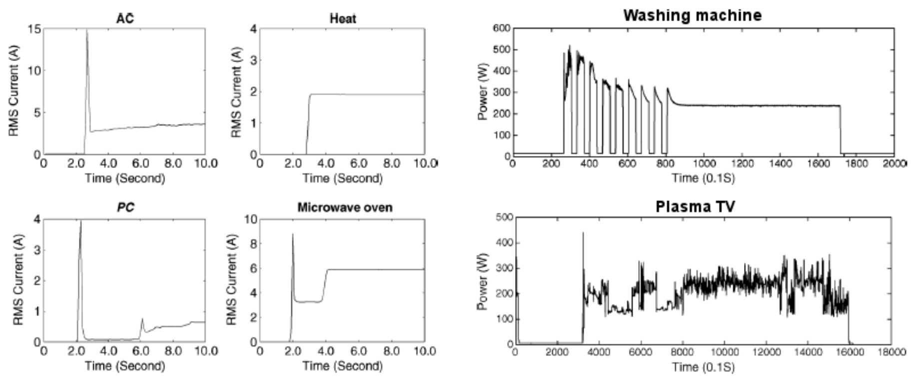

Figure 2-1 Load profiles of exemplary household appliances [25]

Load monitoring techniques are additionally improved with more powerful, modern technology. One example of research in this field is where smart meters and smartphones are utilised to make load monitoring more accurate and accessible [26].

Forecasting load profiles for the residential sector is useful for the planning of infrastructure, or policy design [27]. Load forecasting methodologies can broadly be categorised into bottom-up or top-down. Bottom-up is concerned with establishing a load profile by building it from an intricate knowledge base of the end-user [28, 29]. Top-down disregards specific appliance end-use, and takes into consideration macroeconomic factors and climate [28, 29]. A more indepth distinction is provided at a glance in Figure 2-2.

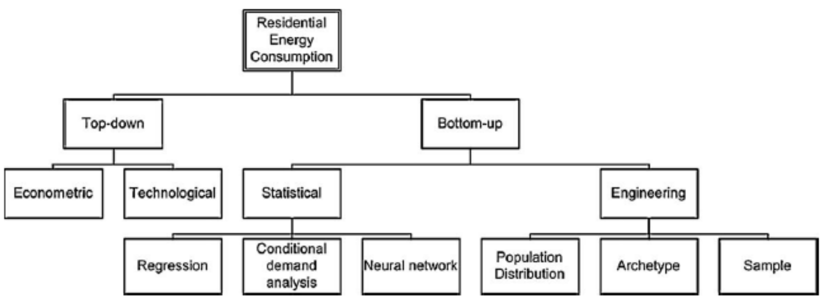

Figure 2-2 Overview of methods used to model or forecast residential loads [29]

Bottom-up load forecasting requires an extensive knowledge base on which a forecasting methodology is designed. For [27], the knowledge base is appliance saturation and working power-level of each appliance, while [30] requires knowledge regarding the members per household. Reference [31] requires knowledge about the appliances in individual households, the ratings of devices with high energy consumption, and average weekly usage patterns of these devices. Reviews of various methodologies show that building type, building age, floor size, etc. are all parameters used by different bottom-up methods [28]. If this information is not available at certain times or in certain locations, methodologies that require this information are most likely irrelevant for the time/location. This necessitates the need to develop bottom-up methodologies to use data that is publicly available or can be gathered, as was done in [27].

Top down considers factors mostly on national scale such as fuel prices, or climate [29]. This is often done on a larger scale than residential level, but the term may be used to describe the methodology used at a residential level, therefore it is included. As before, the input parameters to the methodology at hand vary widely. Two examples using the top-down methodology are given in Figure 2-3.

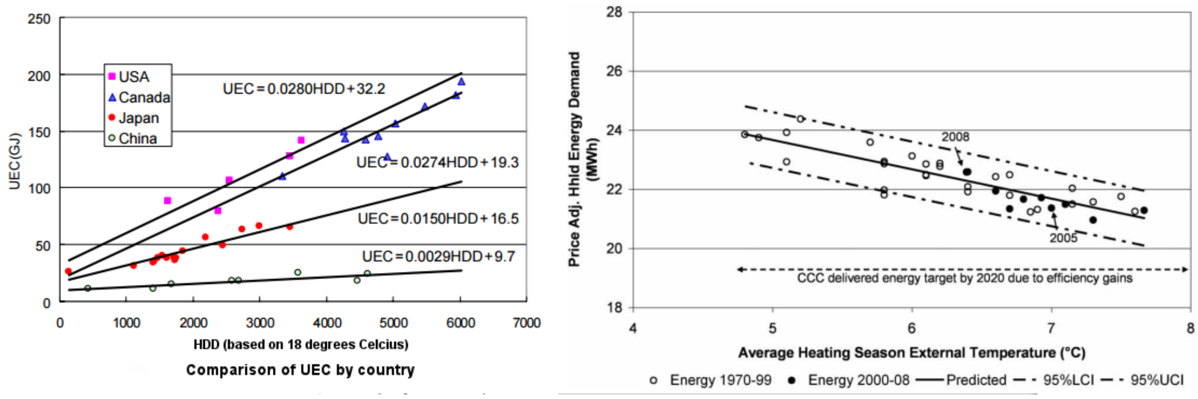

Figure 2-3 Two examples of top-down models to estimate energy consumption [32, 33]

2.3.2 **Load Control and Scheduling**

In research and in practise, a myriad of mechanisms used to implement controllable loads are encountered. A range of automated control mechanisms coupled with scheduling strategies have been explored [34-54]. These mechanisms have different components. One component is the load monitoring or status monitoring of an electrical network to identify when load control is required. This can be done through techniques using power factor, harmonics, load prediction, load identification from aggregate load profiles, etc. In a controllable load, a controller is used to change the load profile of the load or an aggregate of loads. There is often a trade-off between reaching a decided goal and granting end-user acceptance. End-user acceptance can be measured by impact on comfort levels [37]. Controllable appliances have received much attention in literature, however the objectives, method of control, and algorithms were found to vary significantly for each reference. The information available has been summarised in Table 2.1, Table 2.2 and Table 2.3.

The conclusion of the literature on controllable loads is that there is very little consensus on how controllable loads are implemented. This is most likely due to the fact that the objective of optimisation is in very few cases the same. In the cases that the objective is the same, the chosen appliances that will be optimised dictate strongly what controllable methods are possible. Even if these are similar, different optimisation algorithm used to implement the optimisation. It should be note that the adjectives mentioned for the algorithms in Table 2.3 does not explicitly define the optimisation in most cases, only qualifies it. Very few sources explicitly state the exact implementation of the algorithms.

Many of the sources don’t go down to the appliance level to discuss how each appliance can be scheduled (consider [35, 39, 40, 42, 54]). Instead, appliances are categorized (e.g. as time-shiftable or power-shiftable) and further details are abstracted away. The actual implementation of the controlling mechanism of the load is left to the reader concerned with the matter.

Table 2.1 Control methods for controllable loads in literature

Load control method	References
Deferrable Loads	[35, 39, 41, 43, 47]
On-site generators	[45]
Allocating Time Period in which Loads can operate	[34]
Schedulable Loads	[52-54]
Curtailment	[50, 53]
Decreasing requirements of e.g. geysers/aircons	[49]
Battery scheduling	[46, 48, 50, 51]
Power shiftable	[54]
Power + Time shiftable	[51]

Table 2.2 Optimisation objectives for controllable loads in literature

Optimisation objective	References
Adapt Load profile to follow a Target Load Profile	[41, 47]
Turn generator on/off in TOU FIT scheme to minimise cost	[45]
Distribute existing energy (limited energy)	[34]
Minimise cost by Maximising Load Renewable usage	[52]
Minimizing cost through Demand Side source Bidding	[53]
Minimizing cost through load scheduling in with TOU tariffs and peak shaving	[54]
Load Peak Shaving	[46]
Minimize Peak Electricity Usage	[51]
Minimize through load and battery -, just load -, or just battery scheduling	[35, 48, 50]
Minimize cost and minimise deferring period for loads	[43]
Minimize electricity provider's cost of generating electricity	[39]

Table 2.3 Algorithms and techniques for controllable loads in literature

Algorithms/Techniques	References
Model Predictive Control	[38, 45]
Multi-agent Systems	[34]
Greedy Algorithm	[47]
Custom Algorithm	[39, 52]
Heuristic Evolutionary	[41]
Linear Programming	[43, 46]
Tabu Local Search Algorithm	[44, 51]
Particle Swarm Optimisation	[50]
Dynamic Programming	[48]
Pursuit Algorithm	[35]

2.4 Grid connections and tariffs

2.4.1 Tariffs

Initial exploratory research regarding electricity consumption tariffs date back half a century [55, 56]. A review of tariff structures done in 2002 [57] considers the implementation of dynamic pricing, as opposed to more traditional methods such as flat tariffs. The report discussed the tariff structure at the hand of the economics of electricity [57]:

> "Depending on one's view, either the most natural or the most extreme approach to price-responsive demand is real-time pricing of electricity…"

The reason for this contrast is discussed here. The grid requires the capacity to handle the highest demand for electricity. Larger grid capacity implies higher capital cost required to construct this capacity. The capital costs of the electric utility need to be paid by the electricity profits; therefore peak demand causes higher electricity costs. This makes real-time pricing ideal, which implements increased tariffs for energy consumption during peak time periods. However, electricity demand changes almost continuously, implying that consumers could possibly have extreme difficulty managing electricity expenses. This necessitates the need for developing suitable tariff structures such as flat tariffs and TOU tariffs.

The policy decisions regarding tariff structures are in some companies addressed through demand-side management (DSM). Demand side management has been described in the introductory chapter, but in short, it is a type of management that utilities apply to affect load usage patterns to meet objectives such as lowering peak or shifting peaks [16, 58]. DSM addresses grid constraints through various methods, of which one is implementing the correct tariff structure. These objectives of DSM policy implementation are demonstrated in Figure 2-4. DSM does have the potential to produce side-effects [58] and should be applied correctly [16].

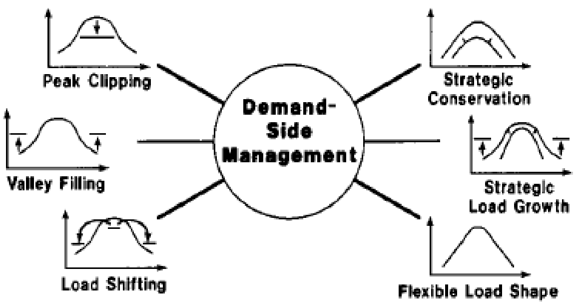

Figure 2-4 Demand Side Management load manipulation objectives [17]

The previous discussion highlighted some of the challenges and reasons for different tariff structures. A list is now given of collected methods, supplemented by [59, 60]:

- Flat tariffs

Throughout the day, a singular tariff is charged for the electricity

- Increasing block pricing

This tariff structure is characterised by the various tiers at which per-unit electricity charge is increased as the consumer passes the specified usage tier.

- Time-of-use tariffs

Electricity is priced at various costs, depending on the time of day. The electricity cost is usually highest at time when the electricity consumption peaks, while during off-peak (usually night) an off-peak tariff is present.

- Critical peak pricing

For a specified duration of time when the electricity peak is highest, tariffs are hiked to discourage consumers from consuming electricity.

- Real-time pricing

Electricity tariffs may be set for a specific hour, half-hour, or moment of the day. Pricing is usually based on the demand for electricity. The tariff is set an agreed-upon time before the tariff is implemented.

The problem of distributing electricity across several income groups lead to apparent problems. To solve the socio-economic problem, block tariffs have been implemented, charging higher tariffs for electricity consumed beyond specified tiers [60, 61].

2.4.2 **Feed-in tariffs**

Feed-in tariffs (FIT) allow electric utilities to remunerate clients for feeding electricity back into the grid. Countries that show quick adoption of PV has shown to most likely have a FIT policy implemented [62, 63]. These policies need to be managed closely to ensure sustainable implementation: As part of the implementation, FIT needs to constantly be adjusted downwards to compensate for cheaper PV systems [63].

The metering infrastructure on the grid connection should be able to support the feed-in of electricity. Different implementations of FIT exist, of which the most common is described here from [9, 64] and is covered in more detail in [8]. One implementation of net metering is where instantaneous power from the grid is measured and the electricity meter starts rolling back if more electricity is generated than used locally. A second implementation of net metering is where energy feed-in and consumption is measured over periods of time, e.g. over a half-hour or hour period. Policies may, in some cases, only remunerate customers as long as more energy is consumed from the grid than is fed into the grid. Opposed to this policy, in an attempt to drive market adoption of renewable technologies, a policy could be implemented where utilities pay a flat rate for electricity fed into the grid, providing stability for customers that purchase a PV system. Policy design for this mechanism faces issues such as whether energy can accumulate into a state of “credit”, and how long the credit is valid for [65]. Countries with established FIT schemes have imposed further regulations to create sustainable and fair tariffs for FIT – holding the grid clients accountable for additional fees that contribute to network maintenance cost, etc [66].

2.5 Photovoltaic Systems

2.5.1 Solar Profiles

The methods to acquire PV system energy output are explored in this section. To predict the economic viability of PV systems, the expected energy output from the PV system is required. To predict the energy collected by PV panels at a specific location, the following methods can be used:

- Obtaining the results from theoretical solar irradiation values [67, 68]

This theoretical approach has been written up meticulously. The theoretical approach uses information derived from knowing the position of the sun at every point of time throughout the year [67, 68]. From the sun’s position, the Direct Beam radiation (I_{BC}), diffuse radiation (I_{DC}) and reflected radiation (I_{RC}) are derived. By knowing the efficiency rating of the panel and other relevant inefficiencies in the PV system, estimates can be obtained for the energy obtained from the solar rays.

Software packages that simulate PV system performance often require measured weather data, as is shown in Table 2.4. This suggests that the results obtained using only theoretical calculations are not adequate to accurately calculate PV system performance.

- Calculating results with irradiance data as measured by satellites [69-71]

Several software packages can accept meteorological data to estimate the performance of PV systems. NASA provides world-wide meteorological data [71]. The smallest granularity of the available data at this point in time is a three hour average.

- Calculating results from ground-level weather station data

Weather station data includes detailed measurements which can’t be obtained through abovementioned methods. These measurements include wind speed, temperature, the effects of cloud cover, etc. Measurements are often done at granularities of 1 minute or 5 minutes. The disadvantage of this data is that a weather station needs to be installed at the site where PV system performance is to be calculated.

Various software packages have been developed to calculate the performance for PV systems. Calculating the PV system performance from measured solar data requires refined models, which has been the sole focus of research projects such as [72]. The software packages in Table 2.4 each has their own methodology and require specific inputs to calculate the PV system performance.

Table 2.4 Software applications to estimate the performance of PV systems

Software	Cost	Origin	Input	Output
PVWatts [73, 74]	Free	Developed at NREL	Not possible to specify our own data. Accepts closest TMY2 weather data file in database. 21/08/14: Closest source to Stellenbosch is Harare, Zimbabwe. 18/07/15: Closest source is Cape Town.	Monthly or Hourly PV system output.
PVsyst [69]	Paid	Commercial Product	Meteorological data.	Monthly yield and detailed system information such as losses.
SAM [75, 76]	Free	Developed at NREL	A variety of weather data files, including TMY2 and TMY3. Also possible to create and input own TMY3 data.	Monthly or hourly yield, system performance, and economic results e.g. payback times.
SunSim [77]	Program not available to the author, software packaged used for University of Cape Town research study			
SolarGIS [70]	Paid	Commercial product offering online access to tools for designing PV systems	Meteorological and Solar data provided at a price.	PV energy calculator and PV performance assessment tool.
HOMER Legacy [78]	Free	NREL. Has been discontinued, no further support is provided, but is still available for academic purposes.	Meteorological data, different options for PV systems, cost of electricity, load profile, etc.	Can optimise PV plant size, provide economic results.
RETScreen	Free	Natural Canada Resources	Has a database with weather station data, and can accept satellite data from the Nasa meteorology data set. Furthermore takes all details regarding electricity cost etc.	Cost and financial analysis, risk analysis, etc.

Each software package provides different results and statistical values. A typical calculation would provide the monthly average of solar energy collected daily, as shown in Figure 2-5.

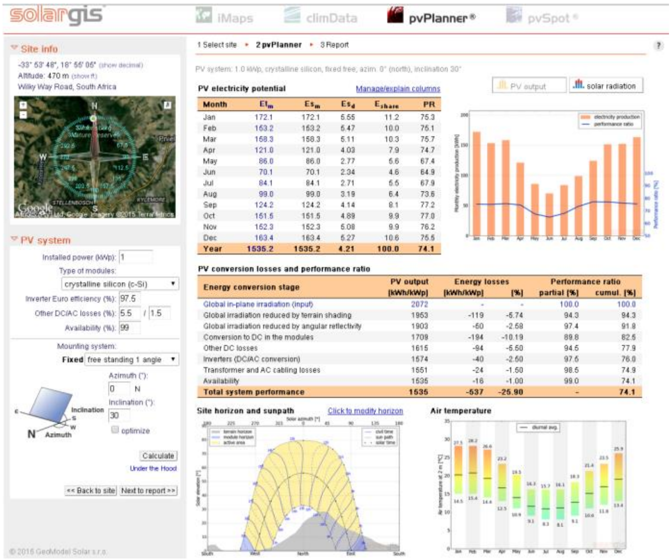

Figure 2-5 PV system performance as calculated by the software package SolarGIS

Providing custom weather data for the SAM program requires the generation of a TMY3 weather file. The SAM help file [75] state that SAM provides assistance for creating TMY3 files. These files require 8760 entries of data points, corresponding to the hourly weather data for non-leap year. The required data measurements are given in Table 2.5.

Table 2.5 Weather data required by a TMY3 weather data file

Column Header	Unit	Description
GHI	W/m^2	Global Horizontal Radiation
DNI	W/m^2	Diffuse Normal Radiation
DHI	W/m^2	Diffuse Horizontal Radiation
Dry bulb	˚C	Dry bulb temperature
Dew-point	˚C	Dew Point temperature
RHum	%	Relative Humidity
Pressure	mBar	Air Pressure
Windspeed	m/s	Windspeed
Albedo	Unitless	Ratio of reflected sunlight to GHI

The SAM help file specifies that the PVWatts model for determining PV system performance is implemented within SAM. This file requires only the following weather data points:

- Diffuse Horizontal Radiation

- Diffuse Normal Radiation
- Albedo (optional)
- Dry bulb temperature
- Wind velocity

The TMY3 file therefore contains all the information necessary to supply information to the PVWatts model, and certain columns in the file can be left unpopulated.

Weather data for South Africa has in its own been a study of various research projects [77, 79, 80], some with the goal of establishing a central database of files with weather data of adequate granularity and accuracy. The available sources have been reviewed and listed:

Table 2.6 Sources of weather data for Stellenbosch

Source	Description	Granularity
Nasa Meteorogical Data [71]	Satellite data	Minimum 3 hours
PVWatts Database [73]	Cape Town. TMY3 file	Hourly
Sonbesie weather data [81]	Stellenbosch, various measuring stations.	Minute/Hour/Day
SAURAN [82]	Various weather stations in South Africa, including: Stellenbosch, Graaff-Reinet, Kwazulu-Natal, Pretoria, etc.	Minute/Hour/Day

2.5.2 PV system installation topology

The energy collected by a grid-connected PV system to be used by appliances should be converted to AC power. Residential users connect electrical appliances to electric wall plugs. The plugs for each country is standardised and can be referenced [83, 84]. For each country, the form and dimension of the plug is specified, but more importantly it is indicated that the standard for home appliances is 50 Hz or 60 Hz AC current. This may not be the case for off-grid residence, which may work on DC electricity.

From quotations for standard solar PV installations, industry standard PV system components [85-87] show similar electrical topologies through which a PV system is installed at a residence: An inverter accepts the DC connection from the PV panels and provides AC power to the distribution box, as shown in Figure 2-6.

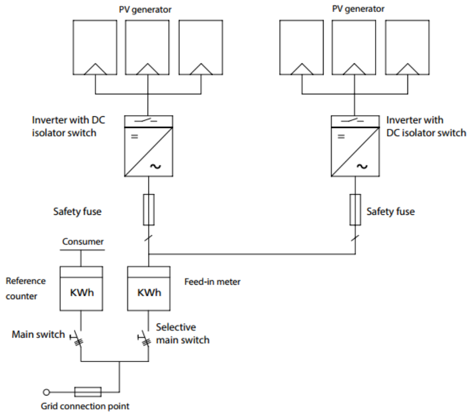

Figure 2-6 Kaco Powador circuit connection overview diagram [86]

PV systems installed on the roof of a residence is installed at a fixed angle. Alternative configurations are single- and double axis tracking, but since this project is concerned with PV installed at residences, no further research is done into the effect of axis tracking.

The question of what optimal orientation and tilt for a PV panels on a residence is, leads to show that 'optimal' needs to be more strictly defined. The amount of irradiance exposure that the panels receive during the course of a year seems to be roughly the same but can vary month-to-month, as shown for the PV system located in the Northern Hemisphere in Figure 2-7. Literature mentions that standard practise is to fix the tilt at the same angle as the latitude of the location where the installation is made [68, 88]. However, energy collection patterns vary as tilt and azimuth is adjusted, and therefore depending on the objective, the "optimal" orientation and tilt may vary. Therefore there is no "optimal" tilt angel at which to install the PV panels – this would have to be determined on a case-by-case basis [88, 89].

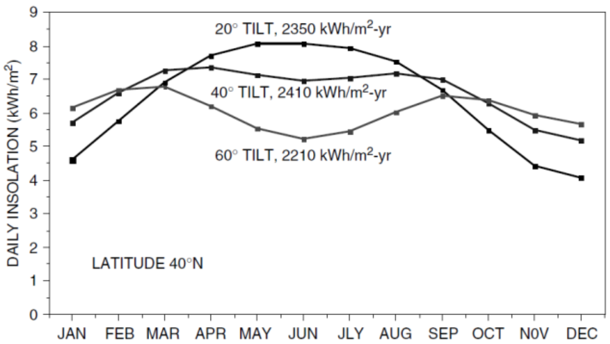

Figure 2-7 PV panel energy collected for various degrees of tilt [68]

The option of using DC power directly in a residence where AC is already installed shows very little advantage [90, 91]. Several reasons can be given for why DC grids can be advantageous, but no reason is adequate to consider DC in conjunction with AC. One specifically major issue is the lack of safety standards imposed on DC microgrid, e.g. regulation of the grounding. This is due to the lack of public and uniform standards for residential DC systems [92].

The topology modifications for adding battery energy storage to the system is now reviewed. Installation manuals of battery system components [87, 93-95] show that battery storage is installed with the standard residential energy system topology. Modern small battery systems allow storage to be integrated with the PV inverter. Larger battery banks require a dedicated bi-inverter, possibly assisted by an energy management system. The bi-inverter acts as an interface between the residential AC power and the battery bank, as shown in Figure 2-8. This allows battery storage to store or provide power depending on the current energy requirements of the system.

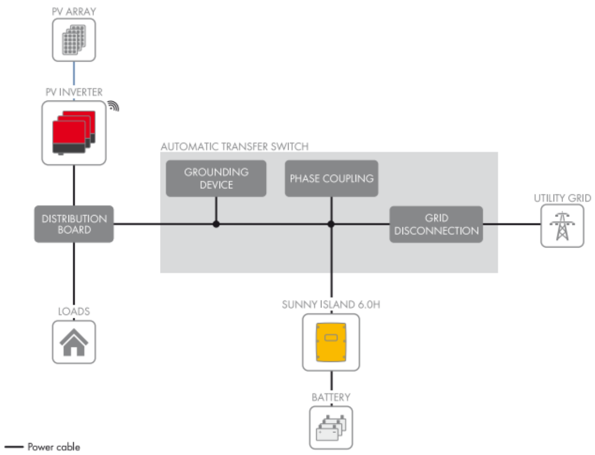

Figure 2-8. Sunny Island circuit connection overview [95]

2.6 **Battery storage**

2.6.1 **Technology**

2.6.1.1 Overview

Literature on residential energy storage almost unanimously considers battery storage as the most viable option currently available. The reasons given are that battery storage has the required energy density, the technology is well developed, and batteries are easily accessible for installation in a residence. Reviews of other technologies for residential energy storage encountered in literature [96-98] show these technologies are impractical for residential application or too expensive at this time. The maturity of various energy storage technologies are given in Figure 2-9. Battery storage is shown to be the only options mature enough for commercial use. Regardless of the maturity of storage technologies excluding batteries, availability remains a barrier to adoption.

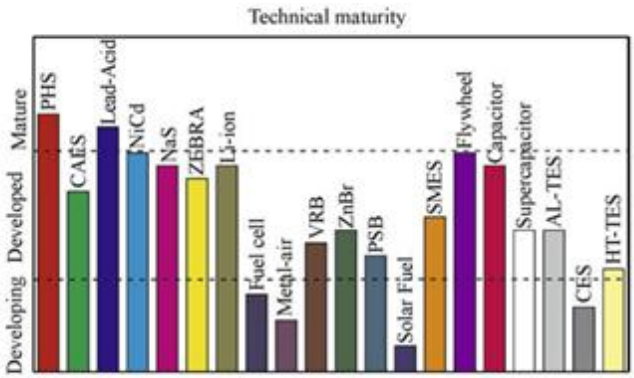

Figure 2-9 Technological Maturity of energy storage system [97]

All viable alternative energy storage methods are shortly reviewed to ensure thorough research is presented. For reverse fuel cells technology, the hydrogen fuel cell is posed as the best alternative for residential energy systems. These cells come at a high cost disadvantage and low round-trip efficiency, and limited life expectancy [96, 97, 99, 100]. Fuel cells can possibly be used in conjunction with batteries, where batteries act as energy buffers [101, 102]. A second technology, super–capacitors, has a high power density, but a low energy density, effective for providing power for short duration [97, 98]. Super capacitors suffer self-discharge of about 5% per day [96, 97]. Thermal storage stores either high or low temperature medium to store energy, but is mostly related to heating and cooling applications [103, 104]. Flywheels store kinetic energy in spinning mass. There is a high cost associated with this technology [98] and its main use is providing power for a short duration, e.g. when smoothing irregular curves [97]. Superconducting magnets keep current in a superconducting coil, but is more related to large scale electricity management [105] especially for short term power supply [106]. Additionally, this technology is still very expensive [107]. Flow batteries are in effect a small chemical plant, consisting (like a normal battery) of electrodes in an electrolyte. The difference is that surplus electrolyte is stored in external reservoirs [97, 98] and this makes flow batteries more suitable for larger applications.

A wide variety of battery storage technologies are available. Li-Ion batteries are favoured for their light weight and high energy density. It has progressively been used for smaller consumer electronic devices (e.g. mp3 players, mobile phones) and then larger systems such as electric vehicle batteries and renewable energy storage [108-110]. NiCd technology is to some extent being replaced by NiMH and Li-Ion. This type of battery does have some advantageous charging characteristics like high discharge capabilities and the ability to withstand overcharge or extensive discharge [111]. NiMH batteries exude a poor discharge performance when compared to NiCd but has a higher energy density [109, 111]. Lead Acid battery types are most widely available and common to use. These batteries are well suited to provide a large amount of power for a brief period of time [109]. Disadvantages when compared to other batteries are the energy density and low depth-of-discharge it can handle: High discharge reduces the useful life of batteries considerably. Other batteries types have been developed from lead acid principle are Valve Regulated Lead Acid (VRLA) batteries. The relationship with Lead Acid batteries are shown in Figure 2-10.

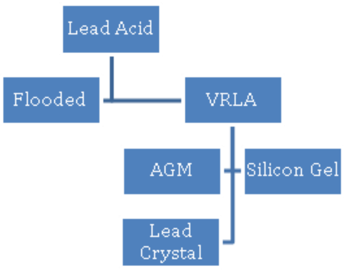

Figure 2-10 Lead acid battery types

Normal lead acid batteries have a positive electrode and negative electrode suspended in a liquid electrolyte, and is known as a flooded battery. The chemical reactions can cause water loss, which necessitates maintenance as the battery has to be topped up with water. A VRLA battery has two main types: Gel Cells and Absorbed Glass Mat (AGM). The chemical reaction is the same as for lead acid batteries. For gel cells, silica gelling agents are added to the electrolyte, causing it to form a gel. For AGM batteries, the electrolyte is absorbed into fibreglass mat. The non-liquid form of the electrolyte allows for lower maintenance, but inhibits power flow. These batteries are then less suitable for e.g. engine starting applications (high power, brief period) and more useful for residential energy storage [109, 112, 113].

A further development that was found to be commercially available was Lead Crystal [114, 115]. For the lack of published literature on these batteries, the study will no further consider these batteries.

2.6.1.2 C-Rating

This rating is used to indicate the tempo of charge or discharge. The formula [111] is given as

$$C = \frac{discharge/charge\ current}{nominal\ capacity}.$$

That implies that if a battery is discharged at 1C, it will take 1 hour to fully discharge the battery, whereas at 0.2 C the battery will take 5 hours to be discharged.

2.6.1.3 Capacity and Charge/Discharge Limits

Battery specifications provide capacity of batteries in *Ah*. In an ideal case, the following relationship exists between the dimensions of capacity and energy:

$$[Wh] = [Ah]\cdot[V]$$

where V is the nominal voltage indicated on the battery. The reason for battery specification provided in Ah rather than Wh is due to the fact that voltage is not constant over the charge/discharge period. This can be seen when the voltage is plotted against time for several constant-current discharges in Figure 2-11.

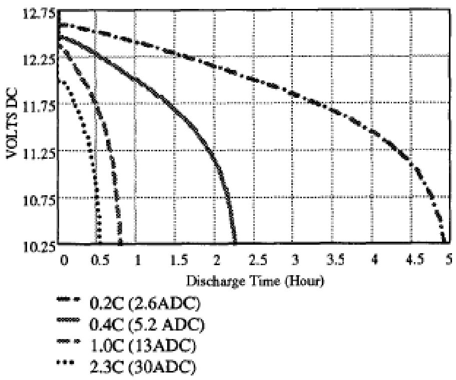

Figure 2-11 Lead acid battery discharge voltage [116]

Higher discharge rates also cause the battery to provide less of its capacity. The capacity of a battery at a given current can be calculated through the use of Peukert's law [117], and informative datasheets of batteries would give some information regarding capacity for their batteries at different discharge rates. Research that requires accurate battery models (such as research concerning the development of charge controllers algorithms) focus on modelling batteries by considering the electrical properties such as voltage, current, state of charge, battery open terminal voltage, internal resistance, etc. [108, 116, 118] or have electrochemical models [111, 119, 120]. The conclusion is that the suggested C-rating is specified to guarantee that the battery can provide the indicated energy capacity.

2.6.1.4 Lifetime cycles

The lifetime of a battery depends on various factors that can the battery's state of health. A single factor consistently raised in battery specifications is the amount of cycles the battery can make for a given depth-of-discharge, shown in Figure 2-12.

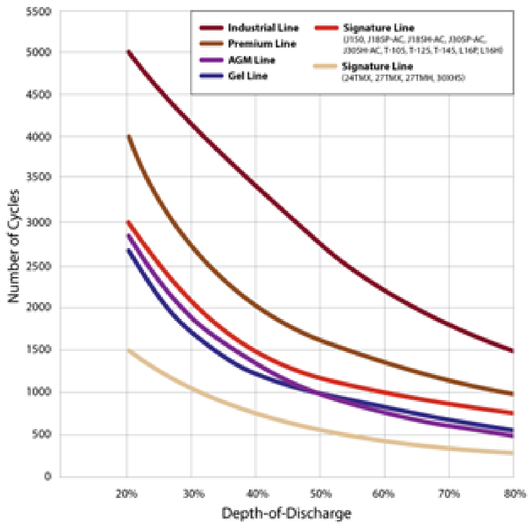

Figure 2-12 Number of cycles vs depth of discharge [121]

2.6.1.5 Charge/Discharge process

The charging process of a battery is most likely controlled by a charge controller. Charge controllers observe the battery for certain indicators to optimally charge and protect it. One indicator is the *voltage regulation set point* which is the voltage beyond which the battery is not charged [122]. A second indicator is the *low voltage disconnect*, the voltage level at which the battery discharge is halted to prevent permanent damage to the battery. Batteries can discharge as the load requires, but charge controllers may limit excessive currents to both protect the charge controller and to prevent damage to the battery.

The charging of the battery is governed by the specific charge algorithm of the charge controller. Battery charging may consist of various stages, of which the three most common stages are presented here [123-125]. The first is the bulk, which charges the battery at maximum rate up to 75% - 90% of its full capacity. The float stage then maintains a fully charged battery at its full capacity as long as energy can be provided to the battery. The equalize stage exposes the battery to a slight overcharge, allowing individual cells within the battery to all charge to the same level of charge. Additionally it causes movements within the acid by cause gas bubbles, a method used to extend the life of the battery in some cases.

2.7 Optimisation methodologies

2.7.1 Introduction

An overview of core optimisation methodologies is presented, mostly supported by the work of Chinneck [126, 127].

2.7.2 Linear programming

Linear programming is the most widely implemented optimisation technique. The "linear" term refers to the fact that each variable to be optimised has a linear contribution (that is, with an exponent of 1) to the objective function, or constraint. An example is modelled in Figure 2-13. Linear programming is well suited to problems that need to be solved with a very large number of variables. Linear programming requires variables, constraints, bounds and an objective function to create a complete model of the problem.

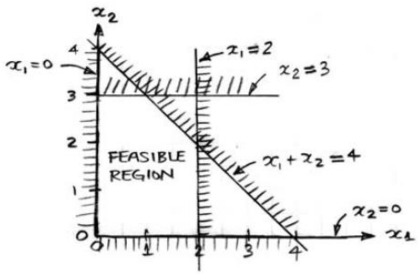

Figure 2-13 A representation of a 2-variable linear problem, with constraints and bounds [126]

Linear programming assumes that variables can be solved with fractional values. Some optimisation problems require a solution in integer values – e.g. when trying to determine how many staff to assign to a project. An important principle is that rounding the solution of linear optimisation does not guarantee to find the optimal solution for an integer problem.

2.7.3 **Integer/Discrete programming**

Finding solutions to problems that require an integer or discrete solution requires a different model than linear programming. If linear programming methods are used to find an optimal solution and then rounded to (supposedly) find something close to the optimal solution, this solution may prove to not be the optimal solution – this is shown in Figure 2-14.

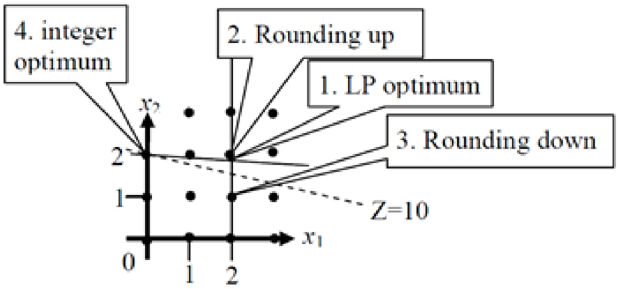

Figure 2-14 A given example for when rounding linear programming solution can provide wrong answers for integer programming [126]

Integer programming provides a finite number of points which can serve as solutions, but simple enumeration through these solutions to find the optimal becomes impossible for large data sets. Algorithms for integer programming explore the finite set of points using different algorithms – the choice of algorithm depends on the nature of the optimisation problem. These algorithms have different approaches for handling breadth first vs. depth first searches, deciding on optimal solutions, and discarding certain sets of options as viable solutions.

2.7.4 **Dynamic programming**

Dynamic programming is a method of optimisation in which an optimisation algorithm explores a set of decisions that needs to be made. At each decision the current best option is chosen as the optimal solution for that decision. Thereafter the algorithm continues to the next decision. Each successive decision that needs to be made is referred to as a state, and a recursive function is implemented to solve the optimisation for each state.

Nonlinear programming

2.7.4.1 Overview

In the simplest of non-linear, continuous problems, derivatives are used to find the optimal solution. Nonlinear problems can also have a discrete/integer nature, in which derivatives are not applicable to the problem. In this case techniques are used to minimise the finite (but possibly very large) set of possible solutions that must be considered. The methods as mentioned will focus on finding the *global* optimum of the objective function, rather than a local optimum.

2.7.4.2 Direct search method: pattern search

Direct search optimisation methods directly calculate the objective function value at each polled point. Gradient values are not considered. Direct search takes as input an initial point. A *poll* is initiated at this point. A mesh is calculated around the initial point, expanding in each direction according to the number of dimensions/variables in the optimisation problem. Depending on the algorithm used in the optimisation optimisation, one of the points in the mesh with an improved objective function value is chosen to be the starting point of the next poll. The algorithms through which points are found [128] are:

- Generalized Pattern Search (GPS) Algorithm
- Generating Set Search (GSS) Algorithm
- Mesh Adaptive Search (MADS) Algorithm

Once the starting point of the next poll is found, the configurations of the search are adjusted for the next poll. If the poll successfully found a more optimal point, the mesh size is expanded. If the poll was unable to find a more optimal value, the mesh size is contracted. The scale at which the mesh is adjusted is configurable. Once a poll determines the surrounding points to be within a given tolerance, the optimal value has been found.

2.7.4.3 Particle swarm optimisation

The particle swarm optimisation (PSO) has numerously been encountered in literature on the topic of load scheduling (refer to section 2-13). The criteria of choosing the particle swarm optimisation as a choice of optimisation is best described by this overview [129] about a decade after the algorithm was first published:

"Areas where PSOs have shown particular promise include multimodal problems and problems for which there is no specialized method available or all specialized methods give unsatisfactory results."

This algorithm distributes a swarm of particles uniformly within the given constraint of the problem space. Each particle is assigned a speed at which it will move through the problem space. For each particle, the value of the objective function is calculated. The objective function values of the surrounding points are then also calculated. According to those results, constraints and bounds, the direction and velocity of the particle is updated. After all particles have been updated, the particles are moved forward one step. This process iteratively continues until a stopping criterion is reached.

2.8 **Financial indicators**

2.8.1 **Introduction**

It is mentioned at the beginning of the project that economic viability is a barrier toward the penetration of PV systems into the market [1-5]. Financial indicators provide potential PV system owners with data to make informed economic decisions regarding the purchase of a PV system. It should be mentioned that concerns have been raised about the unfair comparison between financial indicators of PV systems and the grid connections tariffs or traditional centralized electricity generation prices [130, 131] and this remains a matter of dispute. A further notion is that financial indicators are often generally applicable as found in management books [132], but implementations are derived specifically for residential PV systems [67, 132].

2.8.2 **Simple payback time**

Simple payback time, or equivalently referred to as the payback period, is an indicator that is easily understood by laymen, and it does not require estimations of inflation or discount rates. The simple payback time was found to be the most popular financial indicator by Rai in two of his publications [133, 134]. Simple payback time is defined as [132, 135]:

$$Pb = \frac{C_T}{C_E}$$

where Pb denotes the payback time, C_T denotes the initial cost of installation, and C_E denotes the cost of energy saved by installing the PV system. The payback time indicates the time required to recover the investment cost through the savings or income produced by the investment.

2.8.3 **Present value**

Present value gives the current value that an investment would generate over its lifetime. That is, any value that will be generated is worked back to the current monetary value with consideration of discount/inflation rate. All the values are summed to give the present value. The present value is calculated by [67]:

$$PV = FV * (1 + i_r)^{-n}$$

where PV denotes the present value, FV denotes the future value, i_r denotes the discount or inflation rate and n denotes the number of years.

2.8.4 **Net present value**

Net Present Value (NPV) accounts for all the present and future income and expenditure values. Each value is worked back to its present value using inflation/discount rate. The present income minus expenditure values then give the net present value [135]:

$$NPV = -A_0 + \sum_{i=1}^{n} \frac{B_i - A_i}{(1 + i_r)}$$

where NPV denotes the net present value, A_0 and A_i denote all expense made from year 0 and on, B_i denotes all expenses from the year 1 and on, i_r denotes the inflation/discount rate and n denotes the number of years before the investment expires.

2.8.5 **Internal rate of return**

The Internal Rate of Return (IRR) calculates the discount value that would results the NPV to be zero over the lifetime of the investment [132, 136]. The IRR of an investment can be compared to the IRR of alternative investments. The formula is the same as for the NPV, except that the value of NPV has been set to 0 and the discount/inflation rate now become the internal rate of return:

$$0 = -A_0 + \sum_{i=1}^{n} \frac{B_i - A_i}{(1 + IRR)}$$

where IRR denotes the internal rate of return.

2.8.6 Capital recovery factor

Not found as frequently as NPV and IRR, some research such as [137] does refer to it. The Capital Recovery Factor (CRF) is the discount rate required to generate a given amount of money at a time T years into the future through annual instalments. The formula is given by:

$$P = \sum_{t=1}^{T} A \times (1 + i_r)^{T-t}$$

where P is the value that needs to be paid T years into the future, A is the annual instalment value and i_r is the required CRF.

2.8.7 Levelised Cost of Energy

Levelised Cost of Energy (LCOE) is a popular indicator of the price of generating electricity, as used in [21, 130, 138]. In the case of a PV system, the levelised cost of energy indicates the cost of generating a unit of energy by considering the lifetime costs of the PV system. The calculation is given by [138]:

$$LCOE = \frac{\sum_{t=0}^{T} \frac{C_t}{(1 + i_r)^t}}{\sum_{t=0}^{T} \frac{E_t}{(1 + i_r)^t}}$$

where LCOE is the levelised cost of energy, C_t is the net value of income – expenditure for each year, including the initial investment at t=0, E_t is the total energy collected each year and T is the total lifetime of the investment in years.

2.9 Software development platforms

2.9.1 Optimisation environment

2.9.1.1 Python

Python is a free and open-source programming language [139]. Two main versions of the program is deployed, version 2.7 and version 3.3. Full-featured mathematical libraries can be added through SciPy [140], containing underlying libraries such as NumPy (with mathematical packages) and MatPlotlib (to assist with graphical output). Python is therefore a suitable programming language for data handling, optimisation and creating graphical outputs.

2.9.1.2 Matlab

Matlab is an IDE that features its own native programming language [141]. It's a priced software package that with an assortment of toolboxes that can be purchased for specific uses like optimisation, control system design, signal processing, etc. It includes a powerful simulation/modelling package Simulink. It has powerful graphing capabilities to provide graphical results.

2.9.1.3 Mathematica

Mathematica is, like Matlab, an IDE with its own native programming language [142]. It features extensive mathematical functions for a broad spectrum of possible applications. Mathematica cannot, like Matlab, export programs that can run as stand-alone applications on computers that do not have an installation of the original program.

2.9.2 Graphical User Interface Development

2.9.2.1 Matlab

Matlab does have the ability to create GUI's that interface with Matlab scripts in the background [143]. Matlab does not require that a GUI to display graphs and images – those can be created and displayed as stand-alone figures and images.

2.9.2.2 Visual Studio

Visual Studio is an IDE by Microsoft that allows the user to create GUI's in an assortment of languages, of which the most popular language is Visual C# [144]. Applications can readily be deployed to Windows computers. Visual Studio has a free and paid-for version, with all the necessary tools for a GUI included in the free version.

2.9.2.3 Qt

Qt is a fully integrated framework to create cross-platform applications. It supports the creation of GUI's through C++ libraries, or HTML 5 for web-based development [145]. A PyQt library is available for the creation of GUI's with the Python programming language [146]. Qt has a free community version, and several better-featured paid versions.

2.9.2.4 Delphi

RAD studio is an IDE developed by Embarcadero and can be used to build GUI applications in both C++ and Delphi [147]. Delphi is an extended GUI programming language based on the Pascal programming language [148]. Later versions of Delphi (from 2013, with the XE 6 version) support the development of cross-platform applications, able to run on Windows, Mac OS X, Linux, Android and IOS. All products by Embarcadero require paid licenses.

2.9.2.5 Lazarus

Lazarus is a cross-platform IDE that is based on the Free Pascal programming language [149]. It's a free alternative to the Delphi programming language and RAD studio programming environment. Source code written in Lazarus is not fully compatible with source code written in Delphi. The software is provided under a GPL license, allowing users to create propriety software through the application.

2.9.3 **Databases**

2.9.3.1 SQLite

A SQLite database implements a relational, serverless database engine. The database is simply contained in a file with a .sql extension [150]. Interactions with this file happen through the database engine. Various drivers have been written to interact with the SQlite database from various programming languages such as Python [151], Matlab [152-154] and Delphi [155]. SQlite is an active project with recent updates to the project. SQlite has paid support, and an active community and mailing lists for free support.

2.9.3.2 MySQL

MySQL is the world's most popular open source database [156]. This database is deployed as a MySQL server, through which applications can interact with the relational database. The database has an easy-to-use standalone database server [157]. Paid hosting options are available. Extensive documentation is available for anything from local deployments to cluster deployments.

2.9.3.3 PostegreSQL

PostgreSQL is the world's most advanced open source database [158]. PostgreSQL is highly focused on data integrity, possibly at the cost of fast data reading speeds. The PostgreSQL is advised to be used for experienced database managers that require data integrity for complex applications [157].

2.9.4 UML for software documentation

Unified Modified Language (UML) is notation guidelines to document classes, processes and other concepts in software programming. UML provides various models that enable software developers and other stakeholders in a software project to communicate about program structure and functionality. This section will describe a subset of the notations for UML that will be useful in this project.

2.9.4.1 Use Case Diagrams

Use case diagrams showcase the various manners in which a software application may be used, or demonstrates the various objectives of the application. Typical objectives of the software are described as "use cases", and entities that require the system to have one or more objectives are classified as "actors" [159]. Primary actors are shown as stickmen on the left of the diagram, and the descriptions of the use cases are contained within a modelled box. The box indicates the scope of the project. Each actor is assigned one or more use cases [160].

2.9.4.2 Class Diagrams

Class diagrams describe the classes designed for the software project at hand. In this context classes refer to the concept of classes in object-orientated programming. Class diagrams show the attributes, operations and interrelationships of a class. Two versions of class diagrams exist:

- Analysis class diagrams

These are used to quickly grasp the operations and attributes of a class. It does not showcase the private operations and functions.

- Design class diagrams

These go into the details of the class implementation. Each attribute and operation states its visibility, with special notation for private, package, protected and public visibility [159-161].

Attributes are followed by a colon and provides the type of the attribute (types may be programming language specific, but common types include integers, strings and arrays). Operations specify the input parameters and return types in the form [159]:

name (parameter : type = defaultValue, ...): resultType

Class diagrams avoid showing the scaffolding code, i.e. the getters and setters for the attributes of the class. It's important that class diagrams clearly indicate relationships with other classes. Different relationships exist and are denoted differently in the diagrams [161]:

 This indicates inheritance. In an object-orientated manner, this relationship indicates the relationship between base- and subclasses.

 This indicates dependence. Used in the case where the case is dependent on another class.

 This relationship indicates association. Used when one class has another class as one of its attributes.

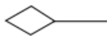 This indicates aggregation. A class may contain another class, but if the container class is destroyed the contained class continues to exist.

 This indicates composition. A class may contain another class, and if the container class is destroyed, the contained class is also destroyed.

The relationship between two classes that is indicated with any of the above relationship qualifiers also has a multiplicity consideration. Multiplicity indicates the amount objects of the class that will be present in the software application. Integers can be used to indicate the multiplicity. If a variable number is expected it can be indicated as *n..m* where n and m indicates the lower and upper bounds for the amount of objects. If the multiplicity exists but the quantity is unknown it can be indicated as *n*..*, where n indicates the lower bound and * indicates "many" [160].

2.9.4.3 Activity Diagrams

Activity diagrams indicate the structure of program flow. Flow chart syntax is used to indicate the logic at each step in the process. Activity diagrams show a singular starting point, various activities through which the program progresses, conditional (decision) blocks and an ending point [161].

2.9.4.4 Component Diagrams

Component diagrams can be used to model the technical infrastructure and domain architecture of the software applications. Components are identified by a recognisable component icon in the top right corner of the rectangle indicating the component [160]. Components have special relationship indicators with other components. The same relationship indicators as discussed in class diagrams are valid when component diagrams are combined with class diagrams.

2.9.4.5 Deployment diagrams

Larger software applications may require various execution environments to operate. A typical example of this is when a software application accesses data on the internet through a webserver, and also accesses its own database through a SQL server. Another example is if the software application requires both Python and the Java Virtual Machine (JVM) installed on the machine where it operates. A deployment diagram can be used to communicate the deployment environment and configuration of a software application.

A deployment diagram indicates the various execution environments or hardware service as rectangular boxes [160]. Components can be placed inside these hardware "nodes" to indicate what parts of the software applications are executed on the relevant nodes. Message busses link the nodes and indicate the message protocol or drivers used for communication within "<< >>" symbols.

3 Mathematical formulation of residential energy system

3.1 Introduction

This chapter defines the mathematical model to meet the objectives as set out in chapter 1. The objectives that must be met by this chapter are:

- Create a mathematical model that is able to contain the required parameters to model the residential energy system.
- Define the optimisation that will be used to determine the optimal PV system rating for which the payback period is a minimum.
- Identify mathematical equations that assist to explore the relationships between the parameters of a residential energy system and the results of the payback period.

Every section in this chapter addresses one, or part of, the objectives as set out above. A mathematical model for a generic electric energy system is created in section 3.2. A residential energy system model is created based on the generic electrical energy system model in section 3.3. Two optimisations are required to meet the objectives of this chapter, namely a load schedule and battery profile optimisation, as well as the PV system rating optimisation. These optimisations are defined in section 3.4. Derivations of mathematical equations that interpret and identify important factors that determine payback time of PV and battery storage systems is presented in section 3.5.

3.2 Mathematical model of an energy system

3.2.1 Overview

The energy balance model is implemented using the principle that energy profiles can be represented by a number of averaging intervals of equal duration. The model is defined using set theory notation to represent the energy profiles. This section starts by defining the notation for energy profiles, demonstrates how energy profiles can describe energy flow within a subsystem and concludes by showing how cost can be associated with energy flow in the model.

3.2.2 Energy and average power

The PV system energy generation and load profiles are represented by sets of timestamps and values. Using set theory notation, the timestamps are expressed as

$$\boldsymbol{T} = \{t_k\} \quad k = 1, 2, 3 \ \cdots \ N_K \tag{3.1}$$

where N_K defines the total number of timestamps. The timestamps give rise to a set of averaging intervals $\boldsymbol{\Delta T}$ given by

$$\boldsymbol{\Delta T} = \{\Delta t_k\} \quad k = 1, 2, 3 \ \cdots \ N_K - 1 \tag{3.2}$$

where

$$\Delta t_k = t_{k+1} - t_k \tag{3.3}$$

and t_k and t_{k+1} denote the beginning and end respectively of the k^{th} averaging interval. A daily power profile $P(t)$ can be expressed as a set of average power values $\tilde{P}$, such that

$$\widetilde{\boldsymbol{P}} = \{\tilde{P}_k\} \quad k = 1, 2, 3 \ \cdots \ N_K - 1 \tag{3.4}$$

where $\tilde{P}_k$ denotes the average power for the k^{th} averaging interval and is given by the relationship

$$\tilde{P}_k = \frac{\int_{t_k}^{t_{k+1}} P(t)dt}{t_{k+1} - t_k} \quad k = 1, 2, 3 \ \cdots \ N_K - 1 \tag{3.5}$$

The energy flow profile E_k associated with the k^{th} averaging interval is related to $\tilde{P}_k$ through the relationship

$$E_k = \tilde{P}_k \, (t_{k+1} - t_k) \tag{3.6}$$

The associated energy flow profile E is given by

$$\boldsymbol{E} = \{E_k\} \quad k = 1, 2, 3 \ \cdots \ N_K - 1 \tag{3.7}$$

3.2.3 **Energy balance model**

The topology of a generic energy system is shown in Figure 3-1. It consists of a total of N_m energy subsystems connected to a common energy bus, where $P_i(t)$ denotes the instantaneous power flow from the i^{th} subsystem to the bus.

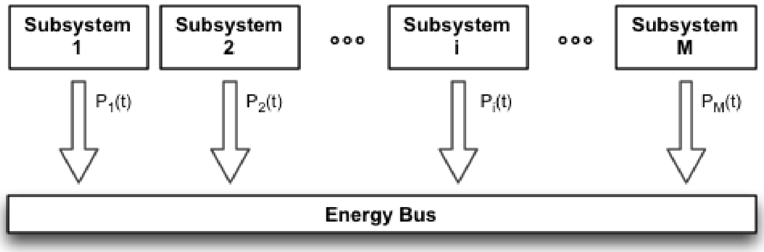

Figure 3-1 Energy system topology for a residential system

Conservation of energy requires that the instantaneous power flowing into the system summates to zero, i.e.

$$\sum_{i=1}^{N_M} P_i(t) = 0 \qquad i = 1, 2, 3 \cdots N_M \tag{3.8}$$

This also holds true for the average power $\tilde{P}_{ik}$ and energy flow profile E_{ik} of the i^{th} subsystem in the k^{th} averaging interval, giving rise to

$$\sum_{i=1}^{N_M} \tilde{P}_{ik} = 0 \qquad i = 1, 2, 3 \cdots N_M \tag{3.9}$$

and

$$\sum_{i=1}^{N_M} E_{ik} = 0 \qquad i = 1, 2, 3 \cdots N_M \tag{3.10}$$

The above relationship gives rise to the following expression for the energy flow profile E_{jk} associated with the j^{th} subsystem in the k^{th} averaging interval

$$E_{jk} = -\sum_{\substack{i=1 \\ i \neq j}}^{N_M} E_{ik} \qquad \begin{matrix} i = 1, 2, 3 \ \ N_M \\ k = 1, 2, 3 \cdots N_M - 1 \end{matrix} \tag{3.11}$$

The relationships given above represent a convenient mathematical model for optimizing energy flow in the system, especially where the objective function can be defined in terms of the energy flow or average power profiles.

3.2.4 Energy cost profiles

Energy can be imported or exported from a subsystem. Different cost profiles may be applicable to the energy imported from a subsystem and the energy exported to a subsystem. For this reason, the energy flow profile for a subsystem is separated into an imported energy profile and an exported energy profile. These separate profiles can be used to calculate total cost associated with the subsystem.

The energy imported from the i^{th} subsystem to the energy bus, $\boldsymbol{E}_i^I$, is given by

$$\boldsymbol{E}_i^I = \{ E_{ik}^I \} \qquad \begin{array}{l} i = 1, 2, 3 \ldots N_M \\ k = 1, 2, 3 \ldots N_K - 1 \end{array} \tag{3.12}$$

where

$$E_{ik}^I = \begin{array}{l} E_{ik} \quad if\ E_{ik} \geq 0 \\ 0\ if\ E_{ik} < 0\,. \end{array}$$

A per-unit cost profile can be associated with energy imported from a subsystem, given by

$$\boldsymbol{R}_i^I = \{ R_{ik}^I \} \qquad \begin{array}{l} i = 1, 2, 3 \ldots N_M \\ k = 1, 2, 3 \ldots N_K - 1 \end{array} \tag{3.13}$$

where R_{ik}^I denotes the per-unit cost for importing energy for subsystem i during the k^{th} averaging interval. The cost of energy exported from the i^{th} subsystem, $\boldsymbol{C}_i^I$, can be represented by

$$\boldsymbol{C}_i^I = \{ c_{ik}^I \} \qquad \begin{array}{l} i = 1, 2, 3 \ldots N_M \\ k = 1, 2, 3 \cdots N_K - 1\text{'} \end{array} \tag{3.14}$$

where

$$c_{ik}^I = R_{ik}^I E_{ik}^I \tag{3.15}$$

and c_{ik}^I denotes the energy cost for energy imported from the i^{th} subsystem on the k^{th} averaging interval. The total cost of imported energy, $C_i^{I\prime}$, given by the relationship

$$C_i^{I\prime} = \sum_{k=1}^{N_K - 1} c_{ik}^I. \tag{3.16}$$

Similarly, the energy $\boldsymbol{E}_i^E$ exported from the i^{th} subsystem to the energy bus, $\boldsymbol{E}_i^E$, can be represented by

$$\boldsymbol{E}_i^E = \{ E_{ik}^E \} \qquad \begin{array}{c} i = 1, 2, 3 \ldots N_M \\ k = 1, 2, 3 \ldots N_K - 1 \end{array}, \tag{3.17}$$

where

$$E_{ik}^I = \begin{array}{c} E_{ik} \;\; if \; E_{ik} < 0 \\ 0 \; if \; E_{ik} \geq 0 \end{array}.$$

A per-unit cost profile can be associated with energy exported to a subsystem, given by

$$\boldsymbol{R}_i^E = \{R_{ik}^E\} \qquad \begin{array}{c} i = 1, 2, 3 \ldots N_M \\ k = 1, 2, 3 \ldots N_K - 1 \end{array} \tag{3.18}$$

where R_{ik}^E denotes the per-unit cost for exporting energy to subsystem i during the k^{th} averaging interval. The cost of energy exported from the i^{th} subsystem, $\boldsymbol{C}_i^E$, can be represented by:

$$\boldsymbol{C}_i^E = \{c_{ik}^E\} \qquad \begin{array}{c} i = 1, 2, 3 \ldots N_M \\ k = 1, 2, 3 \cdots N_K - 1 \end{array}, \tag{3.19}$$

where

$$c_{ik}^E = R_{ik}^E E_{ik}^E \tag{3.20}$$

and c_{ik}^E denotes the energy cost of energy exported from the i^{th} subsystem on the k^{th} averaging interval. The total cost of exported energy, $C_i^{E\prime}$, is given by the following:

$$C_i^{E\prime} = \sum_{k=1}^{N_K - 1} c_{ik}^E \tag{3.21}$$

The net cost associated with the i^{th} subsystem is given by the relationship

$$C_i{}' = C_i^{I\prime} - C_i^{E\prime}. \tag{3.22}$$

3.3 Residential energy system topology

3.3.1 Overview

The generic energy system topology and mathematical model defined in section 3.2 is now applied to a residential energy system. Subsystems associated with a residential system are identified, and a PV subsystem as well as a battery storage subsystem is added to the model. Energy flow constraints of the subsystems are identified. Mathematical constraints associated with the battery storage and controllable load subsystems are given. The cost model for the residential energy system is provided. Finally, the calculation of the payback period of the PV system and battery storage is mathematically defined in terms of the model.

3.3.2 Residential energy system model

The topology chosen for the residential energy system is given in Figure 3-2. The system consists of five subsystems, namely a grid connection, PV energy source, battery storage, a set of uncontrollable loads and a set of controllable loads.

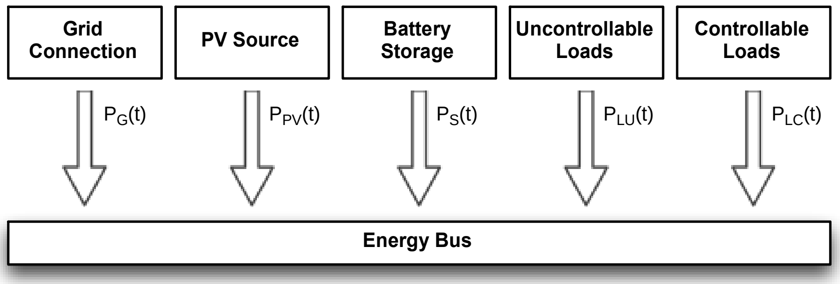

Figure 3-2 Residential Energy System Topology Used in the Case Studies

Uncontrollable loads include loads with fixed operating schedules such as security lighting, cooking appliances, etc. The controllable loads are loads for which the load profile can be adjusted with little or no impact on the behaviour of the end-users (residents). Load profile optimisation will be performed to minimise the cost of energy imported from the grid.

A 24 hour daily profile consists of 49 timestamps from 00:00 and 24:00. A day is thus equally divided into 48 half-hour averaging intervals, for which the energy profiles are calculated. Half-hour intervals provide enough resolution to model the peaks and off-periods associated with residential load profiles, but few enough intervals to optimise the system in a reasonable amount of time. All TOU tariffs can be exactly described using half-hour intervals.

3.3.3 **Power flow constraints for individual subsystems**

Power flow constraints apply to various subsystems and are given by the following:

- *Grid connection:* The power flow can be bidirectional, with

$$-P_{G\,max} \leq P_G(t) \leq P_{G\,max} \tag{3.23}$$

  where $P_{G\,max}$ denotes the power rating of the grid connection.

- *PV source:* The power flow is unidirectional, with

$$0 \leq P_{PV}(t) \leq P_{PV\,max} \tag{3.24}$$

  where $P_{PV\,max}$ denotes the maximum power rating of the PV system.

- *Uncontrollable loads:* The power flow is unidirectional, with

$$-P_{LU\,max} \leq P_{LU}(t) \leq 0 \tag{3.25}$$

  where $P_{LU\,max}$ denotes the sum of the rated values of the uncontrollable loads.

- *Controllable loads:* The power flow is unidirectional, with

$$-P_{LC\,max} \leq P_{LC}(t) \leq 0 \tag{3.26}$$

  where $P_{LC\,max}$ denotes the sum of the rated values of the controllable loads.

- *Battery storage:* The power flow is bidirectional, with

$$-P_{BD\,max} \leq P_B(t) \leq P_{BC\,max} \tag{3.27}$$

  where $P_{BD\,max}$ and $P_{BC\,max}$ denote the maximum discharge rate and maximum charging rate respectively of the battery system.

For the purpose of optimisation, the subsystems shown in Figure 3-2 are characterized in terms of the energy profiles. The power flow constraints listed above translate to constraints for the half-hourly energy profile values in accordance with (3.5) and (3.6). For a half-hourly averaging interval, with energy measured in kWh, this yields the constraints summarized in Table 3.1.

Table 3.1. Energy profile constraints for the residential energy system model

Subsystem	Energy Profile Constraints [kWh]
Grid Connection	$-0.5P_{G\,max} \leq E_{Gk} \leq 0.5P_{G\,max}$
PV source	$0 \leq E_{PVk} \leq 0.5P_{PV\,max}$
Uncontrollable Loads	$-0.5P_{LU\,max} \leq \mathrm{E}_{LUk} \leq 0$
Controllable Loads	$-0.5P_{LC\,max} \leq \mathrm{E}_{LCk} \leq 0$
Battery System	$-0.5P_{BD\,max} \leq E_{Bk} \leq 0.5P_{BC\,max}$

3.3.4 **Battery storage subsystem energy constraints**

Constraints are imposed on the battery storage subsystem to ensure that energy stored cannot exceed the maximum storage capacity. The battery storage should also not be allowed to discharge below a given minimum value. It is further required that the energy profile is energy neutral over the profile timeline. This gives rise to the relationships

$$E_{Bmin} \leq E_{Bstart} + \sum_{k=1}^{\mathrm{M}} E_{Bk} \leq E_{Bmax} \;\; for\; 1 \leq M \leq 48 \tag{3.28}$$

and

$$\sum_{k=1}^{N_K-1} E_{Bk} = 0 \tag{3.29}$$

where E_{Bmin} denotes the minimum charge level for the battery, E_{Bmax} denotes the maximum charge level of the battery, E_{Bstart} denotes the initial energy stored in the battery and E_{Bk} denotes the energy transfer for the k^{th} interval.

The minimum charge level is determined by the allowed depth-of-discharge for the battery. The minimum charge level is given by the relationship

$$E_{Bmin} = B_R(1 - B_{DOD}) \tag{3.30}$$

where B_R denotes the rating of the battery system in kWh and B_{DOD} is the depth-of-discharge allowed for the battery given as a fractional value.

3.3.5 Mathematical model of controllable loads subsystem

To retain the focus of this project on the payback time of PV systems, a simple mathematical model is chosen for the controllable loads. This model can be substituted with a more advanced model if required. Controllable loads are defined to only be *schedulable*. Schedulable loads have a fixed number of times is will operate throughout a day. These are referred to as *operation cycles*. Each operation cycle is associated with a start time and duration. It is assumed that the schedules of each load's operation cycles are known beforehand, and that the start time of operation cycles can be adjusted. The definition of the model is now given. The schedulable loads are defined by a set of power ratings and the set of schedules. The set of power ratings of the schedulable loads, $\boldsymbol{P}_L$, given by the set

$$\boldsymbol{P}_L = \{P_{Lm}\} \qquad m = 1, 2, 3 \ldots N_S \tag{3.31}$$

where P_{Lm} denotes the power rating of an individual schedulable load and N_S denotes the total number of schedulable loads in the energy system. Each load's schedule is defined by one or more operation cycles. The operation cycles of all schedulable loads $\boldsymbol{A}_L$ is a set of sets and is given by

$$\boldsymbol{A}_L = \{\boldsymbol{A}_{Lm}\} \quad m = 1, 2, 3 \ldots\ N_S \tag{3.32}$$

where $\boldsymbol{A}_{Lm}$ denotes the set of operation cycles for load *m*. Each individual operation cycle has two parameters associated with it, namely the start time of the operation cycle and the duration of the operation cycle. An individual schedulable load's set of operation cycles, $\boldsymbol{A}_{Lmn}$, is given by

$$\boldsymbol{A}_{Lmn} = \ \{\, T_{Amn}, D_{Amn}\} \qquad \begin{matrix} m = 1, 2, 3 \ldots N_S \\ n = 1, 2, 3 \ldots N_C \end{matrix} \tag{3.33}$$

where T_{Amn} denotes the starting time of a operation cycle, D_{Amn} denotes the duration of an operation cycle and N_C denotes the total number of operation cycles for the load.

The constraints of the load schedule optimisation is dependent on the start and end time of the day, as well as the sequence in which the start times occur. The parameter of schedulable loads that can be optimised is the starting time of each individual operation cycle, T_{Amn}. The start and end times of operation cycles must conform to the constraints

$$t_1 \leq T_{Amn} \leq t_{N_K} \tag{3.34}$$

and

$$T_{AmN_C} + D_{AmN_C} < t_{N_K} \tag{3.35}$$

where T_{AmN_C} and D_{AmN_C} indicates the starting time and duration of the final operation cycle of the 24 hour period. The operation cycles cannot overlap. This gives rise to the constraint

$$\begin{array}{cc} T_{Am\propto} + D_{Am\propto} < T_{Amn} & m = 1, 2, 3 \ldots N_S \\ or & n, \propto = 1, 2, 3 \ldots N_C \\ T_{Am\propto} > T_{Amn} + D_{Amn} & n \neq \propto \end{array} \tag{3.36}$$

which implies that for each schedulable load *m*, no two operation cycles as indicated by *n* and $\propto$ can overlap. Load schedule optimisation for an individual load is, due to the model defined above, inherently subjected to the constraint that energy consumption before optimisation is equal to the energy consumption after the optimisation.

3.3.6 Cost calculations for residential energy subsystems

The energy cost calculation is now derived for a residential energy system, based on the energy cost calculations for generic energy systems. The subscripts that indicated the subsystems are given in Figure 3-2. From (3.11), the energy exported to or imported from the grid in the k^{th} half-hour interval is given by:

$$E_{Gk} = -(E_{PVk} + E_{LUk} + E_{LCk} + E_{Bk}) \quad k = 1, 2, 3 \cdots 48. \tag{3.37}$$

From (3.12), the energy imported from the grid in the k^{th} half-hour interval is given by

$$\begin{array}{r} E^I_{Gk} = E_{Gk} \ \ if\ E_{Gk} \geq 0 \\ 0\ if\ \ E_{Gk} < 0 \end{array} . \tag{3.38}$$

From (3.17), the energy exported from the grid in the k^{th} half-hour interval is given by

$$\begin{array}{r} E^E_{Gk} = |E_{Gk}| \ \ if\ E_{Gk} < 0 \\ 0\ if\ \ E_{Gk} \geq 0 \end{array} . \tag{3.39}$$

Based on (3.14) and (3.15), the cost of energy imported from the grid connection is given by the relationship

$$\boldsymbol{C}_G^I = R_{Gk}^I E_{Gk}^I \quad k = 1, 2, 3 \cdots 48 \tag{3.40}$$

where R_{Gk}^I is a set containing the grid connection consumption tariffs for each half-hour of the day. Based on (3.19) and (3.20), the cost related to exporting to the grid connection is given by the relationship

$$\boldsymbol{C}_G^E = R_{Gk}^E E_{Gk}^E \quad k = 1, 2, 3 \cdots 48 \tag{3.41}$$

where R_{Gk}^E is a set containing the feed-in tariffs for each half-hour of the day. The net cost of energy exchanged with the grid, C'_G, is given by the net cost equation (3.22) and implementing the grid connection equations (3.40) and (3.41):

$$C'_G = \sum_{k=1}^{48} R_{Gk}^I E_{Gk}^I - R_{Gk}^E E_{Gk}^E \tag{3.42}$$

Equation (3.42) represents a convenient cost function for optimising the payback period of the PV and battery system. This is discussed in the next section.

It must be noted that the assumption is made that energy can either be imported from or exported to grid connection. In practise, exporting energy back into the grid may not be possible depending on the capabilities of the installed network. The PV system is the only subsystem that can cause surplus energy to be exported to the grid connection. In case energy cannot be exported to the grid, the PV system controller can stop energy generation by floating the voltage on the PV panel, or an energy sink can be installed.

3.3.7 **Payback time of installed PV and battery subsystems**

The simple payback period [1] is defined as the time required to recover the capital investment costs through the income or savings produced by the investment. For the purpose of this investigation, the financial savings per day, C', is defined as the reduction of cost of energy imported from the grid connection as a result of the energy supplied by the PV system, giving rise to the relationship

$$C' = C'_{old} - C'_{new} \tag{3.43}$$

where C'_{old} and C'_{new} denote the C'_G cost distinctively before and after the PV and battery storage system has been installed. The simple payback time T_{pb} can be expressed as

$$T_{pb} = \frac{I_C}{C'} \tag{3.44}$$

where I_C denotes cost of investment cost of installing a PV system and/or battery bank at the residence. I_C is represented by

$$I_C = S_C + B_C \tag{3.45}$$

where S_C denotes the solar (PV) system cost and B_C denotes the battery system cost.

3.4 Optimisation of residential energy system

3.4.1 Load schedule and battery profile optimisation

The load schedules of schedulable loads as well as the battery profile can be optimised to minimise electricity cost. Depending on whether schedulable loads, battery storage or both are present in the system, the optimisation optimises different parameters.

The objective function is to minimise cost of energy imported from the grid:

$$minimise\ C'_G = \sum_{k=1}^{48} R^I_{Gk} E^I_{Gk} - R^E_{Gk} E^E_{Gk} \tag{3.46}$$

The load schedule and battery profile is related to the energy costs as given from (3.37) through to (3.42). Three different contexts in which the optimisation could occur, exists. The parameters to optimise in each context is different, hence the three contexts are described:

- Battery storage and load schedule optimisation. The parameters to optimise are

$$E_{Bk}\ for\ k = 1, 2, 3 \dots N_K - 1$$

$$T_{Amn}\ for\ n = 1, 2, 3 \dots N_S\ and\ for\ each\ m = 1, 2, 3 \dots\ N_C$$

- Optimisation of only the load schedules. The parameters to optimise are:

$$T_{Amn}\ for\ n = 1, 2, 3 \dots N_S\ and\ for\ each\ m = 1, 2, 3 \dots\ N_C$$

- Optimisation of only the battery storage profile. The parameters to optimise are:

$$E_{Bk}\ for\ k = 1, 2, 3 \dots N_K - 1$$

3.4.2 PV and battery storage rating optimisation

The objective of this optimisation is to achieve a minimum payback period for the PV and battery system. The payback period is calculated by dividing the total cost of the system by the savings achieved through installation of the PV and battery system, as shown in (3.44). The objective function is

$$minimize\ T_{pb} = \frac{I_C}{C'} \tag{3.47}$$

The optimisation is bounded by the rating limitations on the energy storage and PV system. The battery storage rating constraints are given by

$$B_{Rmin} < B_R < B_{Rmax} \tag{3.48}$$

where B_R denotes the battery system rating and B_{Rmin} and B_{Rmax} denote respectively the minimum and maximum rating for the battery system. The PV system rating constraints are given by

$$S_{Rmin} < S_R < S_{Rmax} \tag{3.49}$$

where S_R denotes the PV system rating and S_{Rmin} and S_{Rmax} denote respectively the minimum and maximum rating for the PV system.

3.5 Introducing the alternative equations for payback period

3.5.1 Overview

This section presents new analysis methods regarding how the payback period of the PV and battery system can be obtained directly from residential energy system parameters such as the load profile, PV system cost and solar energy profile. An equation for the payback period is first derived generically so that it can be applied to calculate the payback period with any tariff structure. It is then shown that simplifications can be made for common tariff structures. These simplifications are used to explore the effect of factors related to the tariff structure, such as the effect on payback time as a function of the relationship between consumption and feed-in tariffs.

3.5.2 Introduction of the utilisation factor

Equation (3.44) provides a simple approach to calculate the PV and battery system payback period. However, factors I_c (total system cost) and C' (total savings per day) does not intuitively give the direct relationship between the input parameters and the results. This is shown explicitly in the first case study in chapter 5. An alternate equation for the payback period is derived, which establishes a direct relationship between the input parameters and results. The equations are first derived for residential energy systems where only a PV system and no battery storage are installed. The payback period equation (3.44) for this residential energy system is rewritten to the investment cost is given by the PV system cost, S_C:

$$T_{pb} = \frac{S_C}{C'} \tag{3.50}$$

Combining the equations for finding the savings of installed PV systems, namely (3.42) and (3.43), the savings achieved by installing a PV system can be given by

$$\begin{aligned} C' &= \sum_{k=1}^{48} (R_{Gk}^{I} E_{Gk}^{I} - R_{Gk}^{E} E_{Gk}^{E})_{old} - \sum_{k=1}^{48} (R_{Gk}^{I} E_{Gk}^{I} - R_{Gk}^{E} E_{Gk}^{E})_{new} \\ &= \sum_{k=1}^{48} R_{Gk}^{I} \Delta E_{k}^{I} + R_{Gk}^{E} \Delta E_{k}^{E} , \end{aligned} \tag{3.51}$$

where

$$\Delta E_k^I = E_{Gk_{old}}^I - E_{Gk_{new}}^I , \tag{3.52}$$

which denotes the change in energy imported from the grid and

$$\Delta E_k^E = E_{Gk_{new}}^E - E_{Gk_{old}}^E , \tag{3.53}$$

which denotes the change in energy exported to from the grid, during the k^{th} half-hour. The payback period given in (3.44) can now, by substituting in (3.51), be rewritten in terms of the per-watt cost of the PV system, the change in energy brought forward by the PV system, and the energy cost tariffs. This is done through the relationship

$$T_{pb}(S_R) = \frac{S_R S_{pu}(S_R)}{\sum_{k=1}^{48} R_{Gk}^{I} \Delta E_k^I + R_{Gk}^{E} \Delta E_k^E} \tag{3.54}$$

where S_R denotes the rating of the PV system, S_{pu} gives the per-watt cost of the PV system and is dependent on S_R, $R_{Gk}^I \Delta E_k^I$ denotes the savings generated by decreasing the energy imported from the grid connection and $R_{Gk}^E \Delta E_k^E$ denotes the savings brought forward by increasing the energy exported to the grid connection, both during the k^{th} half-hour.

The objective of this chapter is to determine the payback period in terms of parameters that describe a residential energy system. Therefore the decrease in imported energy, ΔE_k^I, and increase in exported energy, ΔE_k^E, should be rewritten in terms of parameters such as the PV system energy profile and the grid connection energy profile. Taking the grid connection energy profile *before* PV system installation, $\boldsymbol{E}_G^I$, and PV system energy profile, $\boldsymbol{E}_{PV}$, the energy profile that describes change in imported energy, $\Delta \boldsymbol{E}^I$**,** is found by:

$$\Delta \boldsymbol{E}^I = \boldsymbol{E}_{PV} \cap \boldsymbol{E}_G^I , \tag{3.55}$$

that is

$$\begin{aligned} \Delta E_k^I &= E_{PVk}, \quad if\ E_{PVk} < E_{Gk}^I \\ &= E_{Gk}^I, \quad if E_{Gk}^I < E_{PVk} \end{aligned} \qquad k = 1, 2, 3, \dots 48. \tag{3.56}$$

Equation (3.56) states that ΔE_k^I gives, for the k^{th} half-hour, the PV system energy that will be consumed by subsystems in the residential energy system. Notice that ΔE_k^I can be expressed as a fraction of the E_{PVk} value. To determine the value of this fraction, the following relationship defines the value for each element in the respective sets:

$$\boldsymbol{F}_U = \frac{\boldsymbol{E}_{PV} \cap \boldsymbol{E}_G}{\boldsymbol{E}_{PV}} \tag{3.57}$$

which, when substituted in (3.55), implies

$$\boldsymbol{F}_U = \frac{\Delta \boldsymbol{E}^I}{\boldsymbol{E}_{PV}}. \tag{3.58}$$

$\boldsymbol{F}_U$ is henceforth known as the utilisation factor, because it represents the PV energy that is utilised locally in the residential energy system. The decrease in energy imported from the grid can be defined in terms of the PV system energy profile and utilisation factor, by rewriting (3.58) in the form

$$\Delta \boldsymbol{E}^I = \boldsymbol{E}_{PV} \boldsymbol{F}_U, \tag{3.59}$$

where

$$\Delta E_k^I = E_{PVk}F_{Uk} \qquad k = 1, 2, 3, \dots 48. \tag{3.60}$$

Similarly, the increase in energy exported to the grid can also be defined in terms of the PV system energy profile and the utilisation factor. The change in energy exported to the grid after PV installations is given by

$$\Delta \boldsymbol{E}^E = \boldsymbol{E}_{PV} - \Delta \boldsymbol{E}^I, \tag{3.61}$$

where $\boldsymbol{E}_{PV}$ denotes the PV system energy profile and $\Delta \boldsymbol{E}^I$ denotes the energy of the PV system that is utilised in the residential energy system. This can be further simplified by substituting in (3.59)

$$\Delta \boldsymbol{E}^E = \boldsymbol{E}_{PV} - \boldsymbol{E}_{PV}\boldsymbol{F}_U, \tag{3.62}$$

and factorisation then gives rise to the equation

$$\Delta \boldsymbol{E}^E = \boldsymbol{E}_{PV}(\boldsymbol{1} - \boldsymbol{F}_U). \tag{3.63}$$

If (3.63) is written in terms of half-hour energy it corresponds to

$$\Delta E_k^I = E_{PVk}(1 - F_{Uk}) \qquad k = 1, 2, 3, \dots 48. \tag{3.64}$$

With the derived equations (3.60) and (3.64), the payback period equation given in (3.54) can be rewritten as

$$\begin{aligned} T_{pb}(S_R) &= \frac{S_R S_{pu}(S_R)}{\sum_{k=1}^{48} E_{PVk}F_{Uk}R_{Gk}^I + E_{PVk}(1 - F_{Uk})R_{Gk}^E} \\ &= \frac{S_R S_{pu}(S_R)}{\sum_{k=1}^{48} E_{PVk}[F_{Uk}R_{Gk}^I + (1 - F_{Uk})R_{Gk}^E]} \end{aligned} \qquad k = 1, 2, 3, \dots 48. \tag{3.65}$$

In (3.65) E_{PVk} represents the half-hour energy of PV system energy profile $\boldsymbol{E}_{PV}$. Note that it only gives the total energy collected by the PV system and that the rating of the PV system is not specified. It would be ideal if the payback period could be a function of the PV system rating. Making the assumption that the energy collected by a PV system can be found by scaling the energy collected by a 1 kW PV system, the following equation is created:

$$\boldsymbol{E}_{PV}(S_R) = S_R\boldsymbol{E}_{NPV} \tag{3.66}$$

where $\boldsymbol{E}_{NPV}$ denotes an energy profile of a 1 kW PV system, and S_R is a scalar that denotes the rating of the PV system to be installed. Notice that $\boldsymbol{E}_{PV}$ clearly states that it is a function of the value of the PV system rating S_R. After stating that $\boldsymbol{E}_{PV}$ is a function of S_R in (3.66), it is clear that the utilisation factor is then in turn a function of the PV system rating S_R, i.e

$$\boldsymbol{F}_U(S_R) = \frac{\boldsymbol{E}_{PV}(S_R) \cap \boldsymbol{E}_G}{\boldsymbol{E}_{PV}(S_R)}. \tag{3.67}$$

With all the relevant terms defined, (3.66) and (3.67) is substituted into (3.65), giving rise to:

$$\begin{aligned} T_{pb}(S_R) &= \frac{S_R S_{pu}(S_R)}{\sum_{k=1}^{48} S_R E_{NPVk}[F_{Uk}(S_R)R_{Gk}^I + (1 - F_{Uk}(S_R))R_{Gk}^E]} \\ &= \frac{S_{pu}(S_R)}{\sum_{k=1}^{48} E_{NPVk}[F_{Uk}(S_R)R_{Gk}^I + (1 - F_{Uk}(S_R))R_{Gk}^E]}. \end{aligned} \tag{3.68}$$

Equation (3.68) states that the payback time of a solar system can be expressed in terms of:

- The per-watt purchase cost function of a PV system, $S_{pu}(S_R)$
- The PV solar profile, $\boldsymbol{E}_{NPV}$
- The cost of purchasing electric energy from the grid, $\boldsymbol{R}_G^I$
- The profits made by selling energy to the grid, $\boldsymbol{R}_G^E$
- The fraction of solar energy used by residential loads, $\boldsymbol{F}_{Uk}$

Equation (3.68) is generally applicable to any tariff structure. The equation can be simplified by knowing the state of the tariffs for a residential energy system, e.g. whether a flat or TOU tariff is present and whether any remuneration is given for feeding back into the grid.

3.5.3 **Derivation of simplified payback equation for various tariff structures**

3.5.3.1 Overview

The payback equation in (3.68) can be simplified if the consumption and feed-in tariffs of the grid connection, $\boldsymbol{R}_G^I$ and $\boldsymbol{R}_G^E$, are known. The objective of this section is to stipulate these simplifications in the order as given in Table 3.2.

Table 3.2 The payback equation for the specified tariffs will be derived in the indicated section

Tariff scenario		**Section**
Consumption tariffs	**Feed-in tariffs**	
Flat rate	None	3.5.3.2
Flat rate	Flat rate	3.5.3.3
TOU (2 tariffs)	TOU (2 tariffs)	3.5.3.4

3.5.3.2 Payback equation on flat rate consumption tariffs

The tariffs in this scenario are given by

$$R_{Gk}^{I} = r \qquad k = 1, 2, 3, \dots 48 \tag{3.69}$$

and

$$R_{Gk}^{E} = 0 \qquad k = 1, 2, 3, \dots 48 \tag{3.70}$$

Substituting these values into (3.68), the payback equation is simplified to

$$T_{pb}(S_R) = \frac{S_{pu}(S_R)}{r \sum_{k=1}^{48} E_{NPVk} F_{Uk}(S_R)} \tag{3.71}$$

The tariff simplification allows the summation expression of the denominator to be simplified as well. The denominator is simplified through the equality

$$\sum_{k=1}^{48} E_{NPVk} F_{Uk}(S_R) = E_{NPV} F_U(S_R) \tag{3.72}$$

for which the right hand side factors are given by the sum of the energy in the PV energy profile

$$E_{NPV} = \sum_{k=1}^{48} E_{NPVk} \tag{3.73}$$

and a scalar utilisation factor as the weighted average of the utilisation factor profile

$$F_U(S_R) = \frac{\sum_{k=1}^{48} E_{NPVk} F_{Uk}(S_R)}{\sum_{k=1}^{48} E_{NPVk}}. \tag{3.74}$$

This simplifies (3.71) to the form

$$T_{pb}(S_R) = \frac{S_{pu}(S_R)}{rE_{NPV}F_U(S_R)} \tag{3.75}$$

Equation (3.75) suggests that for flat consumption tariffs, it is not necessary to define $\boldsymbol{F}_U$ in terms of each averaging interval k. To determine the utilisation function, instead of using (3.57), a simpler method of finding the scalar value is given by

$$F_U(S_R) = \frac{\sum_{k=1}^{48} \Delta E_k^I}{\sum_{k=1}^{48} E_{PVk}}. \tag{3.76}$$

3.5.3.3 Payback Equation on flat rate purchase and feed-in tariffs

The tariffs in this scenario are given by

$$R_{Gk}^I = r^I \qquad k = 1, 2, 3, \dots 48 \tag{3.77}$$

and

$$R_{Gk}^E = r^E \qquad k = 1, 2, 3, \dots 48. \tag{3.78}$$

Therefore the payback equation (3.68) can be simplified to

$$T_{pb}(S_R) = \frac{S_{pu}(S_R)}{\sum_{k=1}^{48} E_{NPVk}(F_{Uk}(S_R)r^I + (1 - F_{Uk}(S_R))r^E)}. \tag{3.79}$$

Using the same logic by which (3.71) has been rewritten to (3.75), equation (3.79) is simplified to

$$T_{pb}(S_R) = \frac{S_{pu}(S_R)}{E_{NPV}[F_U(S_R)r^I + (1 - F_U(S_R))r^E]}. \tag{3.80}$$

3.5.3.4 Payback equation on TOU consumption tariffs

The number of defined costs in a TOU tariff structure can vary. An utilisation factor is associated with each cost that is defined in the TOU tariff structure. A simplified equation for payback time with an arbitrary number of defined TOU prices can be derived. The derivation of a generic simplified payback period function for an arbitrary number of defined TOU costs is now given.

Let K_j define a set of averaging intervals which share the same consumption tariff r_j^I. Let N_R give the total number of TOU consumption tariffs. The tariff profile is then given by

$$R_{Gk}^I = r_j^I \qquad for\ all\ k\ in\ set\ K_j \qquad for\ all\ consumption\ tariffs, i.e.\ j = 1, 2 \ldots N_R. \tag{3.81}$$

As a visual example of this, Figure 3-3 presents the case where two tariffs, r_1^I and r_2^I, are defined over the averaging interval sets K_1 and K_2. Since two tariffs are defined, $N_R = 2$.

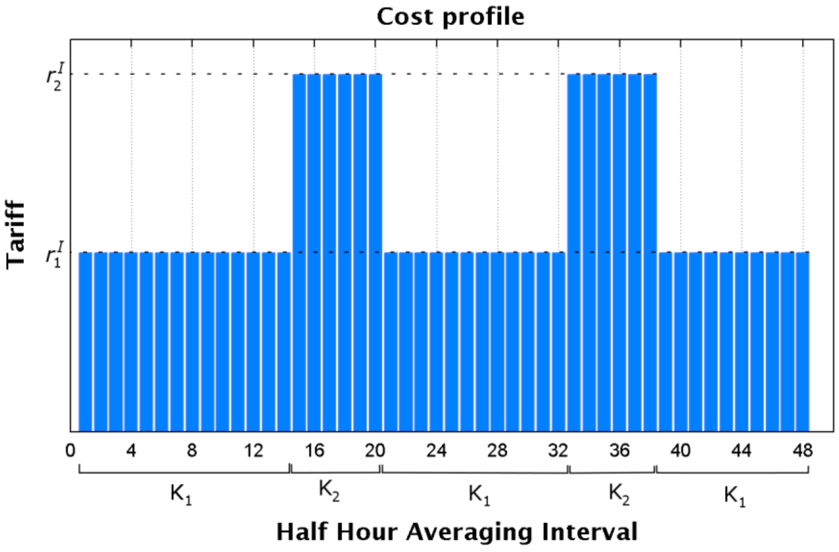

Figure 3-3 Notation definition example

An utilisation factor function is defined for the energy associated with every one of the consumption tariffs. The total energy collected during a given consumption tariff is given by

$$E_{NPVj} = \sum_{K_j} E_{NPVk} \quad for\ all\ j\ in\ N_R. \tag{3.82}$$

where the notation $\sum_{K_j} X_k$ implies that the addition is made for all k in the set K_j. The utilisation factor for each consumption tariff is given by

$$F_{Uj}(S_R) = \frac{\sum_{K_j} E_{NPVk} F_{Uk}(S_R)}{\sum_{K_j} E_{NPVk}} \quad for\ all\ j\ in\ N_R \tag{3.83}$$

Analogous to the simpler practical method for finding utilisation factor as given in (3.76), a practical method with TOU tariffs is given by

$$F_{Uj}(S_R) = \frac{\sum_{K_j} \Delta E_k^I}{\sum_{K_j} E_{NPVk}} \; for\ all\ j\ in\ N_T. \tag{3.84}$$

The payback period of a PV system for a residential energy system with TOU consumption tariffs is then defined by

$$T_{pb}(S_R) = \frac{S_{pu}(S_R)}{\sum_{K_j} E_{NPVj} F_{Uj}(S_R) r_j^I} \quad for\ all\ j\ in\ N_R. \tag{3.85}$$

The practical application of this simplified equation is the payback period equation for a TOU tariff structure with two defined costs. Let r_1^I denote the first cost tariff and E_{NPV1} denote the energy collected by the solar panels during the period r_1^I implemented. Let r_2^I and E_{NPV2} analogously define the associated terms for the second cost tariff. According to the derivation as given in (3.85), the payback period is the given by

$$T_{pb}(S_R) = \frac{S_{pu}(S_R)}{E_{NPV1} F_{U1}(S_R) r_1^I + E_{NPV2} F_{U2}(S_R) r_2^I}. \tag{3.86}$$

3.5.4 Dynamics between per-watt cost, load- and solar profile

3.5.4.1 Overview

One objective of this research project is to explore factors that determine the minimum payback period for the PV and battery system. Preliminary case studies reveal that the payback period, as a function of PV system rating, transitions from a decreasing to increasing function as PV system rating increases. An example is given to demonstrate this. Note that the example is an extract from a case study that will be discussed in detail in Chapter 5. The focus of this section is to point out two features and motivate why mathematical expressions should be derived for these features. The necessary mathematical expressions to investigate the mentioned features are then derived.

Figure 3-4 shows preliminary results for the payback period of a PV system where a flat energy consumption tariff and zero feed-in tariff is considered. The first distinguishable feature, which is present in almost all case studies, is the initial constant value for the utilisation factor function. This constant value is due to the fact that for small PV systems, all the energy is consumed by loads in the residential energy system. A second feature that can clearly be distinguished is that as the PV system rating increases beyond 700 W, the utilisation factor function becomes a decreasing function and the payback period becomes an increasing function. The question that arises is whether payback period becomes an increasing function due to the fact that the utilisation factor function becomes a decreasing function. It should be helpful to understand the exact conditions that give rise to a decreasing payback period function. This section explores these conditions for various tariff structures and identifies the factors that determine a decreasing payback period function.

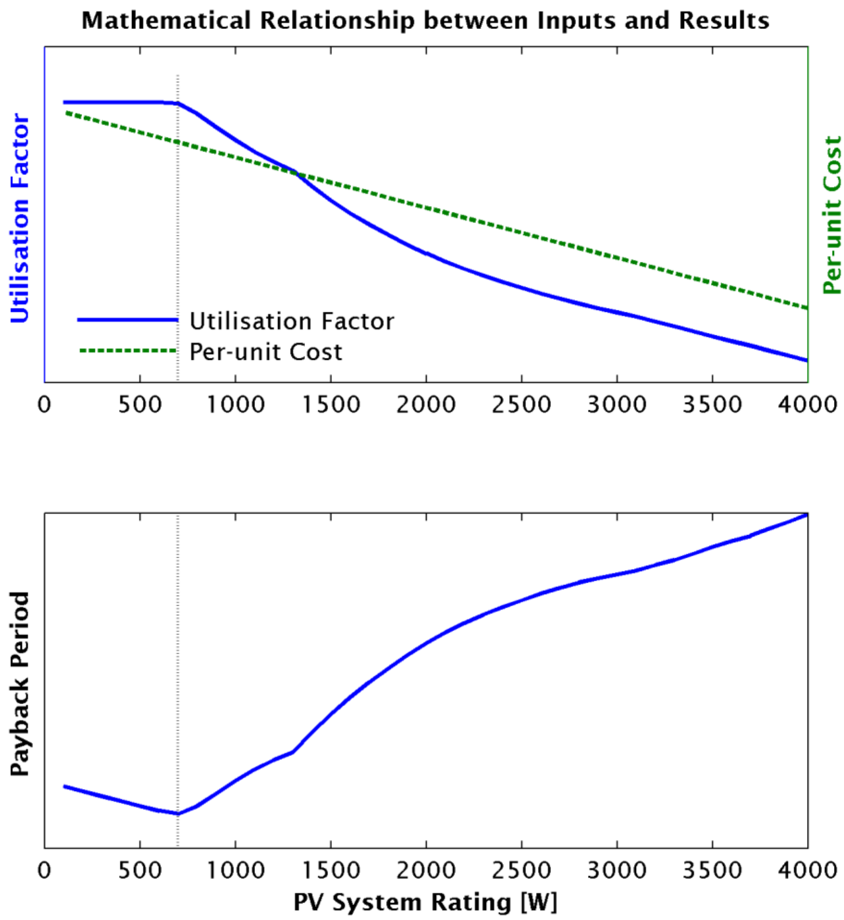

Figure 3-4 Typical analysis results showing relationship between inputs and results. Vertical axis scales intentionally not provided.

3.5.4.2 Derivation of general payback period gradient equation

This investigation considers the effect of a constant utilisation factor and the conditions for an increasing or decreasing payback period, in context of different tariff structures, as given in

Equations (3.75), (3.80) and (3.86). To determine mathematical relationships between the input parameters and the gradient of the payback period, a simplified form of the payback period equations is presented. If r^E and r^I are taken as constants in (3.75), (3.80) and (3.86), the general form of the equations are

$$h(x) = \frac{f(x)}{c.g(x)} \tag{3.87}$$

where x is taken as the dependant variable instead of the PV system rating, $h(x)$ is taken as the payback time, $f(x)$ is taken as the per-unit cost, $g(x)$ represents the denominator, which is mostly dependent on the utilisation factor, and c represents a constant function. The function $g(x)$ and the constant c assume different forms for the different tariff structures as shown in Table 3.3.

Table 3.3 Substituted values through the $g(x)$ function

Environmental parameters description	**Payback Equation**	c	$g(x)$
Flat purchase tariff, no feed-in tariffs	(3.75)	rE_{NPV}	$F_U(S_R)$
Flat purchase tariff, with feed-in tariffs	(3.80)	E_{NPV}	$F_U(S_R)r^I + (1 - F_U(S_R))r^E$
TOU purchase tariffs, no feed-in tariffs	(3.86)	1	$E_{NPV1}F_{U1}(S_R)r_1^I + E_{NPV2}F_{U2}(S_R)r_2^I$

Equations for payback period gradient for different tariff structures will be derived to discuss the effect of constant utilisation factor functions, as well as point out the conditions for decreasing payback time. The equations are valid for any inputs, but logical assumptions based on a practical residential energy system simplify the interpretation of the equations. The first assumption is that when constant c is considered in the light of (3.75), (3.80) and (3.86), it is seen that it constitutes of one or more of the following:

- PV system energy during the day
- consumption tariffs

The values of these two terms are mathematically defined to be:

$$E_{NPVk} > 0 \tag{3.88}$$

and

$$r^{I} > 0. \tag{3.89}$$

This leads to the fact that c is always a positive value. The utilisation factor indicates a fraction (the PV system energy that is utilised within the residential energy system) therefore the value is always positive. The assumption is made that a residential energy system does not have a load of zero. This leads to the condition

$$1 \geq F_U(S_R) > 0. \tag{3.90}$$

The per-unit cost function of the PV system is assumed to be a monotone decreasing function

$$\frac{d}{dS_R} S_{pu}(S_R) < 0. \tag{3.91}$$

If a consumption tariff and a feed-in tariff are present, the assumption is that the feed-in tariff is lower or equal to the consumption tariff, given by

$$\frac{r^E}{r^I} \leq 1. \tag{3.92}$$

The relationship between $h(x)$, $f(x)$ and $g(x)$ is now investigated. The objective is to determine how $f(x)$ and $g(x)$ determine whether $h(x)$ increases or decreases. For this reason, the gradient of $h(x)$ is considered. In the following derivation the quotient rule is applied:

$$\begin{aligned} \frac{d}{dx} h(x) &= \frac{d}{dx}\left(\frac{f(x)}{c.\,g(x)}\right) \\ &= \frac{1}{c}\frac{g(x)\frac{d}{dx}f(x) - f(x)\frac{d}{dx}g(x)}{g(x)^2} \end{aligned} \tag{3.93}$$

From (3.93) a condition can be derived for decreasing payback time:

$$\frac{1}{c}\frac{g(x)\frac{d}{dx}f(x) - f(x)\frac{d}{dx}g(x)}{g(x)^2} < 0$$
$$g(x)\frac{d}{dx}f(x) - f(x)\frac{d}{dx}g(x) < 0 \tag{3.94}$$
$$\frac{\frac{d}{dx}f(x)}{f(x)} < \frac{\frac{d}{dx}g(x)}{g(x)}$$

Equation (3.94) states that if the normalised gradient of the per-unit cost given by $f(x)$ is less that the normalised gradient of $g(x)$, the payback period decreases. The practical implication of this derivation for the different tariff structures are given in subsequent sections. An important consideration is that the case studies will be conducted with discrete intervals, implying that a discrete form of (3.94) is required. The following conditions are specified for the discrete form of (3.94):

$$x_2 > x_1 \tag{3.95}$$

where x_2 and x_1 are two arbitrary values of the dependent variable. The discrete form of the condition for decreasing payback time is the n given by

$$\frac{\left(\frac{f(x_2) - f(x_1)}{x_2 - x_1}\right)}{f(x_1)} < \frac{\left(\frac{g(x_2) - g(x_1)}{x_2 - x_1}\right)}{g(x_1)}$$
$$\frac{f(x_2) - f(x_1)}{f(x_1)} < \frac{g(x_2) - g(x_1)}{g(x_1)}. \tag{3.96}$$

3.5.4.3 Decreasing payback period for flat consumption tariff, zero feed-in tariff

This section represents the first case as mentioned in Table 3.3. To determine the effects of a constant utilisation factor, the residential energy system parameters are substituted into the gradient function (3.93) to give

$$\frac{d}{dS_R}T_{pb}(S_R) = \frac{1}{rE_{NPV}}\frac{F_U(S_R)\frac{d}{dS_R}S_{pu}(S_R) - S_{pu}(S_{R1})\frac{d}{dS_R}F_U(S_R)}{F_U(S_R)^2}. \tag{3.97}$$

Since the utilisation factor is constant over PV system rating, the second term in the nominator is zero. The denominator is a square and since no complex numbers are present, the term is positive. If the simplification assumptions are applied, $\frac{d}{dS_R} S_{pu}(S_R)$ is negative. This implies that as long as the utilisation factor is constant, the payback period gradient is negative. Therefore as long as utilisation factor remains constant, the payback period decreases as PV system rating increases.

Due to the direct relationship between the original form and the general form of the payback period as respectively given in (3.75) and (3.87), the condition for decreasing payback time can be directly be found and is given by

$$\frac{F_u(S_{R2}) - F_u(S_{R1})}{F_u(S_{R1})} > \frac{S_{pu}(S_{R2}) - S_{pu}(S_{R1})}{S_{pu}(S_{R1})}. \tag{3.98}$$

Equation (3.98) states that the payback time increases if the normalised decrease of the utilisation factor is lower than the normalised decrease of the per-unit cost function. The above equations prove that it is possible for the utilisation factor function to be decreasing and still have a decreasing payback period function. In the exemplary Figure 3-4, the payback time immediately increases when the utilisation factor goes below 100%. But here it is noted that payback time can be a decreasing function even if the utilisation function decreases below 100%.

3.5.4.4 Decreasing payback period for flat consumption and feed-in tariff

This represents the second case as mentioned in Table 3.3. To inspect the payback equation gradient as given in (3.99) the various terms are considered.

$$\frac{d}{dS_R} T_{pb}(S_R) = \frac{1}{E_{NPV}} \frac{\left[F_{U1}(S_R) r^I + \left(1 - F_{U1}(S_R)\right) r^E\right] \frac{d}{dS_R} S_{pu}(S_R) - S_{pu}(S_R) \frac{d}{dS_R}\left[F_{U1}(S_R) r^I + \left(1 - F_{U1}(S_R)\right) r^E\right]}{\left[F_{U1}(S_R) r^I + \left(1 - F_{U1}(S_R)\right) r^E\right]^2} \tag{3.99}$$

The constant coefficient is a positive value. The denominator is a square and therefore maintains a positive value. If the assumptions regarding residential energy systems hold, the first numerator term is negative since the gradient of the per-unit cost function is negative and the utilisation factor is positive and smaller than 1. When the derivation operator in the second numerator term is moved into the brackets in the equation, the result is given by

$$-S_{pu}(S_{R1})\left[\frac{d}{dS_R}F_U(S_R)r^I+\left(\frac{d}{dS_R}1-\frac{d}{dS_R}F_U(S_R)\right)r^E\right]. \quad (3.100)$$

Since the utilisation factor function is a constant, the term reduces to 0. Therefore considering all terms in the equation, if the utilisation function is constant and the assumptions as stated are true, the payback period is a decreasing function.

The condition for decreasing payback time for this tariff structure is now derived. The general form of the constraint is given by (3.96). The relationship between the generic and real payback time equations, as respectively given by (3.80) and (3.87), make direct substitution rather unintuitive. The substitution process is given stepwise and the value for substitution is taken from Table 3.3. The substitution value that has to be found is for $g(x_2)-g(x_1)$:

$$\begin{aligned} g(x_2)-g(x_1) &= \left[F_U(S_{R2})(1-\frac{r^E}{r^I})+\frac{r^E}{r^I}\right]-\left[F_U(S_{R1})(1-\frac{r^E}{r^I})+\frac{r^E}{r^I}\right] \\ &= \left(F_U(S_{R2})-F_U(S_{R1})\right)(1-\frac{r^E}{r^I}) \end{aligned} \quad (3.101)$$

With the result from (3.101), the substitution into the right-hand side of the payback period decreasing condition from (3.94) is given by:

$$\frac{g(x_2)-g(x_1)}{g(x_1)} = \frac{\left(F_U(S_{R2})-F_U(S_{R1})\right)(1-\frac{r^E}{r^I})}{F_U(S_{R1})(1-\frac{r^E}{r^I})+\frac{r^E}{r^I}} \quad (3.102)$$

The equation rewritten in (3.103) to make analysis easier, but the new form is not valid for the case where $\frac{r^E}{r^I}=1$. For that specific case, (3.102) can be used to interpret the analysis.

$$\frac{g(x_2)-g(x_1)}{g(x_1)} = \frac{F_U(S_{R2})-F_U(S_{R1})}{F_U(S_{R1})+\frac{\frac{r^E}{r^I}}{(1-\frac{r^E}{r^I})}} \quad (3.103)$$

With the substitutions and derivations in (3.102) and (3.103), the final condition for payback time is given in (3.104).

$$\frac{F_u(S_{R2}) - F_u(S_{R1})}{F_U(S_{R1}) + \frac{\frac{r^E}{r^I}}{(1 - \frac{r^E}{r^I})}} > \frac{S_{pu}(S_{R2}) - S_{pu}(S_{R1})}{S_{pu}(S_{R1})} \tag{3.104}$$

Notice that the different payback equations as given in (3.98) and (3.103) is exactly equal when $\frac{r^E}{r^I} = 0$. This makes perfect sense since the condition for no feed-in tariffs in the payback period in (3.98) imply that $\frac{r^E}{r^I} = 0$.

What does the condition $\frac{r^E}{r^I} = 1$ imply? For each unit of energy the PV system generates, the same amount of cost is avoided by either using it within the residential energy system or feeding it into the grid. Therefore the utilisation factor is eliminated as factor that determines the payback period of the PV system.

Up until this stage, $\frac{r^E}{r^I}$ has only been discussed in terms of being 0 or 1. A discussion is presented on the effect it has for any value between 0 and 1. For the case where $\frac{r^E}{r^I}$ is 0, the payback time's tendency to increase or decrease is heavily influenced by the utilisation factor, as shown in (3.98). For the case where the value is 1, equation (3.102) indicates that utilisation factor's value has no influence. Therefore for an increasing value of $\frac{r^E}{r^I}$, the required constraint on the utilisation factor function to maintain a decreasing payback period is lessened.

3.5.4.5 Decreasing payback period for TOU consumption and zero feed-in tariff

This represents the third case of energy tariffs as mentioned in Table 3.3. Multiple utilisation factor functions are associated with this energy tariff structure. The first derivations will determine the effect of constant utilisation factor function, which in this context imply all utilisation factor functions are constant. The payback period gradient expression is given in (3.105). The first term in the numerator is negative since, by the assumptions, the first factor is positive and the second factor negative. The second term is zero since the gradient of all utilisation factor functions are zero. Therefore the payback period decreases as long as all utilisation factor functions are constant.

$$\frac{d}{dS_R}T_{pb}(S_R) = \frac{\left[\sum_{K_j} E_{NPVj}F_{Uj}(S_R)r_j^I\right]\frac{d}{dS_R}S_{pu}(S_R) - S_{pu}(S_R)\frac{d}{dS_R}\sum_{K_j} E_{NPVj}F_{Uj}(S_R)r_j^I}{\left[\sum_{K_j} E_{NPVj}F_{Uj}(S_R)r_j^I\right]^2} \tag{3.105}$$

The condition for decreasing payback period for TOU tariffs is now derived. The derivation is done with the assumption that 2 consumption tariffs are present, as is shown in the exemplary payback equation given in (3.86). If the condition for decreasing payback time is required for more consumption tariffs, it can be derived analogously. Direct substitution between the general and practical payback period functions, as respectively given in (3.85) and (3.87), is unintuitive and the substitution is therefore given stepwise. The factor that is first found is $g(x_2) - g(\,x_1)$ as per Table 3.3:

$$\begin{aligned} g(x_2) - g(\,x_1) &= E_{NPV1}r_1^I F_{U1}(S_{R2}) + E_{NPV2}r_2^I F_{U2}(S_{R2}) - \\ &\quad [E_{NPV1}r_1^I F_{U1}(S_{R1}) + E_{NPV2}r_2^I F_{U2}(S_{R2})] \\ &= E_{NPV1}r_1^I\big(F_{U1}(S_{R2}) - F_{U1}(S_{R1})\big) + \\ &\quad E_{NPV2}r_2^I\big(F_{U2}(S_{R2}) - F_{U2}(S_{R1})\big) \end{aligned} \tag{3.106}$$

With the result from (3.106) , the substitution into the term right of the operator in (3.94) is given by:

$$\begin{aligned} \frac{g(x_2) - g(x_1)}{g(x_1)} &= \frac{E_{NPV1}r_1^I\big(F_{U1}(S_{R2}) - F_{U1}(S_{R1})\big) + E_{NPV2}r_2^I\big(F_{U2}(S_{R2}) - F_{U2}(S_{R1})\big)}{E_{NPV1}r_1^I F_{U1}(S_{R1}) + E_{NPV2}r_2^I F_{U2}(S_{R2})} \\ &= \frac{F_{U1}(S_{R2}) - F_{U1}(S_{R1})}{F_{U1}(S_{R1}) + \frac{E_{NPV2}r_2^I}{E_{NPV1}r_1^I}F_{U2}(S_{R2})} + \frac{F_{U2}(S_{R2}) - F_{U2}(S_{R1})}{\frac{E_{NPV1}r_1^I}{E_{NPV2}r_2^I}F_{U1}(S_{R1}) + F_{U2}(S_{R2})} \end{aligned} \tag{3.107}$$

The final result substitutes (3.107) into (3.98) to determine the condition for decreasing payback time:

$$\frac{F_{U1}(S_{R2}) - F_{U1}(S_{R1})}{F_{U1}(S_{R1}) + \frac{E_{NPV2}r_2^I}{E_{NPV1}r_1^I}F_{U2}(S_{R2})} + \frac{F_{U2}(S_{R2}) - F_{U2}(S_{R1})}{\frac{E_{NPV1}r_1^I}{E_{NPV2}r_2^I}F_{U1}(S_{R1}) + F_{U2}(S_{R2})} > \frac{S_{pu}(S_{R2}) - S_{pu}(S_{R1})}{S_{pu}(S_{R1})} \tag{3.108}$$

The utilisation factor of each tariff period contributes to the inequality that determines whether the payback period function is increasing or decreasing. The denominators on the left-hand side of (3.108) imply a constraint on the exploratory work that can be done. Each denominator has term that consists of an utilisation factor which is multiplied by a scalar of the solar energy and tariff price associated with each consumption tariff. To change the ratio of the solar energy of the period (i.e. $\frac{E_{NPV1}}{E_{NPV2}}$) the time during which the consumption tariffs are implemented, should be changed. This again leads to a change in the utilisation factor graphs, and changes the problem space completely. However, equation (3.108) can be used to study the effects of adapting the ration of consumption tariffs, i.e. $\frac{r_2^I}{r_1^I}$, and its effect on the payback period of the PV system.

3.5.5 **Battery costs and payback time**

PV systems can be coupled with battery systems to provide backup power and to improve the use of locally generated electricity by storing surplus PV energy. Associated with the battery system are a host of variables that affect performance and the economic viability of the battery storage system. These factors have been stipulated in the literature review, and include the depth-of-discharge and charge rate and their effect on effective lifetime of the battery. To optimise the rating of the battery system requires careful investigation and observation of the performance and economic impact, and this falls outside the scope of this project. In this project, reasonable values for the variables will be assumed and the performance of the battery then measured in the system.

A battery is primarily installed into a residence as a secondary power source in the case of a blackout. However, the battery can assist with saving money in the following manners:

- Charging off surplus solar energy, and then discharging this energy at a later stage to save electricity costs
- In the scenario where TOU tariffs are present, the battery can charge during the cheap tariff periods and then alleviate costs by discharging the expensive periods
- In combination with schedulable loads, the battery offers the optimisation algorithm more options to minimise electricity costs to the residence

This project is concerned with determining if the above techniques can make the battery storage economically viable. For relevant case studies in this project, a battery that has been assigned a maximum charge and discharge rate. Further investigation could consider the values of these variables to determine the exact economic impact thereof, i.e. how it impacts the economic feasibility. This requires careful modelling of the battery storage's utilisation factor function, and is beyond the scope of this study.

The investigation of the economic viability of the battery storage system will combine the investment costs and savings of both the combined battery and PV system. The battery storage affects the electricity cost calculations by changing the energy profile of the grid connection subsystem, as shown in (3.37), and repeated here to aid the discussion.

$$E_{Gk} = -(E_{PVk} + E_{LUk} + E_{LCk} + E_{Bk}) \quad k = 1, 2, 3 \cdots 48$$

The following equations demonstrate how the battery storage energy profile is included in subsystem energy calculations. The grid connection energy profile before the installation of the PV and battery energy systems can be determined from (3.109). The grid energy profile is determined by the loads in the residential energy system. This grid connection energy profile can be used to calculate the residence's electricity expenses before any investment is made into a PV or battery system.

$$E_{Gk} = -(E_{LUk} + E_{LCk}) \quad k = 1, 2, 3 \cdots 48 \tag{3.109}$$

The battery adapts the residential load profile to more effectively utilise the locally generated PV energy profile. The utilisation factor calculations should consider the battery's energy profile as well. Therefore the utilisation factor is calculated based on an intermediary energy profile E_{Rk} expressed in (3.110).

$$E_{Rk} = -(E_{LUk} + E_{LCk} + E_{Bk}) \quad k = 1, 2, 3 \cdots 48 \tag{3.110}$$

The utilisation factor can in this case not be used to calculate the payback period as used in (3.65) or derivations thereof. The assumption was that all the energy indicated by the utilisation function affected the energy exchanged with the grid, while now the utilisation function indicates the energy exchanged both with the grid and the battery storage.

The conclusion is that the addition of the battery storage system requires that the payback period for combined PV and battery systems should be calculated through the traditional equation as given in (3.44). The utilisation factor of PV will still be used to inspect the efficiency increase of the combined battery and PV system.

4 Program Structure

4.1 Introduction

The software application design is presented in this chapter. The mathematical models as given in Chapter 3 are implemented in software structures and integrated into a software application. An activity flow diagram and structure overview of each of the important software modules are given. The objective of the software application is to:

- Determine the energy flows between subsystem in the residential energy system, from which cost can be calculated.
- Calculate the payback time of the PV system.
- Analyse the results to determine cause-and-effect relationships between input and parameters and the results.
- Determine the optimal PV system rating with minimum payback time.

4.2 High-level software overview

The objective of this project is to identify the mathematical factors that influence the PV system payback period in a residential energy system and determine whether a PV system rating exists for which the payback period is a minimum. The software application makes a clear distinction between the two aspects of the objectives of this project:

- Analysis

  Investigate the payback time of the residential PV system as a function of the PV system rating. The focus is to verify the mathematical relationships established in Chapter 3 regarding the payback period of PV and battery systems. A typical set of input parameters therefore include the tariff structures, whether or not to optimise load schedules, and whether or not batteries are installed into the system.

- Optimisation

  For a given set of input parameters, determine whether the PV system rating with the minimum payback period can be found through optimisation.

Multiple case studies will be conducted to accomplish these objectives. The input parameters of initial case studies are simplified to establish simple cause-and-effect relationships between input parameters and results. One example of such a simplification is to use a repeated daily solar and load profile. Using the insight gained from analysing the results based on repeated daily profiles, the studies then proceed to use repeating annual profiles to understand payback time of real PV systems. The abovementioned distinctions give rise to 4 use cases for the software application as shown in Figure 4-1. The use cases are denoted as case A, B, C and D.

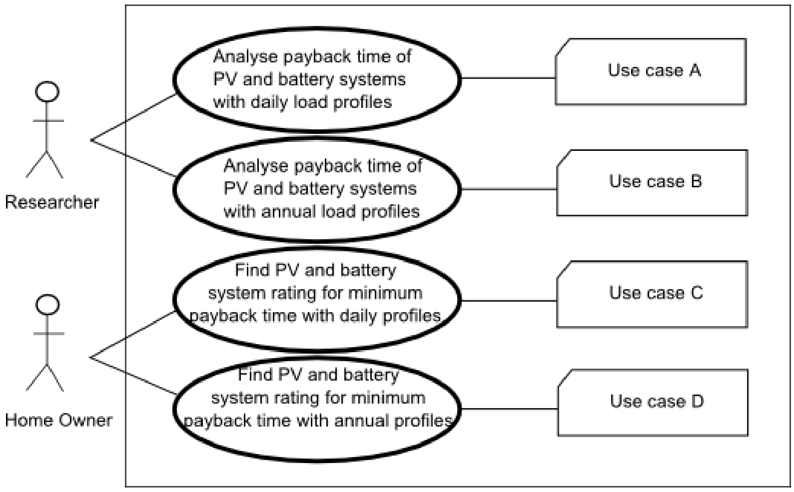

Figure 4-1 Use Case diagram of the residential energy system simulation software

All use cases require the calculation of electricity cost for the residential energy system. This leads to the opportunity to create a reusable code component. It's important to correctly identify which functionality can be reused, and clearly define it by stipulating the expected behaviour and an interface for the input and output parameters. This allows for well-defined and documented code, so it can be re-used in all use cases. To identify the reusable code components, the activity diagrams of all four use cases are presented in Figure 4-2. Each use case is discussed in detail in the relevant sections. From the activity diagrams, it's clear that the *Load schedule optimisation* and *Energy cost calculation* components would be reusable code components.

The following sections describe the software application design. The development environment options are considered in section 4.3. The software implementation of the schedulable load model is presented in section 4.4. The input parameters required to run the software application are shortly discussed in section 5. The design and documentation of the reusable code components, *Load schedule optimisation* and *Energy cost calculation*, is given in section 4.6. The software design for the analysis use cases (use case A and B) are documented in section 4.7. The software design for the optimisation use cases (use case C and D) are discussed in section 4.8. The sections thereafter describe the UI, database and hardware design.

Representations of the software design are given as diagrams in accordance with UML 2.0 specifications. UML 2.0 diagrams types that are used in this project include activity diagrams, class diagrams, component diagrams and deployment diagrams. Object orientated software design structures that are used in this project include interfaces, classes and subclasses.

4.3 **Development environment options**

The development environment for the software implementation of the mathematical model is first considered. An optimisation algorithm is required to find the minimum PV system payback period as a function of PV system rating. The mathematical model indicates that a pattern search optimisation would be appropriate for the optimisation algorithm. Matlab features a *Global optimisation package* that provides a pattern search optimisation. Preliminary development using the pattern search algorithm indicated successful optimisation to find the PV system rating with minimum payback time, even for separate tests for which the input parameters vary significantly. An active community as well as Matlab moderators are available online if support is required. Mathematically, Matlab has good single-row matrix (vector) support which is used extensively for the mathematical modelling. For the given reasons, Matlab was chosen as the environment in which to develop the software application.

The UI component of the application accepts the input parameters from the user. Delphi provides quick UI development capabilities and the ability to exchange information to and from Matlab through the command terminal. Delphi can connect to databases through database connection components. Results can be presented to through available prebuilt UI components such as graphs and text boxes.

The database had to be deployable to microcomputers such as the Raspberri Pi or BeagleBone Black. The database is implemented using a SQLite 3 database as this database format.

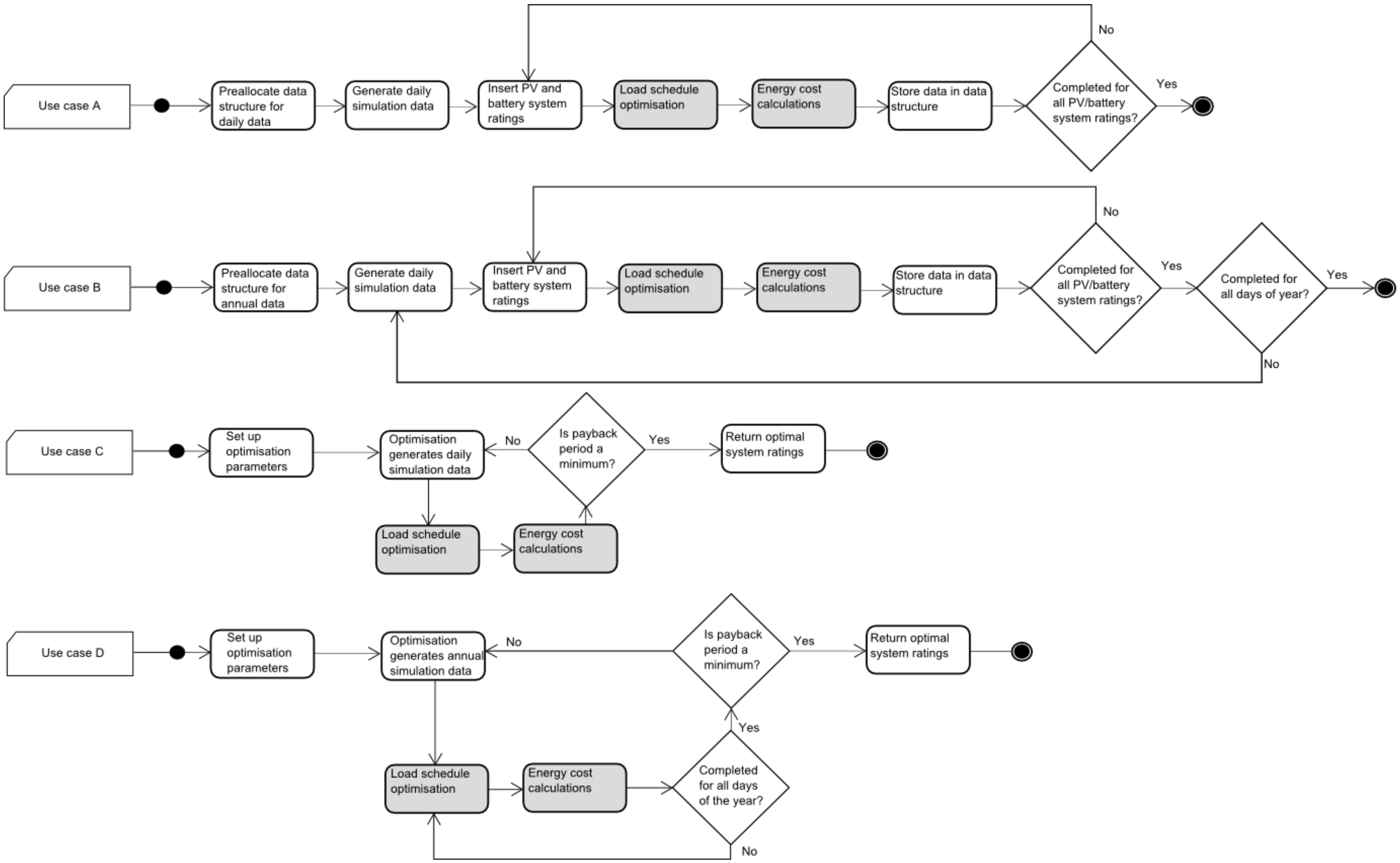

Figure 4-2 Activity Diagrams for the 4 use cases of the residential energy system simulation

4.4 Schedulable load model

This section gives the software implementation of the mathematical model of schedulable loads. The schedulable loads are mathematically defined in section 3.3.5. Each schedulable load has a power rating and a set of operation cycles. Each operation cycle is associated with a start time and duration. The schedulable loads are represented by the *SchedulableLoad* class, as given by the class diagram in Figure 4-3. A description of the class variables is given in Table 4.1. The load profile of a schedulable load is optimised by adjusting the start time of each operation cycle. This implies that the start times in the *startTimes* array of the *SchedulableLoad* class can each be adjusted by an optimisation, with consideration of the constraints imposed by the mathematical model.

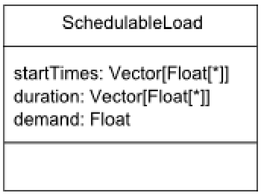

Figure 4-3 Class diagram for a Schedulable load

Table 4.1 Schedulable loads interface parameters

Input parameters	Description
startTimes	The start times of each operation cycle. Each entry associated with the same index entry in the duration vector.
duration	The duration of each operation cycle. Each entry associated with the same index entry in the startTimes vector.
demand	The power rating of the schedulable load

4.5 Residential energy system simulation input parameters

The different use cases as depicted in Figure 4-1 imply that the software application will accept different input parameters depending on the use case. The input parameters for each use case are stipulated by an interface. A set of input parameters exists that is relevant to all of the use cases. These input parameters are given by a common interface and is given in Figure 4-4 as the *SimulationInput* interface. A set of input parameters only relevant to respectively the analysis and optimisation use cases is defined in the *AnalysisSimulation* and *OptimsationSimulation* interfaces. These interfaces are shown to be subclasses to the *SimulationInput* in Figure 4-4. The interfaces of input parameters required for the 4 different use cases are shown in Figure 4-4 but are discussed in more detail in their associated sections. A description of each of the parameters on the *SimulationInput* interface is given in Table 4.2.

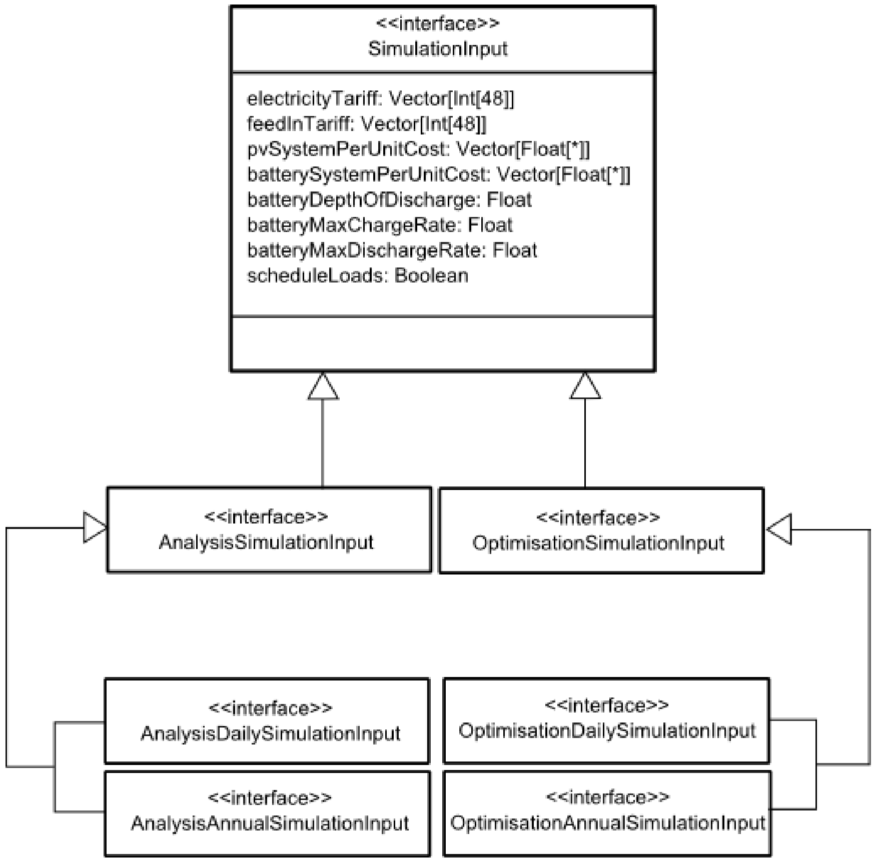

Figure 4-4 Class diagram defining inputs to the residential energy system simulation

Table 4.2 Input parameter description of *SimulationInput* interface

Input parameters	Description
electricityTariff	The electricity consumption tariff for each half-hour
feedInTariff	The electricity feed-in tariff for each half-hour
pvSystemPerUnitCost	The per-watt cost. The number of elements specifies the order of the cost function. Elements give coefficients of equation in decreasing power.
batterySystemPerUnitCost	The per-watthour cost. The number of elements specifies the order of the cost function. Elements give coefficients of equation in decreasing power.
batteryDepthOfDischarge	The depth-of-discharged allowed for the battery bank
batteryMaxChargeRate	The maximum charge rate of the battery specified as the C-rating fraction
batteryMaxDischargeRate	The maximum discharge rate of the battery specified as the C-rating fraction
scheduleLoads	A Boolean value to specify whether load schedule optimisation should be applied to the schedulable load profiles. A value of true stipulates that the load schedule optimisation should be applied.

4.6 Software structure design of *Load schedule optimisation* and *Energy cost calculation* components

4.6.1 Logic flow design

The function of the *Load schedule optimisation* component is to optimise the load schedules of schedulable loads, if it is so specified in the input parameters. If a battery is included in the system, the battery's charge/discharge schedule is optimised to minimise the electricity expenses of the residential energy system. The function of the *Energy cost calculation* component is to calculate the energy costs of a residential energy system for a single day.

Both components are dependent on whether a battery is installed in the energy system and whether load schedule optimisation is applied. These two factors are supplied along with the input parameters and act as logic inputs, as shown in Table 4.3. Since both components need to determine whether a battery is present and whether load optimisation should be optimised, it will be advantageous if this can be determine only once. Considering that the functionality of these two components is coupled in all use cases, the two components were combined to form a *Load schedule optimisation and cost calculation* component.

Table 4.3 Different configurations of a residential energy system

Optimise Load Schedules	Battery rating nonzero	Situation
False	False	The battery rating is zero and no load optimisation is required. This leads to a straightforward calculation of the cost savings produced by the PV system.
False	True	The battery rating is nonzero, so the battery charge/discharge profile should be optimised. No load schedule optimisation.
True	False	The battery rating is zero, but the schedules of the schedulable loads should be optimised.
True	True	The battery rating is nonzero, implying that the charge/discharge profile should be optimised. Additionally the schedules of the schedulable loads should be optimised.

The logic of the *Load schedule optimisation and cost calculation* component is given in the activity diagram in Figure 4-5. Four different control flow branches exist based on the four conditions as set out in Table 4.3. The appropriate branch is selected based on the input parameters provided. If the input parameters specify that the schedulable load profiles should be optimised, the starting times of the schedulable loads are adjusted to minimise the electricity cost of the client. If a battery rating is given in the input parameters, it implies that a battery is present. The charge/discharge profile of the battery will then be optimised to minimise payback time. It is assumed that the input parameters to do this optimisation (such as depth of discharge and charge/discharge limits) are provided. The software application is limited to a maximum of two schedulable loads. This provides the necessary software structure to explore the effect of battery storage and schedulable loads on the payback period of PV and battery storage systems.

Once the necessary load schedule and battery profile optimisations are completed, energy flow and cost associated therewith can be determined. Using the electricity consumption and feed-in tariffs, the cost of electricity for the day is calculated. If the input requested load schedule optimisation, the optimised load schedule is included in the results. If the inputs specified that a battery is present in the energy system, the battery's charge/discharge energy profile is included in the results.

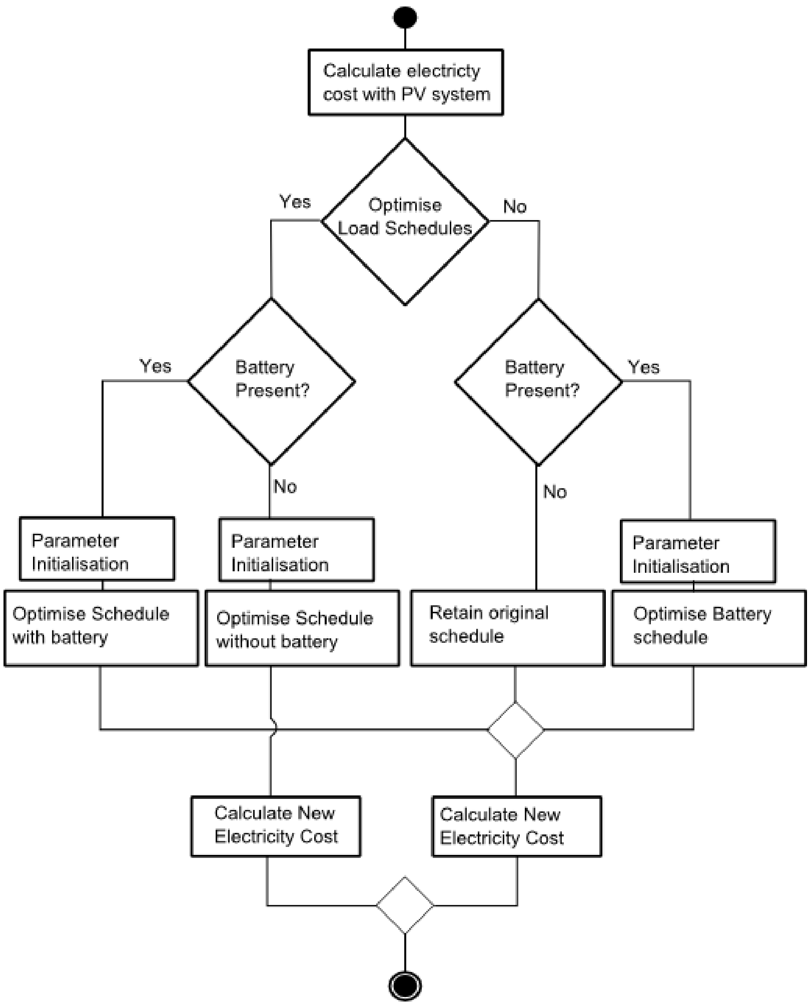

Figure 4-5 Activity diagram for *Load schedule optimisation and cost calculation* component.

4.6.2 Input and output interface

The interface design for the *Load schedule optimisation and cost calculation* component is given in Figure 4-6. The inputs are specified by the *DailyParameters* interface. A description of the input parameters is given in Table 4.1.

The output that the component should provide is specified by the *DailyPerformanceResults* interface as given in Figure 4-6. More details on the variable names are provided in Table 4.5. Preliminary analysis of the results from residences showed that it's insightful to understand the savings achieved by installing the PV system before the optimisation, and the amount that is additionally saved from load schedule and battery optimisation. Therefore the output provides both these parameters.

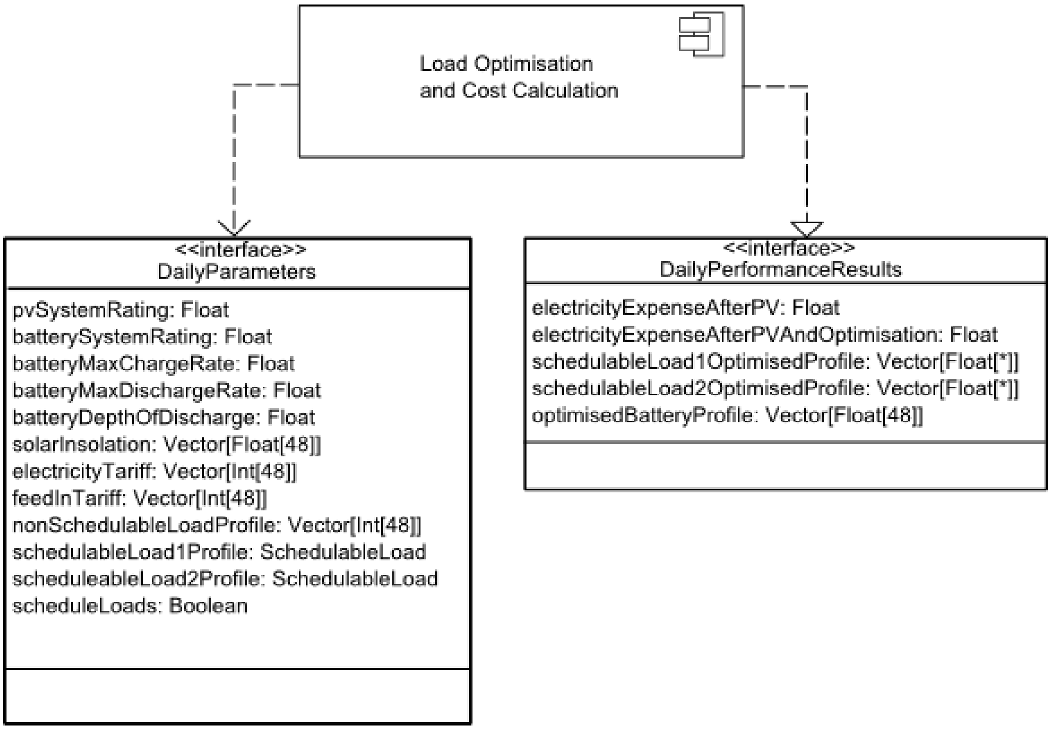

Figure 4-6 Component diagram for the *Load schedule optimisation and cost calculation* component

Table 4.4 Input interface parameters description for *Load schedule optimisation and cost calculation* component

Input parameter	Description
pvSystemRating	The rating of the PV system in the residential energy system
batterySystemRating	The rating of the battery storage in the residential energy system
batterymaxChargeRate	The maximum charge rate of the battery specified as the C-rating fraction
batteryMaxDischargeRate	The maximum discharge rate of the battery specified as the C-rating fraction
batteryDepthOfDischarge	The depth-of-discharged allowed for the battery bank
solarInsolation	Daily solar energy, normalised to energy received by 1 kW PV system
electricityTariff	The electricity consumption tariff for each half-hour
feedInTariff	The electricity feed-in tariff for each half-hour
nonSchedulableLoadProfile	The load profile of the non-schedulable loads
schedulableLoad1Profile, schedulableLoad2Profile	Two objects of the SchedulableLoad class with the necessary information to model schedulable loads and their associated operation cycles
scheduleLoads	A Boolean value to specify whether load schedule optimisation should be applied to the schedulable load profiles. A value of true stipulates that the load schedule optimisation should be applied.

Table 4.5 Results interface for the *Load schedule optimisation and cost calculation* component

Output parameter	Description
electricityExpenseAfterPv	The electricity expense after a PV system is installed in the residential energy system
electricityExpenseAfterPvAnd-Optimisation	The electricity expenses after a PV system is installed and the load and battery profile optimisation in the residential energy system
schedulableLoad1Optimised-LoadProfile, schedulableLoad2Optimised-LoadProfile	The optimised start times of the schedulable load operation cycles.
optimisedBatteryProfile	The charge and discharge profile of the battery

4.7 Software structure design for analysis of PV and battery system payback time

4.7.1 Overview

The objective of the analysis use case in this software application is to inspect the payback periods over a range of PV and battery system ratings. For each PV/battery system rating combination, a simulation of the residential energy system is done to determine the performance and payback period of the PV and battery storage subsystems. The results are stored in a data structure, from where an interpretation API is used to explore relationships between the input parameters and results. The analysis is either done with repeated daily profiles or repeated annual profiles, depending on the use case. The software design for these respective use cases is different, considering that different input parameters and different results data structures are used. The design and definition of the repeated daily profile optimisation is given in section 4.7.2 and of the repeated annual profiles optimisation is given in section 4.7.3.

A common set of input parameters for the analysis case studies are defined in the *AnalysisSimulationInput* interface as given in Figure 4-7. A short description of the variables in the interface is provided in Table 4.6. The input parameters, two vectors respectively for the PV and battery subsystems, specify the ratings at which the payback period should be calculate. These vectors are used to calculate a matrix of all possible PV/battery system combinations.

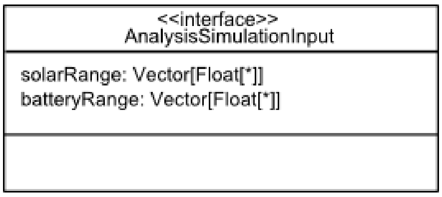

Figure 4-7 The class diagram define input parameters required for analysis simulations

Table 4.6 Input interface parameter descriptions for *AnalysisSimulationInput*

Input parameter	Description
solarRange	A vector of PV system ratings for which the residential energy systems is simulated.
batteryRange	A vector of battery system ratings for which the residential energy systems is simulated.

4.7.2 Residential energy system simulation with daily repeated profiles

The input to the daily analysis use case is defined by a subclass of the *SimulationInput* and *AnalysisSimulationInput* interfaces. The final properties required for this case study is given in the *AnalysisAnnualSimulationInput* interface as shown in Figure 4-8. A short description of the variables of the *AnalysisAnnualSimulationInput* is given in Table 4.7. The input parameters give the daily non-schedulable load profile, the schedulable load profiles and the solar profile. This defines the complete set of input parameters for this use case.

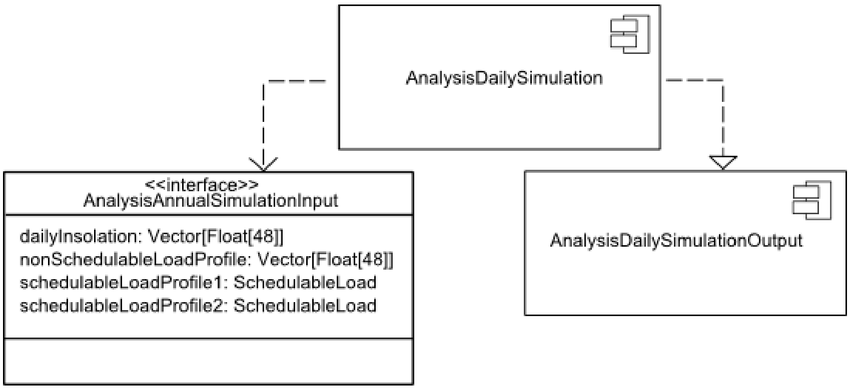

Figure 4-8 Component diagram indicating inputs and outputs for system rating optimisation with repeated daily profiles

Table 4.7 Input interface parameters description for *AnalyisDailySimulationInput*

Input parameter	Description
dailyInsolation	Daily solar energy, normalised to energy received by 1 kW PV system
nonSchedulableLoadProfile	Daily load profile of non-schedulable loads
schedulableLoadProfile1, schedulableLoadProfile2	Two objects of the SchedulableLoad class with the necessary information to model schedulable loads the their associated operation cycles

When the software application is run with this set of input parameters, the actions as set out for use case A in the activity diagram in Figure 4-2 is executed. The residential energy system is constructed with the load profiles as required. A matrix is created for each PV/battery system combination for which the payback period should be calculated. For each PV/battery system combination, a residential energy system is created with the associated rated PV and battery systems. For each PV/battery system combination, the residential energy system simulation is run to calculate the energy flow between the different subsystems. When the simulation is completed, the electricity costs associated with the grid connection subsystem is calculated. The final calculation determines the payback time. All the results of the simulation and cost calculations are then exported to the data structure *AnalysisDailySimulationOutput* component from Figure 4-8. The simulation completes when the cost calculations for every PV/battery system combination has been completed.

The internal structure of the *AnalysisDailySimulationOutput* component is given in Figure 4-9. The data structure is the only data persistently stored after the simulation and therefore contains all necessary details of the simulation, including the input parameters. Parameters that are applicable to the simulation are stored in the *SystemResults* class. A description of each of the variables is provided in Table 4.8. Results of each PV/battery system combination are stored in an *IterationDailyResults* class. These results include the payback period and utilisation factor function of the associated with the PV/battery system combination. A short description of each of these variables is given in Table 4.9.

An extensive API has been written to access this data structure and interpret the simulation results. The data is then presented in most cases graphical form for easy inspection.

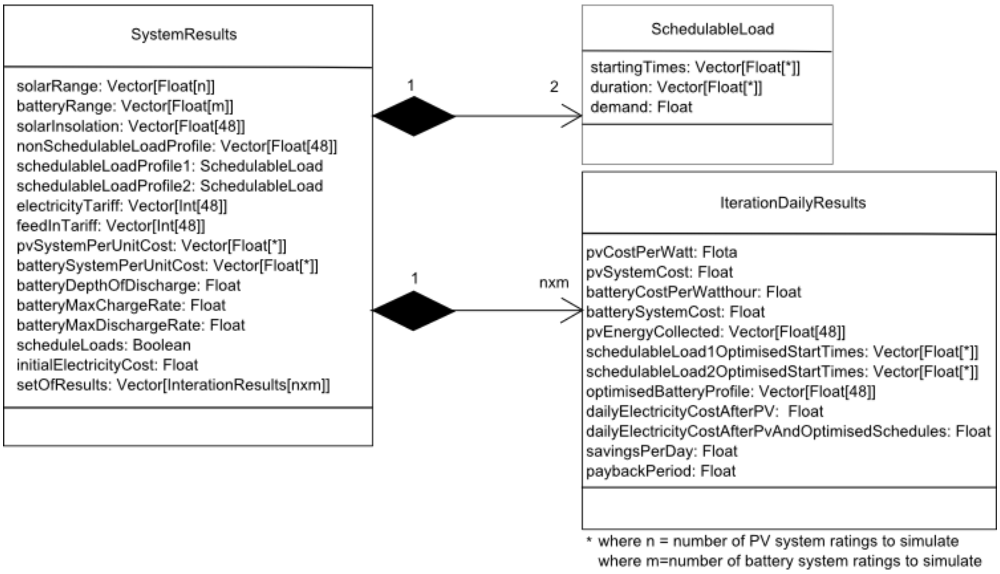

Figure 4-9 Class diagram of the data structure component *AnalysisDailySimulationOutput*

Table 4.8 *SystemResults* parameter descriptions

Parameter	Description
solarInsolation	Daily solar energy, normalised to energy received by 1 kW PV system
nonSchedulableLoadProfile	Daily load profile of non-schedulable loads
schedulableLoadProfile1, schedulableLoadProfile2	Two objects of the SchedulableLoad class with the necessary information to model schedulable loads the their associated operation cycles
electricityTariff	The electricity consumption tariff for each half-hour
feedInTariff	The electricity feed-in tariff for each half-hour
pvSystemPerUnitCost	The per-watt cost. The number of elements specifies the order of the cost function. Elements give coefficients of equation in decreasing power.
batterySystemPerUnitCost	The per-watthour cost. The number of elements specifies the order of the cost function. Elements give coefficients of equation in decreasing power.
batteryDepthOfDischarge	The depth-of-discharged allowed for the battery bank
batterymaxChargeRate	The maximum charge rate of the battery specified as the C-rating fraction
batteryMaxDischargeRate	The maximum discharge rate of the battery specified as the C-rating fraction
scheduleLoads	A Boolean value to specify whether load schedule optimisation should be applied to the schedulable load profiles. A value of true stipulates that the load schedule optimisation should be applied.
initialElectricityCost	The electricity expense before any PV or battery system is installed into the residential energy system
setOfResults	A matrix that contains the results of each PV and battery rating system combination. The result of each PV and battery system rating combination is stored in an object based on the IterationResults class.

Table 4.9 *IterationDailyResults* parameters description

Parameter	Description
pvCostPerWatt	The per-unit cost of the PV system based on the associated PV system rating.
pvSystemCost	The total cost of the PV system based on the associated PV system rating.
batteryCostPerWatthour	The per-unit cost of the battery storage based on the associated battery system rating.
batterySystemCost	The total cost of the battery storage based on the associated battery system rating.
pvEnergyCollected	The energy profile providing the energy provided by the PV system
schedulableLoad1OptimisedStartTimes, schedulableLoad2OptimisedStartTimes	An array containing the optimised start times of the schedulable loads
optimisedBatteryProfile	The optimised charge/discharge profile of the battery for each half-hour during the day
dailyElectricityCostAfterPv	Electricity expense after only applying PV, before applying the effects of load schedule and battery optimisation
dailyElectricityCostAfterPvAndOptimisedSchedules	Electricity expense after applying PV and battery and load schedule optimisation
savingsPerDay	The savings achieved by installing PV and optimising load schedules and the battery profile.
paybackPeriod	The payback period of the associated PV and battery system

4.7.3 Residential energy system simulation with annual repeated profiles

The input interface to this simulation inherits the input parameters stipulated from the discussed *SimulationInput* and *AnalysisSimulation* interfaces as shown in Figure 4-4 and Figure 4-7. The input interface for the annual repeated profiles is stipulated in the *AnalysisAnnualSimulationInput* as shown in Figure 4-10. A short description of the variables are given in Table 4.10. It is shown that an annual load profile and solar profile is required for this simulation.

When the software application is run with this set of input parameters, the actions as set out for use case B in the activity diagram in Figure 4-2 is executed. The residential energy system is constructed with the annual load profiles and annual solar profile. A matrix is created for each PV/battery system combination for which the payback period should be calculated. For each day of the year, the residential energy system is simulated for each PV/battery system combination. For each of the PV/battery system combinations, the residential energy system simulation is run to calculate the energy flow between the different subsystems. When the simulation is completed, the electricity costs associated with the grid connection subsystem is calculated. When all PV/battery system combinations have been completed for a single day, the process is repeated for the next day. This continues until the results for 365 days of the year have been considered. The payback period for each PV/battery system combination is then calculated by iterating over the results for each of the 365 days.

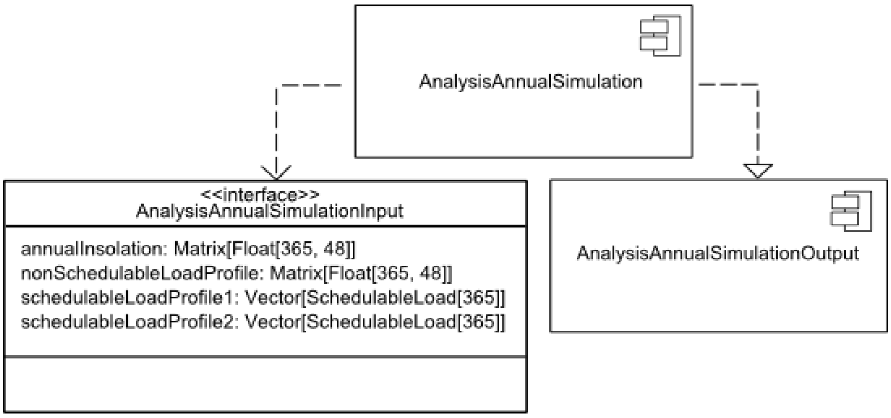

Figure 4-10 Component diagram indicating inputs and outputs for system rating optimisation with repeated annual profiles

Table 4.10 Input interface parameters description for *AnalyisAnnualSimulationInput*

Input parameter	Description
annualInsolation	Annual solar energy, normalised to energy received by 1 kW PV system
nonSchedulableLoadProfile	A matrix containing a daily load profile for each day of the year
schedulableLoadProfile1, schedulableLoadProfile2	Each schedulable load profile is given by a vector of daily schedule for each day of the year.

All the results of the simulation and cost calculations are exported to the data structure *AnalysisAnnualSimulationOutput* as shown in Figure 4-10. The internal structure of the *AnalysisDailySimulationOutput* component is given in Figure 4-11. The data structure is the only persistent data stored after the simulation and therefore contains all details of the simulation, including the input parameters. Parameters that are applicable to the simulation are stored in the *SystemResults* class. A description of each of the variable in this class is provided in Table 4.11. The set of results containing the payback period of each PV/battery system combination is also kept in this class. The total set of results for each day is contained in the *DailyResults* class. A description of each of the variables in this class is given in Table

4.12. Results of each PV/battery system combination for an associated day are stored in the *IterationAnnualResults* class. The variable descriptions for the *IterationAnnualResults* class are the same as given for the *IterationDailyResults* in Table 4.9.

The extent of this annual profile simulation is greater than that of the daily profile simulation, as the performance for 365 days are evaluated. In the case where the battery or profiles of the schedulable loads require optimisation, this script needs to optimise 365 problems. This requires many hours of simulation, which is one reason the repeated daily profiles are initially used to explore relationships between input parameters and the results.

An extensive API has been written that accesses the annual result's data structure and interprets the simulation results. The data is then presented in most cases graphical form for easy inspection.

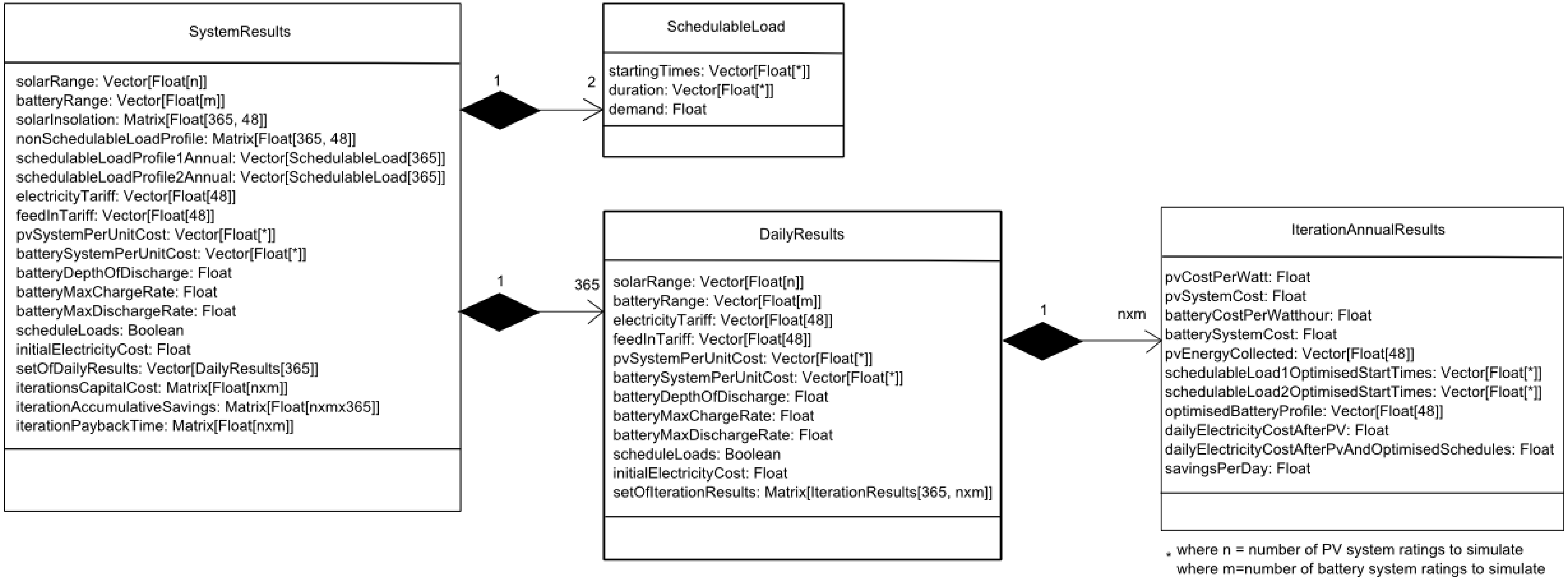

Figure 4-11 Class diagram of the data structure used to hold to results of the *AnnualAnalysisSimulationScript*

Table 4.11 *SystemResults* variable descriptions

Parameter	Description
solarRange	A vector of PV system ratings for which the residential energy systems is simulated.
batteryRange	A vector of battery system ratings for which the residential energy systems is simulated.
solarInsolation	Annual solar energy, normalised to energy received by 1 kW PV system
nonSchedulableLoadProfile	A matrix containing a daily load profile for each day of the year
schedulableLoadProfile1, schedulableLoadProfile2	Each schedulable load profile is given by a vector of daily schedule for each day of the year.
electricityTariff	The electricity consumption tariff for each half-hour
feedInTariff	The electricity feed-in tariff for each half-hour
pvSystemPerUnitCost	The per-watt cost. The number of elements specifies the order of the cost function. Elements give coefficients of equation in decreasing power.
batterySystemPerUnitCost	The per-watthour cost. The number of elements specifies the order of the cost function. Elements give coefficients of equation in decreasing power.
batteryDepthOfDischarge	The depth-of-discharged allowed for the battery bank
batterymaxChargeRate	The maximum charge rate of the battery specified as the C-rating fraction
batteryMaxDischargeRate	The maximum discharge rate of the battery specified as the C-rating fraction
scheduleLoads	A Boolean value to specify whether load schedule optimisation should be applied to the schedulable load profiles. A value of true stipulates that the load schedule optimisation should be applied.
initialElectricityCost	The electricity expense before any PV or battery system is installed into the residential energy system
setOfDailyResults	The simulation results for every day of the year.
iterationCapitalCost	A set containing total purchase cost for each battery and PV system rating combination
iterationAccumalativeSavings	A set containing accumulative daily savings for each battery and PV system rating combination
iterationPaybackTime	A set containing payback time for each battery and PV system rating combination

Table 4.12 ***DailyResults*** **variable descriptions**

Parameter	Description
solarRange	A vector of PV system ratings for which the residential energy systems is simulated.
batteryRange	A vector of battery system ratings for which the residential energy systems is simulated.
solarInsolation	Daily solar energy, normalised to energy received by 1 kW PV system
electricityTariff	The electricity consumption tariff for each half-hour
feedInTariff	The electricity feed-in tariff for each half-hour
pvSystemPerUnitCost	The per-watt cost. The number of elements specifies the order of the cost function. Elements give coefficients of equation in decreasing power.
batterySystemPerUnitCost	The per-watthour cost. The number of elements specifies the order of the cost function. Elements give coefficients of equation in decreasing power.
batteryDepthOfDischarge	The depth-of-discharged allowed for the battery bank
batterymaxChargeRate	The maximum charge rate of the battery specified as the C-rating fraction
batteryMaxDischargeRate	The maximum discharge rate of the battery specified as the C-rating fraction
scheduleLoads	A Boolean value to specify whether load schedule optimisation should be applied to the schedulable load profiles. A value of true stipulates that the load schedule optimisation should be applied.
initialElectricityCost	The electricity expense before any PV or battery system is installed into the residential energy system
setOfIterationResults	A matrix that contains the results of each PV and battery rating system combination. The result of each PV and battery system rating combination is stored in an object based on the IterationResults class.

4.8 Software structure design for optimisation of PV and battery system payback time

4.8.1 Overview

The goal of this optimisation is to determine, given the necessary inputs, which PV system rating and battery system rating, constrained to given ranges, would result in the minimum payback time. A set of configurations is supplied to the optimisation. The configuration parameters assist to find the optimal point accurately while searching through a minimal number of PV and battery system combinations. The optimisation is either done with repeated daily profiles or repeated annual profiles, depending on the use case. The software design for these respective use cases is different as different input parameters and control logic is used for the respective optimisations. The design and definition of the repeated daily profile optimisation is given in section 4.8.2 and of the repeated annual profiles optimisation is given in section 4.8.3.

A common set of input parameters for the optimisation case studies are defined in the *OptimisationSimulationInput* interface as given in Figure 4-12. The input parameters of the optimisations are scalar values. These parameters provide the upper and lower boundaries of the optimisation, and the initial ratings which the optimisation will optimise. A short description of the variables in the interface is provided in Table 4.13.

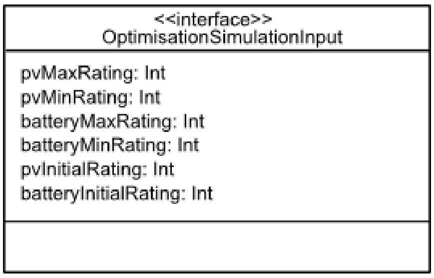

Figure 4-12 The class diagram define input parameters required for optimisation simulations

Table 4.13 Input interface parameters description for *OptimisationSimulationInput*

Input parameter	Description
pvMaxRating	The upper limit for the PV system rating optimisation
pvMinRating	The lower limit for the PV system rating optimisation
batteryMaxRating	The upper limit for the battery system rating optimisation
batteryMinRating	The lower limit for the battery system rating optimisation
pvInitialRating	The initial value for the PV system rating. This is required by the optimisation.
batteryInitialRating	The initial value for the PV system rating. This is required by the optimisation.

4.8.2 **Residential energy system simulation with daily repeated profiles**

The optimisation takes the required parameters to calculate the payback time of a PV and battery system. It is assumed that the load and solar profile is repeated for each day. The lower and upper bounds of the optimisation is provided as part of the input. The optimisation requires an initial value for the parameters to the optimised, which is also provided as part of the input. The component diagram in Figure 4-13 shows the interfaces for the input parameters and results. A description of what the variable names represent is given for the input parameters in Table 4.14 and for the results in Table 4.15.

When the software application is run with this set of input parameters, the actions as set out in Figure 4-2 for use case C is executed. The optimisation algorithm is configured based on the input parameters as provided. This sets the constraints by which the optimisation is bound, the initial value of the optimisation, etc. The optimisation then executes. The optimisation adjusts the rating of the PV system optionally the battery storage. The load schedule optimisation is performed if so specified by the input parameters. The cost of energy for the day is found. Since the load and PV energy profile is repeated, the cost of energy for the single day can be used to determine the payback period of the PV and battery system. The optimisation determines whether the payback period is a minimum value. If not, another iteration with an adjusted PV and battery system rating is performed. Once the optimisation determines that the minimum payback period has been found, the optimisation concludes by outputting the results as givenin the *OptimisationDailySimulationOutput* interface.

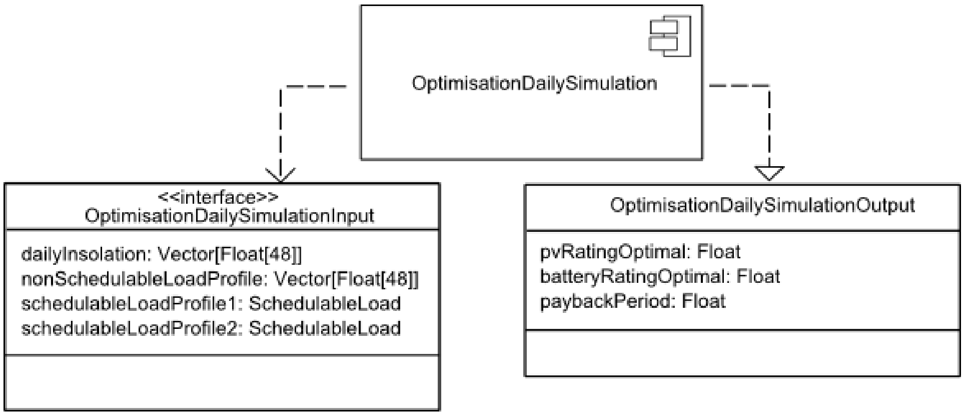

Figure 4-13 Component diagram indicating inputs and outputs for system rating optimisation with a daily timeline

Table 4.14 Input interface parameters description for *OptimisationDailySimulation*

Input parameter	Description
dailyInsolation	Daily solar energy, normalised to energy received by 1 kW PV system
nonSchedulableLoadProfile	A matrix containing a daily load profile for each day of the year
schedulableLoadProfile1, schedulableLoadProfile2	Two objects of the SchedulableLoad class with the necessary information to model schedulable loads the their associated operation cycles

Table 4.15 Results interface parameters description for *OptimisationDailySimulation*

Results parameter	Description
pvRatingOptimal	The rating of the PV system for which the payback time is a minimum
batteryRatingOptimal	The rating of the battery system for which the payback time is a minimum
paybackPeriod	The payback period of the PV and battery systems installed into the residential energy system.

4.8.3 Residential energy system simulation with annual repeated profiles

This optimisation takes the required parameters to calculate the payback time of a PV and battery system, given an annual load and solar profile. The component diagram in Figure 4-14 shows the interfaces of the input and results. A description of what the variable names represent is given for the input parameters in Table 4.16 and for the results parameters in Table 4.17. The lower and upper bounds of the optimisation is provided as part of the input. The optimisation requires an initial value for the parameters to the optimised, which is also provided as part of the input.

When the software application is run with this set of input parameters, the actions as set out for use case D in the activity diagram given in Figure 4-2 is executed. The optimisation algorithm is configured based on the input parameters. This sets the constraints by which the optimisation is bound, the initial value of the optimisation, etc. The input parameters specify annual load and PV energy profiles. The load schedule optimisation and energy cost calculation is performed for every day of the year, to determine annual energy cost. Based on the annual energy cost, the payback period of the PV and optional battery system is found. The optimisation determines whether the payback period is a minimum value. If not, another iteration with an adjusted PV and battery system rating is performed. Once the optimisation determines that the minimum payback period has been found, the results of the optimisation are provided in the output interface.

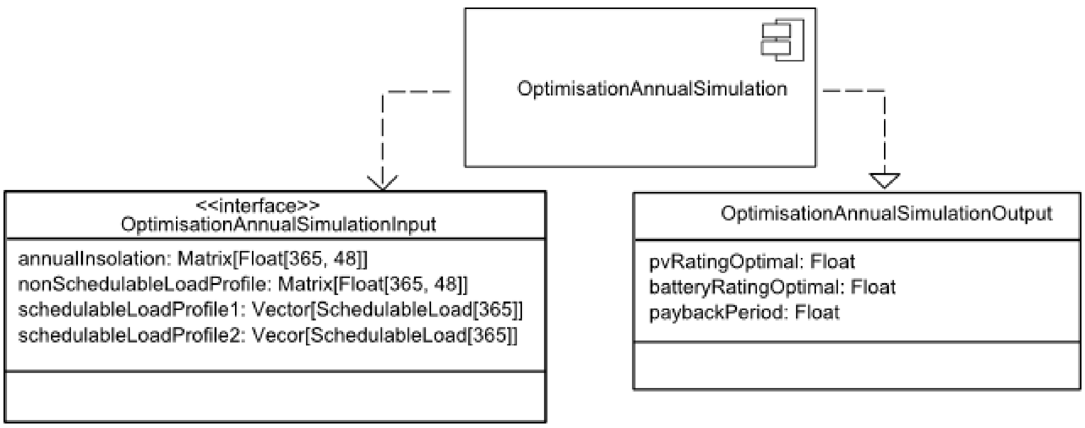

Figure 4-14 Component Diagram indicating inputs and outputs for system rating optimisation with a daily timeline

Table 4.16 Input interface parameters description for *OptimisationAnnualSimulation*

Input parameter	Description
annualInsolation	Annual solar energy, normalised to energy received by 1 kW PV system
nonSchedulableLoadProfile	A matrix containing a daily load profile for each day of the year
schedulableLoadProfile1, schedulableLoadProfile2	Each schedulable load profile is given by a vector of daily schedule for each day of the year.

Table 4.17 Results interface parameters description for *OptimisationDailySimulation*

Results parameter	Description
pvRatingOptimal	The rating of the PV system for which the payback time is a minimum
batteryRatingOptimal	The rating of the battery system for which the payback time is a minimum
paybackPeriod	The payback period of the PV and battery systems installed into the residential energy system.

4.9 Database design

The load data for is captured in a database, which lists typical load use schedules for the residence from this list. Storing this data in a database required denormalisation of the data. Denormalisation of the data showed that two tables would be required to represent the data.

The first table, titled *Loads*, contain the list of loads in the residence. The table qualifies each load with regards to the rated power use, typical duty cycle, and whether the load is schedulable. The header column of this table is indicated in Table 4.18.

Table 4.18 Column headers for the *Loads* specification table in the database

LoadId	Designation	Rating	DutyCycle	Schedulable

The second table, titled *LoadSchedules*, contain the schedules of typical operational times expected for each of the loads. Each schedule references the specific *LoadId* as specified in the *Loads* table. The structure of the database allows for multiple operational periods for each of the loads. The header column of this table in indicated in Table 4.19.

Table 4.19 Column headers for the *LoadSchedules* table in the database

ScheduleId	Description	StartTime	EndTime	LoadId

Due to different needs during the development of the software application, scripts have been written both in Delphi and Python to interpret the data and convert it to usable load profiles. The output of the scripts are a 48-element vector that indicates the energy used during each averaging period throughout a 24 hour period

4.10 Software deployment architecture

This section presents the overall application architecture, indicating clearly how the use cases for this software application is achieved by combining a user interface, mathematical operations and persistent storage on database. A deployment diagram is used to present how the various components work together to achieve this software application. The deployment diagram in Figure 4-15 show how various programs were more fitted for specific purposes in satisfying the use cases for this software application.

The Optimise.exe is the Windows application written in Delphi. This application accepts the input form the user, relays this information to a Matlab script for the mathematical processing, and displays the returned result to the user. A preliminary interface design for this application is shown in Figure 4-16.

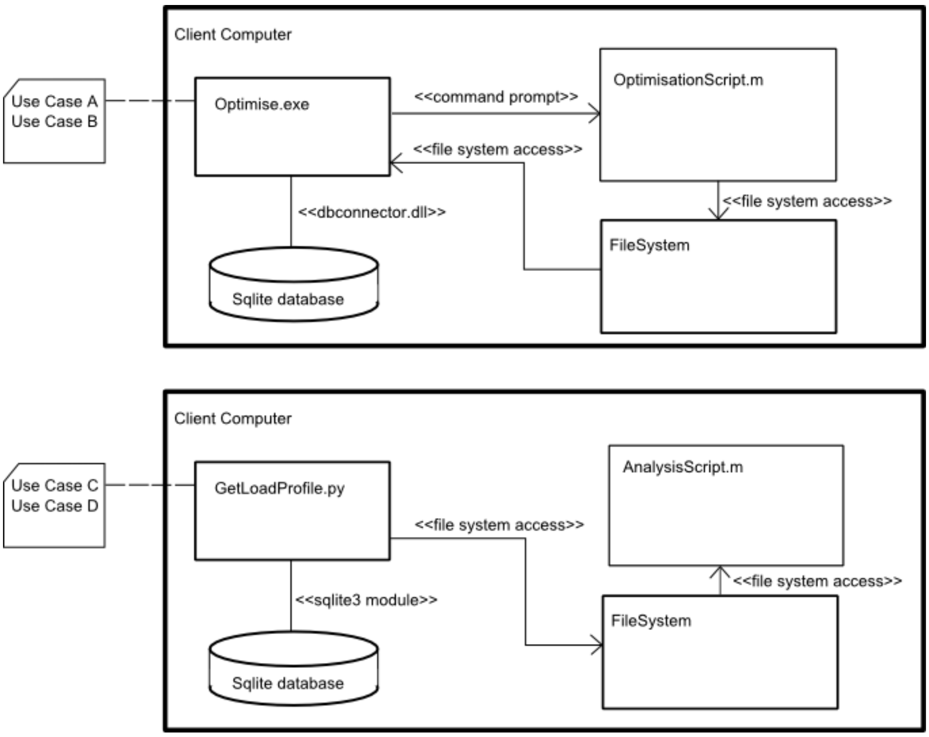

Figure 4-15 A deployment diagram showing how the various components achieve the use cases

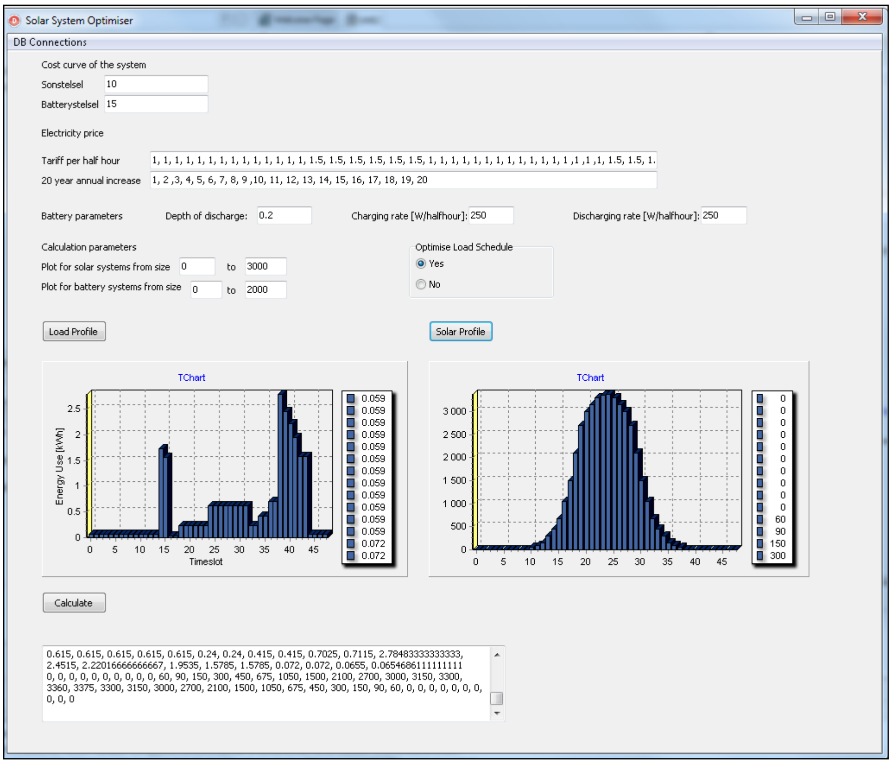

Figure 4-16 Preliminary user interface design which returns the optimal PV and battery system rating for a residence

4.11 **Hardware design**

4.11.1 **Overview**

The use of schedulable loads necessitates the need for load switching hardware. This hardware can be built into the load, or be controlled via external hardware. A feasible method of communicating optimised load schedules to schedulable loads is to have a central controller optimise the loads, and relay the necessary information wirelessly to the loads in the residence. This section aims to build the necessary hardware for this implementation.

4.11.2 **Architecture**

From previous work, the architecture in Figure 4-17 has been chosen to switch controllable loads. A Matlab environment allows for optimisation of schedulable loads. The optimised schedules are written to a Beaglebone Black microcomputer. The microcomputer wirelessly communicates with remote switches to switch schedulable loads. In previous word, remote switches simply switched LED’s to demonstrate load switching capability. Communication with real loads would require a more robust design, implementing current isolation between the 3,3 V Xbee output and load voltage. Referring to Figure 4-17, this implies the design of and insolation interface where the Xbee module interacts with schedulable loads through general purpose input/output (GPIO) pins.

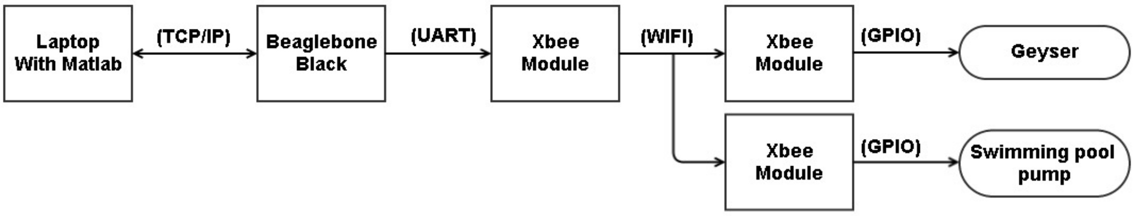

Figure 4-17 Architecture for schedule optimisation and control signal communication to loads

4.11.3 **Design**

A circuit board was designed and built to host the Xbee modules, and provide power to the components. The circuit board required a 2 layer design, as indicated in Figure 4-18 and Figure 4-19. The power supply to the circuit board is supplied by a 5 V input or a battery. This provides the necessary power for the Xbee, allowing it to listen for signals. The Xbee has a non-standard 2 mm pin spacing, which is broken out to the standard 2,14 mm ping spacing on the bottom layer (Figure 4-19). Two of the pins lead to two separate output screw terminals. These two output pins have been designed to have electric isolation from the output. For the first pin, this was achieved using an optocoupler. The second pin achieves the same electrical isolation with a reed relay.

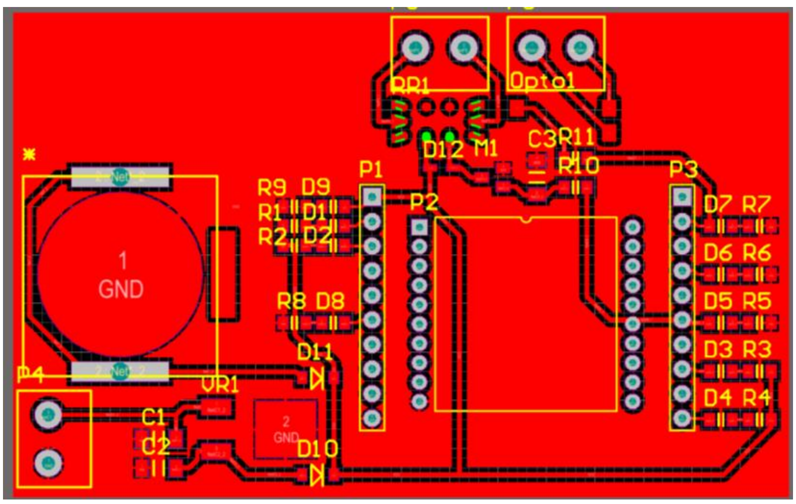

Figure 4-18 Top layer of the signal receiver circuit board

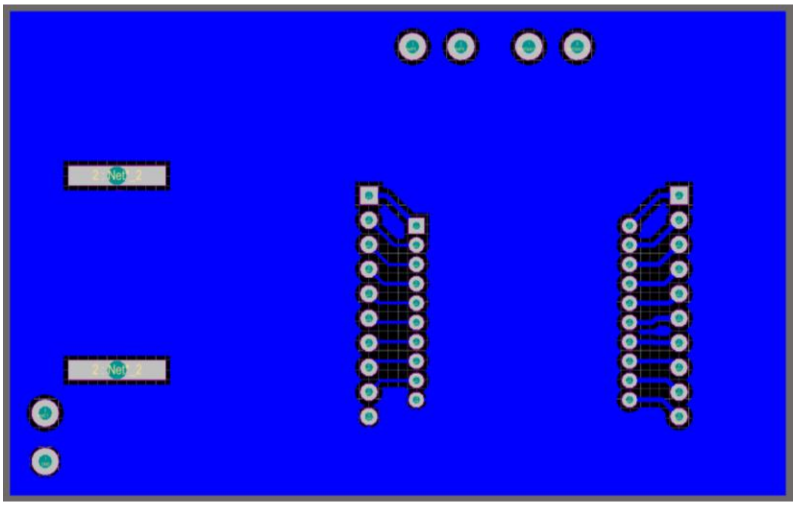

Figure 4-19 Bottom layer of the signal receiver circuit board

The hardware as designed allows for the successful relaying of control messages to schedulable devices. The manufactured prototype is shown in Figure 4-20. The handling of the control signals is device-dependent. Commercial implementations that allow for controlling loads, built by manufacturers such as SMA, is becoming viable methods for non-technical residents to have schedulable loads in their residence.

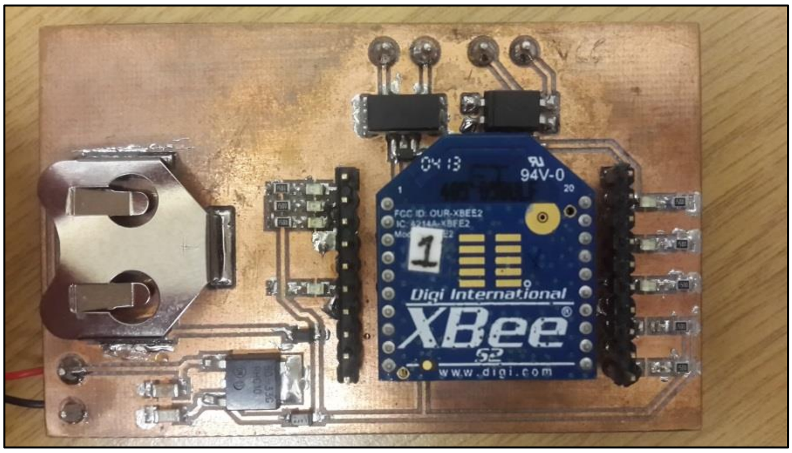

Figure 4-20 The manufactured prototype of the hardware used to switch loads

5 Case studies, parameter effects and results

5.1 Overview

Two sets of case studies are presented. The first set of case studies is exploratory, with the goal to determine confirm cause-and-effect relationships between input parameters and the results as mathematically established in chapter 3. The input parameters are chosen to be realistic, but simple. The second set of case studies use input parameters based on real measured values. The second set of case studies demonstrates the practical application of the findings presented in this project.

5.2 Case study set 1

5.2.1 Introduction

This set of case studies use different input parameters and presents the typical outputs that can be expected. The objectives of this set of case studies are the following:

- To observe results for the simplest possible input parameters.
- At each case study, analyse the effects of changes in the output due to one or more input parameters changes such as TOU tariffs, feed-in tariffs, load profile, solar profile, or using battery storage.
- Show correlation between cause-and-effect relationships observed and the mathematical equations derived in chapter 3.
- Analyse to which extent optimised schedulable load profiles benefit the economic viability of installed PV systems.

This set of case studies demonstrate relationships between input parameters and results that can be observed in real PV systems. The inputs for this case study had been simple models to assist clarity and understanding. The important observations are clearly shown, discussed and can be applied to real PV systems. Some simplifications cause secondary results that are not practically applicable to real PV systems. An example of such a simplification is the assumption of a first-order decreasing per-unit cost of PV systems. Practical PV systems per-unit cost is often better modelled using a higher order function with a gradient that approaches zero as the rating increases. Due to this simplification of per-unit PV system cost, higher rated PV systems seem more favourable than they would be for real PV systems.

5.2.2 **Input parameters**

5.2.2.1 Load profile

Three different load profiles are used for the first set of case studies.

The first load profile is defined for a single day and includes schedulable and non-schedulable loads. The load profile is fabricated but is based on realistic values. The energy consumption for each half-hour is within bounds of what a real house in South Africa uses. The maximum usage is 1 575 Wh per half-hour, which at 24 V_{ACrms} gives an average current of 13,125 A, well within the typical breaker limit of 60 A. The daily consumption is 37,4 kWh. This is a bit lower than the 42,84 kWh average daily use of the high-end residential energy users in the Western Cape Province, as can be calculated from [162]. The load profile has a similar shape to real households, mimicking the morning and afternoon peak and lower energy consumption the rest of the day. The schedulable loads in the household are the geyser and the pool pump. The schedules are given in Table 5.1 and the associated load profiles in Figure 5-1 and Figure 5-2. If no load schedule optimisation is done for the household, the load profiles of the geyser and pump will remain as given. The non-schedulable loads for the residence are given in Figure 5-3 and the exact values presented in Appendix Table A.2. The total load profile is given in Figure 5-4.

Table 5.1 Schedulable load schedules for demonstration case studies

Load	Rating [W]	Operation cycle 1	Operation cycle 2
Pool pump	750	06:00-12:30	19:00 – 23:30
Geyser	3 000	04:00 – 11:00	16:30 – 20:30

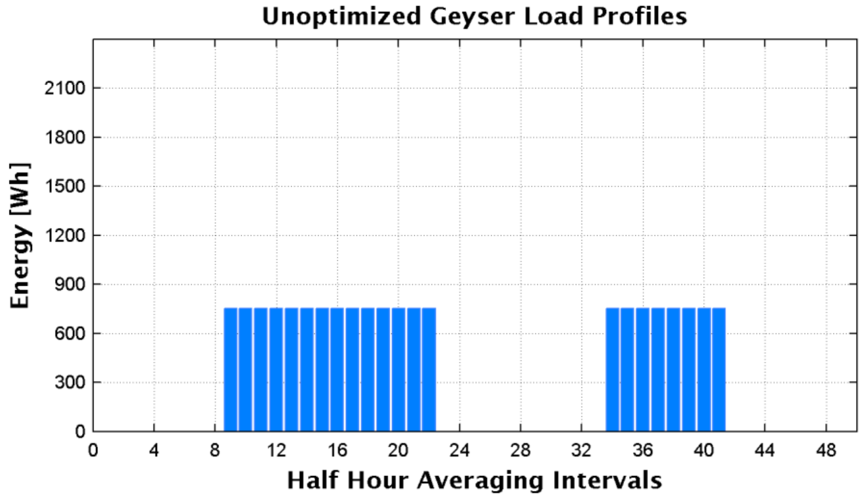

Figure 5-1 Geyser initial load profile

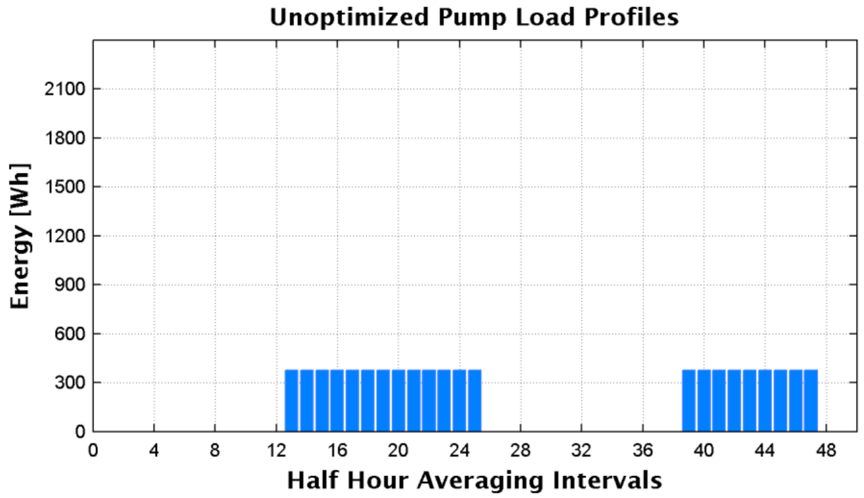

Figure 5-2 Pool pump initial load profile

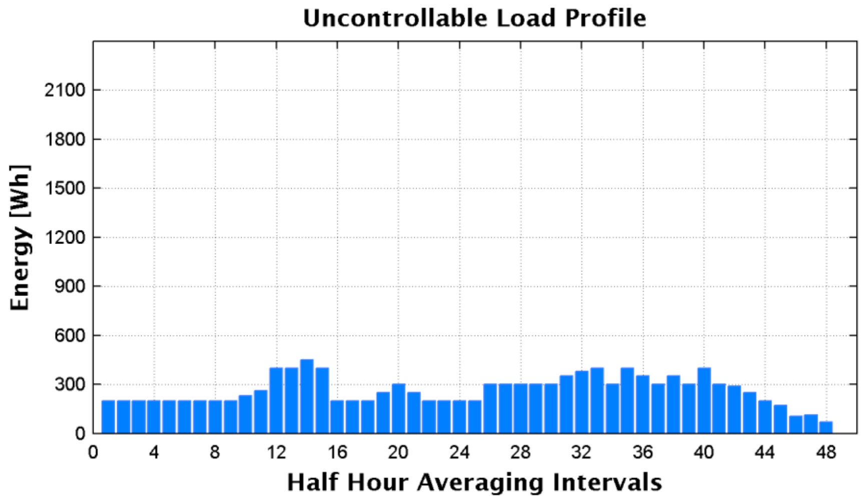

Figure 5-3 Non-schedulable load profile

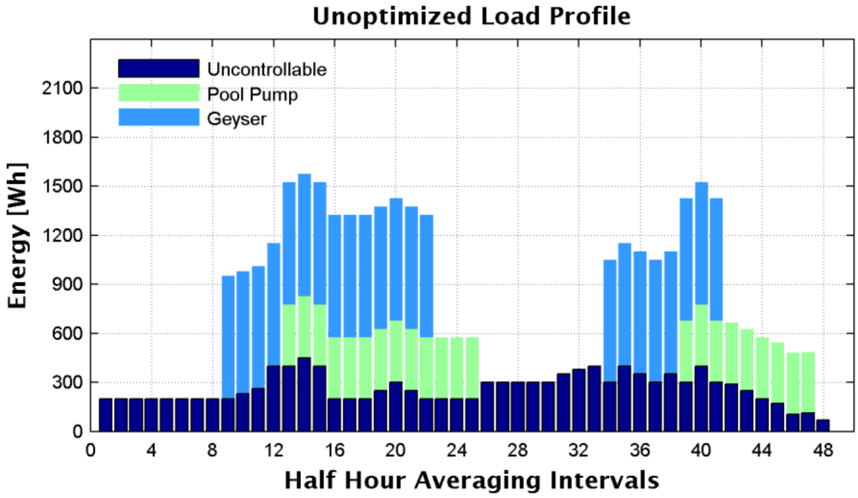

Figure 5-4 Total load profile of the demonstration case studies

The second load profile used in this set of case studies only contains non-schedulable loads. The load profile is only defined for a single day and is given in Figure 5-5. The numerical values are given in Appendix Table A.3. This load profile has a peak energy consumption of 2 025 Wh per half-hour, translating to an average current of 16,88 A, within the typical 60 A breaker limit. The daily energy consumption is 28,78 kWh, which is between the middle and high energy consumption groups as can be calculated from [162].

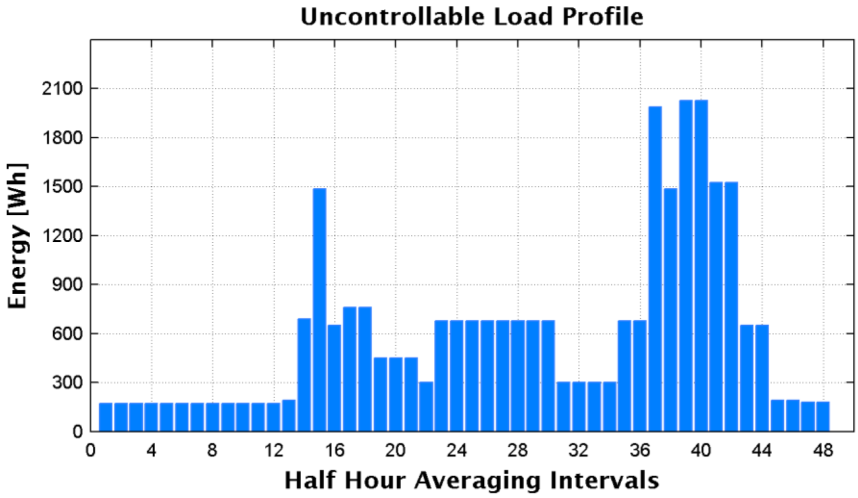

Figure 5-5 Total load profile for case study 2

The last load profile is defined over a year. Two daily load profiles have been constructed which is each repeated for 6 months of the year. The first load profile is representative of a summer profile, used for the months January, February, and September through to December. The second load profile is representative of a winter profile, used for the months March through to August. The swimming pool pump and geyser are again used as the schedulable loads. For the summer profile, the pool pump operates for extended periods of time and the geyser for shorter durations, when compared to the winter profile.

For the summer profile, the schedules of schedulable loads are given in Table 5.2 and the schedulable load profiles are given in Figure 5-6 and Figure 5-7. The non-schedulable load profile is given Figure 5-8 and the numerical values given in Appendix Table B.1. The total load profile is given in Figure 5-9. The daily energy consumption is 29,83 kWh and the peak consumption is 2 048 Wh per half-hour, both of which is within realistic bounds.

Table 5.2 Schedulable load profiles during summer

Load	Rating [W]	Operation cycle 1	Operation cycle 2
Pool pump	750	10:00 – 14:00	17:00 – 21:00
Geyser	900	06:00 – 08:00	19:00 – 20:00

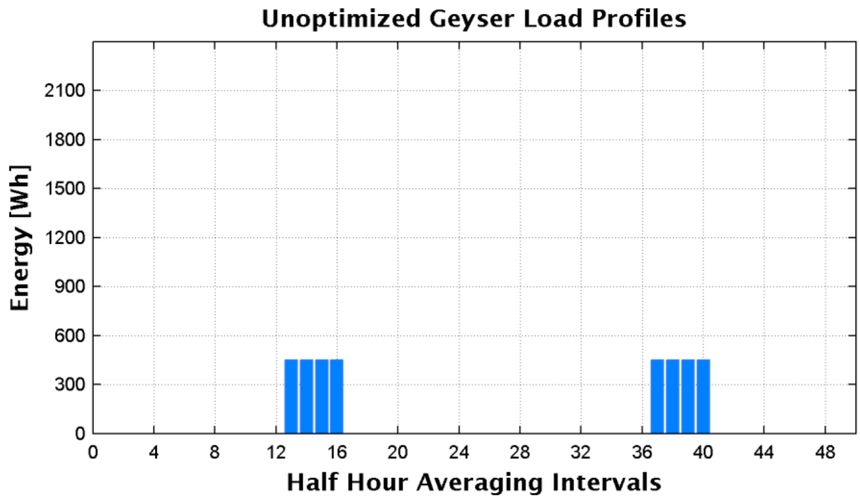

Figure 5-6 Geyser initial summer load profile

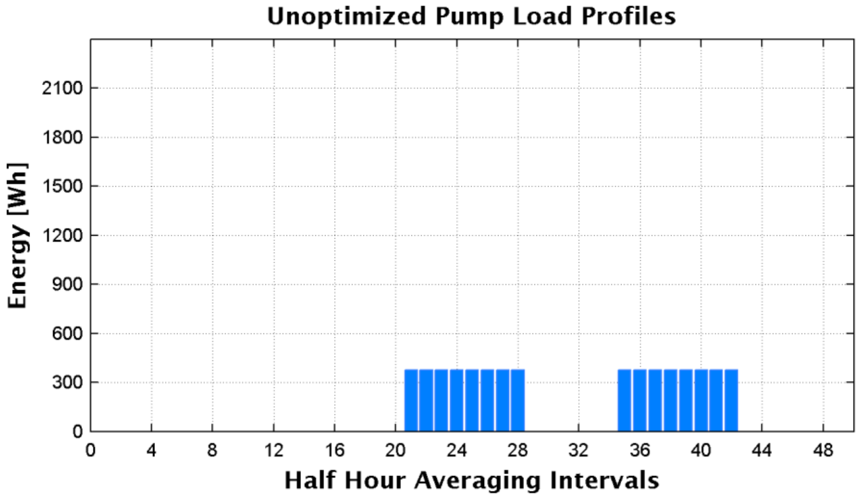

Figure 5-7 Pool pump initial summer load profile

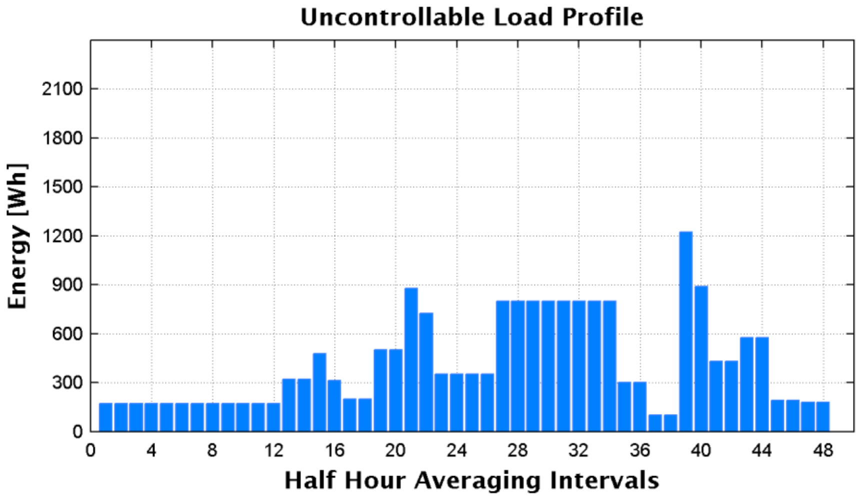

Figure 5-8 Non-schedulable load profile for summer

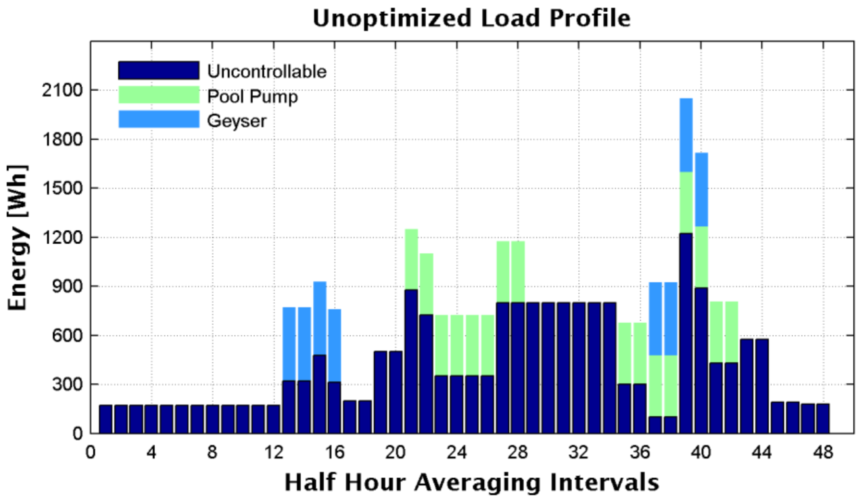

Figure 5-9 Total load profile for summer

For the winter profile, the schedules of schedulable loads are given in Table 5.3, and the schedulable load profiles in Figure 5-10. The non-schedulable load profile is given in Figure 5-12 and the numerical values given in Appendix Table B.2. The total load profile is given in Figure 5-13. The daily energy consumption is 26,68 kWh and the peak consumption is 1 985 Wh per half-hour, both of which is within realistic bounds.

Table 5.3 Schedulable load profiles during winter

Load	Rating [W]	Operation cycle 1	Operation cycle 2
Pool pump	750	11:00 – 13:00	17:00 – 19:00
Geyser	900	06:00 – 09:00	18:00 – 22:00

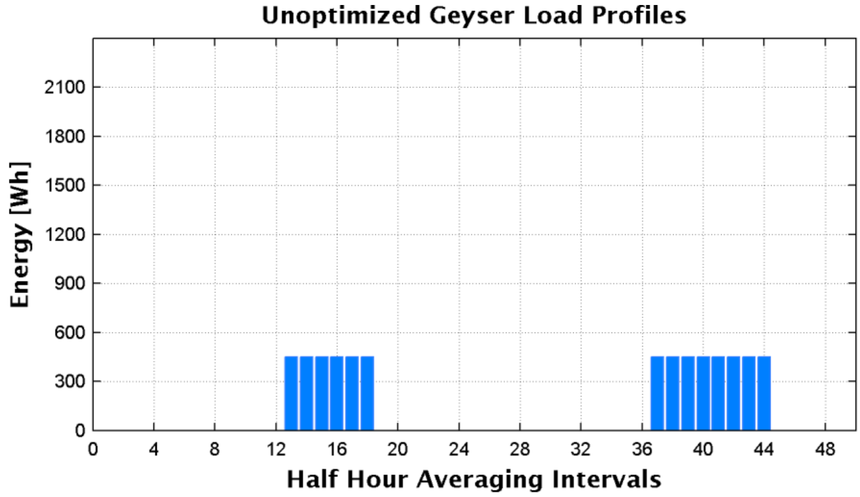

Figure 5-10 Geyser initial winter load profile

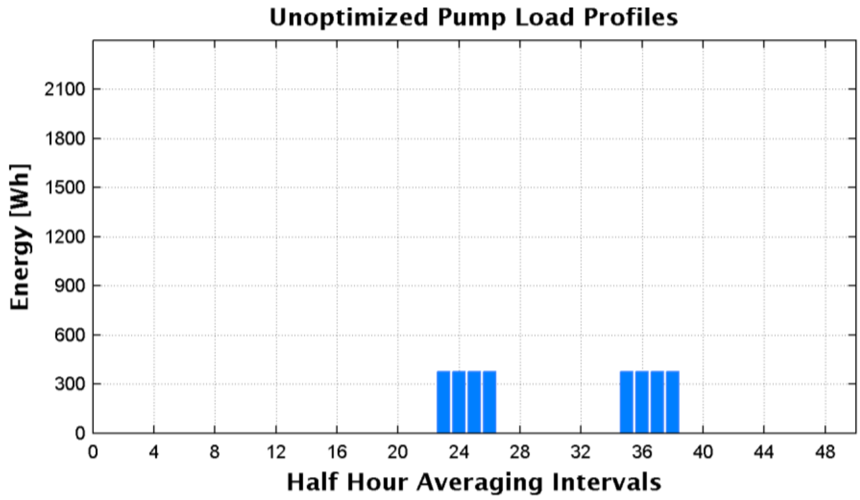

Figure 5-11 Pump initial winter load profile

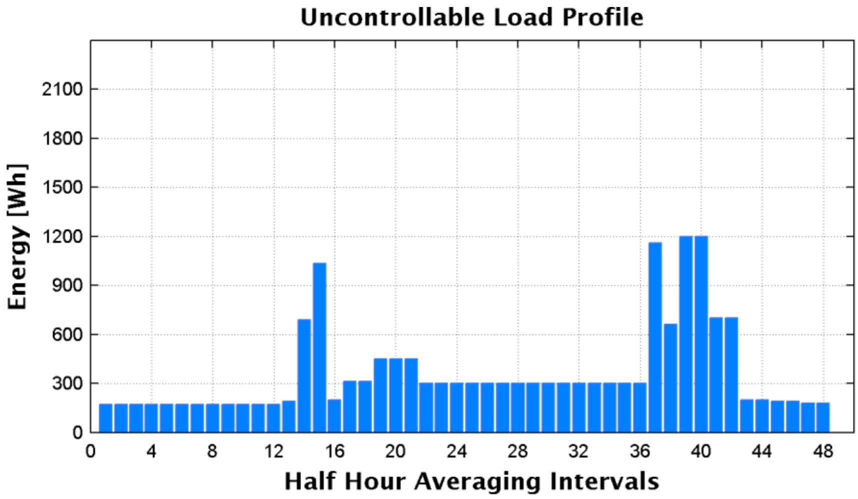

Figure 5-12 Non-schedulable load profile for winter

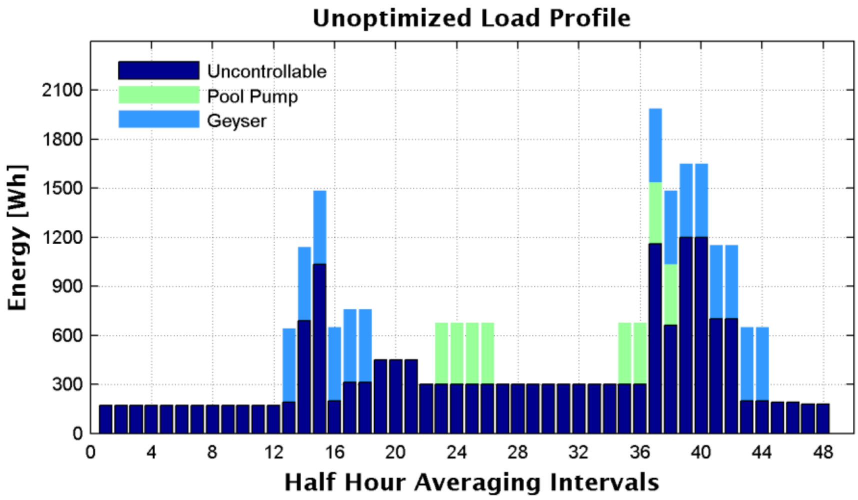

Figure 5-13 Total load profile for the annual profile case studies

5.2.2.2 Solar profile

A daily and an annual solar profile are defined for this set of case studies. The daily solar profile is fabricated based of observed values for a weather station in Randburg, Johannesburg, South Africa, accessed per [163]. The observed values are based on an ideal day's solar profile. The profile shows the energy collected each half-hour of the day for a 1 kW PV system. The solar profile is given in Figure 5-14. The numerical values are given in Appendix Table A.1. The total energy collected during the day is 6 535 Wh.

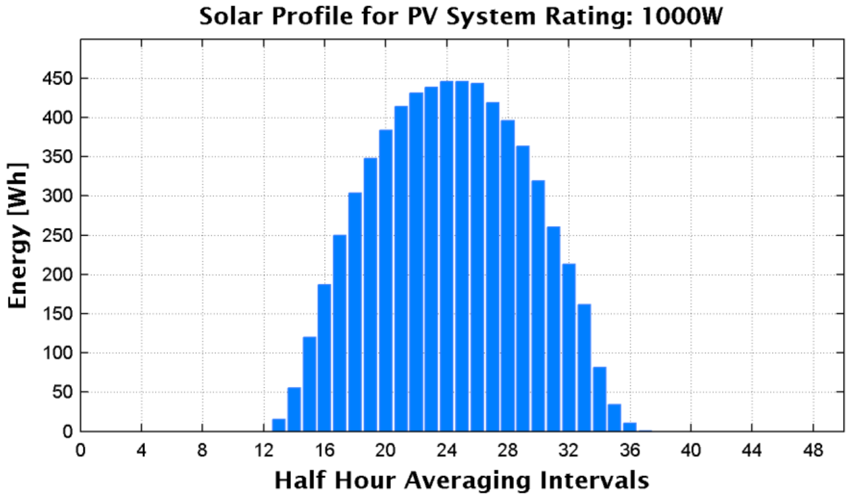

Figure 5-14 Daily solar profile

The annual solar profile is based on measured PV system results for observed for Stellenbosch in the year 2012, available on the SAURAN database [82]. The origin, collection and processing of the data is recounted along with providing graphical representation of the data in Appendix C.

5.2.2.3 Tariff structure

Two tariff structures are discussed here: the consumption tariff, for purchasing energy from the grid, and the feed-in tariff, for selling energy back to the grid. Costs are calculated based on the net energy into the grid for each half-hour. If the consumption is higher than the feed-in for the respective half-hour, the consumption tariff is applied on the net energy drawn off the grid. If the feed-in is larger than the consumption for the half-hour, the feed-in tariff is applied on the net energy fed into the grid.

Two consumption tariffs are used in this set of case studies. The first is a flat tariff, where energy is purchased from the grid at R1/kWh. The second is TOU tariffs, where the off-peak tariff is referred to as $r_1^I$and the expensive peak tariff as r_2^I. The cost of electricity throughout the day is shown in Figure 5-15. The exact times at which r_1^I and r_2^I are implemented is given in Table 5.4. The exact prices charged for electricity is given in Table 5.5. The chosen values provide nice rounded figures and an pricing ratio of $\frac{2}{3}$. These values are fabricated but realistic when compared with real tariffs [164].

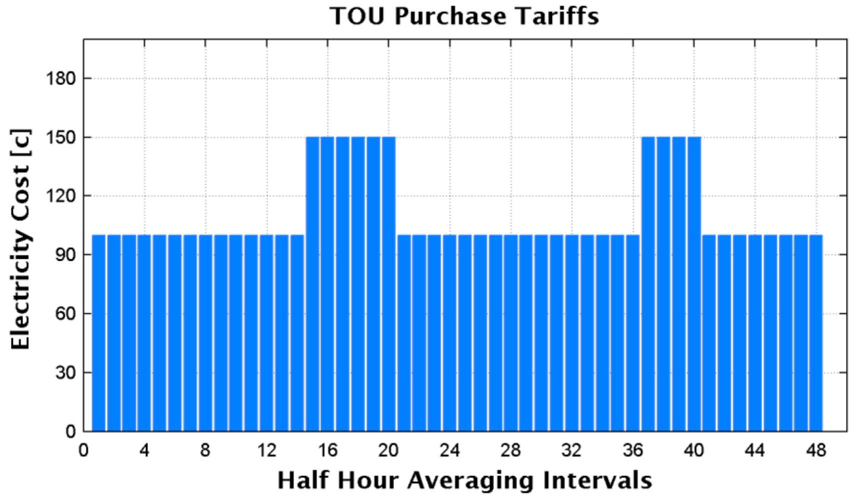

Figure 5-15 Time-of-use tariff structure for the demonstration case study

Table 5.4 TOU tariff implementation times

Parameter	Start time	End time
T2 morning times	07:00	10:00
T2 afternoon times	18:00	20:00

Table 5.5 TOU tariff prices

Tariff	Electricity cost [R/kWh]
r_1^I	1
r_2^I	1,50

For the feed-in tariffs, only flat tariffs will be used. Case studies that explores the effect of feed-in tariffs specifies what tariffs are used.

5.2.2.4 Battery storage

Limits to impose on the battery were chosen to ensure reasonable battery lifetime. These values are provided in Table 5.6.

Table 5.6 Battery configurations for the demonstration case study

Battery parameter	Value
Max bat discharge rate	C/10
Max bat charge rate	C/20
Max battery DOD	0,2

5.2.2.5 System installation cost

The investments costs comprise of the cost of acquiring a PV system and optionally a battery system. The price for installing a PV system is determined from prices taken from [115], from which a linear function derived in Appendix D. The linear model was chosen to approximate the cost trend in a simple manner for the demonstration purposes. The price can be represented by the linear equation given in (5.1) and is shown graphically in Figure 5-16.

$$S_{pu}(S_R) = (-2{,}09.10^{-3}S_R + 31{,}47)\ [R/W] \tag{5.1}$$

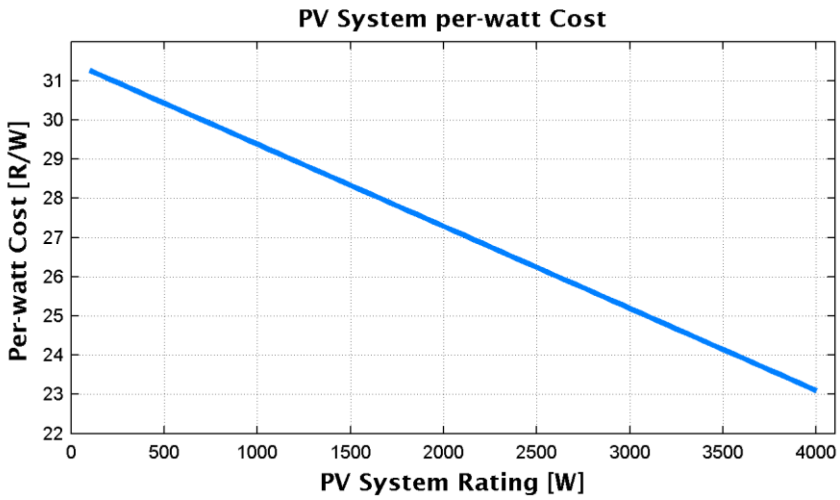

Figure 5-16 Per-watt cost of installing PV for the demonstration case study

The price of the battery system for the demonstration was also obtained from [115]. Quotes from alternative providers revealed these prices to be exaggerated especially for higher rated systems, therefore the rating is constrained to smaller systems for the first set of case studies. The formula to calculate per-watthour costs for the battery system in (5.2).

$$S_{pu}(S_R) = (-2.00.10^{-3}S_R + 33.25)\ [R/Wh] \tag{5.2}$$

5.2.3 Case study progression

The case studies initially explore simple system configurations and determine the effect of changing input parameters. Case study set one input parameters are presented in Table 5.7.

Table 5.7 Set 1 of case studies with associated input parameters

Case study	Tariff		Load Profile optimisation	Battery storage	Timeline
	Consumption	Feed-in			
1	Flat	No	No	No	Daily
2	Flat	No	No	No	Daily
3	Flat	No	Yes	No	Daily
4	TOU	No	No	No	Daily
5	TOU	No	Yes	No	Daily
6	Flat	Flat	No	No	Daily
7	Flat	No	No	Yes	Daily
8	Flat	No	No	No	Annual
9	Flat	No	Yes	No	Annual

5.2.4 Case study 1

5.2.4.1 Inputs parameters

The first case study uses the simplest input parameters. The input parameters used in this study are

- *Load profile* – The daily load profile as set out in Figure 5-4
- *Solar profile* – The daily solar profile as set out in Figure 5-14
- *PV system cost* – The cost as given in (5.1)
- *Load schedule optimisation* – Not applied
- *Consumption tariffs* – R1/kWh
- *Feed-in tariff* – R0/kWh

5.2.4.2 Results

The payback period of the PV system is given for a range of PV system ratings in Figure 5-17. Figure 5-17 indicates that the payback period function is initially a decreasing function. When the payback period is considered, the minimum is found to be at about 700 W, with a payback period of about 12,6 years. After this point, the payback period increases as the PV system ratings increases.

The PV system rating optimisation is able to determine the minimum payback period, as shown in Figure 5-18. The results from the optimisation algorithm show that the optimal PV system rating is 676,4 W with a payback period of 12,6 years.

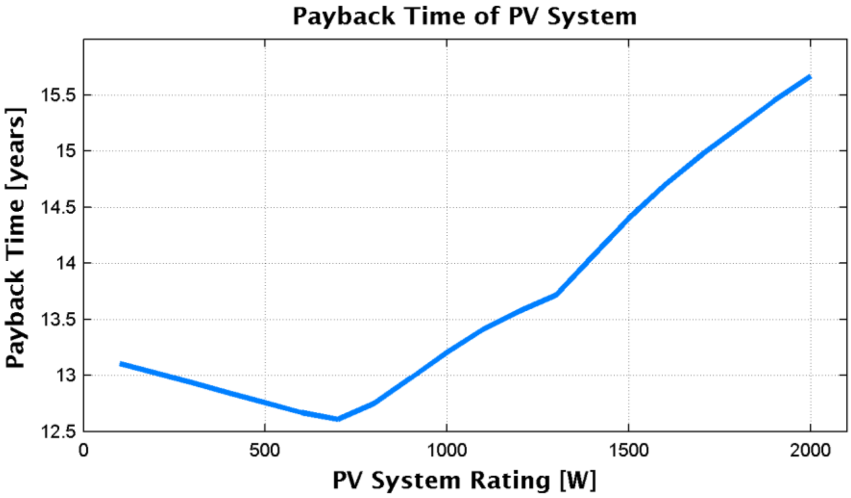

Figure 5-17 Case study 1 PV system payback time

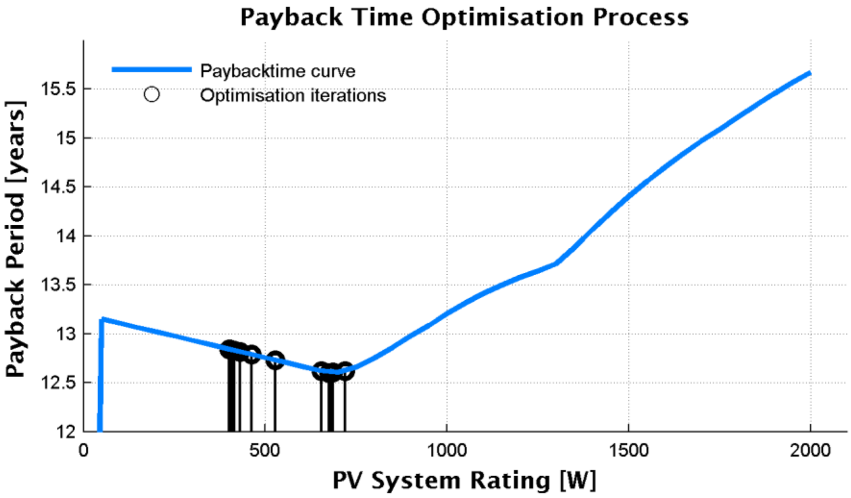

Figure 5-18 Optimisation algorithm progress for case study 1

5.2.4.3 Analysis

To analyse how the input parameters lead to payback period as found in Figure 5-17, inspection is made into the payback period equation. Since in this case study the investment costs consists of only the PV system cost the payback period is expressed by (3.50) and is given here as a function of PV system rating:

$$T_{pb} = \frac{S_C(S_R)}{C'(S_R)} \tag{5.3}$$

where T_{pb} denotes the payback period, S_C denotes the purchase cost of the PV system, C' denotes the savings achieved per day by installing the PV system and S_R denotes the PV system rating. The values for these functions are shown in Figure 5-19 and Figure 5-20.

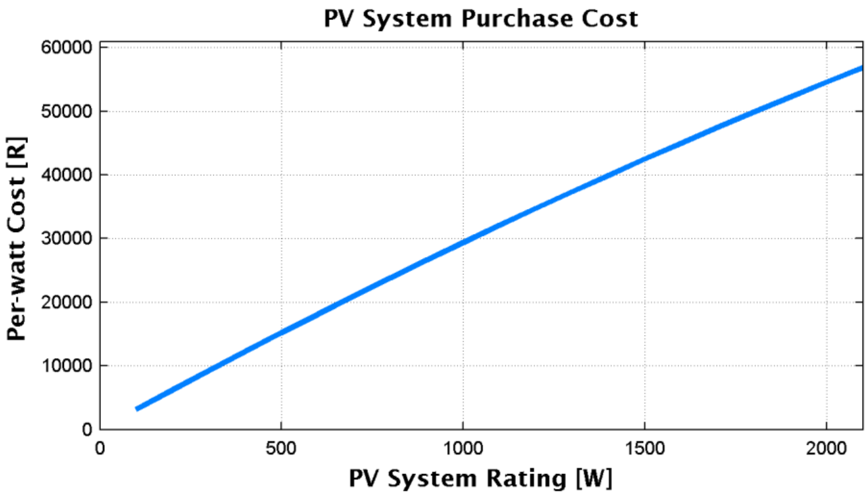

Figure 5-19 PV system cost as a function of system rating

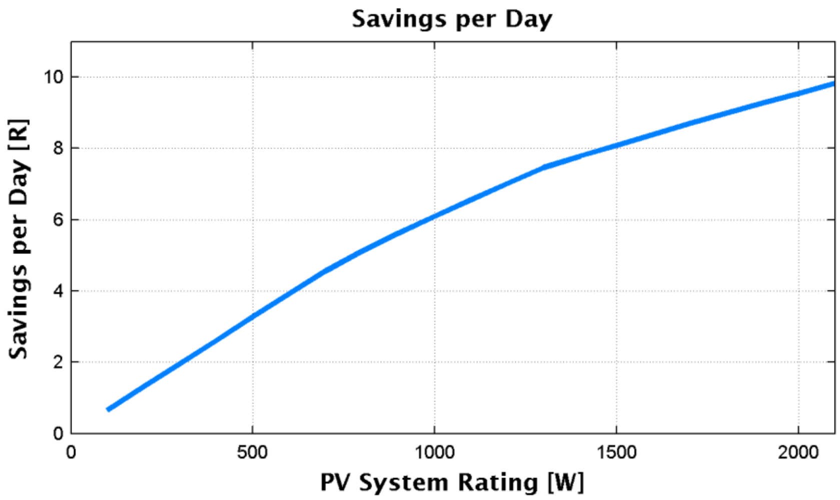

Figure 5-20 Savings achieved by the PV system as a function of system rating

It's difficult to intuitively grasp the reason for the payback period function curve in Figure 5-17 from the graphical results in Figure 5-19 and Figure 5-20. A next attempt to provide a graphical result that leads to an intuitive interpretation of the payback period function is the savings per-day per-watt brought forward by the PV system. This is given in Figure 5-21.

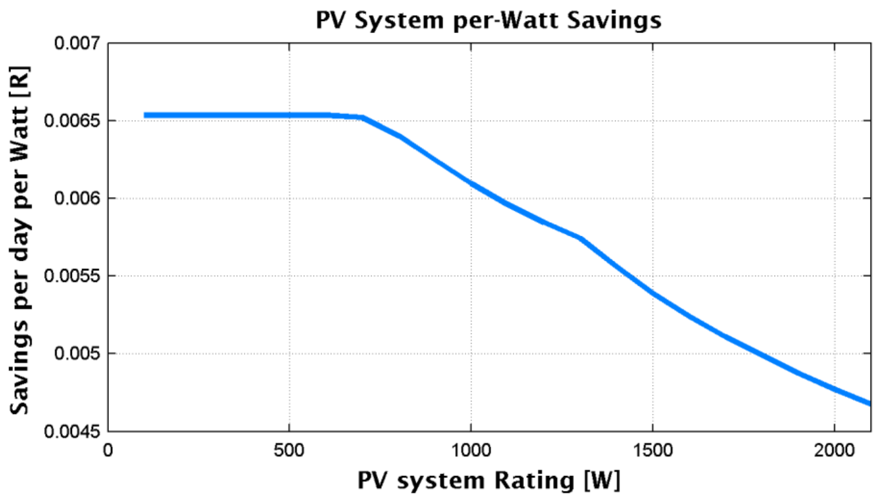

Figure 5-21 Daily savings achieved per watt of PV system rating

Note the following similarities from the savings per-day per-watt graph given in Figure 5-21 and the payback period function graph given in Figure 5-17:

- While the PV system savings per-day per-watt remains constant, the PV system payback period decreases linearly.
- There exists a point (here, about 700 W) where the PV savings per-day per-watt starts decreasing. Similarly, at this point the PV system payback period changes from a decreasing to an increasing function.

Two analyses are now presented with regards to the PV system per-day per-watt savings. The first analysis considers the curvature of the PV system per-day per-watt curve given in Figure 5-21. The second considers the mathematical reasons for the observed corresponding patterns between the per-watt savings and the payback period of the PV system.

The curve of the per-watt per-day savings initially has a constant value. To investigate this, the PV system energy profile and the load profile consumption are given in Figure 5-22. In this graph it is seen that for PV systems rated lower than 500 W, all the generated energy is consumed by loads in the residential energy system. As the PV system rating increases beyond 500 W, a rating will be reached where the generated energy is not entirely consumed in the residential energy system. This is shown in Figure 5-23, where the solar energy yield exceeds the load consumption energy profile. The surplus solar energy has to be fed into the grid for no remuneration. Only a fraction of the total generated solar energy is utilised to offset electricity cost. Figure 5-21 suggests that 100% of the solar energy is as PV system rating increases until a rating of about 700 W is reached, after which the fraction of utilised solar energy decreases.

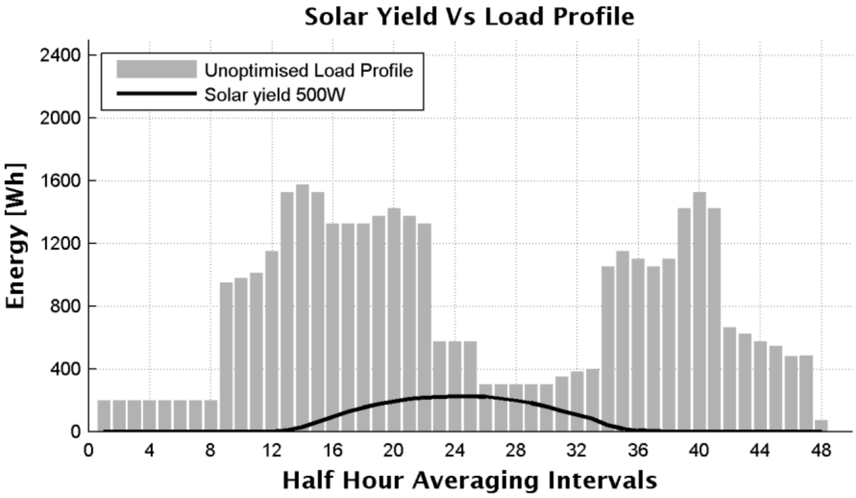

Figure 5-22 PV system and load consumption energy profile for 500 W PV system

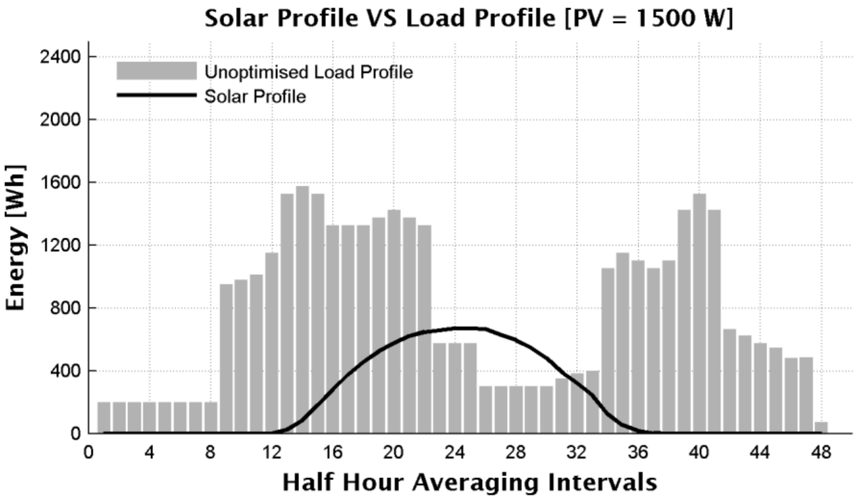

Figure 5-23 PV system and load consumption energy profile for 1000 W PV system

A simple mathematical derivation based on the observed behaviour will be presented. This derivation shows how the observed behaviour is fully described by the mathematics derived in section 3.5. This indicates that the equations from section 3.5 can subsequently be utilised to analyse payback period results. The savings per-day per-watt for the PV system can, in the case where 100% of the solar energy is utilised, be calculated by

$$C' = rE_{PV} \tag{5.4}$$

where r is the electricity consumption tariff and E_{PV} is the total energy in the PV system energy profile. To model the savings for systems where less than 100% of the energy is utilised, an utilisation factor is introduced that gives the fraction of solar energy that is consumed by the load profile in the residential energy system. The utilisation factor is a function of the PV system rating:

$$C' = rE_{PV}F_U(S_R) \tag{5.5}$$

where $F_U(S_R)$ is the utilisation factor. Figure 5-21 is a graphical representation of (5.5). This leads to a payback period equation when substituted into the payback equation given in (5.3):

$$T_{pb} = \frac{S_C(S_R)}{rE_{PV}F_u(S_R)} \tag{5.6}$$

Equation (5.6) approaches the payback period function form derived during the formal mathematical derivations in chapter 3. Applying the simplification of removing the PV system rating from the numerator and denominator as shown in (3.68), the payback equation is derived to the form given in (3.75):

$$T_{pb} = \frac{S_{pu}(S_R)}{rE_{NPV}F_u(S_R)}$$

where $S_{pu}(S_R)$ denotes the per-watt cost of the PV system, $F_u(S_R)$ denotes the utilisation factor of the system and rE_{NPV} is a constant factor determined from the electricity cost r and the solar energy collected throughout the day E_{NPV}.

Investigating the graphs of the numerator and the denominator in (3.75) leads to new insights. The numerator is the per-unit cost of the PV system. The denominator contains a constant value and the utilisation factor function. The per-unit cost function is plotted against the utilisation factor function in Figure 5-24. This should be closely compared to the payback period function given in Figure 5-17. Initially the payback period decreases linearly – this can be attributed to the fact that per-watt cost of PV systems linearly decreases, while the utilisation factor stays constant at 100%. As the PV system rating increases beyond 700 W, the utilisation factor function decreases. This implies that for any PV system rated higher than 700 W, only a fraction of the energy that is generated by the PV system is utilised locally in the residential energy system. An inherent property of energy is that it cannot be stored and without battery storage, the only option is to export surplus energy to the grid. For this case study, the grid connection feed-in tariffs are zero, implying that energy exported to the grid does not contribute to savings. An interesting but logical observation is then that the point where the utilisation factor drops below 100% the payback period of the PV system starts to increase, as can be seen in Figure 5-17. This implies that a relationship exist between the payback period and the residential energy system's ability to utilise the generated PV energy. The next case study considers this in more detail, focusing on whether the payback period necessarily starts increasing when the utilisation factor starts decreasing from 100%.

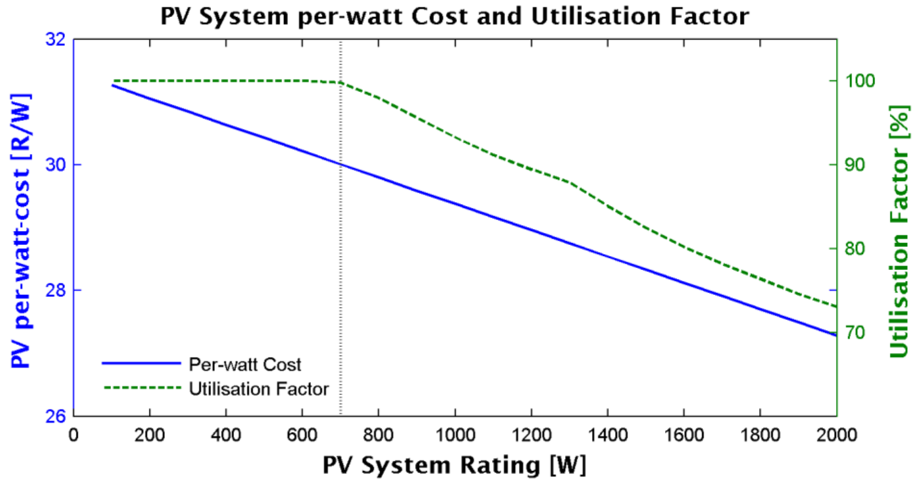

Figure 5-24 Compared utilisation factor and per-watt cost at different PV system ratings

5.2.5 **Case study 2**

5.2.5.1 Input parameters

This case study will use an alternative load profile to showcase an important aspect of the work – to determine the exact point at which the minimum payback occurs. The input parameters used in this study are

- *Load profile* – The daily load profile as set out in Figure 5-5
- *Solar profile* – The daily solar profile as set out in Figure 5-14
- *PV system cost* – The cost as given in (5.1)
- *Load schedule optimisation* – Not applied
- *Consumption tariffs* – R1/kWh
- *Feed-in tariff* – R0/kWh

5.2.5.2 Results

The graph of the payback period is shown in Figure 5-25 and identifies three corner cases: 700 W, 1 100 W, and 1 525 W. These cases are explored further in the analysis section.

The optimisation script could successfully determine the system rating with the minimum payback period. The iterations of the optimisation are shown in Figure 5-26. The PV system rating for minimum payback period is 1 088,27 W, with a payback period of 12,53 years.

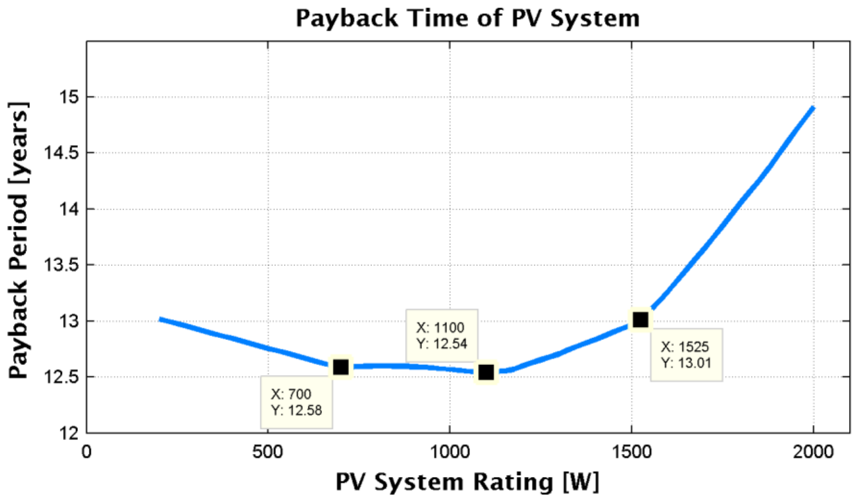

Figure 5-25 Payback time of system for case study 2

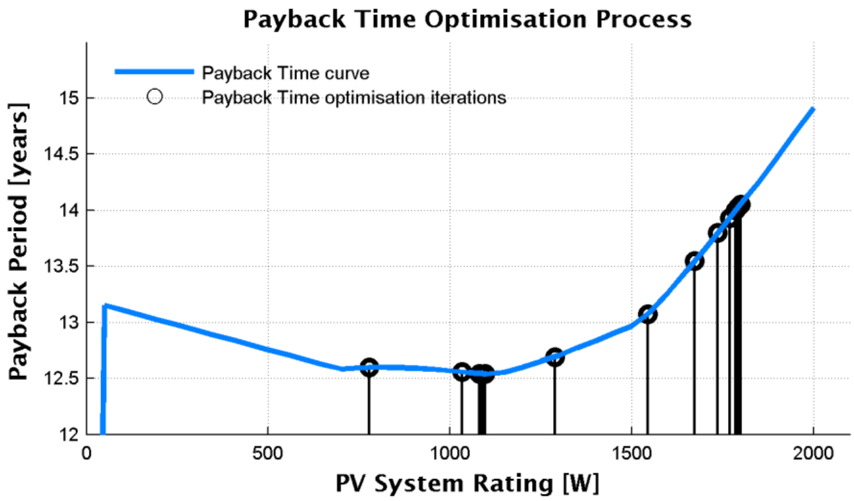

Figure 5-26 Optimisation algorithm progress for case study 2

5.2.5.3 Analysis

Case study 1 indicated the importance of the utilisation factor function and indicated that it is related to the payback period. The utilisation function is given in Figure 5-27. The utilisation factor goes below 100% at about 700 W. At this time the payback does start to increase, but at about 1 000 W the payback method again has a decreasing function, even though the utilisation factor is also a decreasing function – clearly indicating that the payback period *can* still decrease even after the utilisation factor has fallen below 100%.

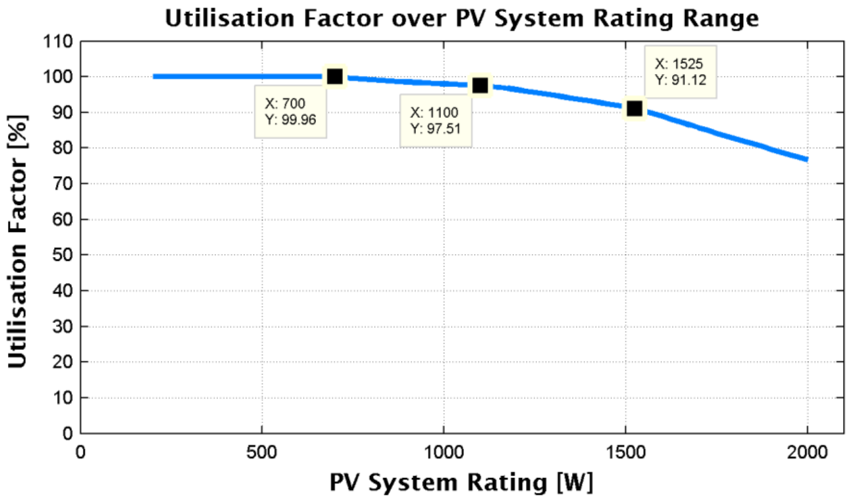

Figure 5-27 Utilisation factor for case study 2

The reason for this is found in (3.98), and the validity of (3.98) can be demonstrated by using the results from this case study. Equation (3.98) is repeated here to aid the discussion. It states that the required condition to achieve a decreasing payback period is

$$\frac{F_u(S_{R2}) - F_u(S_{R1})}{F_u(S_{R1})} > \frac{S_{pu}(S_{R2}) - S_{pu}(S_{R1})}{S_{pu}(S_{R1})}$$

where and S_{R1} and S_{R2}denotes two instances of PV system ratings where $S_{R2} > \; S_{R1}$, $F_u(S_R)$ denotes the utilisation factor and $S_{pu}(S_R)$ denotes the per-watt cost of the PV.

To verify (3.98), the left and right side of the condition is given graphically in Figure 5-28. The graph is given along with the payback graph. It can be seen that as long as the left side of the equation (corresponding to the "utilisation normalised decrease" line) is larger than the right side of the equation ("per-unit cost normalised decrease") the payback period decreases. This proves that the relationship established between the solar profile, the local consumption as specified by the load profile and the cost of the PV system.

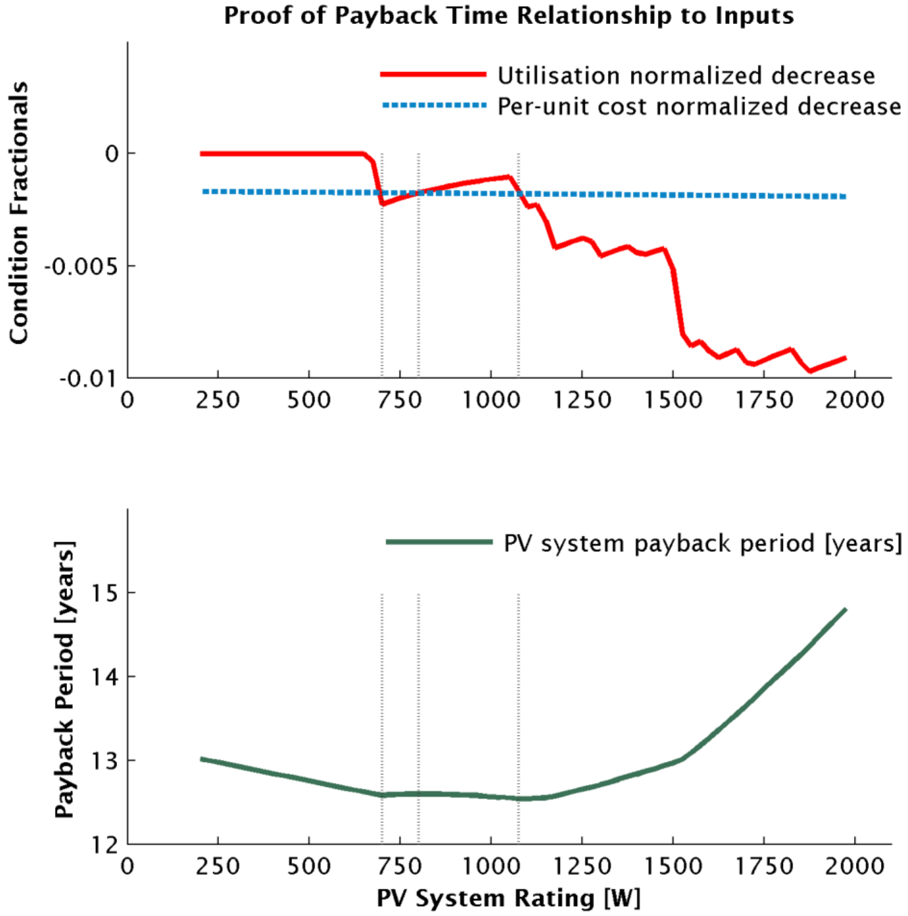

Figure 5-28 Input parameter relationship to payback time

5.2.6 **Case study 3**

5.2.6.1 Inputs parameters

This case study investigates the effect of using a load schedule controller to optimise the load profile of schedulable loads. The input parameters used in this study are

- *Load profile* – The daily load profile as set out in Figure 5-4
- *Solar profile* – The daily solar profile as set out in Figure 5-14
- *PV system cost* – The cost as given in (5.1)
- *Load schedule optimisation* – Applied
- *Consumption tariffs* – R1/kWh
- *Feed-in tariff* – R0/kWh

5.2.6.2 Results

The payback period curve for this case study is given in Figure 5-29. The optimisation algorithm is able to find the PV system rating with minimal payback period successfully. The iterations of the optimisation are shown in Figure 5-30. The minimum payback period was found to be 10,55 years at a PV system rating of 3 074 W.

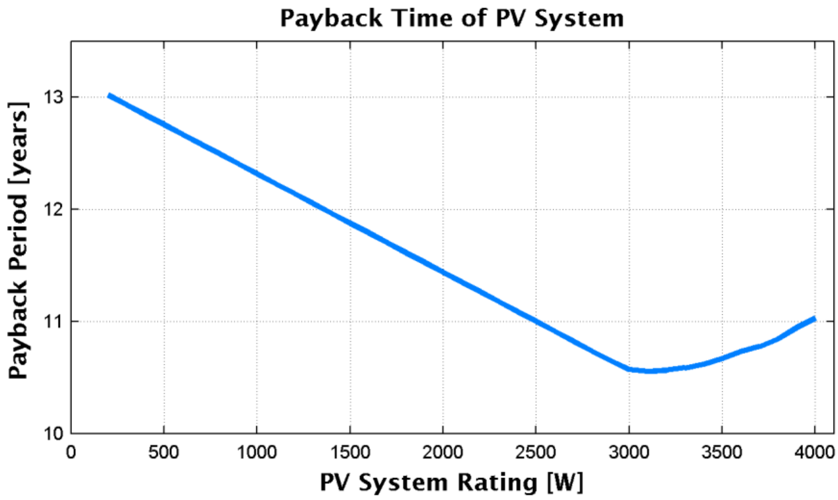

Figure 5-29 Payback time of system for case study 3

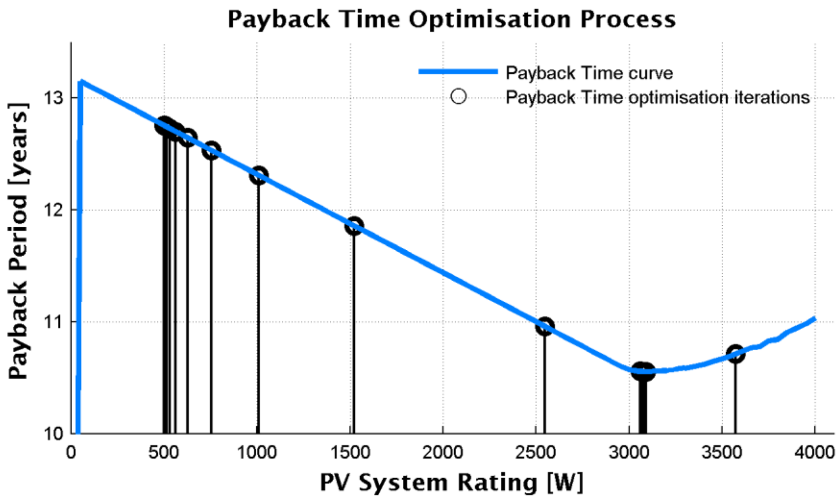

Figure 5-30 Optimisation algorithm progress for case study 3 (initial value 500 W)

5.2.6.3 Analysis

The difference in results between case study 3 and case study 1 is quite apparent. The solar profile and load profile in this case study is the same as in case study 1. The only difference is the fact that the schedules of schedulable loads are optimised. In case study 1, the optimal PV system rating is 676 W while for this case study it's 3 074,25 W. For case study 1, the minimum payback period is 12.6 years while for this case study it's 10.55 years. Comparing the results of case study 3 against case study 1, the PV system's rating is 5 times as high, with a payback period decreased by 2 years.

To identify the reason for the improved payback period, the utilisation factor is considered. The utilisation factor shows that 100% of the energy that is collected by the PV panels is utilised for systems of up to 3 050 W. In case study 1, the residence started using less than 100% of the collected energy at about 670 W. By optimising the load scheduling, the collected solar energy is utilised more effectively as PV system rating increases. Since the per-watt cost of the PV systems decrease for PV system rating increases, the payback period decreases. The residence only starts to use less than 100% of the energy at about 3000 W.

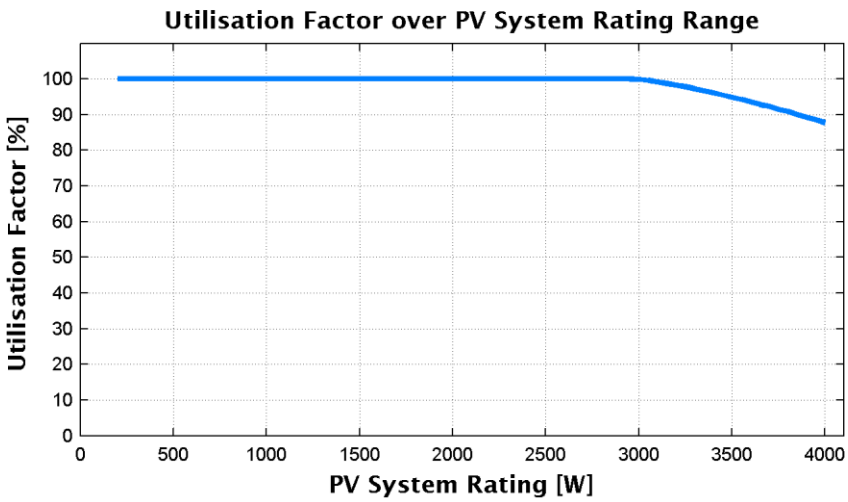

Figure 5-31 Utilisation factor for case study 3

To understand how the load scheduling can achieve more effective utilisation of solar energy, the energy collected vs load profile graphs is compared for case study 1 and case study 3. With a PV system rating of 500 W, the residential energy system in both case study 1 and 3 utilise 100% of the PV energy, as shown in Figure 5-32. In case study 1 the utilisation factor of the decreases as the PV system rating increases beyond 670 W. At a PV system rating of 1 500 W, a significant fraction of PV system energy is not utilised, as shown in Figure 5-33. For case study 3, the load schedule optimisation algorithm reallocates loads ensuring that a high fraction of the solar energy is utilised. At a PV system rating of 1 500 W, all of the generated solar energy is utilised, as shown in Figure 5-34. The utilisation factor graph of Figure 5-31 shows that 100% of energy is utilised up to a PV system of 3 000 W. The load profile and solar profile at this rating is given in Figure 5-35. As the per-watt cost decreases as the PV system rating increases, decreased payback periods for the PV systems are achieved, as shown in Figure 5-29.

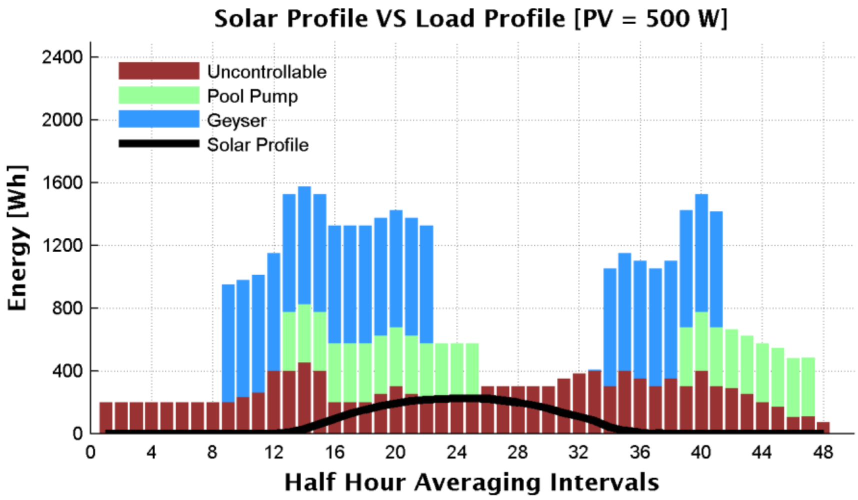

Figure 5-32 The load profile utilises 100% of a small PV system's energy

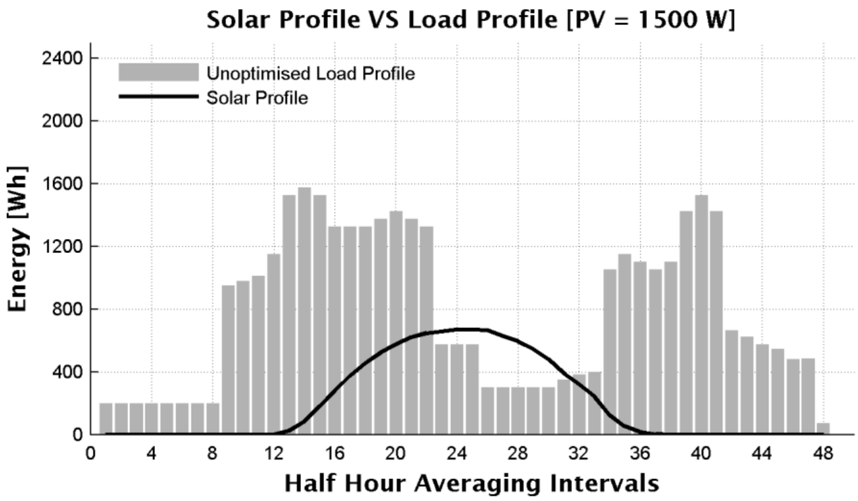

Figure 5-33 The load profile utilises less than 100% of a 1500 W PV system's energy

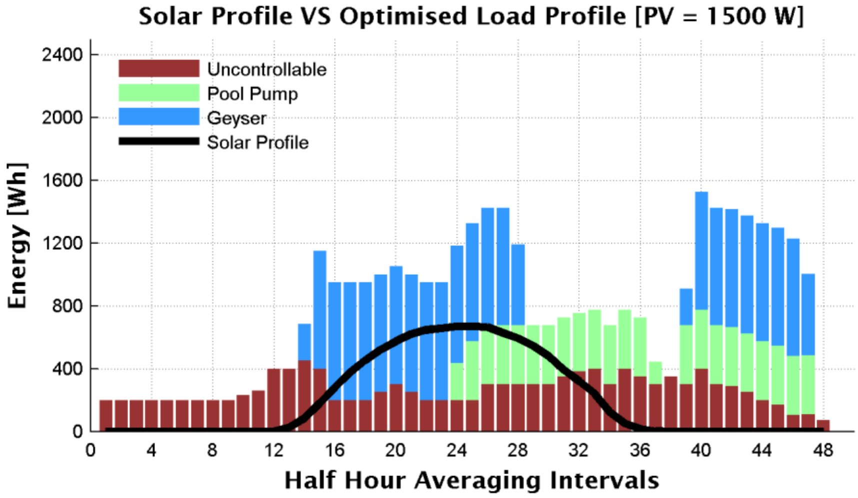

Figure 5-34 The optimised load profile utilises 100% of a 1500 W PV system's energy

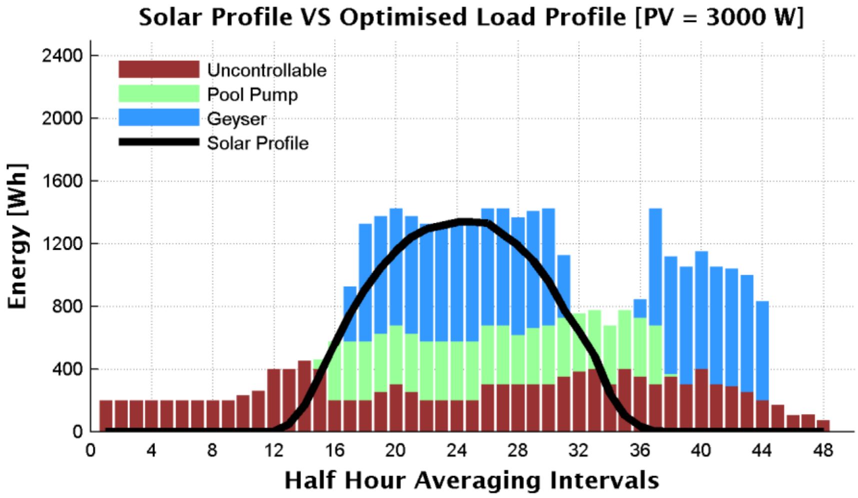

Figure 5-35 The optimised load profile utilises 100% of a 3000 W PV system's energy

5.2.7 **Case study 4**

5.2.7.1 Inputs parameters

This case study investigates the effect of TOU tariffs on the payback period of a residence where the load profile is not optimised. The input parameters used in this study are

- *Load profile* – The daily load profile as set out in Figure 5-4
- *Solar profile* – The daily solar profile as set out in Figure 5-14
- *PV system cost* – The cost as given in (5.1)
- *Load schedule optimisation* – Not applied
- *Consumption tariffs* – TOU tariffs as given in Figure 5-15

- *Feed-in tariff* – R0/kWh

5.2.7.2 Results

The payback period is given in Figure 5-36. It follows a similar form as the payback period curve for a flat rate tariff: An initial decrease in and then a gradual increase of the payback period. The system rating optimisation is able to determine the optimal system rating, as shown in Figure 5-37. The optimal system rating is 676 W and the payback period 11.23 years. The rating is the same as for case study 1, but with the more expensive tariff in this case study, the payback period is less than the payback period in case study 1 of 12.4 years.

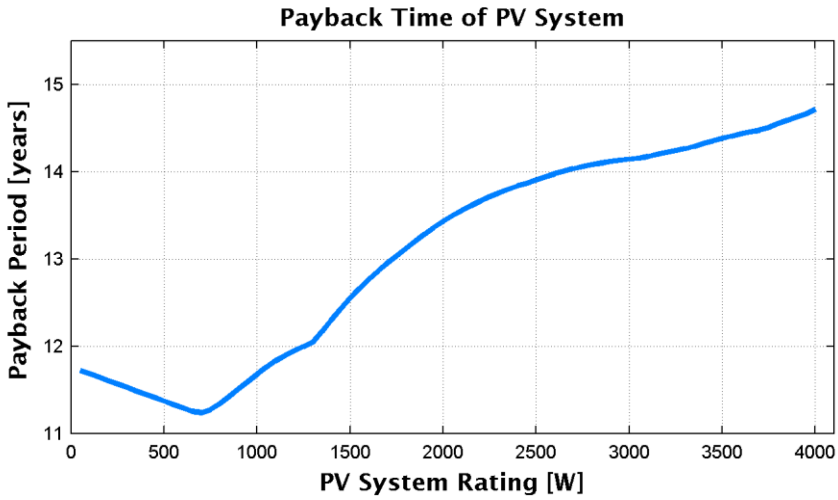

Figure 5-36 Payback time for case study 4

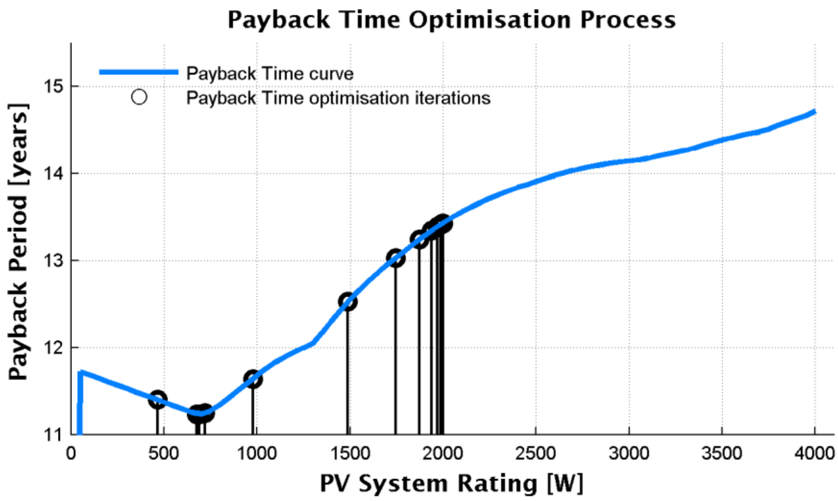

Figure 5-37 Optimisation algorithm progress for case study 4 (initial value 2000 W)

5.2.7.3 Analysis

This analysis will focus on understanding the role of the $\frac{r_2^I}{r_1^I}$ pricing in the payback period of this system. According to the formulas derived for payback period for TOU system, as in (3.83), each tariff period has its own utilisation factor function. If the overall utilisation factor of the system is considered, it's the same utilisation factor as in case study 1, as given in Figure 5-38. The periods for which the which the r_1^I and r_2^I tariffs are active are respectively referred to as K_1 and K_2. Visual representation of the utilisation factors during K_1 and K_2 is given by Figure 5-39 and Figure 5-40.

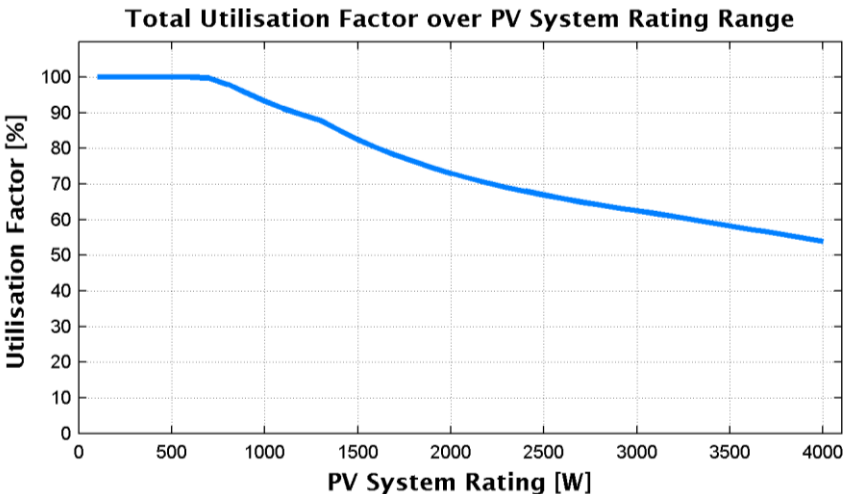

Figure 5-38 Total utilisation factor for case study 4

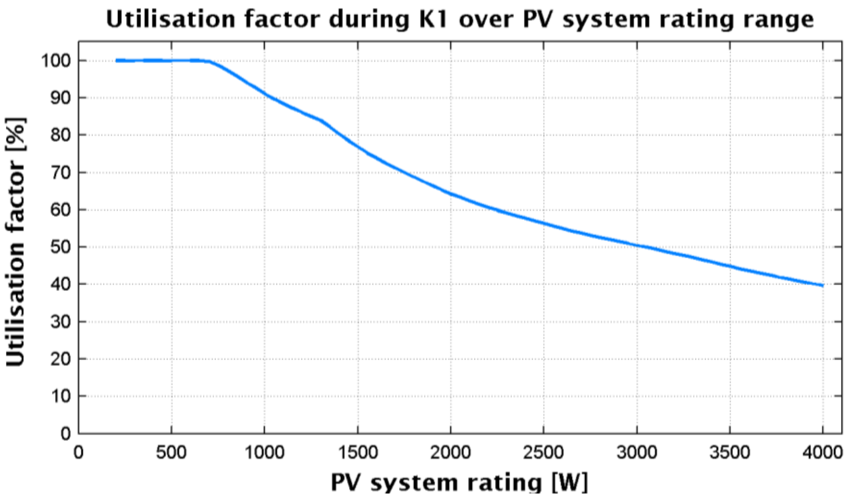

Figure 5-39 Utilisation factor for the K_1 tariff for case study 4

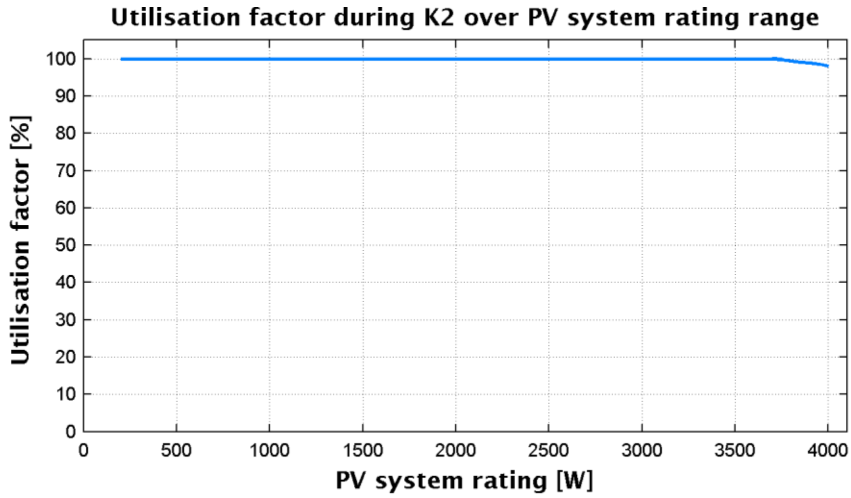

Figure 5-40 Utilisation factor for the K_2 tariff for case study 4

The first observation from inspection is that the utilisation factor of K_2 only goes below 100% when at a PV system rating of about 3 750 W. This is due to the fact that the K_2 is defined during the mornings and late evenings. Only a small amount of energy is collected by the PV system during this time. Furthermore, the loads peak at this time. The loads in the residential energy system uses all the energy generated by the PV system until a PV system rating of about 3 750 W, as suggested by Figure 5-40. At a PV system rating of 4000 W, it can be seen from Figure 5-41 that during averaging interval 20 less than 100% of the collected solar energy is used.

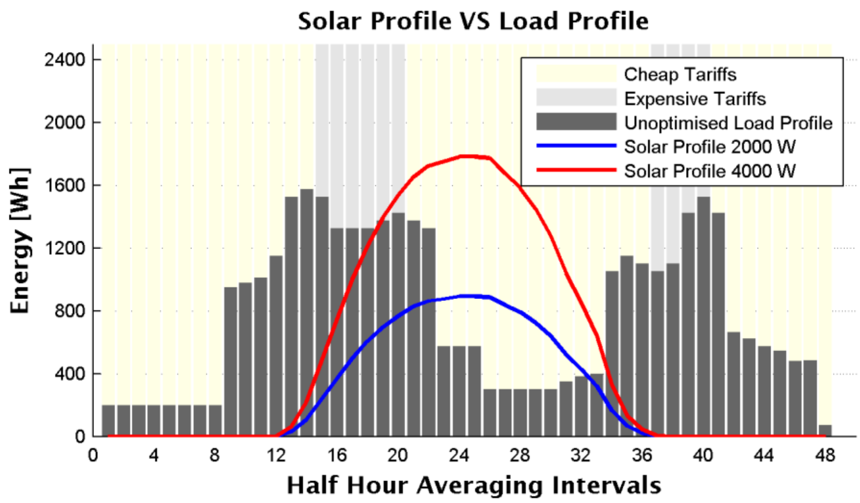

Figure 5-41 Load Profile vs PV energy collected shown against tariffs K_1 and K_2

The payback period for TOU systems is derived in (3.86). The utilisaiton factor functions for K_1 and K_2 is respectively given by $F_{u1}(S_R)$ and $F_{u2}(S_R)$. Consider that the two terms of the denominator is weighted by two factors:

1. The price of electricity during the tier (i.e. r_1^I and r_2^I)
2. The amount of PV energy collected during each of the tariff periods (E_{NPV1} and E_{NPV2})

The equation is not well suited to study the effect of adjusting the periods over which r_1^I and r_2^I are implemented (K_1 and K_2), since this changes both the E_{NPV} and $F_u(S_R)$ factors throughout the equation and requires an entire new simulation. The equation is however well suited to study the effect of $\frac{r_2^I}{r_1^I}$. The condition for decreasing payback period is given in (3.108) and is repeated here to aid the discussion:

$$\frac{F_{U1}(S_{R2}) - F_{U1}(S_{R1})}{F_{U1}(S_{R1}) + \frac{E_{NPV2}r_2^I}{E_{NPV1}r_1^I}F_{U2}(S_{R2})} + \frac{F_{U2}(S_{R2}) - F_{U2}(S_{R1})}{\frac{E_{NPV1}r_1^I}{E_{NPV2}r_2^I}F_{U1}(S_{R1}) + F_{U2}(S_{R2})} > \frac{S_{pu}(S_{R2}) - S_{pu}(S_{R1})}{S_{pu}(S_{R1})}$$

To verify (3.108), the data from the simulation is inserted into the equation and graphed as shown in Figure 5-42. The left side of (3.108) is given by the “Utilisation normalized decrease” and the right side by “Per-unit cost normalized decrease”. It can be seen that when the left-hand side becomes smaller than the right-hand side as happens at 676 W, the payback period increases. This proves that the relationship established between the solar profile, the local consumption as specified by the load profile, the influence of TOU and the cost of the PV system.

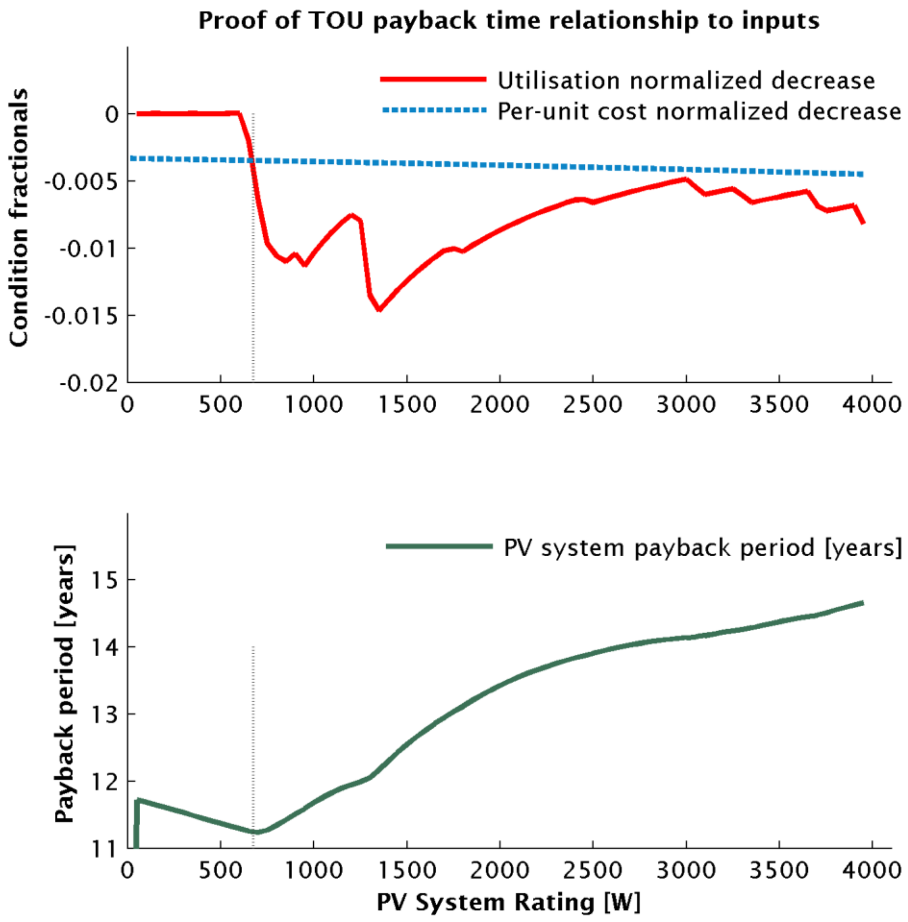

Figure 5-42 Input parameter relationship to payback time

5.2.8 Case study 5

5.2.8.1 Inputs Parameters

This case study investigates the effect of TOU tariffs on the payback period of a residence where the load profile is optimised. The input parameters used in this study are

- *Load profile* – The daily load profile as set out in Figure 5-4
- *Solar profile* – The daily solar profile as set out in Figure 5-14
- *PV system cost* – The cost as given in (5.1)
- *Load schedule optimisation* – Applied
- *Consumption tariffs* – TOU tariffs as given in Figure 5-15
- *Feed-in tariff* – R0/kWh

5.2.8.2 Results

The payback period curve for this case study has very little in common with payback curves of previous case studies. The payback curve is provided in Figure 5-43. The curve is erratic, with many minima and maxima on the curve, of which the major ones are indicated.

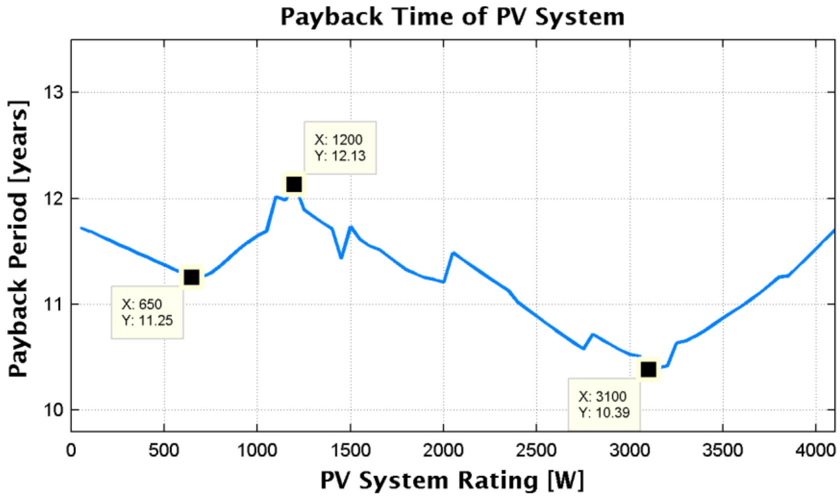

Figure 5-43 Payback time of case study 5

The PV system rating optimisation algorithm does not consistently find the PV system rating with the minimum payback period. This is confirmed when the optimisation is run with three different initial system rating values. The first optimisation starts with an initial value of 400 W and wrongfully finds the first local minima as the absolute minima, shown in Figure 5-44. The second optimisation, shown in Figure 5-45, starts at 1 300 W, and manages to successfully ignore the minor local minima. This implies that, once the payback period curve approximately known, the optimisation algorithm can be configured to possibly successfully ignore local minima and find the absolute minimum from any initial value. The last optimisation successfully finds the correct minimum since as given in Figure 5-46. This is due to the fact that, from an initial value of 4 000 W, the first encountered local minimum is also the absolute minimum.

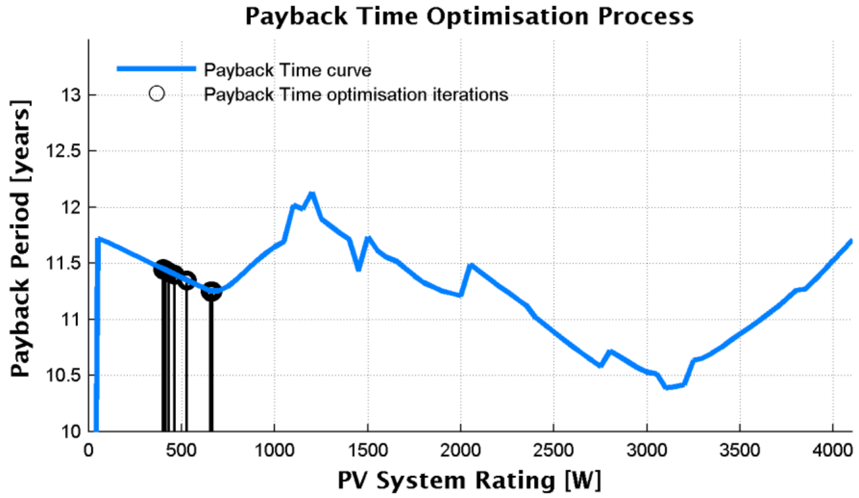

Figure 5-44 Optimisation algorithm progress for case study 5 (initial value 400 W)

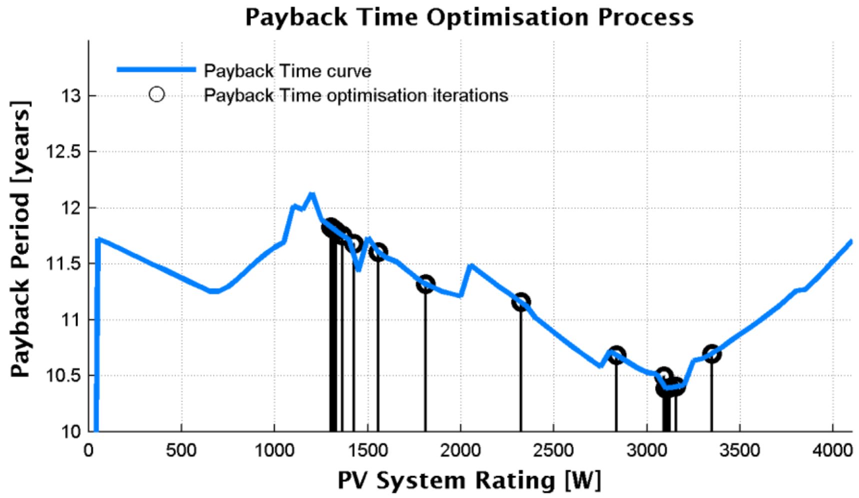

Figure 5-45 Optimisation algorithm progress for case study 5 (initial value 1 300 W)

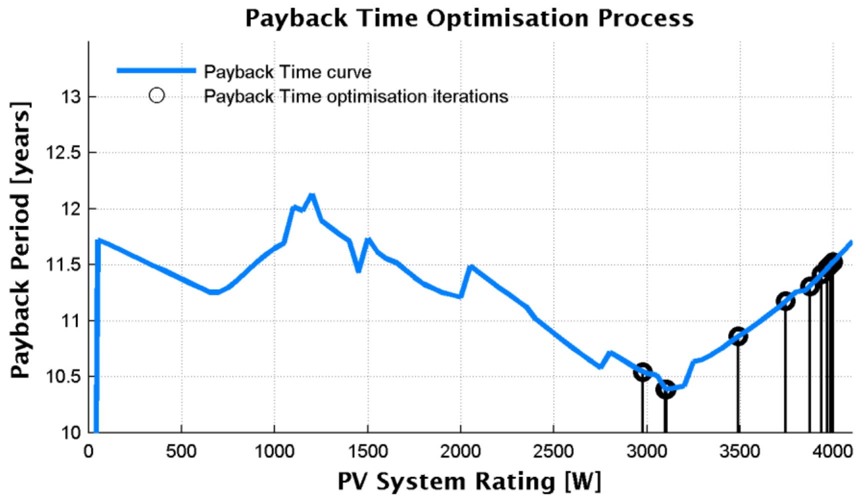

Figure 5-46 Optimisation algorithm progress for case study 5 (initial value 4 000 W)

5.2.8.3 Analysis

Due to the fact that TOU tariffs are present, schedulable loads can be rescheduled to save costs before any PV system has been installed in the residence. This is indicated in Figure 5-47 and Figure 5-48, showing how schedulable loads are clearly rescheduled to save costs on electricity expenses before a PV system is been installed. The financial savings achieved by this optimisation is given in Table 5.8. Therefore the savings achieved by the PV system is not measured against the electricity cost of a residential energy system where no PV system has been installed, but against a residential energy system where no PV system is installed and where schedulable loads have been optimised to minimise costs.

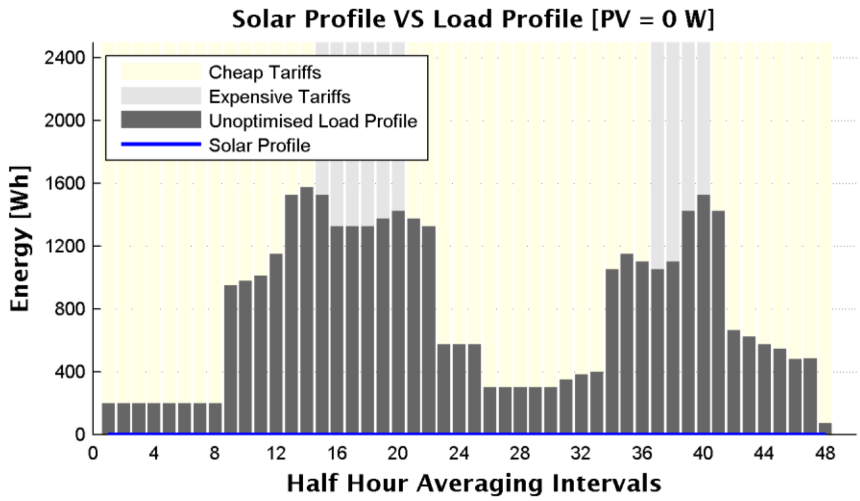

Figure 5-47 Unoptimised load profile graphed against the TOU tariffs for case study 5

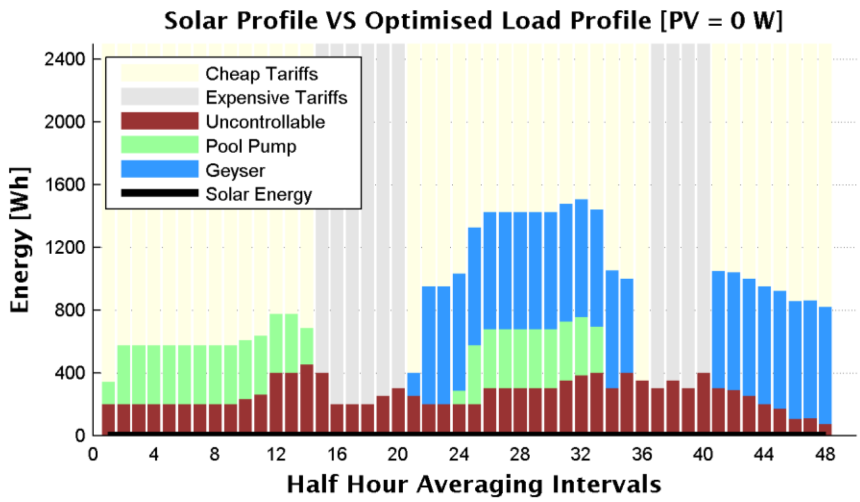

Figure 5-48 Optimised load profile graphed against the TOU tariffs for case study 5

Table 5.8 Savings achieved by optimising load schedules of schedulable loads

Parameter	Graph
Initial residence electricity cost	R44.11 per day
Electricity cost after load schedule optimisation	R38.86 per day
Savings due to load scheduling	R5.25 per day

Before inspecting the how the starting times of schedulable loads are optimised, an important trade-off must be discussed. This concerns the load scheduling optimisation with TOU tariffs. An example is given of why the load scheduling optimisation is more complex when TOU tariffs are present. A significant amount of energy is collected by the PV system during the period where the expensive morning peak tariffs are charged. In this case study, no remuneration is given for the excess energy exported to the grid connection. The objective function of the load scheduling algorithm is to minimise the electricity cost of the residential energy system, not to maximise the use of collected PV system energy. If any surplus energy from the PV system is available, using that surplus energy would ensure savings. But if a rescheduled load profile requires more energy than what the PV system can provide, electricity from the expensive tariff is used. In this simulation, the scheduling algorithm avoided using the surplus energy for the 1 000 W PV system (Figure 5-49) but used it at the cost of also using expensive electricity for the 2 000 W and 3000 W systems (Figure 5-50 and Figure 5-51).

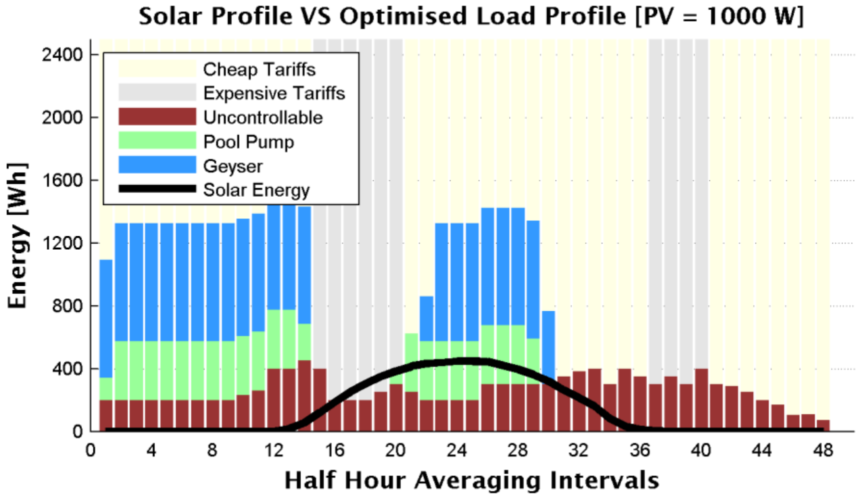

Figure 5-49 Optimised Load schedule in for a residence with a 1 000 W PV system

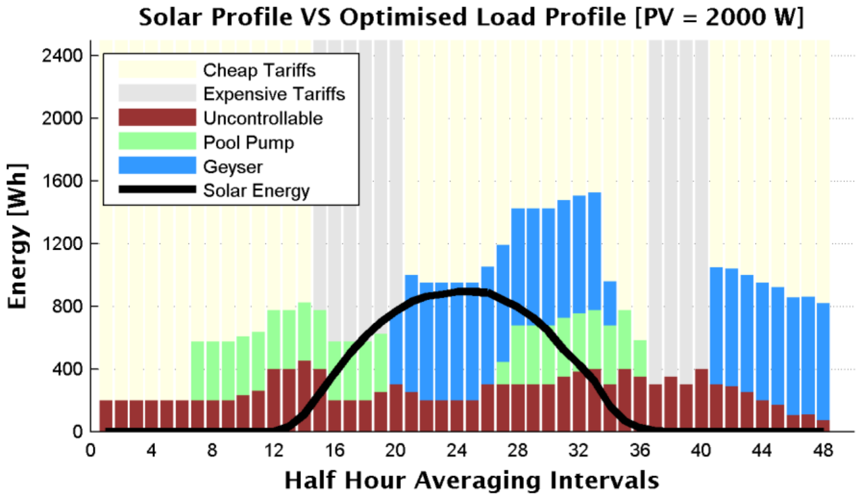

Figure 5-50 Optimised Load schedule for a residence with a 2 000 W PV system

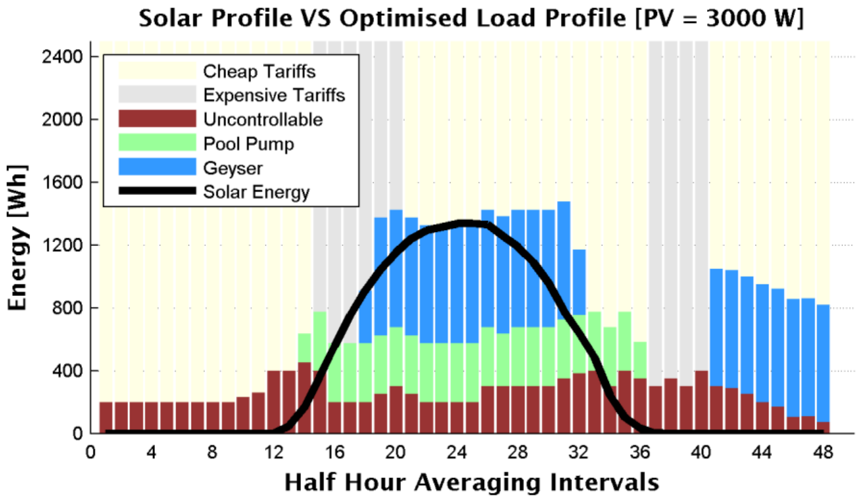

Figure 5-51 Optimised load schedule for a residence with a 3 000 W PV system

As in case study 4, it is useful to consider the utilisation curves of the PV for the normal tariff period K_1 and the expensive tariff period K_2, as shown in Figure 5-52 and Figure 5-53. As observed from Figure 5-52, the utilisation of PV system energy during the cheaper tariffs is effective up to a PV system rating of 3 000 W. An interesting observation is made from the utilisation curve of the solar profile in K_2, as shown in Figure 5-53, where the utilisation factor suddenly drops on two occasions around 1 000 W. This drop is most likely caused by the free energy/cheap energy trade-off as previously discussed.

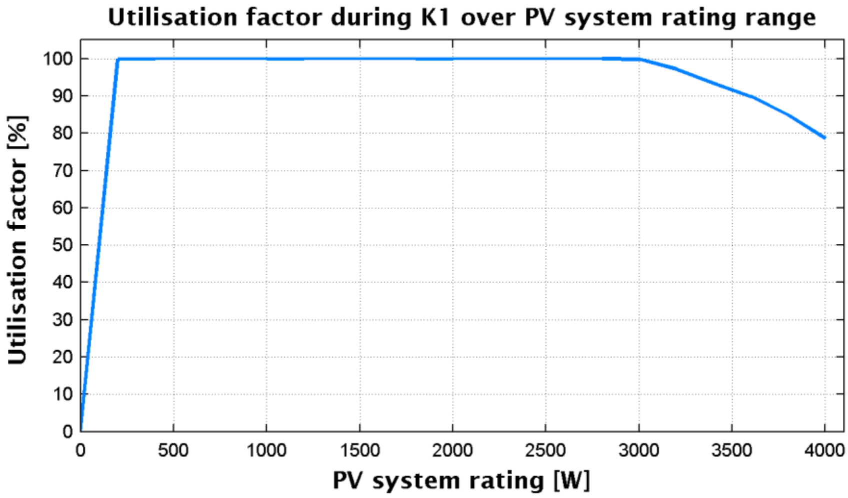

Figure 5-52 Utilisation factor for the K_1 tariff for case study 5

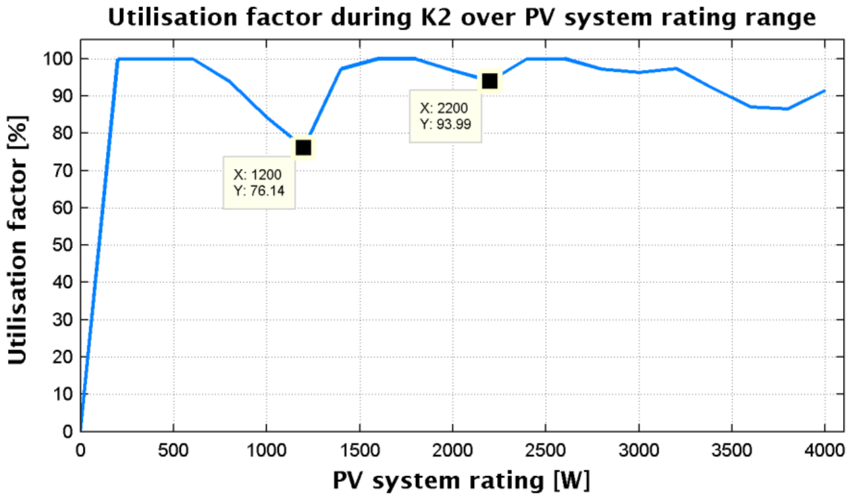

Figure 5-53 Utilisation factor for the K_2 tariff for case study 5

Following the discussions on load schedule optimisation, the payback period of the residential energy system with a non-optimised load schedule is compared to the payback period of the residential energy system with an optimised load schedule in Figure 5-54. It can be seen that the optimised load schedule has an incrementally longer payback period at around 1 000 W. This suggests that the dip in utilisation function observed in Figure 5-53 is caused by the load scheduling optimisation failing to find the optimal schedule for the system.

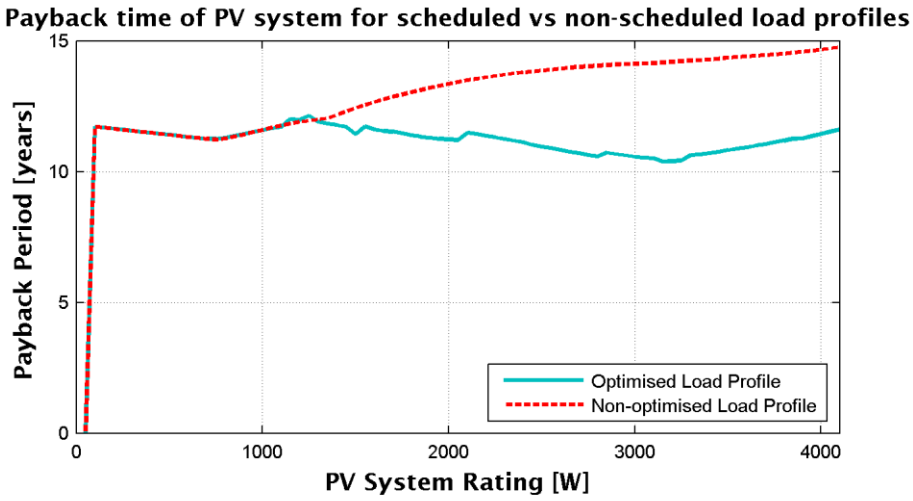

Figure 5-54 Comparison of payback time for non-optimised and optimised load schedules

The optimal payback period at 3 097 W in Figure 5-54 indicates that it has an even shorter payback period than the 676 W system from case study 4. This shows the power of the combined factors of decreasing per-unit cost and improvement of utilisation factor through improved load scheduling.

5.2.9 **Case study 6**

5.2.9.1 Inputs Parameters

This case study investigates the effect of a feed-in tariff on payback period. The input parameters used in this study are

- *Load profile* – The daily load profile as set out in Figure 5-4
- *Solar profile* – The daily solar profile as set out in Figure 5-14
- *PV system cost* – The cost as given in (5.1)
- *Load schedule optimisation* – Not applied
- *Consumption tariffs* – R1/kWh
- *Feed-in tariff* – Multiple flat tariffs

5.2.9.2 Results

Payback period curves are shown in Figure 5-55 for the following feed-in tariffs: 0c, 25c, 50c, 75c and 100c. The results for the 0c, 25c show an initial lowering in payback period, followed by an increase. The 50c curve shows an initial decrease until 676 W, then an increase until about 2 100 W, then decreases again. The 75c curve shows a noticeable change in gradient at 1 000W to about 1 700W, but the payback period consistently decreases. For the 100c curve, payback period is a straight decreasing function.

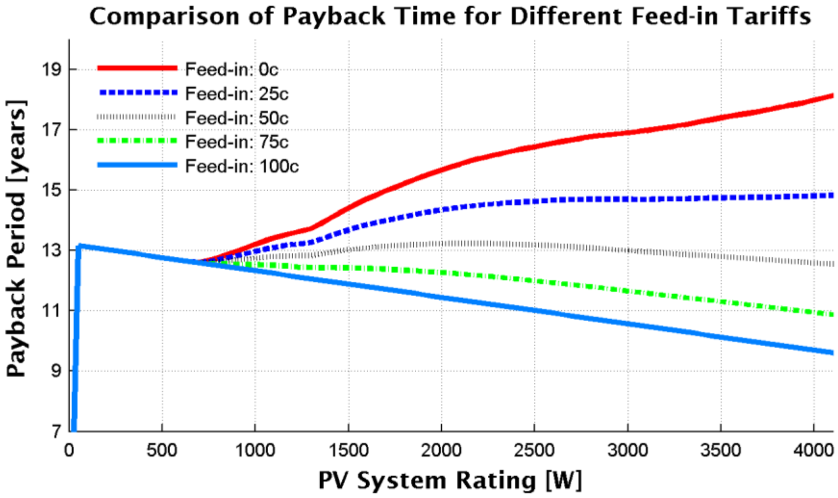

Figure 5-55 Payback time plots for 0c, 25c, 50c, 75c and 100c feed-in tariff simulations

The PV system rating optimisation may find the wrong optimal values depending on the curve and the initial value. The PV system rating with minimum payback period is always successfully found for the 0c and 25c curves, which has a single minimum. The system rating optimisation attempts for the 25c feed-in tariff is shown in Figure 5-56.

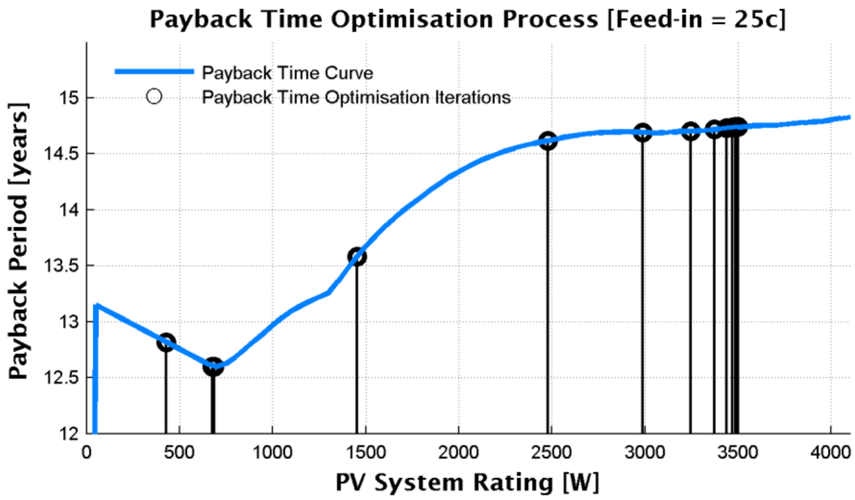

Figure 5-56 Optimisation algorithm progress for feed-in tariffs of 25c (initial value 3500W)

The curve for the 50c feed-in tariffs has two minima and the wrong minimum may be found depending on the initial starting point of the optimisation. With an initial value of 3 000 W the correct PV system rating is found, as shown in Figure 5-57. With an initial value of 2 000 W, the wrong value is found, as shown in Figure 5-58.

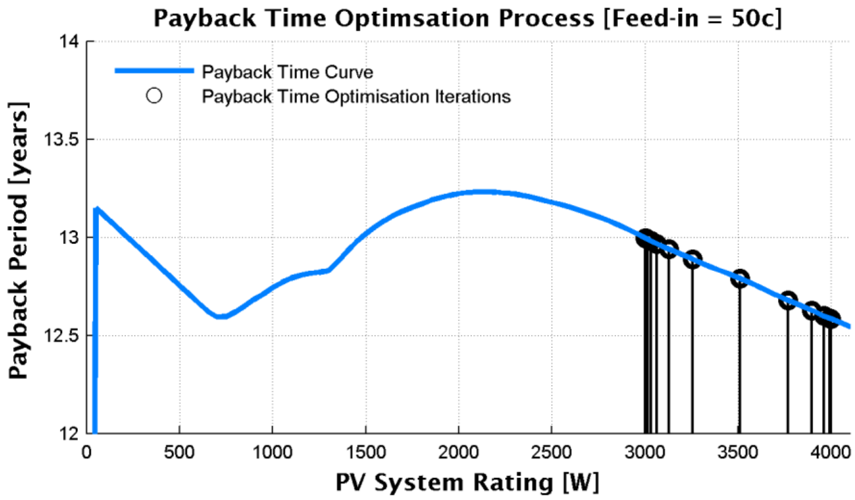

Figure 5-57 Optimisation algorithm progress for feed-in tariffs of 50c (initial value 3 000 W)

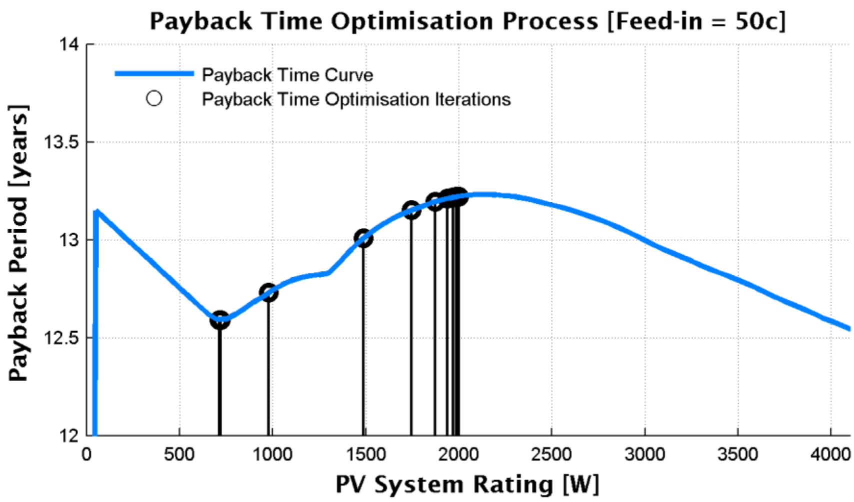

Figure 5-58 Optimisation algorithm progress for feed-in tariffs of 50c (initial value 2 000 W)

The payback period curves for the 75c and 100c feed-in tariff systems each have only single minima, which the optimisation algorithm is successfully able to detect. The optimisation process for the 75c feed-in tariff is shown in Figure 5-59.

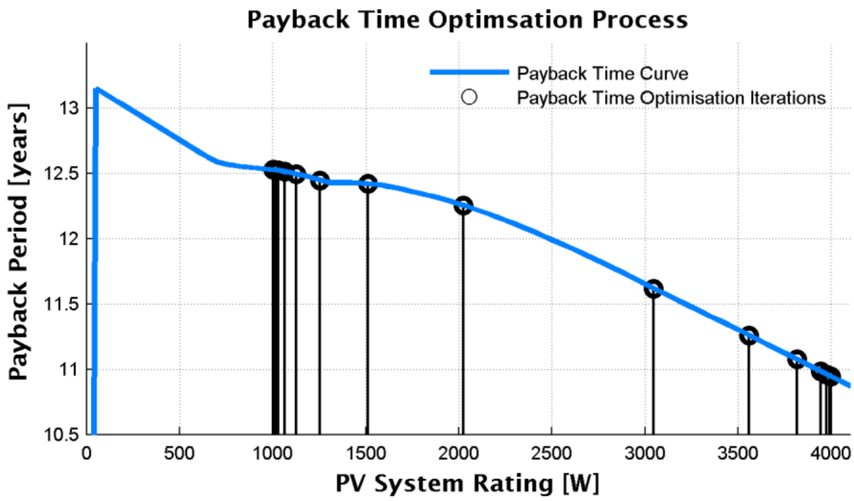

Figure 5-59 Optimisation algorithm progress for feed-in tariffs of 75c (initial value 1 000 W)

5.2.9.3 Analysis

The challenge for this case study is to determine the exact reason for the form of the payback period curvatures noted in the 25c, 50c, 75c and 100c curves. The effect of the feed-in tariff on the increasing or decreasing gradient for the payback is derived for formula (3.104). The equation is repeated here to aid the discussion:

$$\frac{\left(F_U(S_{R2}) - F_U(S_{R1})\right)}{F_U(S_{R1}) + \frac{\frac{r^E}{r^I}}{(1-\frac{r^E}{r^I})}} > \frac{S_{pu}(S_{R2}) - S_{pu}(S_{R1})}{S_{pu}(S_{R1})}$$

The utilisation factor for this case study is also important. The utilisation factor function for this case study is the same as for case study 1 and is shown in Figure 5-60.

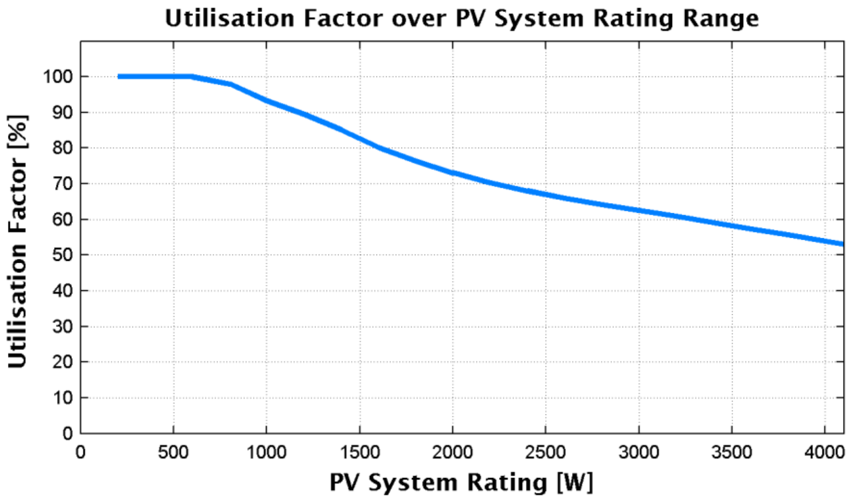

Figure 5-60 Utilisation factor for case study 6

To understand the curvature of the payback curve for the 100c (i.e. $\frac{r^E}{r^I} = 1$), consider the payback equation derived for feed-in systems given in (3.80). The formula is repeated in (5.7) to aid the derivation, and the value $\frac{r^E}{r^I} = 1$ is substituted into the equation:

$$\begin{aligned} T_{pb} &= \frac{S_{pu}(S_R)}{E_{NPV}[F_U(S_R)r^I + \left(1 - F_U(S_R)\right)r^E]} \\ &= \frac{S_{pu}(S_R)}{E_{NPV}r^I} \end{aligned} \tag{5.7}$$

Given that $S_{pu}(S_R)$ is a decreasing function as shown as part of the input parameters, the payback period should simply be that decreasing function scaled with $\frac{1}{E_{NPV}r^I}$. This simple concept explains the curvature of payback period graph for the 100c feed-in tariff.

The focus now shifts to the curvature of the 25c, 50c and 75c feed-in tariff payback period simulations. If the curvature of one of the feed-in tariffs is fully understood, the reasoning will hold for the other tariffs. The 50c tariff is chosen, as its payback period showcases the most peculiar behaviour as seen in Figure 5-55: An initial decrease, then an increase, and finally a decrease. To explain this, first the total system cost and savings achieved per day is considered. These are the two factors to calculate payback period in a simple manner, as shown in (3.44). The two values are graphed in Figure 5-61. A glance at the graphs give no immediate intuitive clue as to why the 50c feed-in tariff would lead to the payback period curvature as found. Having found little to no clues from the savings per day or the utilisation graphs, the analysis is further dependent on (3.104) to explain the payback period curvature.

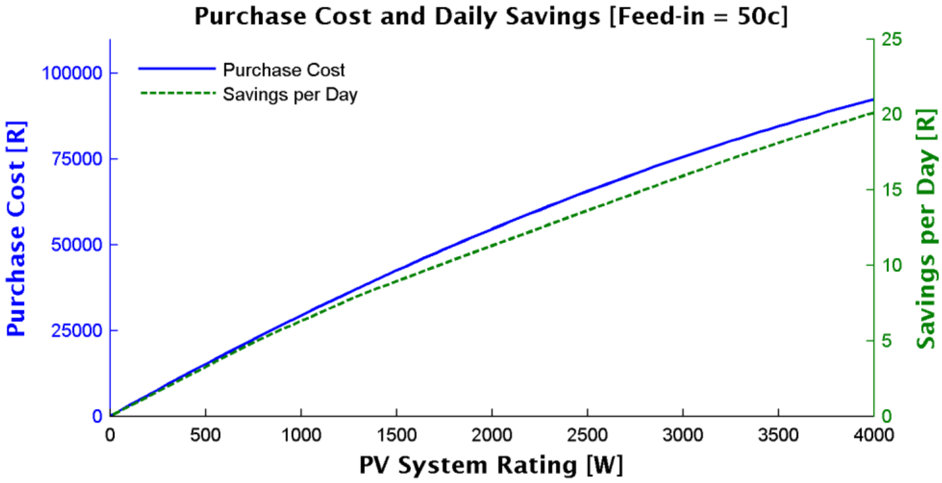

Figure 5-61 Comparison of investment cost and daily savings with a 50c feed-in tariff

To prove that equation (3.104) gives the condition for decreasing payback period, the left and right side of the equation is plotted and shown alongside the payback period in Figure 5-62. The left side of (3.108) is given by the "Utilisation normalized decrease" and the right side by "Per-unit cost normalized decrease". It can be seen that when the left-hand side becomes smaller than the right-hand side as happens at 676 W and 2 100 W, the payback period increases. This proves that the relationship established between the solar profile, the local consumption as specified by the load profile, the influence of feed-in tariffs and the cost of the PV system.

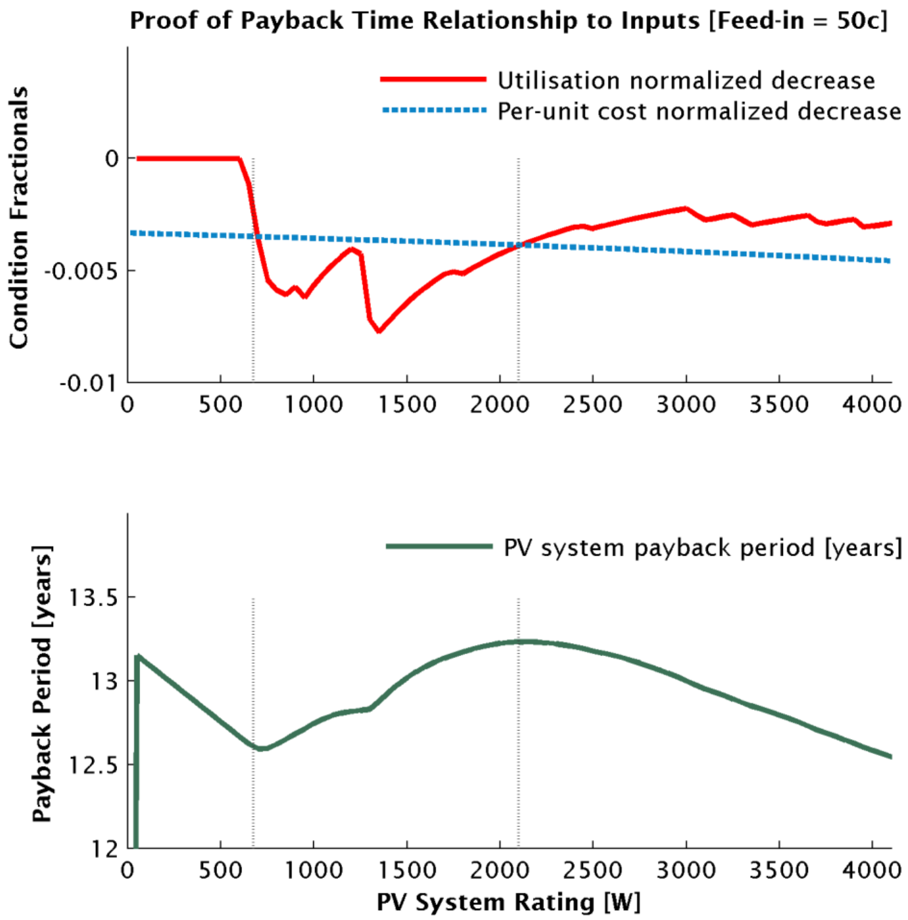

Figure 5-62 Input parameter relationship to payback time

Exactly the same reasoning can be made for the system with the 25c and 75c feed-in tariff. The "Utilisation normalised decrease", as given for the 50c feed-in in Figure 5-62, is repeated in Figure 5-63 with this curve plotted for the 0c, 25c, 50c, 75c and 100c feed-in tariffs. In previous case studies, as long as the utilisation factor function remained constant or its decreasing gradient was not too severe, the payback period would decrease. The results in Figure 5-63 show that as feed-in tariffs increase, the contribution of the normalised utilisation function to determine an increasing or decreasing payback period as given by (3.104), decreases. When the feed-in tariff equals the consumption tariff, the normalised utilisation factor function gradient does not contribute the payback period increase/decrease condition. Feed-in tariffs can therefore greatly assist to decrease the need to effectively utilise the energy collected by the PV system.

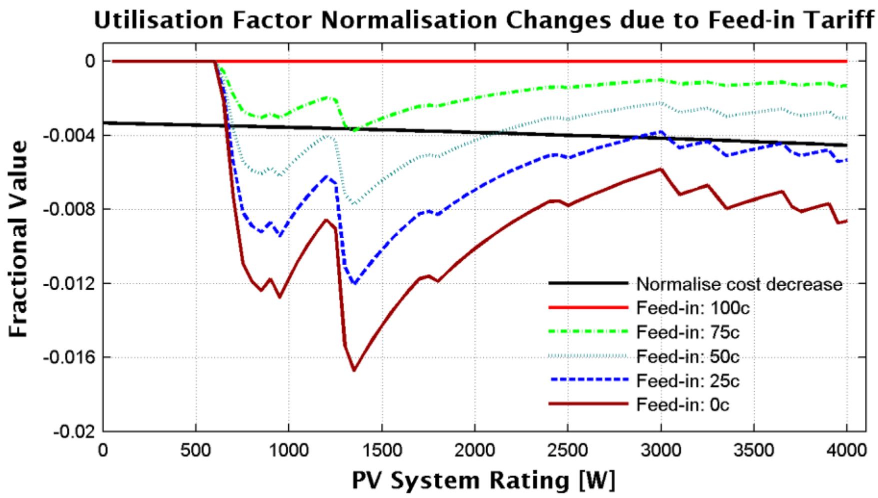

Figure 5-63 Feed-in tariffs influence the values that determine decreasing payback time

5.2.10 **Case study 7**

5.2.10.1 Input Parameter

This case study investigates the economic implications of including a battery in the system. The battery that is used in this study is chosen to be a more expensive deep cycle battery. The input parameters used in this study are

- *Load profile* – The daily load profile as set out in Figure 5-4
- *Solar profile* – The daily solar profile as set out in Figure 5-14
- *PV system cost* – The cost as given in (5.1)
- *Battery system cost* – The cost as given in (5.2)
- *Load schedule optimisation* – Not applied
- *Consumption tariffs* – R1/kWh
- *Feed-in tariff* – R0/kWh

5.2.10.2 Results

The payback period result is given as a surface graph in Figure 5-64. The payback period is dependent on two dimensions in this case study: The rating of the PV system, and the rating of the battery system. The payback periods as found are impractical, but the results are given in the interest of analysing and interpreting it. The graph cuts off any values larger than 50 years.

The PV and battery system rating with the minimum payback period is a 0Wh battery system rating and 676 W PV system, with a payback period of 12.59 years.

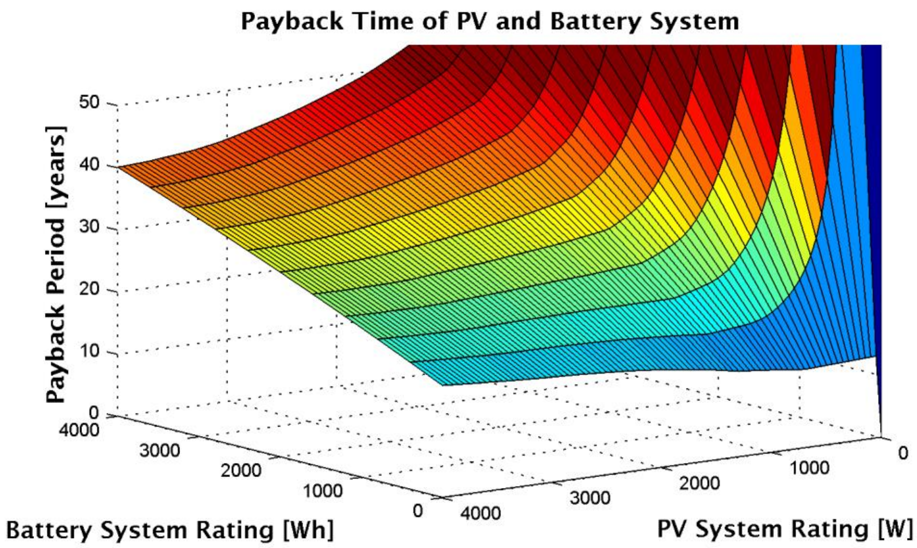

Figure 5-64 Payback time for a combined PV and battery system

5.2.10.3 Analysis

The payback period found in Figure 5-64 shows increasing payback period for higher rated battery systems. The battery system in its own does not create any savings, therefore the payback period of battery systems combined with small PV systems approach infinity. The batteries improve their economic viability when coupled with PV system of a more substantial rating.

An analysis is done to show how a battery system assists a PV system to minimise electricity cost to the residence. This discussion will make use of the results for 3kW PV system as an example. If only the PV system's effect is considered on the load profile, the energy withdrawn from the grid is given in Figure 5-65. In this case study no feed-in tariffs are present and no remuneration is received for the substantial energy fed back into the grid.

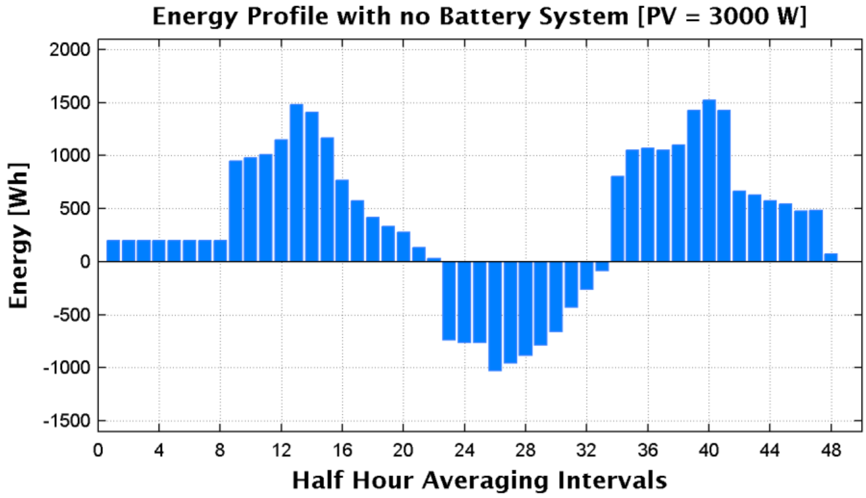

Figure 5-65 Energy is drawn from and pumped back into the grid throughout the day

With the addition of the battery, energy from the solar energy that would have been exported to the grid is stored. This energy is then used to offset energy usage at a later time during the day. The effect of the battery on the same load/PV profile is shown in Figure 5-66 with the 3 200 Wh battery system rating. The allowed depth-of-discharge of 20% gives the battery an effective capacity of 640 Wh. The battery starts the day at half the charged capacity (this is chosen to be the convention). To ensure satisfactory performance each day, the net energy from the battery should be zero, as shown in (3.29). Therefore the battery discharges at a small tempo for the first 23 half-hours of the day. This decreases the energy that needs to be purchased from the grid. As soon as surplus energy becomes available from the PV system, the battery utilises this energy and charges. This decreases the energy exported into the grid over midday, as shown in Figure 5-66. The battery recharges with this energy as shown in Figure 5-67. The battery continues to lessen the load for the remainder of the day. The battery returns to the initial state-of-charge at the end of the day.

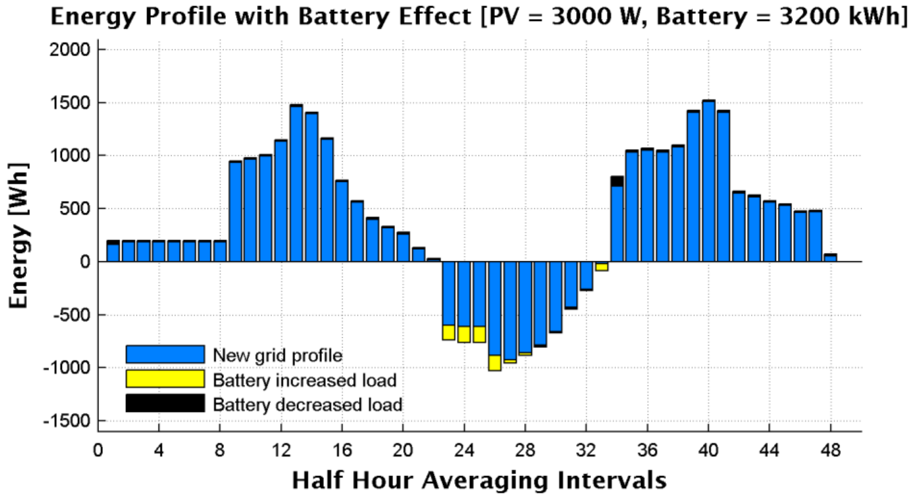

Figure 5-66 The battery captures PV energy and uses it to offset energy purchased from the grid

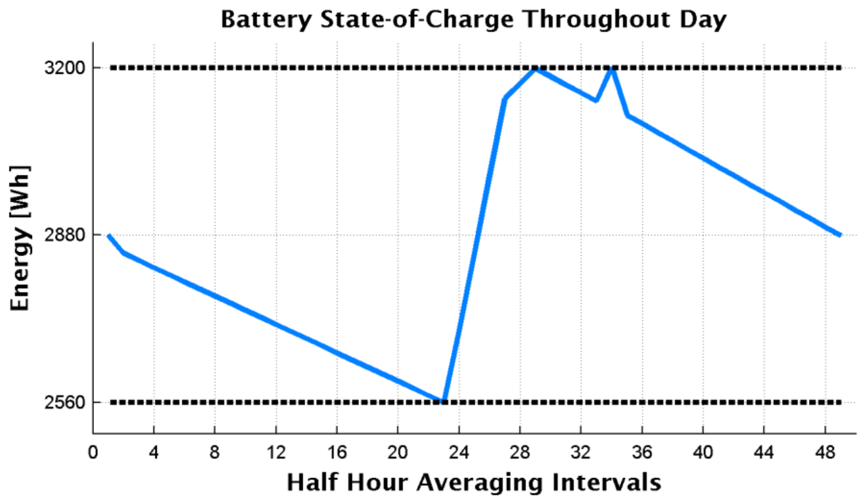

Figure 5-67 Battery state-of-charge show utilisation of PV energy over mid-day

The energy that the battery can shift throughout the day can be more significant if higher rated battery systems are installed. It should be noted that the battery's lifetime is limited by the amount of charge cycles, implying that charging and discharging at such a tempo would not be optimal to sustain a long lifespan. This factor should be considered when a detailed study is done on optimal rating of battery systems.

5.2.11 **Case study 8**

5.2.11.1 Input parameters

This case study simulates the performance of a PV system using an annual load and solar profile. The input parameters used in this study are

- *Load profile* – The summer load profile as given by Figure 5-9 and the load profile as given by Figure 5-13
- *Solar profile* – Annual measured values which is given graphically in Appendix Figure C.1 and Appendix Figure C.2
- *PV system cost* – The cost as given in (5.1)
- *Load schedule optimisation* – Not applied
- *Consumption tariffs* – R1/kWh
- *Feed-in tariff* – R0/kWh

5.2.11.2 Results

The payback period of the system show that it features the same curvature as found in previous results such as case study 1: An initial decline in payback period, where it reaches a minimum, and then payback period increases.

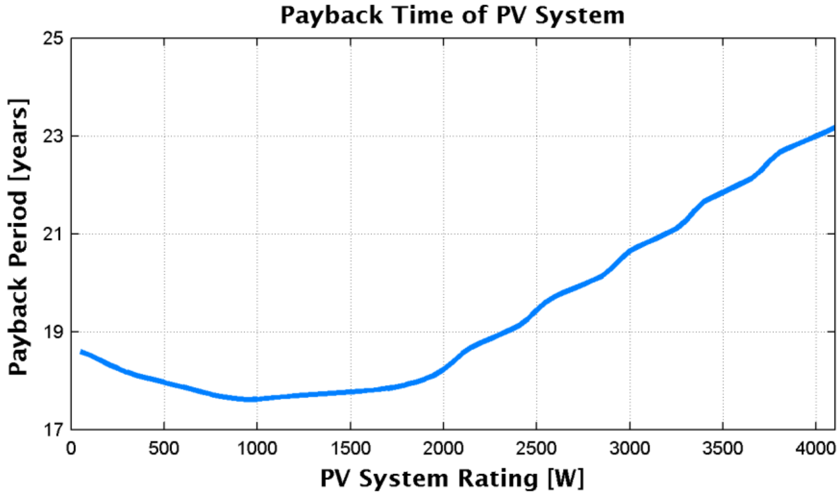

Figure 5-68 Payback time for PV system for case study 8

The optimisation is able to determine the optimal system rating for an annual profile. The iterations of the optimisation are shown in Figure 5-69. The optimal PV system rating is found to be 961 W and the payback period about 17.61 years.

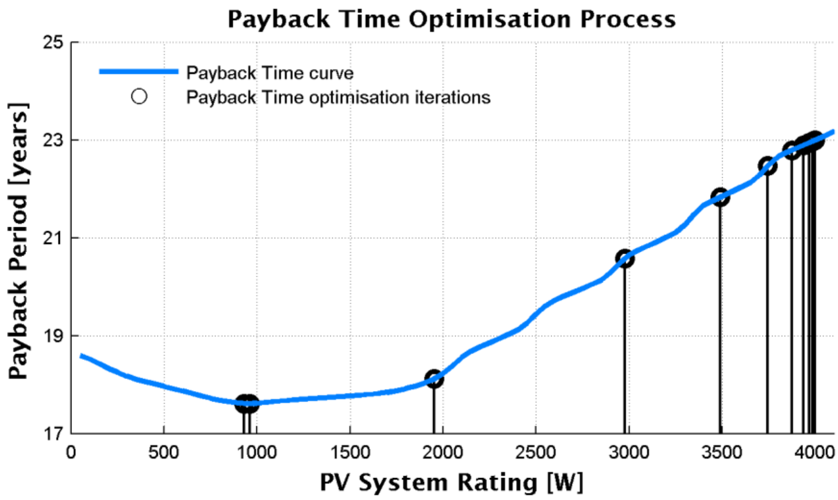

Figure 5-69 Optimisation algorithm progress for case study 8 (initial value 4 000 W)

5.2.11.3 Analysis

The curvature of the payback period has been seen before and properly analysed during the case studies with daily load and solar profiles. A noticeable change in the results is increased payback period. The main reason for the increased payback period is the use of an ideal solar profile for previous case studies, whereas in this study a real solar profile was used. The energy collected by the real system is much less on average over the course of a year, as less energy is generated due to non-ideal weather conditions such as cloud cover. Therefore much less energy is generated at the same cost of the PV system as in previous case studies. As discussed for the input parameters, the energy in the daily solar profile used for previous case studies is 6.54 kWh/day, which is significantly more than for the real annual profile with an average of 4.64 kWh/day.

5.2.12 **Case study 9**

5.2.12.1 Input parameters

This case study simulates the performance of a PV system using an annual load and solar profile and applies load schedule optimisation for each day of the year. The input parameters used in this study are

- *Load profile* – The summer load profile as given by Figure 5-9 and the load profile as given by Figure 5-13

- *Solar profile* – Annual measured values which is given graphically in Appendix Figure C.1 and Appendix Figure C.2
- *PV system cost* – The cost as given in (5.1)
- *Load schedule optimisation* – Applied
- *Consumption tariffs* – R1/kWh
- *Feed-in tariff* – R0/kWh

5.2.12.2 Results

Simulating the performance of the residential energy system over a range of PV system ratings gives the payback period results as shown in Figure 5-70. Payback period increases for PV systems until a rating of about 3 000 W. At this stage the payback period is about 15.3 years. The payback period increases as the PV system rating increases beyond 3 000 W.

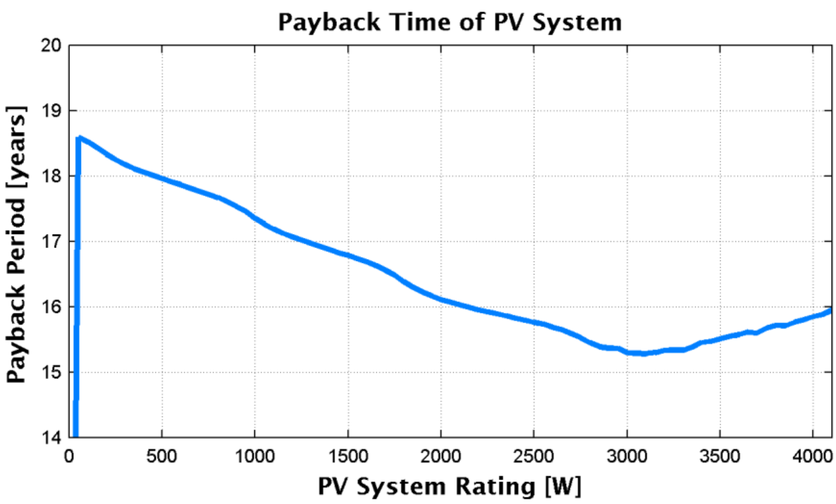

Figure 5-70 Payback time for the PV system for case study 9

The PV system rating optimisation algorithm successfully manages to find the optimal PV system rating. The optimisation algorithms iterations are shown in Figure 5-71. The minimum payback period is 15.26 years, with a PV system rating of 3063 W. With the same load profile and solar profile as case study 8, load schedule optimisation decreased from 17.61 years to 15.26 years, while simultaneously allowing for a higher rated PV system to be installed. The optimisation of the PV system rating in previous case studies completed within less than a minute. This simulation takes about 3 hours to complete.

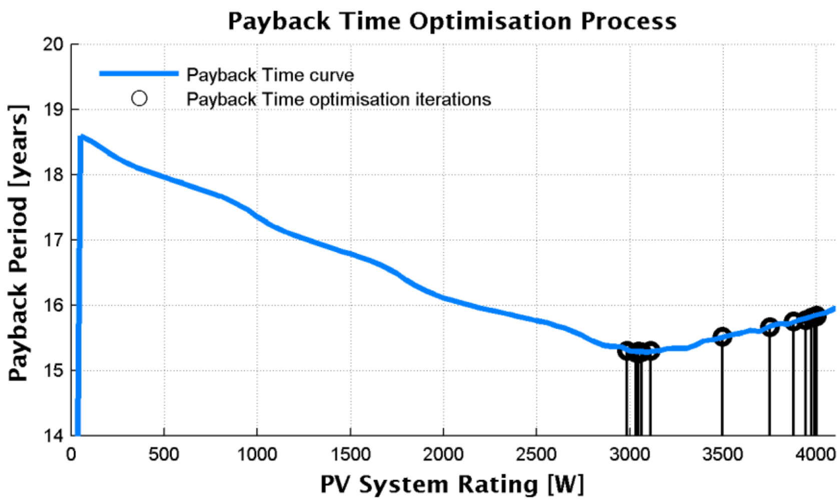

Figure 5-71 Optimisation algorithm process for case study 9 (initial value 4000 W)

5.2.12.3 Analysis

This case study showcases a powerful feature of the simulation: To calculate expected payback period where annual solar and load profiles are used with optimised schedulable load profiles. The curvatures of the payback periods are similar to the payback periods encountered in the daily load and solar profile case study with optimised schedulable load profiles, as in case study 3. The same analysis principles found in case study 3 is applicable here.

The time duration of the optimisation might lead to further considerations regarding the type of optimisation used to find the optimal scheduling algorithm. The reason for the extended duration is that the load schedule optimisation is done for each day of the year. One of two solutions is proposed to this problem. The first is to reconfigure the configuration options of the optimisation to ensure less iteration is required to find the optimal results. The second solution would be to consider using a heuristic algorithm, to ensure that a decent (though not necessary most optimal) solution is found in a shorter amount of time.

5.3 Case study set 2

5.3.1 Introduction

A single case study is presented that uses real, measured residential data for the input parameters. The objectives of this case study is the following:

- To identify residential energy systems with different categories of average energy consumption to compare the payback periods.
- To find the payback period of PV systems in real residential energy systems.
- To use the knowledge gained from case study set 1 to analyse payback period of PV systems in real residential energy systems.

5.3.2 **Input Parameters**

5.3.2.1 Load profile

Attaining a realistic load profile has proved to be a major challenge in the South African context. Very few studies make the data publicly available.

The first attempt was to collect this data from research in the field. Ongoing studies in South Africa do measure the electricity usage of residences, but the data of these studies is inaccessible. Research has been published on top-down methods of generating load profiles, but the common shortcoming is that data required for the inputs is not available, and the outputs that the top-down method generates is not applicable to this study.

The second attempt to find a suitable annual load profile was to collect the raw data from a similar study that has been metering data for some years. In this study, various types of meters are installed in a residence to log major load on-and-off times, as well as total electricity usage. During the process of data processing and validation, the dataset proved too erroneous to extract data specific to this project.

A third solution was to create a load profile from a bottom-up approach. The load profile would assume an average load profile for winter and an average load profile for summer. The derivation of the load profiles would be based on expected appliance usage schedules. The attempt is recollected in Appendix E. The final averaged load profile for summer is given by Appendix Figure E.1and the averaged load profile for winter by Appendix Figure E.2. The load profile did not resemble realistic energy usage. The absences of the many random small appliances in the household, as well as the simplification of loads lead to almost no energy consumption during off peak time and very high consumption during peak times.

A final attempt to acquire a load profile was to establish a confidentiality agreement with the local national electric utility for residential load profile data. Half-hour electric consumption data has been collected from about 700 residences over the course of two years. Data cleansing was applied and confidence levels established with regards to the amount of missing data entries. A final set of 89 house load profiles where the confidence of data (valid data measurements) of more than 98% were chosen as adequate to work from.

Load profiles used for this case study needed to have an average energy consumption of a financially middle or upper class residence. Relevant data for this was acquired from a study in South Africa with residential energy consumption data [162]. This study shows that energy consumption can be divided into four categories, and the two categories containing the largest electricity consumers, respectively uses 28 kWh and 40 kWh per day. Therefore a set of load profiles has been selected with this range of average daily electricity consumption. One load profile from this selection (chosen arbitrarily) is shown in Appendix Figure F.1 and Appendix Figure F.2.

5.3.2.2 Solar profile

The solar profile for this study is based on real collected weather data for Stellenbosch, South Africa. The processing to find the energy collected by the PV system is shown in Appendix C. The final energy collected by a normalised 1kW PV system is given in Appendix Figure C.1 and Appendix Figure C.2.

5.3.2.3 PV system and battery system purchase costs

To understand the payback period of real PV and battery systems, the definition of “costs” of the system is clearly defined here. For this case study, it will include all the necessary components to install a PV system onto a residence, including mounting and brackets, as well as the labour. The exact derivations have been shown in Appendix D. The final PV system per-watt cost is taken from a curve-fit regression polynomial as indicated on Appendix Figure D.4. The battery system cost has been found in the same manner and is shown in Appendix Figure D.7. As the costs are based on real prices for available systems, the PV system price is only defined for PV systems rated higher than 1.5 kW and lower than 5.5 kW.

5.3.2.4 Electricity costs

The electricity tariffs for two cities in South Africa are compared to find realistic tariffs. The first tariffs are taken from the Cape Town electricity tariffs [165]. Cape Town allows residents to offset their electricity purchase with small-scale generation, valid as long as over the course of a day, electricity usage exceeds generation. The tariffs are given in Table 5.9. Johannesburg residents can apply for TOU tariffs [164]. Johannesburg has different tariffs for winter and summer. Three TOU tariffs exist for Johannesburg - a peak, standard, and off-peak period. The exact time at which the residential tariffs are implemented is not specified, but it is specified for industrial systems, and these times will be used here. The tariff is given in Table 5.10.

Table 5.9 Cape Town electricity tariffs

Parameter	Tariff [c/kWh, incl VAT]
Energy charge, for month consumption <600 kWh	179.5
Energy charge, for month consumption >600 kWh	213.90
Feed-in Tariff	64.97

Table 5.10 Johannesburg electricity tariffs

Energy charge	Summer Tariff [c/kWh]	Winter Tariff [c/kWh]
Peak	123,29	294,04
Standard	97,53	117,41
Off-peak	76,73	82,33

The tariffs are implemented with block tariffs. For the case study at hand, the block tariff is ignored. The tariffs chosen for this set of case studies are based on the Cape Town tariffs, but the feed-in tariff is taken as zero. This is shown in Table 5.11.

Table 5.11 Tariffs as used for the current case study

Parameter	Tariff [c/kWh, incl VAT]
Energy charge	180
Feed-in tariff	0

5.3.2.5 Load schedule optimisation

Load schedule optimisation will not be implemented in this case study.

5.3.2.6 Battery parameters

A battery will not be included in this case study.

5.3.3 **Case study 10**

5.3.3.1 Input parameters

This case study will investigate the payback period of different residential energy systems using input parameters collected from real environments in South Africa:

- *Load profile* – Load profiles of 4 households, with respective average daily energy consumption of 20 kWh/day, 31 kWh/day, 32 kWh/day and 40 kWh/day
- *Solar profile* – Annual measured values which is given graphically in Appendix Figure C.1 and Appendix Figure C.2
- *PV system cost* – A third order cost function, as given in Appendix Figure D.4
- *Load schedule optimisation* – Not applied
- *Consumption tariffs* – R1, 80/kWh
- *Feed-in tariff* – R0/kWh

5.3.3.2 Results and Analysis

The comparison of the payback periods and utilisation factors is shown in Figure 5-72 and Figure 5-73. Observations based on the comparison between the respective payback period and utilisation rates are made.

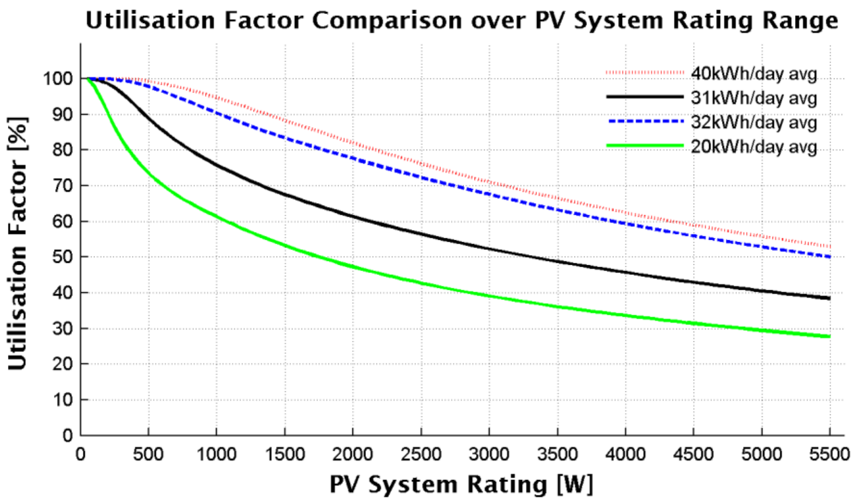

Figure 5-72 Comparison of payback time for various residences

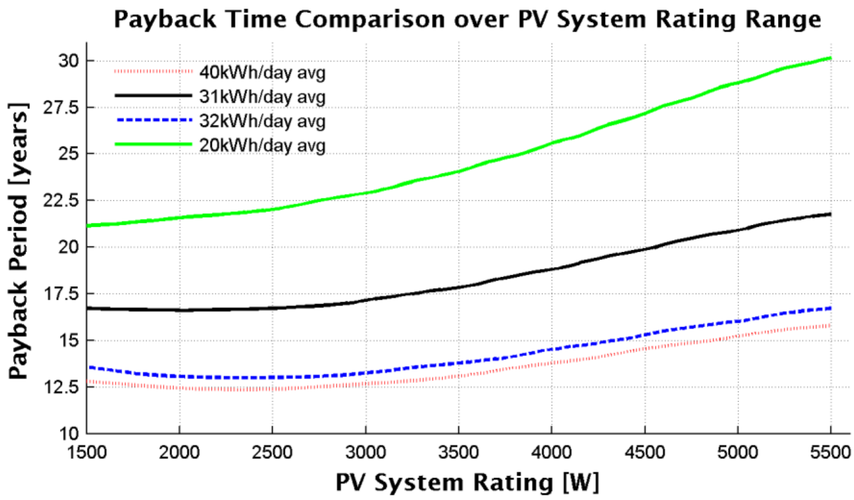

Figure 5-73 Comparison of utilisation factor for various residences

The PV system investment cost is only valid for PV systems rated higher than 1.5 kW and lower than 5.5 kW. Only that range has been included in the graph.

The utilisation factor functions for all residences showcase aspects pointed out during the exploratory case studies in set 1. For low rated PV systems, the utilisation factor is 100%. As soon as the PV system rating increases so that the PV system energy is greater than the load profile, the utilisation factor starts decreasing. The payback periods of the 31 kWh/day, 32 kWh/day and 40 kWh/day residences as given in Figure 5-73 initially decreases, reaches a minimum and the increases. Two important observations regarding the payback periods of the residential energy systems can be made. The first is that the payback period for the 20 kWh/day residence most likely also follows the same curve as the payback period for other residences. The minimum payback period is for the 20 kWh/day residence is a PV system rated lower than 1500 W, which is unavailable commercially and thus not shown on the graph. The second observation is that payback period varies very little over a wide range of PV system ratings around the optimal system rating. Consider as an example the residence with the 32 kWh/day energy consumption The range over which the PV system for the residence remains within 10% of a year around the minimum payback period is almost 1kW – from about 1 950 W to 2 800 W, as indicated on Figure 5-73. This is most likely due to the fact that the load profile in this case study is a real load profile with a much higher variability between daily and half-hour energy consumption measurements than in previous case studies. The effect of variability in the load profile and the effect of payback period can be a focus of a further study. Another conclusion that can be made is that this result necessitates research into alternative financial indicators to determine economic viability of PV systems.

The optimisation to find minimum payback period and the related PV system ratings proved successful, even with the new third-order PV system rating cost-per-watt equation. The results are given in Table 5.12.

Table 5.12 Optimisation results

Residence average consumption [kWh/day]	Minimum payback period [years]	Associated PV system rating [W]
20	Not in range	n/a
31	16.75	
32	12.99	2 337
40	12.4	2 250

Two important observations are made when comparing the payback periods of different residences. These observations are:

- Observation 1: For two residences with very similar energy consumption, the 31 kWh/day residence and 32 kWh/day residence's payback period varies significantly.

The difference here is the **instantaneous value** of utilisation factor.

The instantaneous utilisation factor plays a role in calculating payback period, as mathematically shown in (3.75). Compare the payback period results of the 31 kWh/day and 32 kWh/day. Although the daily energy use of the two residences differs with about 1kWh, the payback periods differs greatly. This can be seen from the utilisation curves in Figure 5-73. As an example, take the PV system rated at 2 000 W: The utilisation of the 32 kWh/day profile is about 0.77 and the utilisation factor of the 31 kWh/day profile is about 0.61. This difference leads to the payback period for the PV systems for these residences differ with more than two years at any given PV system rating, as seen in Figure 5-72. Practically, this implies that the 32 kWh/day residence makes more optimal use of the energy generated by the PV panels, whilst the 31 kWh/day residences load profile makes less effective use of this energy.

The conclusion from this is that similar energy consumption is no guarantee of similar optimal payback periods.

- Observation 2: For two residences with very different energy consumption, the 32 kWh/day residence and 40 kWh/day residence's payback period is very similar.

The difference here is the **rate of decrease of utilisation factor** relative to the current value of the utilisation factor.

The rate at which the utilisation factor is decreasing plays a role in determining what the optimal PV system rating is for minimum payback period, as proven mathematically in (3.98). The utilisation curves of the residences with 32 kWh/day and 40 kWh/day energy consumption follows each other extremely closely, albeit with a constant difference, as seen in Figure 5-73. The *instantaneous difference* leads to a difference in the payback period, while the *gradient similarity* leads to the residences having almost the same optimal PV system rating, as can be seen in Figure 5-72.

The conclusion is therefore that high energy consumption is no guarantee of requiring a higher rated PV system for optimal payback period

6 Recommendations and Conclusion

6.1 Conclusions

An overview is presented to show how the thesis addressed the objectives as set out in Chapter 1. These were:

- Creating a mathematical model that is able to contain the required parameters to model a residential energy system.
- Develop simulation software to calculate the performance of the residential PV system, using the developed mathematical model.
- Analysing, understanding and logically explaining observations made through simulation of energy flow in residential energy systems with PV installed.
- Investigate the possibility of using an optimisation algorithm to find the optimal PV system rating with minimal payback time.

6.1.1 Create a mathematical model that is able to accept the required parameters to model a residential energy system

A comprehensive literature review regarding the various components of a PV system that should be included in the mathematical model was presented. A mathematical model was created to model the residence, the load profile, the PV system, energy storage, and the grid connection. The concept of utilisation factor was presented and mathematically modelled.

A novel set of equations is presented to show how the payback period is deduced from the per-watt PV system cost function and the utilisation factor function. The process to arrive at this conclusion is summarised here: First a payback period equation is developed for a generic residence in terms of the utilisation factor. Common tariff structures scenarios are presented and it is shown that the payback equation can be simplified according to the tariff structures. An investigation is made to determine what the condition is for payback period to decrease or to increase. These conditions are simplified for common tariff structures.

Through this work, a direct link is established between the load profile of the residence, the solar profile of the local climate, and the purchase price of PV systems. A discussion on how this information can be used to determine a specific residence's compatibility with solar and the expected economic impact is given in the *Further Work* section in Recommendations.

6.1.2 **Develop simulation software to calculate the performance of the residential PV system, using the developed mathematical model**

An extensive software application was developed to implement the mathematical model and determine PV system performance over a range of PV system ratings. The development and layout was discussed in Chapter 4. The software application is designed to be modular and the re-use code for common functionalities. The application accepts relevant inputs to address the given use cases and calculates the performance and savings achieved by the PV system. A data structure for the results was designed and is used extensively to output the results in both numeric and graphical form for the analysis done in this project.

6.1.3 **Analysing, understanding and logically explaining observations made through simulation of energy flow in residential energy systems with PV installed**

A selection of case studies in chapter 5 demonstrates the direct relationships that can be observed between input parameters and results for PV system performance. The first set of case studies uses simplified (but realistic) input data to present a clear link between the input and results of the simulation. Progressively the case studies have more complex inputs whilst building upon observations from previous case studies to identify new trends and patterns. After concluding the case study set with simplified parameters, a case study using realistic data is done for four different residences with various different energy consumptions. The results are compared and observations made to reflect how the mathematical model and patterns observed in the simplified case studies provide the necessary groundwork to interpret the results.

An extensive analysis API has been developed to interpret the data from the simulation and provide the results in numeric and graphical form. The API is used in chapter 5 to provide the results of case studies in an insightful manner. Using this API, the important aspects of the results are clearly shown and discussed.

The case study results confirmed the observations made whilst developing the mathematical model with regards to the payback period of PV systems. The mathematical model showed that the value and rate of change of the utilisation factor determine is compared to the to the value and rate of change of the per-unit cost of the PV system to determine whether the payback period of the PV system is increasing or decreasing.

It is observed that scheduling loads to minimise the electricity cost to the client dramatically increases the PV system rating where payback period is a minimum. The schedulable loads ensure good local utilisation for the energy generated from higher rated PV systems.

6.1.4 **Investigate the possibility of using an optimisation algorithm to find the optimal PV system rating with minimal payback time**

The optimisation extends the work already presented on the PV system performance analysis. The optimisation is included in the mathematical modelling presented in chapter 3 to specify the objective function and constraints of the optimisation. The optimisation is integrated into the software application as presented in chapter 4. It's found that the optimisation can find the optimal PV system rating for minimum payback period, in chapter 5. It is shown that the implemented payback period function succeeds when only one local minimum exists. Complications arise when multiple local minima exist, e.g. in the case where the schedules of schedulable loads are optimised. A discussion on how optimisation can be implemented differently to be more robust the minimum is given in the Further Work section in the Recommendations.

6.2 **Recommendations**

6.2.1 **Further work**

The thesis extensively studies the relationship between the utilisation factor (influenced by the load profile of the residence and solar profile of the environment) against the purchase cost of the PV and battery system. In this lies the greatest opportunity to extend the work presented in this thesis. If bottom-up factors can statistically be linked to utilisation factors, then it can become very easy to determine which for which residences a PV system will be economically viable. This effectively then creates a direct link from the behaviour of residence member (which leads to the load profile) taking into consideration the local solar profile and PV system prices, and predict for a specific household the economic viability of a PV system.

After having studied the payback period functions for different input parameters, the optimisation algorithm used to determine the optimal PV system rating can be reconsidered. The payback function exposes certain characteristics for which alternative non-linear optimisation methodologies may be more appropriate. The pattern search optimisation used in this thesis can be perfectly adequate, but requires configuration of the optimisation parameters. Consideration should be given to the trade-off between runtime, accuracy, and expected local minima in the payback period function.

Based on the literature review conducted for battery energy storage, the battery storage deserves optimisation of its own parameters to determine financial viability of the system. Certain parameters with regards to batteries within this project have been chosen from best-practise guidelines or suggested ratings. Specifically, these parameters are

- Battery Charge and Discharge rate
- Battery Depth-of-discharge

The absolute maximum limits can discharge or charge is orders of magnitude higher than the suggested limits, but results in lower capacity or decreased lifetime. A further optimisation model can be constructed that finds optimal charge and discharge rates, while considering the fact that faster charge/discharge rates use increasingly less of the full capacity of the battery. The optimisation can investigate the trade-off between charging the battery at a slow rate awhile using more of its capacity vs charging the battery at a faster rate, but all the while utilise less of the available capacity. Additionally the optimisation can investigate the trade-off between lower depths of discharge using a large battery system versus a higher depth of discharge where the system needs more regular replacement due to less lifetime cycles.

References

[1] D. Noll, C. Dawes and V. Rai, "Solar Community Organizations and active peer effects in the adoption of residential PV," *Energy Policy,* vol. 67, pp. 330-343, 2014.

[2] P. Lorenz, D. Pinner and T. Seitz, "The economics of solar power," *The McKinsey Quarterly*, 2008.

[3] W. Jager, "Stimulating the diffusion of photovoltaic systems: A behavioural perspective," *Energy Policy,* vol. 34, pp. 1935-1943, 2006.

[4] P. Balcombe, D. Rigby and A. Azapagic, "Motivations and barriers associated with adopting microgeneration energy technologies in the UK," *Renewable and Sustainable Energy Reviews*, vol. 22, pp. 655-666, 2013.

[5] E. Drury, M. Miller, C. M. Macal, D. J. Graziano, D. Heimiller, J. Ozik and T. D. Perry IV, "The transformation of southern California's residential photovoltaics market through third-party ownership," *Energy Policy,* vol. 42, pp. 681-690, 2012.

[6] C. S. King, "The economics of real-time and time-of-use pricing for residential consumers," *American Energy Institute*, *Tech.Rep*, 2001.

[7] A. Faruqui, D. Harris and R. Hledik, "Unlocking the €53 billion savings from smart meters in the EU: How increasing the adoption of dynamic tariffs could make or break the EU’s smart grid investment," *Energy Policy,* vol. 38, pp. 6222-6231, 2010.

[8] T. Couture and Y. Gagnon, "An analysis of feed-in tariff remuneration models: Implications for renewable energy investment," *Energy Policy,* vol. 38, pp. 955-965, 2010.

[9] M. Mendonca, D. Jacobs and B. K. Sovacool, *Powering the Green Economy: The Feed-in Tariff Handbook.* London, UK: Earthscan, 2010.

[10] H. Farhangi, "The path of the smart grid," *Power and Energy Magazine, IEEE,* vol. 8, pp. 18-28, 2010.

[11] D. G. Hart, "Using AMI to realize the smart grid," in *Power and Energy Society General Meeting-Conversion and Delivery of Electrical Energy in the 21st Century, 2008 IEEE,* 2008, pp. 1-2.

[12] F. Li, W. Qiao, H. Sun, H. Wan, J. Wang, Y. Xia, Z. Xu and P. Zhang, "Smart transmission grid: Vision and framework," *Smart Grid, IEEE Transactions On,* vol. 1, pp. 168-177, 2010.

[13] T. Ackermann, G. Andersson and L. Söder, "Distributed generation: a definition," *Electr. Power Syst. Res.*, vol. 57, pp. 195-204, 2001.

[14] G. Pepermans, J. Driesen, D. Haeseldonckx, R. Belmans and W. D'haeseleer, "Distributed generation: definition, benefits and issues," *Energy Policy,* vol. 33, pp. 787-798, 2005.

[15] R. Ramakumar and P. Chiradeja, "Distributed generation and renewable energy systems," in *Energy Conversion Engineering Conference, 2002. IECEC'02. 2002 37th Intersociety,* 2004, pp. 716-724.

[16] C. W. Gellings and W. M. Smith, "Integrating demand-side management into utility planning," *Proc IEEE,* vol. 77, pp. 908-918, 1989.

[17] C. W. Gellings, "The concept of demand-side management for electric utilities," *Proc IEEE,* vol. 73, pp. 1468-1470, 1985.

[18] P. Palensky and D. Dietrich, "Demand side management: Demand response, intelligent energy systems, and smart loads," *Industrial Informatics, IEEE Transactions On,* vol. 7, pp. 381-388, 2011.

[19] A. Faiers, C. Neame and M. Cook, "The adoption of domestic solar-power systems: Do consumers assess product attributes in a stepwise process?" *Energy Policy,* vol. 35, pp. 3418-3423, 2007.

[20] N. R. Darghouth, G. Barbose and R. Wiser, "The impact of rate design and net metering on the bill savings from distributed PV for residential customers in California," *Energy Policy,* vol. 39, pp. 5243-5253, 2011.

[21] H. Ren, W. Gao and Y. Ruan, "Economic optimization and sensitivity analysis of photovoltaic system in residential buildings," *Renewable Energy,* vol. 34, pp. 883-889, 2009.

[22] X. Gong and M. Kulkarni, "Design optimization of a large scale rooftop photovoltaic system," *Solar Energy,* vol. 78, pp. 362-374, 2005.

[23] G. W. Hart, "Nonintrusive appliance load monitoring," *Proc IEEE,* vol. 80, pp. 1870-1891, 1992.

[24] H. Najmeddine, K. El Khamlichi Drissi, C. Pasquier, C. Faure, K. Kerroum, A. Diop, T. Jouannet and M. Michou, "State of art on load monitoring methods," in *Power and Energy Conference, 2008. PECon 2008. IEEE 2nd International,* 2008, pp. 1256-1258.

[25] Z. Wang and G. Zheng, "Residential appliances identification and monitoring by a nonintrusive method," *Smart Grid, IEEE Transactions On,* vol. 3, pp. 80-92, 2012.

[26] M. Weiss, A. Helfenstein, F. Mattern and T. Staake, "Leveraging smart meter data to recognize home appliances," in *Pervasive Computing and Communications (PerCom), 2012 IEEE International Conference On,* 2012, pp. 190-197.

[27] J. V. Paatero and P. D. Lund, "A model for generating household electricity load profiles," *Int. J. Energy Res.,* vol. 30, pp. 273-290, 2006.

[28] M. Kavgic, A. Mavrogianni, D. Mumovic, A. Summerfield, Z. Stevanovic and M. Djurovic-Petrovic, "A review of bottom-up building stock models for energy consumption in the residential sector," *Build. Environ.,* vol. 45, pp. 1683-1697, 2010.

[29] L. G. Swan and V. I. Ugursal, "Modeling of end-use energy consumption in the residential sector: A review of modeling techniques," *Renewable and Sustainable Energy Reviews,* vol. 13, pp. 1819-1835, 2009.

[30] A. Capasso, W. Grattieri, R. Lamedica and A. Prudenzi, "A bottom-up approach to residential load modeling," *Power Systems, IEEE Transactions On,* vol. 9, pp. 957-964, 1994.

[31] M. Aydinalp, V. I. Ugursal and A. S. Fung, "Modeling of the appliance, lighting, and space-cooling energy consumptions in the residential sector using neural networks," *Appl. Energy*, vol. 71, pp. 87-110, 2002.

[32] A. Summerfield, R. Lowe and T. Oreszczyn, "Two models for benchmarking UK domestic delivered energy," *Build. Res. Inf.*, vol. 38, pp. 12-24, 2010.

[33] Q. Zhang, "Residential energy consumption in China and its comparison with Japan, Canada, and USA," *Energy Build.*, vol. 36, pp. 1217-1225, 2004.

[34] S. Abras, S. Pesty, S. Ploix and M. Jacomino, "An anticipation mechanism for power management in a smart home using multi-agent systems," in *Information and Communication Technologies: From Theory to Applications, 2008. ICTTA 2008. 3rd International Conference On*, 2008, pp. 1-6.

[35] S. Ali, S. Maqbool, T. I. Ahamed and N. Malik, "Pursuit algorithm for optimized load scheduling," in *Power Engineering and Optimization Conference (PEDCO) Melaka, Malaysia, 2012 Ieee International*, 2012, pp. 193-198.

[36] S. Barker, A. Mishra, D. Irwin, P. Shenoy and J. Albrecht, "Smartcap: Flattening peak electricity demand in smart homes," in *Pervasive Computing and Communications (PerCom), 2012 IEEE International Conference On*, 2012, pp. 67-75.

[37] D. S. Callaway and I. A. Hiskens, "Achieving controllability of electric loads," *Proc IEEE*, vol. 99, pp. 184-199, 2011.

[38] M. D. Galus, S. Koch and G. Andersson, "Provision of load frequency control by PHEVs, controllable loads, and a cogeneration unit," *Industrial Electronics, IEEE Transactions On*, vol. 58, pp. 4568-4582, 2011.

[39] C. Joe-Wong, S. Sen, S. Ha and M. Chiang, "Optimized day-ahead pricing for smart grids with device-specific scheduling flexibility," *Selected Areas in Communications, IEEE Journal On*, vol. 30, pp. 1075-1085, 2012.

[40] D. Li, S. K. Jayaweera, O. Lavrova and R. Jordan, "Load management for price-based demand response scheduling-a block scheduling model," in *International Conference on*

Renewable Energies and Power Quality (ICREPQ'11), Las Palmas de Gran Canaria, Spain, 2011.

[41] T. Logenthiran, D. Srinivasan and T. Z. Shun, "Demand side management in smart grid using heuristic optimization," *Smart Grid, IEEE Transactions On,* vol. 3, pp. 1244-1252, 2012.

[42] A. Mamat, Y. Lu, J. Deogun and S. Goddard, "Real-time divisible load scheduling with advance reservation," in *Real-Time Systems, 2008. ECRTS'08. Euromicro Conference On,* 2008, pp. 37-46.

[43] A. Mohsenian-Rad and A. Leon-Garcia, "Optimal residential load control with price prediction in real-time electricity pricing environments," *Smart Grid, IEEE Transactions On,* vol. 1, pp. 120-133, 2010.

[44] G. Morganti, A. Perdon, G. Conte, D. Scaradozzi and A. Brintrup, "Optimising home automation systems: A comparative study on tabu search and evolutionary algorithms," in *Control and Automation, 2009. MED'09. 17th Mediterranean Conference On,* 2009, pp. 1044-1049.

[45] R. R. Negenborn, M. Houwing, B. De Schutter and H. Hellendoorn, "Adaptive prediction model accuracy in the control of residential energy resources," in *Control Applications, 2008. CCA 2008. IEEE International Conference On,* 2008, pp. 311-316.

[46] A. Nottrott, J. Kleissl and B. Washom, "Energy dispatch schedule optimization and cost benefit analysis for grid-connected, photovoltaic-battery storage systems," *Renewable Energy,* vol. 55, pp. 230-240, 2013.

[47] G. O'Brien and R. Rajagopal, "A method for automatically scheduling notified deferrable loads," in *American Control Conference (ACC), 2013,* 2013, pp. 5080-5085.

[48] Y. Riffonneau, S. Bacha, F. Barruel and S. Ploix, "Optimal power flow management for grid connected PV systems with batteries," *Sustainable Energy, IEEE Transactions On,* vol. 2, pp. 309-320, 2011.

[49] S. Shao, M. Pipattanasompornand S. Rahman, "Development of physical-based demand response-enabled residential load models," *Power Systems, IEEE Transactions On,* vol. 28, pp. 607-614, 2013.

[50] E. Sortomme and M. El-Sharkawi, "Optimal power flow for a system of microgrids with controllable loads and battery storage," in *Power Systems Conference and Exposition, 2009. PSCE'09. IEEE/PES,* 2009, pp. 1-5.

[51] K. Tanaka, A. Yoza, K. Ogimi, A. Yona, T. Senjyu, T. Funabashi and C. Kim, "Optimal operation of DC smart house system by controllable loads based on smart grid topology," *Renewable Energy,* vol. 39, pp. 132-139, 2012.

[52] R. Teng and T. Yamazaki, "Bit-watt home system with hybrid power supply," in *The 2nd International Conference on Computer and Automation Engineering (ICCAE),* 2010, pp. 59-63.

[53] A. G. Tsikalakis and N. D. Hatziargyriou, "Centralized control for optimizing microgrids operation," in *Power and Energy Society General Meeting, 2011 IEEE,* 2011, pp. 1-8.

[54] Y. Taeyoon, S. Dong and S. Sung-Yong, "Home appliance scheduling optimization with time-varying electricity price and peak load limitation," in *The 3rd International Conference on Information Science and Technology,* 2013, pp. 196-197, 198, 199.

[55] H. S. Houthakker, "Electricity tariffs in theory and practice," *The Economic Journal,* pp. 1-25, 1951.

[56] P. O. Steiner, "Peak loads and efficient pricing," *The Quarterly Journal of Economics,* pp. 585-610, 1957.

[57] S. Borenstein, M. Jaske and A. Rosenfeld, "Dynamic pricing, advanced metering, and demand response in electricity markets," 2002.

[58] G. Strbac, "Demand side management: Benefits and challenges," *Energy Policy,* vol. 36, pp. 4419-4426, 2008.

[59] P. C. Reiss and M. W. White, "Household electricity demand, revisited," *The Review of Economic Studies,* vol. 72, pp. 853-883, 2005.

[60] S. Borenstein, "Equity effects of increasing-block electricity pricing," in *Center for the Study of Energy Markets Working Paper Series,* Berkely, 2008.

[61] J. A. Herriges and K. K. King, "Residential demand for electricity under inverted block rates: Evidence from a controlled experiment," *Journal of Business & Economic Statistics,* vol. 12, pp. 419-430, 1994.

[62] A. Klein, A. Held, M. Ragwitz, G. Resch and T. Faber, "Evaluation of different feed-in tariff design options: Best practice paper for the International Feed-in Cooperation," *Karlsruhe, Germany and Laxenburg, Austria: Fraunhofer Institut Für Systemtechnik Und Innovationsforschung and Vienna University of Technology Energy Economics Group*, 2007.

[63] J. Prest, "The Future of Feed-in Tariffs: Capacity Caps, Scheme Closures and Looming Grid Parity," *ANU College of Law Research Paper,* 2012.

[64] Y. Yamamoto, "Pricing electricity from residential photovoltaic systems: A comparison of feed-in tariffs, net metering, and net purchase and sale," *Solar Energy,* vol. 86, pp. 2678-2685, 2012.

[65] C. Eid, J. R. Guillén, P. F. Marín and R. Hakvoort, "The economic effect of electricity net-metering with solar PV: Consequences for network cost recovery, cross subsidies and policy objectives," *Energy Policy,* vol. 75, pp. 244-254, 2014.

[66] A. Picciariello, J. Reneses, P. Frias and L. Söder, "Distributed generation and distribution pricing: Why do we need new tariff design methodologies?" *Electr. Power Syst. Res.,* vol. 119, pp. 370-376, 2015.

[67] R. Foster, M. Ghassemi and A. Cota, *Solar Energy: Renewable Energy and the Environment.* Boca Raton, Florida: CRC Press, 2010.

[68] G. M. Masters, *Renewable and Efficient Electric Power Systems.* Hoboken, New Jersey: John Wiley & Sons, 2004.

[69] PVSyst - PhotoVoltaic Software. "PVSyst" [online]. Available: http://www.pvsyst.com/en/ (accessed 18 July 2015).

[70] SolarGIS. "SolarGIS - Online data and tools for solar energy projects" [online]. Available: http://solargis.info/ (accessed 18 July 2015).

[71] Surface meteorology and Solar Energy. "Surface meteorology and Solar Energy" [online]. Available: https://eosweb.larc.nasa.gov/cgi-bin/sse/sse.cgi?skip@larc.nasa.gov+s03#s03 (accessed 19 July 2015).

[72] D. L. King, J. A. Kratochvil and W. E. Boyson, *Photovoltaic Array Performance Model.* Albuquerque, New Mexico: Citeseer, 2004.

[73] NREL's PVWatts Calculator. "PVWatts Calculator" [online]. Available: http://pvwatts.nrel.gov/ (accessed 18 July 2015).

[74] A. P. Dobos, "PVWatts version 5 manual," *National Renewable Energy Laboratory, September*, 2014.

[75] SAM. *"System Advisor Model Help Files"* [online]. Available: https://sam.nrel.gov/sites/sam.nrel.gov/files/content/documents/pdf/sam-help.pdf (accessed: 18 July 2015).

[76] N. Blair, A. P. Dobos, J. Freeman, T. Neises, M. Wagner, T. Ferguson, P. Gilman and S. Janzou, "System Advisor Model General Description," *System Advisor Model, SAM 2014.1.14: General Description*, 2014.

[77] B. Bekker, "Irradiation and PV array energy output, cost and optimal positioning estimation of South Africa," *Journal of Energy in Southern Africa*, vol. 18, pp. 16-25, 2007.

[78] Homer Energy. "HOMER - Hybrid Renewable and Distributed Generation System Design Software" [online]. Available: http://www.homerenergy.com/ (accessed 18 July 2015).

[79] D. Ciolkosz, "SASRAD: An hourly-timestep solar radiation database for South Africa," *Journal of Energy in Southern Africa*, vol. 20, pp. 25, 2009.

[80] E. Zawilska, M. Brooks and A. Meyer, "A review of solar resource assessment in south africa: The case for a national network," in *Proceedings: The World Renewable Energy Forum,* Denver, Colorado, 2012.

[81] Download Weather Data. "Sonbesie Weather Data" [online]. Available: http://weather.sun.ac.za/downloadList.php (accessed 19 July 2015).

[82] Welcome To SAURAN - Southern African Universities Radiometric Network. "SAURAN - Solar radiometric data for the public" [online]. Available: http://www.sauran.net/ (accessed 19 July 2015).

[83] World Standards. "Plug, socket & Voltage by country" [online]. Available: http://www.worldstandards.eu/electricity/plug-voltage-by-country/ (accessed 7/18/2015).

[84] International Electrotechnical Commission. "World Plugs: List view by location" [online]. Available: http://www.iec.ch/worldplugs/list_bylocation.htm (accessed 7/18/2015).

[85] Fronius. *"Fronius IG Plus Advanced Operating Instructions"* [online]. Available: http://www.fronius.com/cps/rde/xbcr/SID-0F54DA89-FB5DC62B/fronius_usa/42_0426_0158_EA_294276_snapshot.pdf (accessed: 18 July 2015).

[86] Kaco. *"Kaco Powador 2002 | 3002 4202 | 5002 6002 Operating Instructions"* [online]. Available: http://kaco-newenergy.com/fileadmin/data/downloads/products/Galvanically%20Isolated%20String%20Inverters%20Powador%202002-6002/Instruction%20Manuals/MNL_PW_2002-6002_en_08a.pdf (accessed: 18 July 2015).

[87] SMA. *"Operating Manual Sunny Boy 3600 / 5000 Smart Energy"* [online]. Available: http://files.sma.de/dl/21567/SB36-50SE-BE-en-11.pdf (accessed: 18 July 2015).

[88] I. H. Rowlands, B. P. Kemery and I. Beausoleil-Morrison, "Optimal solar-PV tilt angle and azimuth: An Ontario (Canada) case-study," *Energy Policy,* vol. 39, pp. 1397-1409, 2011.

[89] G. Lewis, "Optimum tilt of a solar collector," *Solar & Wind Technology,* vol. 4, pp. 407-410, 1987.

[90] K. Engelen, E. L. Shun, P. Vermeyen, I. Pardon, R. D'hulst, J. Driesen and R. Belmans, "The feasibility of small-scale residential DC distribution systems," in *32nd Annual Conference on IEEE Industrial Electronics*, Paris, 2006, pp. 2618-2623.

[91] D. J. Hammerstrom, "AC versus DC distribution systemsdid we get it right?" in *Power Engineering Society General Meeting, 2007. IEEE*, 2007, pp. 1-5.

[92] D. Dong, F. Luo, X. Zhang, D. Boroyevich and P. Mattavelli, "Grid-interface bidirectional converter for residential DC distribution systems—Part 2: AC and DC interface design with passive components minimization," *Power Electronics, IEEE Transactions On*, vol. 28, pp. 1667-1679, 2013.

[93] Kaco. *"Blueplanet Gridsave 14.0 TL3 Data Sheet"* [online]. Available: http://kaco-newenergy.com/fileadmin/data/downloads/products/Energy%20Systems%20Technology/Powador-gridsave/Data_Sheets/DTS_bp_gridsave_14_TL3_en.pdf (accessed: 18 July 2015).

[94] Kaco. *"Blueplanet Gridsave Eco 5.0 TR1 Bidirectional Battery Inverter Operating Instructions"* [online]. Available: http://kaco-newenergy.com/fileadmin/data/downloads/products/Energy%20Systems%20Technology/Powador-gridsave_eco/Instruction_Manuals/MNL_PW_gridsave-eco_en_03a.pdf (accessed: 18 July 2015).

[95] SMA. *"Installation - Quick Reference Guide - SMA Flexible Storage System with Battery Backup Function"* [online]. Available: http://files.sma.de/dl/20472/Ersatzstrom-IS-en-30W.pdf (accessed: 18 July 2015).

[96] H. Ibrahim, A. Ilinca and J. Perron, "Energy storage systems—characteristics and comparisons," *Renewable and Sustainable Energy Reviews*, vol. 12, pp. 1221-1250, 2008.

[97] H. Chen, T. N. Cong, W. Yang, C. Tan, Y. Li and Y. Ding, "Progress in electrical energy storage system: A critical review," *Progress in Natural Science*, vol. 19, pp. 291-312, 2009.

[98] P. J. Hall and E. J. Bain, "Energy-storage technologies and electricity generation," *Energy Policy*, vol. 36, pp. 4352-4355, 2008.

[99] B. Sørensen, *Hydrogen and Fuel Cells: Emerging Technologies and Applications.* Kidlington, Oxford: Academic Press, 2012.

[100] A. Veziroglu and R. Macario, "Fuel cell vehicles: State of the art with economic and environmental concerns," *International Journal of Hydrogen Energy,* vol. 36, pp. 25-43, 2011.

[101] A. Bilodeau and K. Agbossou, "Control analysis of renewable energy system with hydrogen storage for residential applications," *J. Power Sources*, vol. 162, pp. 757-764, 2006.

[102] J. D. Maclay, J. Brouwer and G. S. Samuelsen, "Dynamic modeling of hybrid energy storage systems coupled to photovoltaic generation in residential applications," *J. Power Sources,* vol. 163, pp. 916-925, 2007.

[103] A. Arteconi, N. Hewitt and F. Polonara, "State of the art of thermal storage for demand-side management," *Applied Energy,* vol. 93, pp. 371-389, 2012.

[104] L. Chidambaram, A. Ramana, G. Kamaraj and R. Velraj, "Review of solar cooling methods and thermal storage options," *Renewable and Sustainable Energy Reviews,* vol. 15, pp. 3220-3228, 2011.

[105] M. Ali, B. Wu and R. A. Dougal, "An overview of SMES applications in power and energy systems," *Sustainable Energy, IEEE Transactions On,* vol. 1, pp. 38-47, 2010.

[106] F. Rahman, S. Rehman and M. A. Abdul-Majeed, "Overview of energy storage systems for storing electricity from renewable energy sources in Saudi Arabia," *Renewable and Sustainable Energy Reviews,* vol. 16, pp. 274-283, 2012.

[107] M. Zheng, C. J. Meinrenken and K. S. Lackner, "Agent-based model for electricity consumption and storage to evaluate economic viability of tariff arbitrage for residential sector demand response," *Appl. Energy*, vol. 126, pp. 297-306, 2014.

[108] S. Lee, J. Kim, J. Lee and B. Cho, "State-of-charge and capacity estimation of lithium-ion battery using a new open-circuit voltage versus state-of-charge," *J. Power Sources,* vol. 185, pp. 1367-1373, 2008.

[109] M. Root, *The TAB Battery Book: An in-Depth Guide to Construction, Design, and Use.* McGraw Hill Professional, 2010.

[110] W. van Schalkwijk and B. Scrosati, *Advances in Lithium-Ion Batteries.* New York: Kluwer Academic Publishers, 2007.

[111] J. O. Besenhard, *Handbook of Battery Materials.* Weinheim, Germany: Wiley VCH, 2008.

[112] M. Fernandez, A. Ruddell, N. Vast, J. Esteban and F. Estela, "Development of a VRLA battery with improved separators, and a charge controller, for low cost photovoltaic and wind powered installations," *J. Power Sources,* vol. 95, pp. 135-140, 2001.

[113] D. A. J. Rand, *Valve-Regulated Lead-Acid Batteries.* Elserivier, 2004.

[114] "Exsolar - Exsolar" [online] (accessed 3/6/2015).

[115] "Renewable Energy Systems & Green Solutions | SA's No. 1 Online Eco Store - Sustainable.co.za" [online] (accessed 3/6/2015).

[116] R. Rynkiewicz, "Discharge and charge modeling of lead acid batteries," in *Applied Power Electronics Conference and Exposition, 1999. APEC'99. Fourteenth Annual,* 1999, pp. 707-710.

[117] D. Doerffel and S. A. Sharkh, "A critical review of using the Peukert equation for determining the remaining capacity of lead-acid and lithium-ion batteries," *J. Power Sources,* vol. 155, pp. 395-400, 2006.

[118] H. Kim and K. G. Shin, "Scheduling of battery charge, discharge, and rest," in *Real-Time Systems Symposium, 2009, RTSS 2009. 30th IEEE,* 2009, pp. 13-22.

[119] J. Ross, T. Markvart and W. He, "Modelling battery charge regulation for a stand-alone photovoltaic system," *Solar Energy,* vol. 69, pp. 181-190, 2000.

[120] D. Mayer and S. Biscaglia, "Modelling and analysis of lead acid battery operation," in *Telecommunications Energy Conference, 1989. INTELEC'89. Conference Proceedings., Eleventh International*, 1989, pp. 23.3/1-23.3/6 vol. 2.

[121] "Trojan Battery Company" [online]. Available: http://www.trojanbattery.com/markets/renewable-energy-re/ (accessed 3 June 2015).

[122] S. Harrington and J. Dunlop, "Battery charge controller characteristics in photovoltaic systems," *Aerospace and Electronic Systems Magazine, IEEE*, vol. 7, pp. 15-21, 1992.

[123] Microcare. *"LCD MPPT User Documentation"* [online]. Available: http://gbsynergy.co.za/micro/wp-content/uploads/2014/10/LCD-MPPT-Charge-Controller-Manual.pdf (accessed: 6 March 2015).

[124] Outback Power. *"FLEXmax Series Charge Controller Owners Manual"* [online]. Available: http://www.outbackpower.com/downloads/documents/flexmax_6080/owner_manual.pdf (accessed: 6 March 2015).

[125] Steca. *"Solar Charge Controller"* [online]. Available: file:///C:/Users/16082370/Downloads/Steca_Tarom4545-48_Manual_DE-GB.pdf (accessed: 6 March 2015).

[126] Chinnek J W. *"Practical optimization: A gentle introduction"* [online]. Available: http://www.sce.carleton.ca/faculty/chinneck/po.html (accessed: 29 November 2015).

[127] J. W. Chinneck, *Feasibility and Infeasibility in Optimization: Algorithms and Computational Methods*. US: Springer, 2007.

[128] MathWorks Documentation. "How pattern search polling works" [online]. Available: http://www.mathworks.com/help/gads/how-pattern-search-polling-works.html (accessed 1 August 2015).

[129] J. Kennedy, R. Poli and T. Blackwell, "Particle swarm optimization: An overview," *Swarm Intelligence*, vol. 1, pp. 33, 2007.

[130] M. Bazilian, I. Onyeji, M. Liebreich, I. MacGill, J. Chase, J. Shah, D. Gielen, D. Arent, D. Landfear and S. Zhengrong, "Re-considering the economics of photovoltaic power," *Renewable Energy,* vol. 53, pp. 329-338, 2013.

[131] W. Patterson, *Keeping the Lights on: Towards Sustainable Electricity.* London, UK: Routledge, 2012.

[132] R. H. Garrison, E. W. Noreen and P. C. Brewer, *Managerial Accounting.* McGraw-Hill/Irwin New York, 2003.

[133] V. Rai and K. McAndrews, "Decision-making and behavior change in residential adopters of solar PV," in *World Renewable Energy Forum,* 2012.

[134] V. Rai and B. Sigrin, "Diffusion of environmentally-friendly energy technologies: buy versus lease differences in residential PV markets," *Environmental Research Letters,* vol. 8, pp. 014022, 2013.

[135] V. Quaschning, *Understanding Renewable Energy Systems.* London, UK: Earthscan, 2005.

[136] S. Tudisca, A. M. Di Trapani, F. Sgroi, R. Testa and R. Squatrito, "Economic analysis of PV systems on buildings in Sicilian farms," *Renewable and Sustainable Energy Reviews,* vol. 28, pp. 691-701, 2013.

[137] P. P. Singh and S. Singh, "Realistic generation cost of solar photovoltaic electricity," *Renewable Energy,* vol. 35, pp. 563-569, 2010.

[138] K. Branker, M. Pathak and J. M. Pearce, "A review of solar photovoltaic levelized cost of electricity," *Renewable and Sustainable Energy Reviews,* vol. 15, pp. 4470-4482, 2011.

[139] Python. "Python" [online]. Available: https://www.python.org/ (accessed 1 August 2015).

[140] SciPy.org. "SciPy.org" [online]. Available: http://www.scipy.org/ (accessed 1 August 2015).

[141] MathWorks. "Matlab" [online]. Available: http://www.mathworks.com/products/matlab/ (accessed 1 August 2015).

[142] Wolfram. "Wolfram Mathematica" [online]. Available: http://www.wolfram.com/mathematica/ (accessed 1 August 2015).

[143] MathWorks Documentation. "GUI Building" [online]. Available: http://www.mathworks.com/help/matlab/gui-development.html (accessed 1 August 2015).

[144] Visual Studio. "Visual Studio" [online]. Available: https://www.visualstudio.com/ (accessed 1 August 2015).

[145] Qt. "The framework and tools" [online]. Available: http://www.qt.io/qt-framework/ (accessed 1 August 2015).

[146] Python Wiki. "PyQt" [online]. Available: https://wiki.python.org/moin/PyQt (accessed 1 August 2015).

[147] Embarcadero. "Delphi XE 8" [online]. Available: http://www.embarcadero.com/products/delphi (accessed 1 August 2015).

[148] About Tech. "Delphi History" [online]. Available: http://delphi.about.com/cs/azindex/a/dhistory.htm (accessed 1 August 2015).

[149] Lazarus. "About Lazarus project" [online]. Available: http://www.lazarus-ide.org/index.php?page=about (accessed 1 August 2015).

[150] Sqlite. "About Sqlite" [online]. Available: https://www.sqlite.org/about.html (accessed 1 August 2015).

[151] Python Documentation. "DB interface for SqLite databases" [online]. Available: https://docs.python.org/2/library/sqlite3.html (accessed 1 August 2015).

[152] Github: Kyamagu, sqlite3 driver. "Matlab Sqlite3 Driver" [online]. Available: https://github.com/kyamagu/matlab-sqlite3-driver (accessed 1 August 2015).

[153] SourceForge. "mksqlite" [online]. Available: http://sourceforge.net/projects/mksqlite/ (accessed 1 August 2015).

[154] MathWorks Documentation. "SQlite JDBC for Windows" [online]. Available: http://www.mathworks.com/help/database/ug/sqlite-jdbc-windows.html (accessed 1 August 2015).

[155] Embarcadero Wiki. "Tutorial: Connecting to a sqlite database" [online]. Available: http://docwiki.embarcadero.com/RADStudio/XE5/en/Tutorial:_Connecting_to_a_SQLite_Database_(Delphi) (accessed 1 August 2015).

[156] MySql. "MySql - The world's most popular open source database" [online]. Available: https://www.mysql.com/ (accessed 1 August 2015).

[157] Digital Ocean. "SQLite vs MySQL vs PostgreSQL: A Comparison Of Relational Database Management Systems" [online]. Available: https://www.digitalocean.com/community/tutorials/sqlite-vs-mysql-vs-postgresql-a-comparison-of-relational-database-management-systems (accessed 1 August 2015).

[158] PostgreSql. "About" [online]. Available: http://www.postgresql.org/about/ (accessed 1 August 2015).

[159] J. Hunt, *Guide to the Unified Process Featuring UML, Java and Design Patterns.* London, UK: Springer Verlag, 2003.

[160] S. W. Ambler, *The Elements of UML (TM) 2.0 Style.* New York, USA: Cambridge University Press, 2005.

[161] D Banas. "UML 2.0 Tutorial," *Youtube,* Nov 5, 2012 [Video file]. Available: https://www.youtube.com/watch?v=OkC7HKtiZC0 [Accessed: 1 August 2015].

[162] D. Mayr, E. Schmid, H. Trollip, M. Zeyringer and J. Schmidt, "The impact of residential photovoltaic power on electricity sales revenues in Cape Town, South Africa," *Utilities Policy,* vol. 36, pp. 10-23, 2015.

[163] MeteoControl. "MeteoControl Energy and Weather Service" [online]. Available: http://www.meteocontrol.com/en/ (accessed 1 September 2015).

[164] City of Johannesburg. *"Approved Tariffs for 2015/2016"* [online]. Available: http://joburg.org.za/images/stories/2015/May/2015-16%20tariffs%20for%20approval.pdf (accessed: 29 September 2015).

[165] City of Cape Town. *"Utility Service - Electricity Service (Consumptive)"* [online]. Available: https://www.capetown.gov.za/en/electricity/Elec%20Tariffs%20201516/Utility%20Services%20Electricity%20Consumptive%201516_PUB.pdf (accessed: 29 September 2015).

Appendix A: Case study daily input parameter values

Appendix Table A.1 Energy collected by the 1kW solar system

Halfhour	Energy [Wh]
1	0
2	0
3	0
4	0
5	0
6	0
7	0
8	0
9	0
10	0
11	0
12	0
13	15.5
14	55
15	119.5
16	186.5

Halfhour	Energy [Wh]
17	250
18	303.5
19	348
20	383.5
21	413.5
22	431
23	438
24	445.5
25	445.5
26	443.5
27	419
28	395.5
29	363
30	319
31	260
32	213

Halfhour	Energy [Wh]
33	161
34	81.5
35	33.5
36	10.5
37	0.5
38	0
39	0
40	0
41	0
42	0
43	0
44	0
45	0
46	0
47	0
48	0

Appendix Table A.2 Non-schedulable load profile for case studies 1, 3, 4, 5, 6 and 7

Halfhour	Energy [kWh]
1	200
2	200
3	200
4	200
5	200
6	200
7	200
8	200
9	200
10	230
11	260
12	400
13	400
14	450
15	400
16	200

Halfhour	Energy [kWh]
17	200
18	200
19	250
20	300
21	250
22	200
23	200
24	200
25	200
26	300
27	300
28	300
29	300
30	300
31	350
32	380

Halfhour	Energy [kWh]
33	400
34	300
35	400
36	350
37	300
38	350
39	300
40	400
41	300
42	290
43	250
44	200
45	170
46	104
47	110
48	70

Appendix Table A.3 Non-schedulable load profile for case study 2

Halfhour	Energy [kWh]
1	170
2	170
3	170
4	170
5	170
6	170
7	170
8	170
9	170
10	170
11	170
12	170
13	190
14	690
15	1483
16	650
17	760
18	760
19	450
20	450
21	450
22	300
23	675
24	675
25	675
26	675
27	675
28	675
29	675
30	675
31	300
32	300
33	300
34	300
35	675
36	675
37	1985
38	1485
39	2025
40	2025
41	1525
42	1525
43	650
44	650
45	190
46	190
47	180
48	179

Appendix B: Case study annual load profile input parameters

Appendix Table B.1 Non-schedulable summer load profile for case study 8 and 9

Halfhour	Energy [kWh]	Halfhour	Energy [kWh]	Halfhour	Energy [kWh]
1	170	17	760	33	300
2	170	18	760	34	300
3	170	19	450	35	675
4	170	20	450	36	675
5	170	21	450	37	1985
6	170	22	300	38	1485
7	170	23	675	39	2025
8	170	24	675	40	2025
9	170	25	675	41	1525
10	170	26	675	42	1525
11	170	27	675	43	650
12	170	28	675	44	650
13	190	29	675	45	190
14	690	30	675	46	190
15	1483	31	300	47	180
16	650	32	300	48	179

Appendix Table B.2 Non-schedulable winter load profile for case study 8 and 9

Halfhour	Energy [kWh]
1	170
2	170
3	170
4	170
5	170
6	170
7	170
8	170
9	170
10	170
11	170
12	170
13	190
14	690
15	1483
16	650

Halfhour	Energy [kWh]
17	760
18	760
19	450
20	450
21	450
22	300
23	675
24	675
25	675
26	675
27	675
28	675
29	675
30	675
31	300
32	300

Halfhour	Energy [kWh]
33	300
34	300
35	675
36	675
37	1985
38	1485
39	2025
40	2025
41	1525
42	1525
43	650
44	650
45	190
46	190
47	180
48	179

Appendix C: **Annual solar profile data**

Solar Data Acquisition

Weather data for 2012 was acquired from the SAURAN database for the Stellenbosch weather station. Data is provided as a CSV file. Data is checked for integrity and conditioned where invalid data is found.

The complete weather file is then used to a TMY3 weather file (discussed in the literature study) and provided as an input to the SAM solar software package. A TMY3 file has a resolution of 1 hour and a timespan of 1 year In SAM, a PV system installation is configured with default (typical) values for a residential PV plant, with no shade falling on the panels. SAM generates the expected energy collected from the PV system for each hour of the day during the year.

This dataset is then exported to Excel, where the time-string is conditioned to a suitable format for Matlab, and saved as a CSV. After the data is imported to Matlab, a script is used to convert the hourly data energy collected data from to half-hourly power data. This is done by keeping the on-the-hour values as is, and then inserting averaged values on the half-hour. That is, the data has been transformed from the set in Appendix Table C.1 to Appendix Table C.2.

Appendix Table C.1 Original PV system energy collected hourly data

Time	Energy collected [Wh]
14:00	400
15:00	300

Appendix Table C.2 Adapted PV system power half-hourly data

Time	Power [W]
14:00	400
14:30	350
15:00	300

These values are then used as inputs to the residential PV system electricity cost simulation. The final data as conditioned and discussed above is shown in the figures below. Data ranges from 1 January 00:00 2012 to 31 December 2012 24:00.

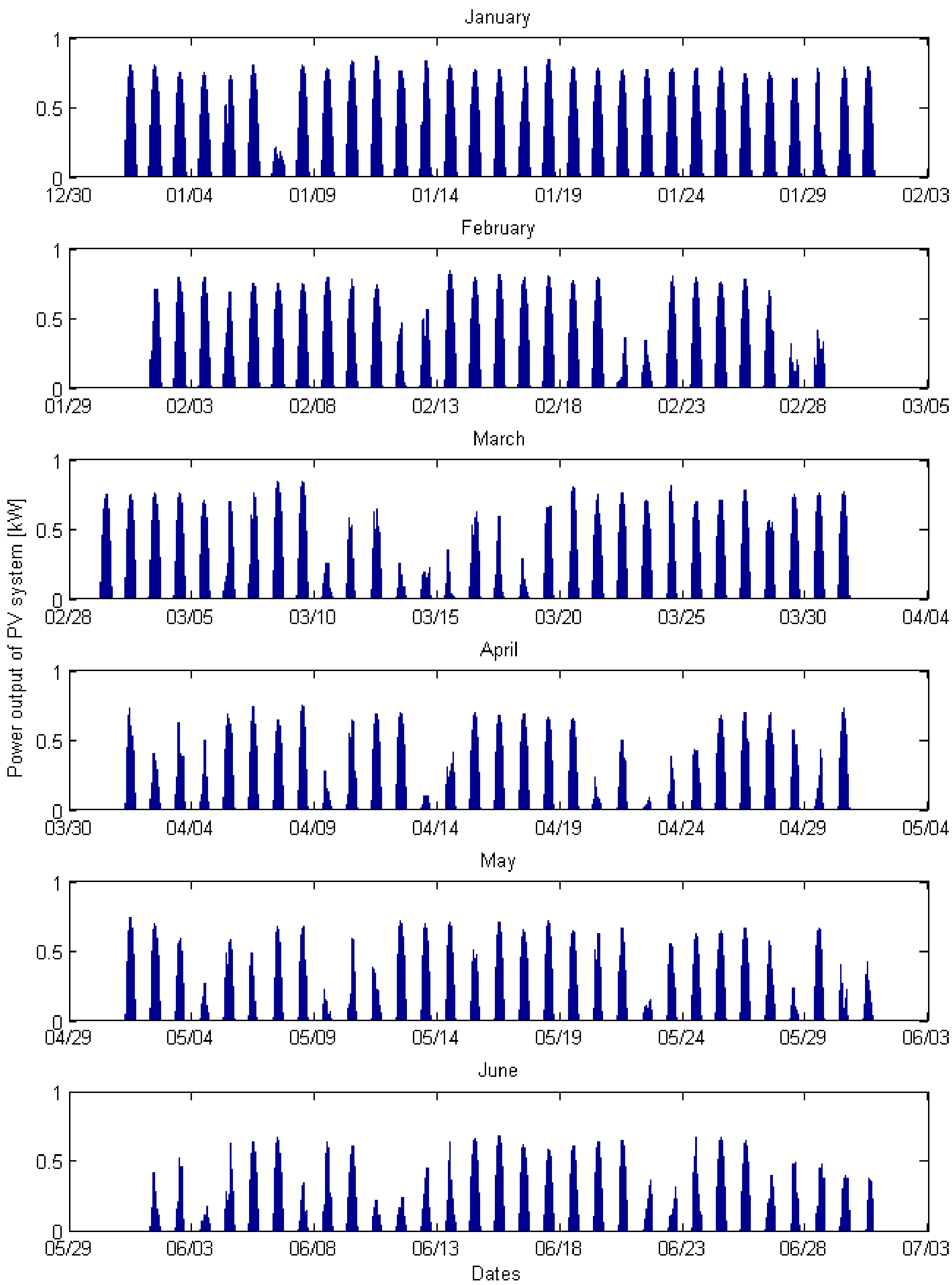

Appendix Figure C.1 PV system power profiles for the first six months of 2012

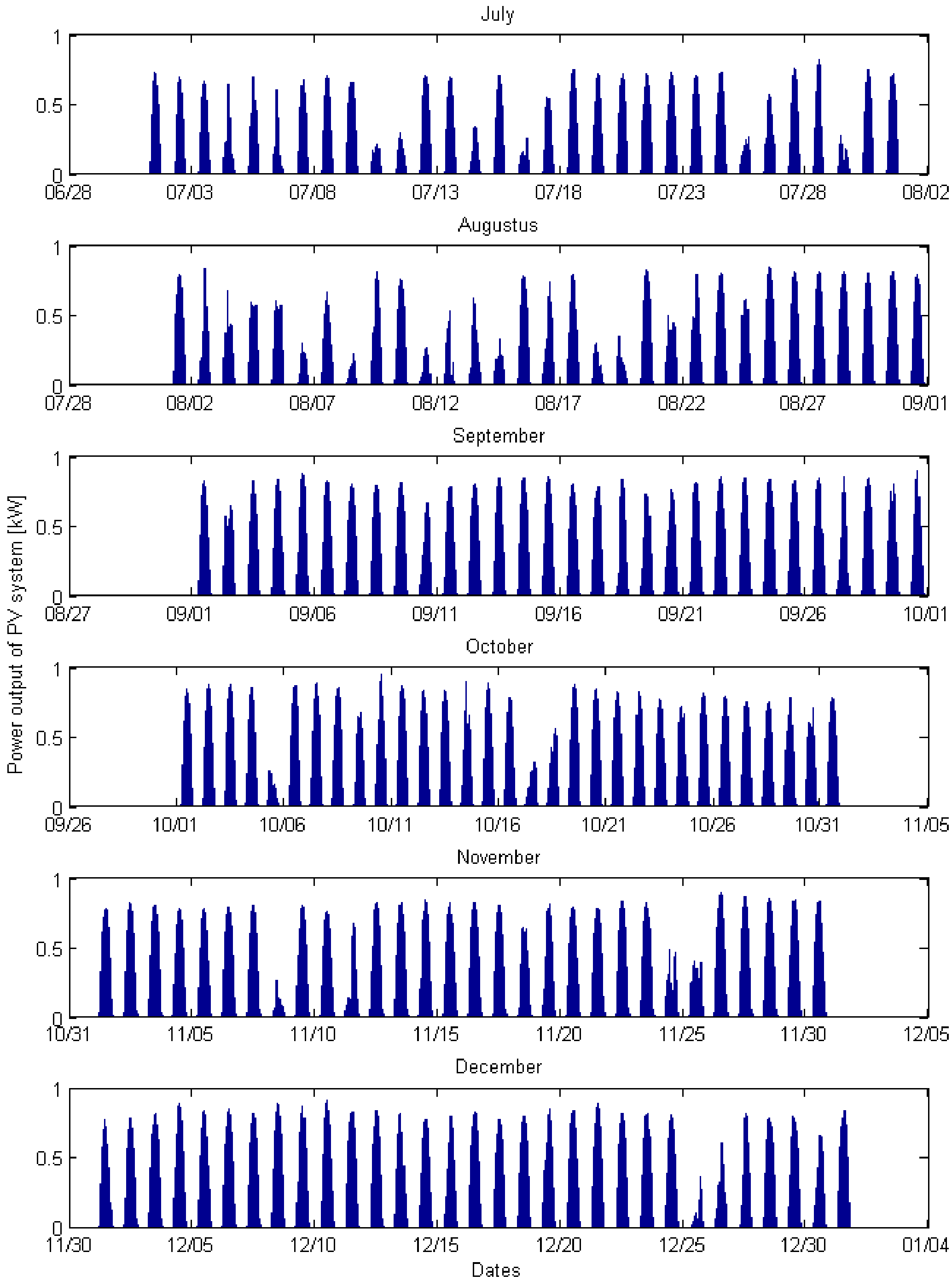

Appendix Figure C.2 PV system power profiles for the last six months of 2012

Appendix D: **PV and battery system cost derivation**

The project at hand requires a model whereby the cost of a solar system can easily be determined for each rating of system that needs to be installed. Three major factors contribute to the cost of the installation:

- The components of the solar system. These are shown in Appendix Figure D.1
- Mounting, structural and connection costs. These include the roof mounts, cabling and fittings to install the system
- Labour cost of the installation

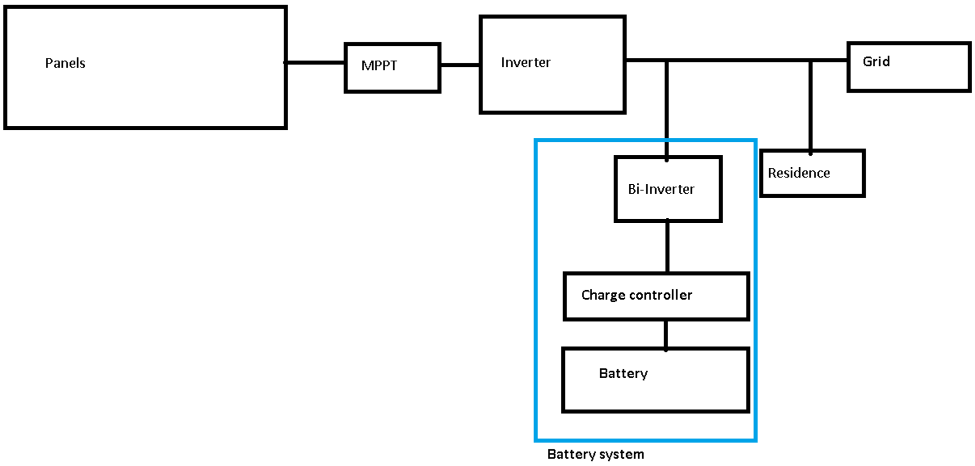

Appendix Figure D.1 PV system required components with optional battery system

Depending on factors such as location and resources available to the installer, the costs can be different at each location. A general price curve for solar systems is found by collection and analysis of readily available and accessible equipment and components, or inquiring quotes from respective providers. As exporting energy to the grid is not supported by older metering equipment, smart PV generation meters are included in some quotes to actively monitor PV generation and prevent grid feed-in. For the purpose of this study, the smart meter is not included as the research is conducted for more general cases. Different service providers have a different set of services they offer and therefore the quotes are not directly comparable, but adjustments can be made to compare prices.

Appendix Figure D.2 show how the prices compare for three different providers according to quotes or website prices: ExSolar, Current Automation and sustainable.co.za. Appendix Table D.1 indicates what is included in each of the prices.

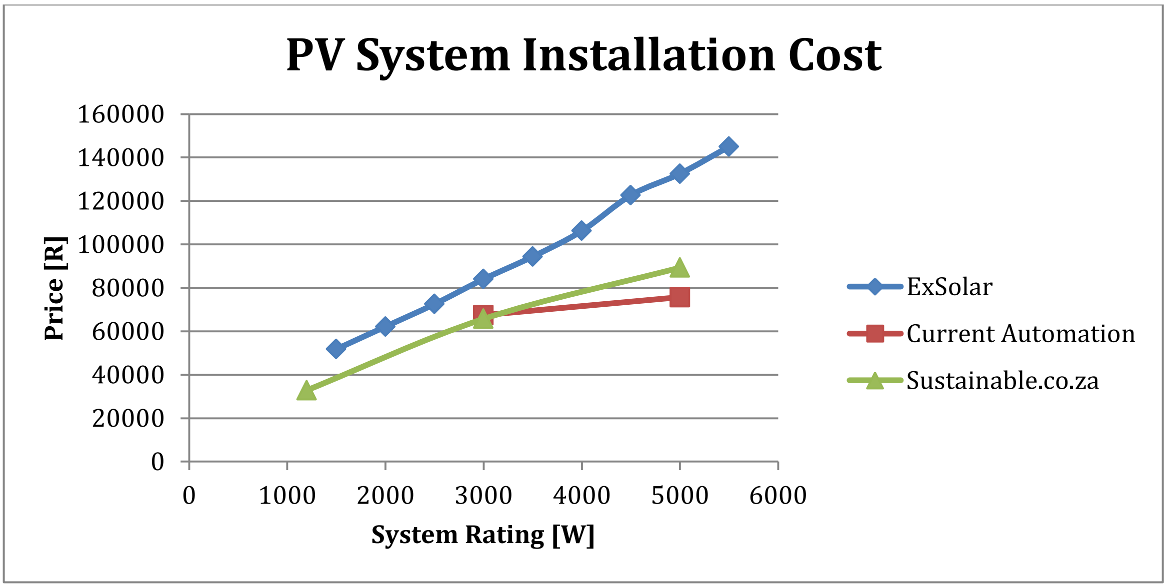

Appendix Figure D.2 Price comparison of PV system installation by different providers

Appendix Table D.1 Service provider inclusions in price of installation

	Components	**Mounting $ Brackets**	**Labor**
ExSolar	✓	✓	✓
Current Automantion	✓	✓	
Sustainable.co.za	✓		

A per-unit cost for the PV system is determined for the prices available from sustainable.co.za. The per-unit cost only includes the components necessary for the PV system. The prices for three different rated systems are calculated in Appendix Table D.2 and graphically shown in Appendix Figure D.3.

Appendix Table D.2 Per unit cost calculation of PV system purchase cost

	1300W	3000W	5000W
Grid-tied inverter	16794	27702	35836
PV panels	15336	34749	53460
Roof mountings	2000	4000	6000
Inverter and panel connectors	3213	6245.1	8929.6
Total	37343	73696.1	104225.6
Per-unit	28.73	24.23	20.84

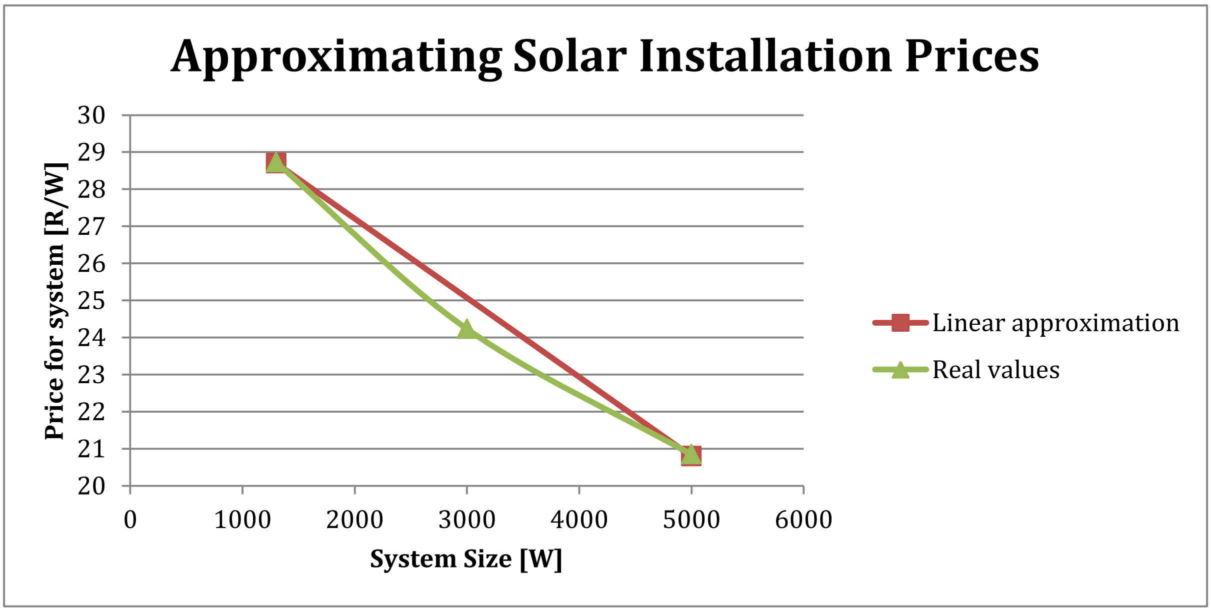

Appendix Figure D.3 Linear function to approximate per-unit cost

The same calculations are applied to the purchase prices from ExSolar, as shown in Appendix Figure D.4. A regression function is used to find a function that fits these points and model the per-watt installation cost of the system as a continuous function. Linear Regression has been done in Excel to find a curve-fitting equation. A third-order polynomial follows the line quite well and is indicated on the figure.

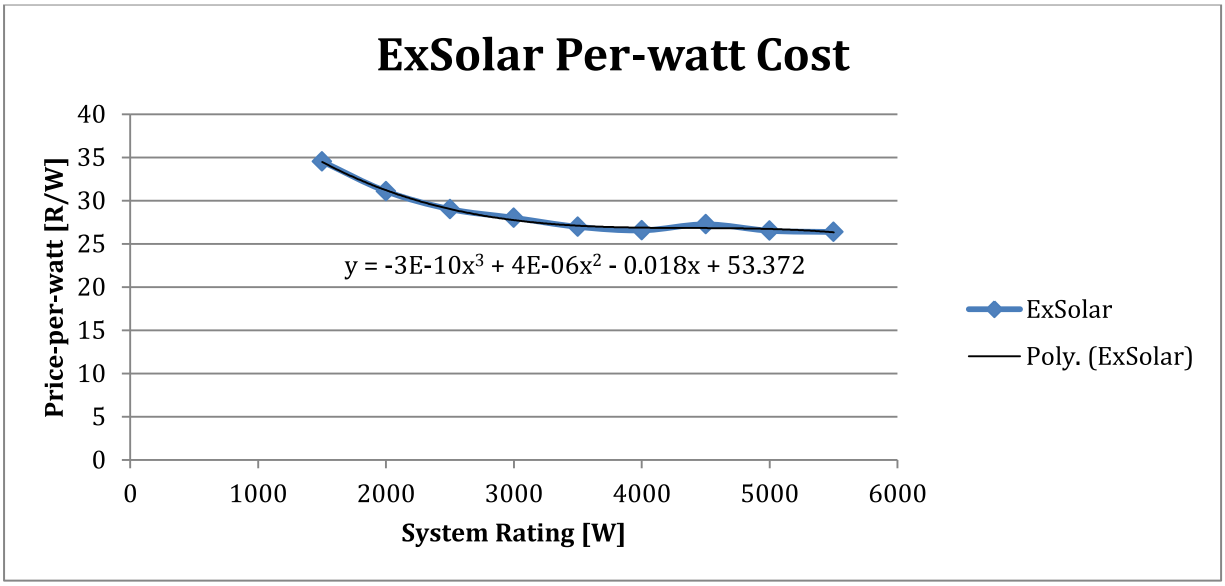

Appendix Figure D.4 Per-watt total cost of the PV system

Repeating the previous process for only the battery components the total purchase price of battery systems are shown in Appendix Figure D.5. The service provider's offering is the same as given in Appendix Table D.1.

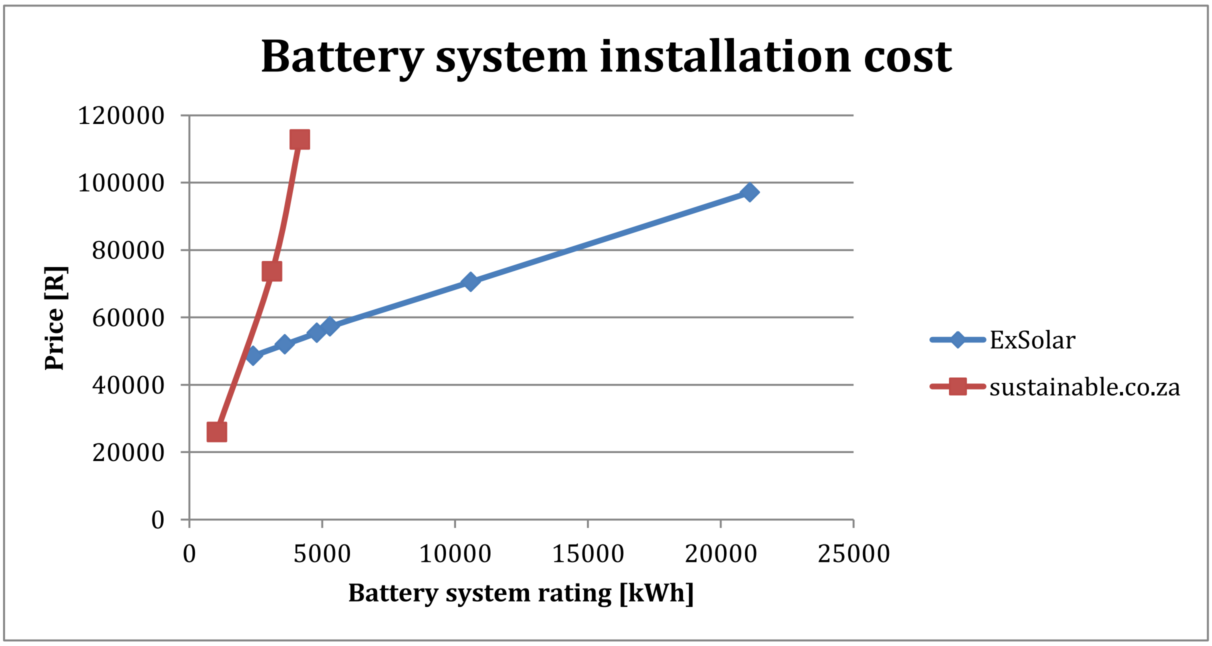

Appendix Figure D.5 Comparison of battery installation cost from different vendors

A per-watthour battery purchase price is calculated for the prices attained from sustainable.co.za [115]. The derivation of the per-unit price is given in Appendix Table D.3 and graphically in Appendix Figure D.6.

Appendix Table D.3 Per unit cost calculation of battery system purchase cost

	1kW inverter/ 2500Wh	3kW inverter/7500Wh	5kW inverter/12500Wh
Bi-Inverter	7965	19391	23400
Batteries	21250	63750	106250
Connectors	2921.5	8314.1	8153.6
Total	32136.5	91455.1	137803.6
Per-Unit cost	32.14	30.48	27.56

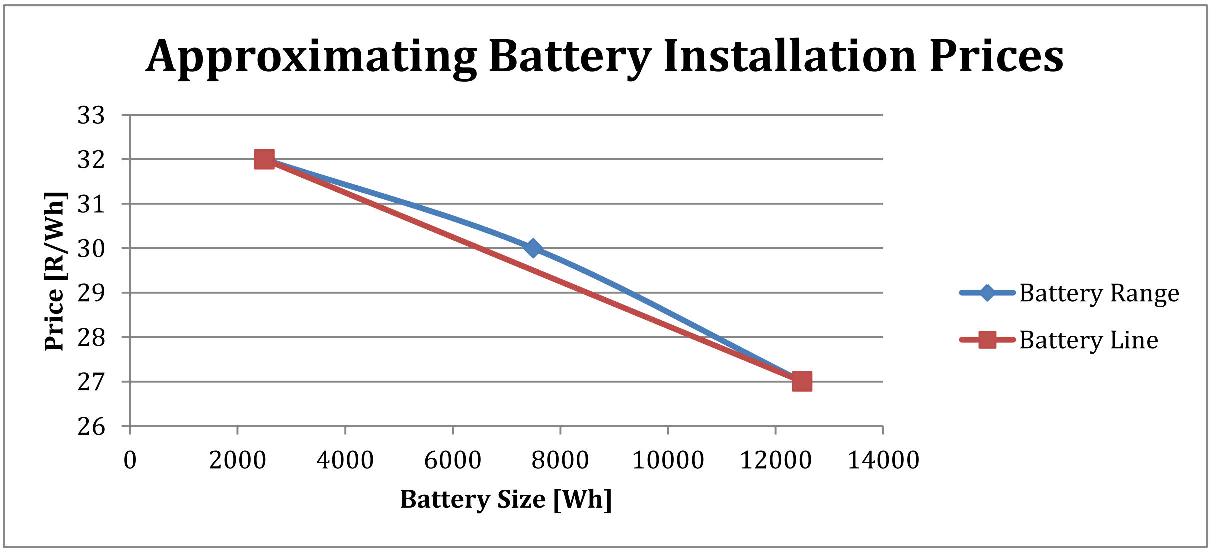

Appendix Figure D.6 Linear function to approximate per-unit cost

A per-watthour price is found for ExSolar, applying linear regression to find the function indicated on Appendix Figure D.7. A power-based function followed the data best and was chosen to use for the function.

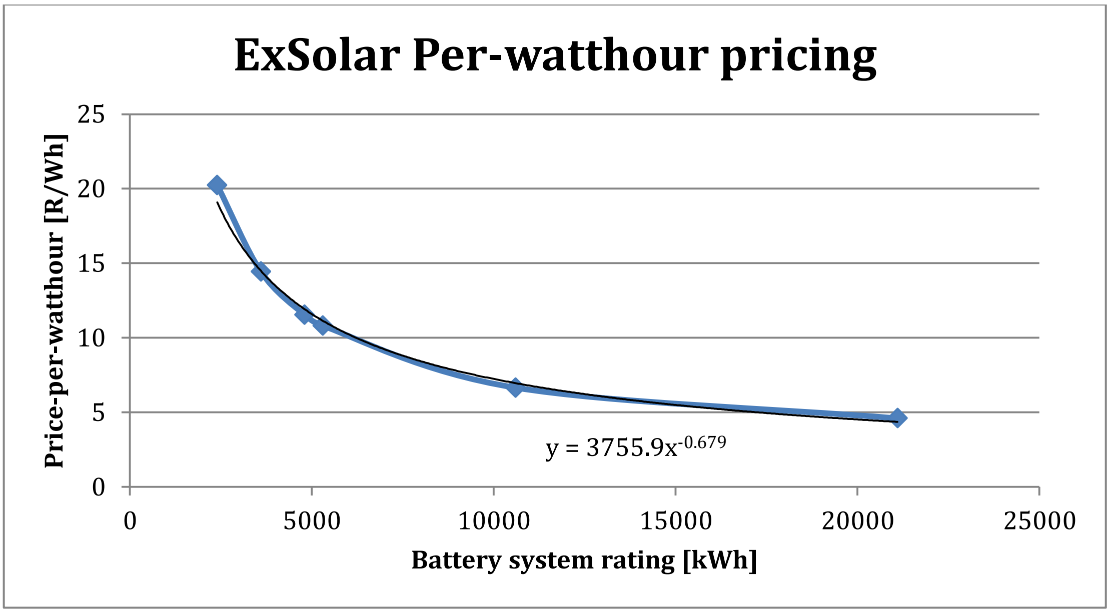

Appendix Figure D.7 Per-watthour total cost of the battery system

Appendix E: Load Profile Derivation

Overview

This section documents the attempt to create a load profile through a bottom-up approach. Each load has been documented to reflect the defense for choosing the appropriate load parameters. The outcome of this is a load schedule representing the averaged winter and summer load profile.

Load profile schedule

The load schedule found for winter and summer is shown in Appendix Table.E.1. The load profiles generated from this load schedule for the averages summer profile is given in Appendix Figure E.1 and the load profile for winter by Appendix Figure E.2. A description of each load is subsequently given to defend the choices made regarding the parameters for the schedule.

Appendix Table.E.1 Load schedules for bottom-up generated load profile

Appliance	Rating [kW]	Duty Cycle	Schedulable	Summer	Winter
Outside					
Pool pump	0.75	1	Yes	09:00 – 13:00	10:00 – 12:00
				17:00 – 21:00	17:00 – 19:00
Light 1 Outside	0.015	1		19:30 – 06:00	17:45 – 08:00
Light 2 Outside	0.015	1		19:30 – 06:00	17:45 – 08:00
Light 3 Outside	0.015	1		19:30 – 06:00	17:45 – 08:00
Light 4 Outside	0.015	1		19:30 – 06:00	17:45 – 08:00
Light 5 Outside	0.015	1		19:30 – 06:00	17:45 – 08:00
Water heating					
Geyser	3	1	Yes	06:15 – 07:45	06:00 – 09:00
				19:00 – 21:00	18:00 – 22:40
Bedroom 1					
Light 1 Bedroom 1	0.015	1			06:00 – 07:00
				20:00 - 22:00	20:00 - 22:00
Bedroom 2					
Light 1 Bedroom 2	0.015	1			06:00 – 07:00
				20:00 - 22:00	20:00 - 22:00

Bedroom 3					
Light 1 Bedroom 3	0.015	1			06:00 – 07:00
				20:00 - 22:00	20:00 - 22:00
Bathroom					
Light 1 Bathroom	0.015	1			06:00 - 07:30
					19:00 -20:00
Kitchen					
Refrigerator+Freezer	0.037	Incl.		00:00 - 24:00	00:00 - 24:00
Kettle	2.2	1		07:00 - 07:05	07:00 - 07:10
				19:00 -19:10	18:00 - 18:15
Light 1 Kitchen	0.03	1			06:00 - 07:30
				19:00 - 20:00	18:00 - 20:00
Microwave	1.5	1		06:00 - 06:15	06:00 -06:15
				18:00 - 18:15	18:00 - 18:15
Oven	2.3	0.8		18:00 – 19:00	18:00 – 19:00
Washing Machine	2.3	0.6		06:00 - 06:40	06:00 - 06:40
Tumble Dryer	1.75	0.75			06:15 - 07:00
Dishwasher	2.3	0.75		06:00 - 07:30	06:00 - 07:30
				18:00 - 19:30	18:00 - 19:30
Entertainment area					
Light 1 Ent	0.015	1		19:00 - 20:00	19:00 - 20:00
Aircon	2.5	0.5		18:00 - 19:00	18:00 - 20:00
Standby loads					
Router,Alarm systems etc	0.025			00:00 – 24:00	00:00 – 24:00

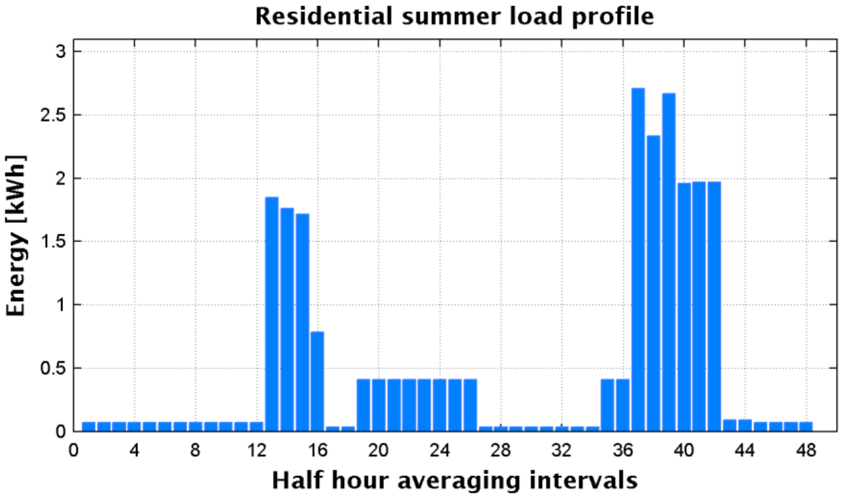

Appendix Figure E.1 Load profile generated for summer without (left) and with (right) the geyser

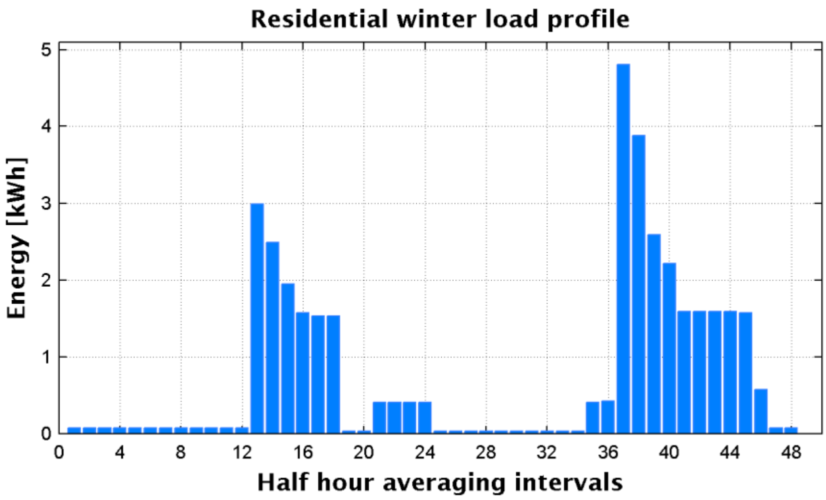

Appendix Figure E.2 Load profile generated for winter

Water Heating

The following sources were used to construct the geyser profile:

1. Meyer, JP. "A review of domestic hot-water consumption in South Africa," *R&D Journal*, pp. 55-61, 2000.
2. I Dincer, M A Rosen. *Thermal energy Storage: Systems and Applications*. Wiley: West Sussex, England. 2002.
3. Davis, S. "Measuring the rebound effect of energy efficiency initiatives for the future", Energy Research Centre, Cape Town. 2010.

The energy available through thermal storage in a medium is given by

$$E = C(T_2 - T_1)V$$

where E denotes energy, C denotes the specific het per unit volume, T_2 and T_1 denotes temperature and V denotes the volume of the substance.

The heating capacity of water is

$$C = 4.19 \frac{kJ}{kgK} at\ 15°C.$$

The objective is to determine the energy requirements of the geyser during winter and summer. A household with 4 members is assumed. Per person, the typical hot water requirements (at 65 degrees Celsius) for a middle –to-high income household is taken as 90*l* during the winter and 60*l* during the summer. During the winter, the temperature of the water flowing into the geyser is taken as 10 degrees Celsius, and during the summer it's taken as 20 degrees Celsius. The conversion rate for 1 joule of energy to kWh is $2.778x10^{-7}$. Therefore, the energy required to provide the house with warm water during winter is given by

$$\begin{aligned} E &= 4.19 \times (65 - 10) \times 360 \\ &= 82\ 962\ kJ \\ &= 23.05\ kWh \end{aligned}$$

and in summer

$$\begin{aligned} E &= 4.19 \times (65 - 20) \times 200 \\ &= 37\ 310\ kJ \\ &= 10.48\ kWh. \end{aligned}$$

Generating a geyser load profile for a single household can be difficult due to the high variability between load profiles of different houses. Taking into account that geyser usage is high in the morning and afternoon, the geyser is assigned to operate at full power for during the mornings and during the afternoon. Assuming a geyser of 3kW, that would imply 10,48 kWh/3 kW = 3.5 hours in summer, and 23,0.5 kWh/3 kW = 7.66 hours.

Lights

Sources:

1. Matlab Suncycle. “suncycle” [online]. Available: http://mooring.ucsd.edu/software/matlab/doc/toolbox/geo/suncycle.html (accessed 29 November 2015).

The light schedules in the house have been modelled according to behaviour expected by residents according to the the sunrise and –set times of winter and summer. The table below give the average sunset and sunrise times for winter and summer

Appendix Table E.2 Sunrise and sunset times for Stellenbosch, South Africa.

	Winter	**Summer**
Sunrise	7:42	5:55
Sunset	17:53	19:44

All residents wake up at 06:00 and leave the house at 07:30. At night, residents spend time in the kitchen and entertainment area. Before going to sleep, residents are in their bedrooms. The light schedules were designed around the given sunset/sunrise details and the living pattern. The lights were chosen to be 15 W fluorescent lights, except the light installed in the kitchen, which is a 30 W fluorescent tubular bulb.

Refrigerator and Freezer

The data is extracted from databases containing typical appliance ratings. A large refrigerator/freezer was chosen for this family. The data for the 410l refrigerator/freezer shows expected annual consumption of 325kWh. As the refrigerator runs consistently, to load was modelled to consume a constant amount of power throughout the year. This is calculated by

$$325\ kWh \times \frac{1}{365\ days} \times \frac{1}{24\ hours} = 0.037kW \tag{6.1}$$

Therefore the refrigerator/freezer is modelled as a load with a constant power consumption of 37 W.

Kettle

The following sources were used to research the kettle profile:

1. Dong M, Meira PCM, et al. “Non-Intrusive Signature Extraction for Major Residential Loads”, *IEEE Transactions on smart grid,* vol 4, 2013.

The kettle draws its rated amount of power during the full time it is on. An example of a kettle load profile is given in Appendix Figure E.3. The usage of the kettle is shown to be during the mornings and the afternoons. When the kettle is used, it operates at 100% duty cycle. The kettle is chosen to be rated at 2200W.

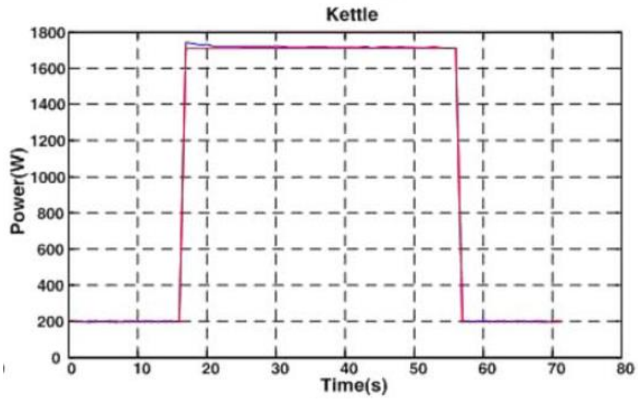

Appendix Figure E.3 Measured load profile of a kettle (Dong, Meira, 2013)

Microwave

A local database of appliance ratings is used to select a rating for the microwave. A 1500 W microwave was chosen for this family. The microwave is used primarily for the preparation of meals; therefore it operates mornings and during the afternoon.

Oven

The following sources were used to research the oven energy profile:

1. Gonzalez M, Debusshere, et al. "A Load Identification Method for Residential Building Applications", *IEEE International Conference on Industrial Technology*, pp 84- 88, 2012.
2. Pipattanasomporn M, Kuzlu M, et al. "Load Profiles of Selected Major Household Appliances and Their Demand Response Opportunities", *IEEE Transactions on smart grid*, pp 742 – 750, 2014.

The stove hob in this residence operates is chosen to use gas as an energy source, therefore the stove plates are not considered in the energy profile. The oven is electrical, and is used during the evenings for cooking. A load profile acquired for oven electricity use show initially a lower power rating, then full power, and then maintains the heat by intermittently switching on and off again. The load profiles are shown in Appendix Figure E.4 and Appendix Figure E.5.

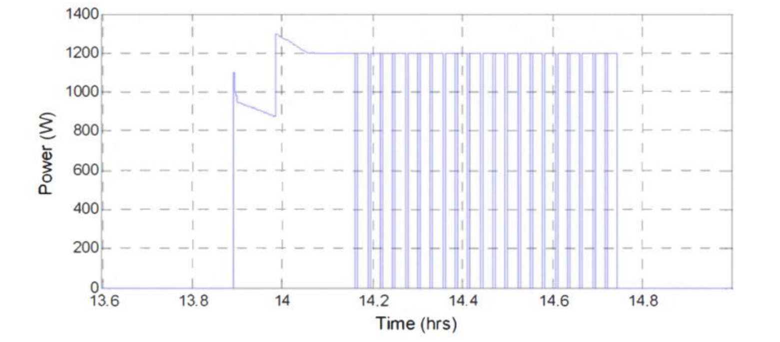

Appendix Figure E.4 Electric stove energy profile (Gonzalez, Debusshere, 2012)

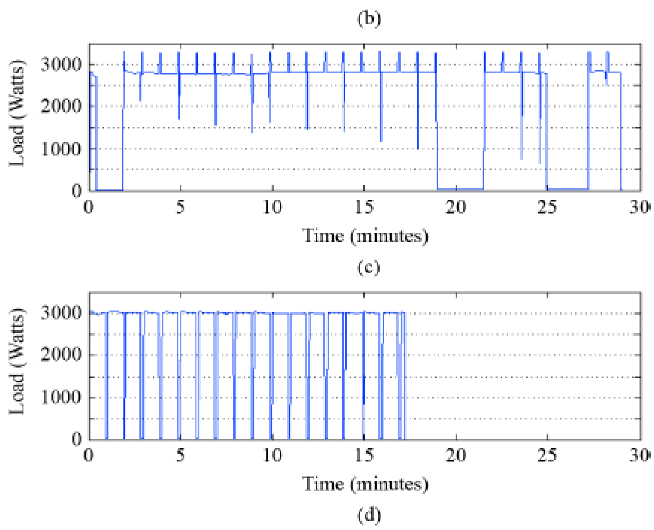

Appendix Figure E.5 An extract from (Pipattanasomporn, Kuzlu, 2014) showing electric oven bake and groil energy profiles.

For this residence at hand, the oven will be used for food preparation at night. The mimicked load profile will be taken to operate at 80% duty cycle for the duration of the hour. The oven is chosen to be a relatively small model at 2 300 W.

Washing machine

The following sources were used to research the microwave energy profile:

1. Stephen B, Galloway S, et al. "Self-learning load characteristic model for smart appliances," *IEEE Transactions on smart grid*, vol 5, pp 2432 – 2439, 2014.

From a database of appliance rating data, a 2 300 W washing machine is selected to be used in this residence. A study on residential appliances identified a washing machine load profile as shown in Appendix Figure E.6. The load profile shows a large initial energy use for about 17 minutes, an insignificant energy use for about 17 minutes, and a small energy used during the last 5 minutes. The typical cycle is then about 40 minutes. The same behaviour is somewhat simplified and mimicked by modelling the load as a 2.3kW load, active for 25 minutes, with a 100% duty cycle.

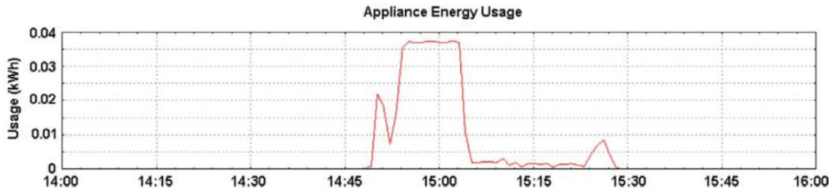

Appendix Figure E.6 Measured washing machine energy profile (Stephen, Galloway, 2014)

Tumble dryer

The following sources were used to research the tumble dryer energy profile:

1. Stephen B, Galloway S, et al. "Self-learning load characteristic model for smart appliances," *IEEE Transactions on smart grid*, vol 5, pp 2432 – 2439, 2014

From a database of appliance rating data, a 1 750 W tumble dryer is selected to be used in this residence. The tumble dryer is active only during the mornings, to dry clothes that need to be worn on the day. A load profile for a tumble dryer has been measured in the referenced report, and is shown in Appendix Figure E.7. The cycle is active for almost 45 minutes, but the most energy is consumed within the first 38 minutes of operation. The load profile is simplified and mimicked by modelling the 1.75 kW tumble dryer as a load that is on for 45 minutes with a duty cycle of 75%.

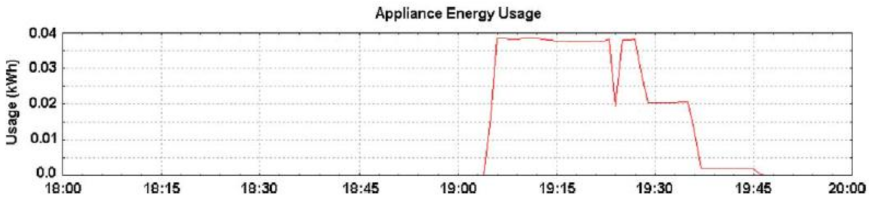

Appendix Figure E.7 Measured tumble dryer energy profile (Stephen, Galloway, 2014)

Dishwasher

The following sources were used to research the dishwasher energy profile:

1. Stephen B, Galloway S, et al. "Self-learning load characteristic model for smart appliances," *IEEE Transactions on smart grid*, vol 5, pp 2432 – 2439, 2014

2. North West Univeristy. "Practical guidelines on how to save energy at home" [online]. Available: http://www.nwu.ac.za/faculty-engineering-energy-saving-home-dishwasher (accessed 29 November 2015).

The dishwasher in this residence is used to clean dishes every morning and every night. The energy load profile of the dishwasher as given in (Stephen, Galloway, 2014) is given in Appendix Figure E.8. The measured dishwasher had the functionality to do a rinse cycle apart from the normal washing cycle. In the model that is used to mock this software, this will all be done in a single cycle.

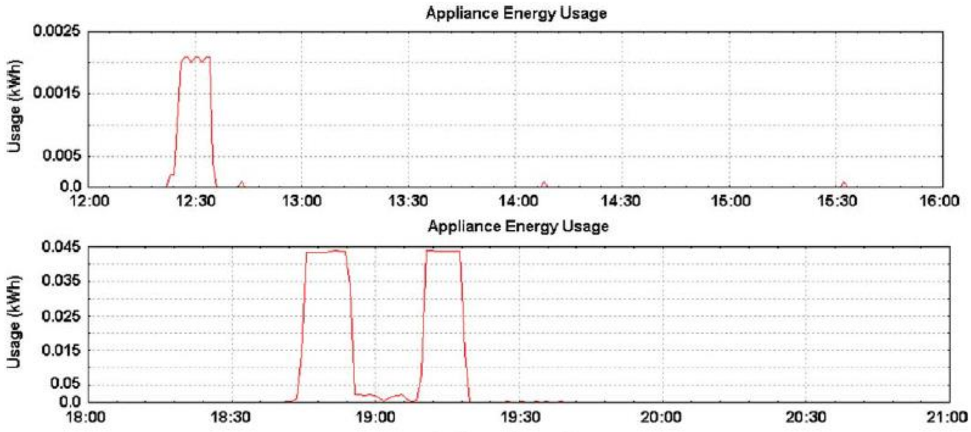

Appendix Figure E.8 Measured dishwasher energy profile (Stephen, Galloway, 2014)

Appliance data for South African dishwashers is provided by the North West University's data. An extract of the data is given in Appendix Figure E.9. This gives the energy consumption of an older dishwasher model at 1,15 kW. Using a 2,3 kW dishwasher with a washing cycle of 1,5 hours (from the appliance data) this corresponds to a device operating at a mean duty cycle of 33%.

Dishwasher Consumer Profile

Criteria	Unit	Dishwashers		
Capacity in place settings	N	12	12	14
Electrical energy consumption per three part cycle	kWh	1.15	1.02	0.93
Water consumption per three part cycle	ℓ	16	14	9.5
Noise emission	dB	54	52	46
Overall class		A	A+	A++
Drying efficiency class		A	A+	A
Annual electrical energy consumption (280 Three part cycles)	kWh	322	285.6	260.4
Annual water consumption (280 Three part cycles)	ℓ	4480	3920	2660
Cost of electrical energy	R	1.51	1.51	1.51
Annual cost of electrical energy	R	486.22	431.26	393.20
Cost of dishwasher	R	4299	5299	5999
Typical lifecycle	y	10	10	10
Total lifecycle cost	R	7519	8155	8603
Breakeven point	y	0	18.2	18.28

Appendix Figure E.9 Extract from North West University data on dishwashers

Air conditioner

The following sources were used to research the air conditioner energy profile:

1. Chanana S, Arora M. "Demand Response from Residential Air Conditioning Load Using a Programmable Communication Thermostat", *International Journal of Electrical, Computer, Energetic, Electronic and Communication Engineering*, vol 7, pp 1180 – 1186, 2013.
2. South Africa National Standards. 54511-3:2010.
3. Powerknot. "COPs, EERs, and SEERs" [online]. Available: http://www.powerknot.com/how-efficient-is-your-air-conditioning-system.html (accessed 29 November 2015).

Air conditioners come in a variety of different forms: Central units, window units, and split units. For this residence a split unit is used. The air conditioner is also capable of heating. When cooling, the efficiency of the air conditioner is dictated by the energy efficiency ratio (EER). This indicates the effective cooling power against the power input to the unit.

When operating in heating mode, the efficiency of the air conditioner is given by the coefficient of performance (COP). This gives the effective output energy over the electrical energy input by the user.

An air conditioner works as a heat pump as demonstrated in . Effectively it takes electrical energy E_{in} as input. This electrical energy is applied to remove heat energy from the household. The combined removed heat and electrical input is deliver it to the outside environment as E_{out}.

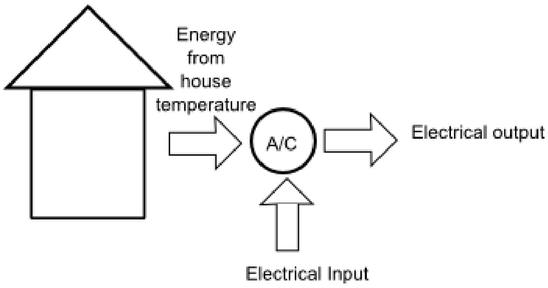

Appendix Figure E.10 An air conditioner can be modelled as a heat pump (Powerknot)

The process is shown in the figure below. The EER is then calculated as

$$EER = \frac{E_{out}}{E_{in}}$$

The process for COP is the exact opposite, where electrical energy is used to take heat energy from the environment, heat the air further, and pump it into the residence. The EER and COP rating of air conditioners is indicated on the energy label, as specified by the SANS standards:

Appendix Table E.3 SANS standards for air conditioners

Energy Efficiency Class	EER (at full load, T1 conditions)	Power consumption P [W]
A	$EER > 3{,}20$	$P < 3\,750$
B	$3{,}20 \geq EER > 3{,}00$	$3750 \leq P < 4000$

Given the standards as given in Appendix Table E.3, an A rated air conditioner/heat unit is chosen for the household. For simplicity, the heating and cooling is taken to use the same amount of energy at the same duty cycle. A study conducted on controlling the temperature control on air conditioners gives a typical load profile as shown in Appendix Figure E.11. In the residence that this project models, the air conditioner and heater is run at night when the family is at home – taking a rough estimate when the figure below is considered, the air conditioner and heater is taken to be operating at a 50% duty cycle. The air conditioner/heating unit is taken to be a 3,5 kW unit.

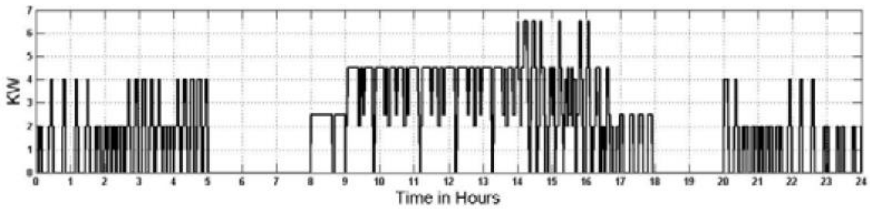

Appendix Figure E.11 Air conditioner power consumption over 24 hours (Chanana, Arora, 2013)

Pool pump

The following sources were used to research the pool pump energy profile:

1. World Health Organisation. "Guidelines for safe recreational water environments: Volume 2" [online]. Available: http://apps.who.int/iris/bitstream/10665/43336/1/9241546808_eng.pdf?ua=1 (accessed 29 November 2015).
2. Center for Disease Control and Prevention. "Healty housing reference manual" [online]. Available: http://www.cdc.gov/nceh/publications/books/housing/housing_ref_manual_2012.pdf (accessed 29 November 2015)
3. Penguin Pools. "Fibreglass Pools" [online]. Available: http://www.penguinpools.co.za/fibreglass-pools.html (accessed 29 November 2015)

The cleaning mechanism for bacterial infections in swimming pools is chlorine, whilst the removal of particles from the pool is achieved by the filter. The water is pumped from the swimming pool, through the filter and redeposited into the swimming pool. The amount of filtering necessary is calculated by the amount of times it's required to filter through the entire volume of water of the pool during a single day, which is called the turnover rate.

A pool pump's energy rating shows the amount of output power from the pump. The pump also indicates the flow rate that it is able to handle. With regards to efficiency, a large number of studies are concerned with lowering the flow rate of the pump. This project will not focus on lowering the flow rate – that is either subjected to further studies, or the responsibility of the user. The optimisation algorithm for all loads in this study is to reschedule specified operation times of loads to minimise the cost of purchasing electricity from the grid.

During the summer, pools are more often used and therefore a larger turnover of water is required. Pool pumps will then operate for longer periods of time in summer than in winter.

Therefore the pool is modelled with a 750W pool pump that requires 4 hours of operation during the winter, and 8 hours of operation during the summer.

Standby Loads

The following sources were used to research the standby loads energy profile:

1. Hardware info. "Linksys WRT1900AC" [online]. Available: http://us.hardware.info/productinfo/214507/linksys-wrt1900ac/testresults (accessed 29 November 2015).
2. Bredekamp AJ, Uken EA, et al. "Standby power consumption of domestic appliances in South Africa", *Domestic use of Energy Conference*, 2006.
3. Shuma-Iwisi MV, "Estimation of standby power load in South Africa domestic sector: initial survey results" Ph.D. dissertation, Engineering Faculty, University of Witwatersrand, Johannesburg, Gauteng, 2009.

From the sources as listed, the standby power in a residence is insignificant. The combined standby power of the microwave, router and media devices is taken as 25W.

Appendix F Real residential load profile

Introduction

The national electric utility, Eskom, provided confidential data that contains half-hour load profiles of about 700 houses, measured for 2013 and 2014. The data had not been validated and integrity-checked; therefore this still needed to be done. This section describes the process.

Data structure transformation

As received, the data was stored in CSV files, one for each month of 2013 and 2014, containing in the rows the consecutive readings of all half-hour energy consumption measurements for each house. This is indicated in Appendix Table F.1, with mocked data.

Appendix Table F.1 Data structure of energy consumption data

Service Point	Timestamp	Energy [kWh]
HouseId1	DD/MM/YYYY HH:MM	10
HouseId1	DD/MM/YYYY HH:MM	10

This data was captured and transformed to show the load profile of every house for an entire year. Negative and exceptionally high values were replaced with average values if isolated or with data of the following week if an interval of data was missing. The transformed data structure is indicated in Appendix Table F.2, with ellipses indicating in-between values which are not included for the sake of brevity.

Appendix Table F.2 Transformed data structure of consumption data

Service Point	01/01/2013 00:00	…	31/12/2013 23:30
HouseId1	10	…	10
HouseId2	10	…	10

A confidence factor was calculated for each household to indicate the amount of missing or unrealistic high values in the dataset for each season. This indicator was used to assist in using only credible data for simulations .Each residence was assigned an average daily energy consumption to get some idea of the energy requirements of each house.

Residential load profiles used for case studies were taken from this data set. As per the confidentiality agreement, the raw data is not published, but the load profile of a single residence is shown graphically for demonstration purposes. The data has been interrogated and cleansed. The load profile is given in Appendix Figure F.1 and Appendix Figure F.2.

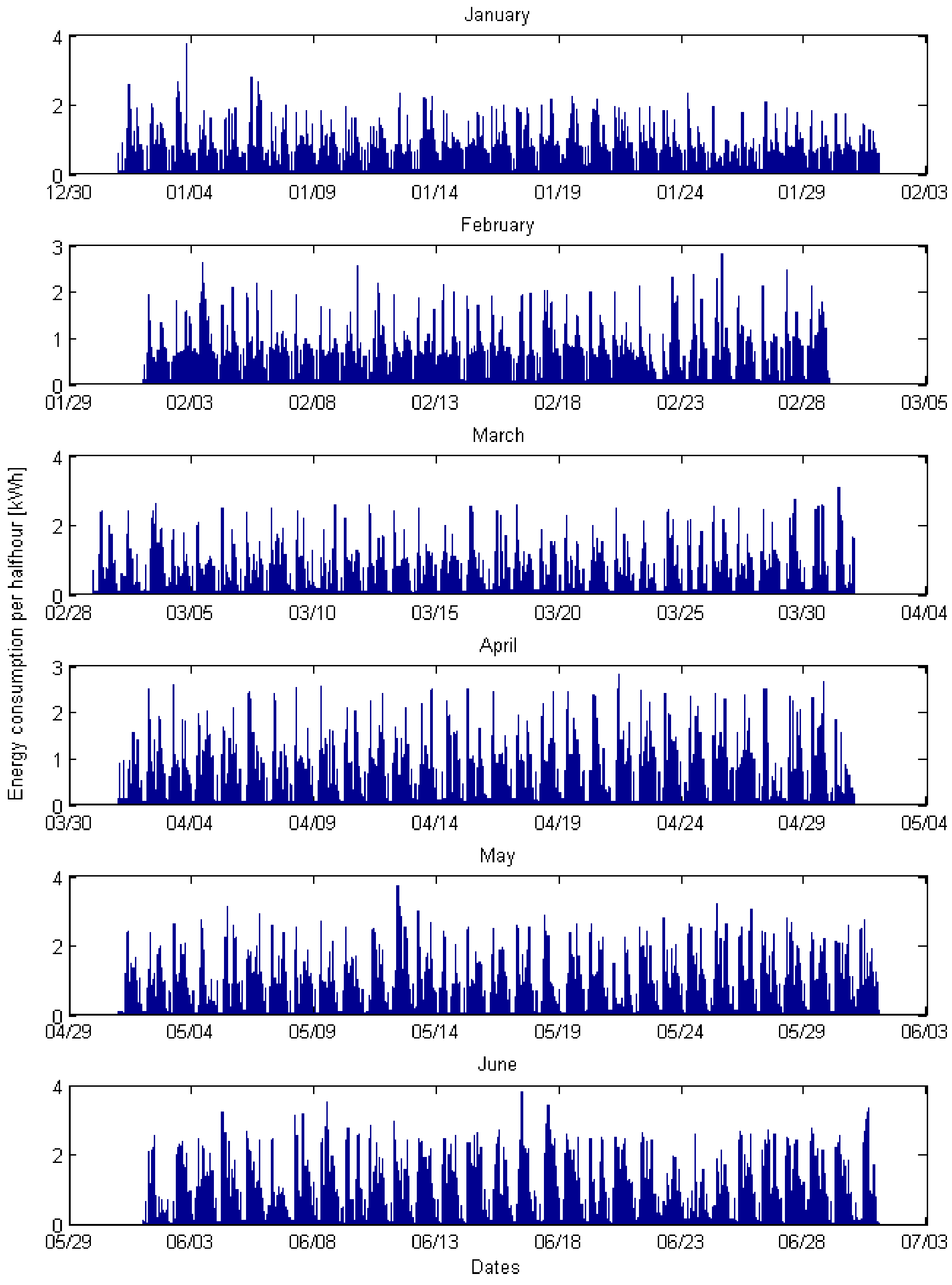

Appendix Figure F.1 Residential load profile for the first six months of 2013

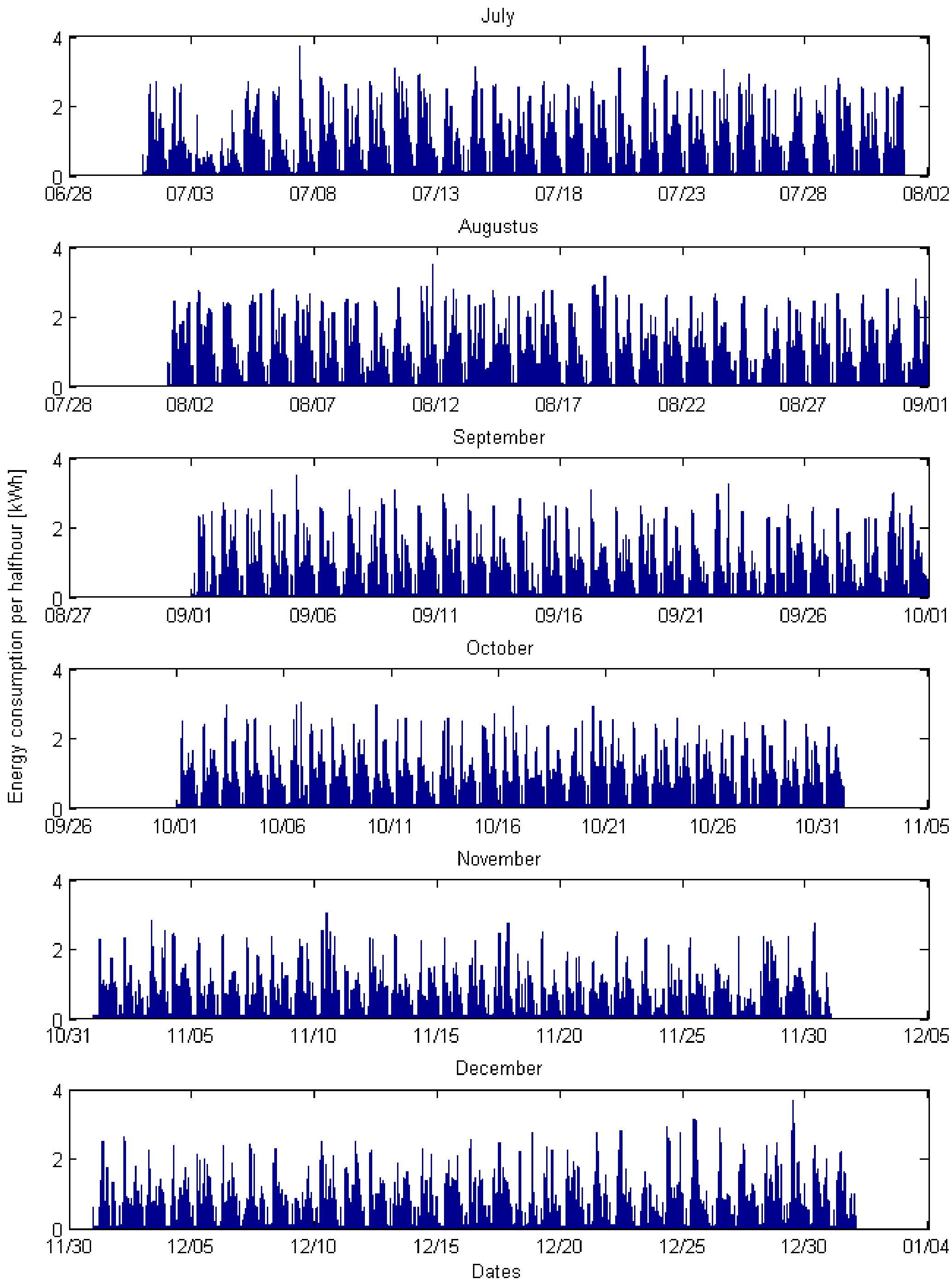

Appendix Figure F.2 Residential load profile for the last six months of 2013